

# Development of innovative in situ forming gels for topical ophthalmic delivery

---

Krtalić, Iva

Doctoral thesis / Disertacija

2018

Degree Grantor / Ustanova koja je dodijelila akademski / stručni stupanj: **University of Zagreb, Faculty of Pharmacy and Biochemistry / Sveučilište u Zagrebu, Farmaceutsko-biokemijski fakultet**

Permanent link / Trajna poveznica: <https://urn.nsk.hr/urn:nbn:hr:163:959202>

Rights / Prava: [In copyright](#)/[Zaštićeno autorskim pravom.](#)

Download date / Datum preuzimanja: **2024-07-18**



Repository / Repozitorij:

[Repository of Faculty of Pharmacy and Biochemistry University of Zagreb](#)





University of Zagreb

University of Zagreb  
FACULTY OF PHARMACY AND BIOCHEMISTRY

Iva Krtalić

**DEVELOPMENT OF INNOVATIVE IN SITU  
FORMING GELS FOR TOPICAL  
OPHTHALMIC DELIVERY**

DOCTORAL DISSERTATION

Zagreb, 2018



University of Zagreb

UNIVERSITY OF ZAGREB  
FACULTY OF PHARMACY AND BIOCHEMISTRY

Iva Krtalić

**DEVELOPMENT OF INNOVATIVE *IN SITU*  
FORMING GELS FOR TOPICAL  
OPHTHALMIC DELIVERY**

DOCTORAL DISSERTATION

Supervisor:  
Jasmina Lovrić, Ph.D.

Zagreb, 2018



University of Zagreb

SVEUČILIŠTE U ZAGREBU  
FARMACEUTSKO-BIOKEMIJSKI FAKULTET

IVA KRTALIĆ

**RAZVOJ INOVATIVNIH *IN SITU*  
GELIRAJUĆIH PRIPRAVAKA ZA  
TOPIKALNU PRIMJENU OFTALMIČKIH  
LIJEKOVA**

DOKTORSKI RAD

Mentorica:  
izv. prof. dr. sc. Jasmina Lovrić

Zagreb, 2018.

The doctoral thesis was submitted to the Faculty Council of the Faculty of Pharmacy and Biochemistry, University of Zagreb in order to acquire a PhD degree in the area of Biomedicine and Health, the field of Pharmacy, the branch of Pharmacy.

The work presented in this doctoral thesis was performed at the Faculty of Pharmacy and Biochemistry and PLIVA CROATIA Ltd. under supervision of Associate Prof. Jasmina Lovrić, PhD. The research conducted was financed by the project „Development of *in vitro* and *ex vivo* models for the permeability testing of new topical ophthalmic formulations“ (04.01/56, „Partnership in research“, Croatian Science Foundation and PLIVA CROATIA Ltd.).

## ZAHVALE / ACKNOWLEDGEMENTS

Na kraju ovoga izazovnoga, ali i ispunjujućega te poprilično dugoga putovanja koje je snažno obilježilo moj život, željela bih zahvaliti dragim ljudima, bez kojih ono ne bi bilo isto, a do čijega bi kraja bilo značajno teže stići.

Prvenstveno, od srca veliko hvala mojoj mentorici izv. prof. dr. sc. Jasmini Lovrić na iznimnoj pomoći u nastajanju ove disertacije, na jasnoj viziji i vodstvu tijekom našega istraživanja, savjetima, potpori i strpljenju. Hvala na svemu što si me naučila, ostavilo je veliki trag u meni.

Hvala kolegicama i kolegama iz I&R, mojim Fizikalkama (Liljani, Dunji i Ivani) kojima nije bilo teško montirati haubicu na reometar po milijunti put. Dragoj Ani i Nikolini velika zahvala na pomoći pri izradi uzoraka - vjerojatno će još dugo i naširoko zaobilaziti ledene kupelji.

Hvala Senki na nemjerljivoj pomoći u svijetu statistike. Tvrtku zahvala na lijepim grafičkim idejama i rješenjima. Tanja, hvala puno na logističkoj, a često i na emocionalnoj potpori kada mi je bila potrebna.

Mojim Pliva-curkama - Ivani, Jasmini, Ivi, Mihaeli, Maji, Marini te cimeru - veliko hvala za potporu sve ove godine, lako je raditi kada si okružen prijateljima. Hvala dugogodišnjim prijateljima (mojim Metkovicima, curama iz Gorjanske i trešnjevačkoj ekipici) – dugo su slušali o *nekim* gelovima i davali mi potporu da ustrajem u ovom cilju.

Neizmjerne sam zahvalna mojoj obitelji, najdražim Ujdurima – mami, tati, Kati i Tomi što su, bez iznimke, uvijek i u svakom smislu, pravo značenje izraza "biti tu", lijepo je biti dio ove obitelji.

Hvala i mojoj "novoj" obitelji, Krtalićima, na velikoj podršci tijekom nastajanja ovoga rada.

I na kraju, hvala mojim dečkima Viti i Vedranu, dvojcu najvrjednijem u mom životu, mojoj radosti, veselju, miru i snazi... hvala na podršci, razumijevanju, razgovorima, zagrljajima, toplini, ljubavi...hvala na svemu, nije bilo lako i trebalo (me) je izdržati.

## TABLE OF CONTENTS

SUMMARY .....	1
SAŽETAK .....	3
1. INTRODUCTION .....	8
2. THEORETICAL PART .....	11
2.1. Ophthalmic drug delivery .....	12
2.1.1. Topical ophthalmic drug delivery .....	13
2.2. Topical ophthalmic dosage forms .....	20
2.2.1. Innovative ophthalmic drug delivery systems.....	22
2.3. Hydrogels in ophthalmic drug delivery.....	25
2.3.1. <i>In situ</i> forming ophthalmic gels .....	26
2.3.2. pH-responsive <i>in situ</i> forming gels .....	30
2.3.3. Ion-responsive <i>in situ</i> forming gels.....	31
2.3.4. Temperature-responsive <i>in situ</i> forming gels.....	33
2.4. Poloxamer-based <i>in situ</i> forming ophthalmic gels.....	36
2.5. Considerations for formulation development of poloxamer-based <i>in situ</i> forming ophthalmic gels .....	40
2.6. Chitosan in ophthalmic drug delivery .....	42
2.7. Rheological characterization of <i>in situ</i> forming gels .....	44
2.8. Quality by Design and Design of Experiments in pharmaceutical development .....	51
2.8.1. DoE workflow .....	53
2.9. Ocular tolerability assessment.....	55
3. AIMS OF THESIS .....	57
4. MATERIALS AND METHODS .....	59
4.1. Materials.....	60
4.2. Methods.....	61
4.2.1. Preparation of <i>in situ</i> forming ophthalmic gels.....	61
4.2.2. Osmolality, pH and transparency determination.....	61
4.2.3. Measurement of temperature of gelation and complex viscosity .....	62
4.2.4. Design of experiments.....	63
4.2.5. Oscillatory rheological characterization – strain sweep, frequency sweep and gelation time testing.....	65

4.2.6.	Rotational rheological characterization.....	66
4.2.7.	Sterilization .....	66
4.2.8.	Physical stability of samples at room temperature.....	67
4.2.9.	In vitro release testing .....	67
4.2.9.1.	Solubility testing and choice of IVR medium.....	69
4.2.9.2.	Membrane selection study.....	69
4.2.9.3.	Data presentation and statistical analysis.....	70
4.2.10.	UPLC analyses .....	70
4.2.10.1.	Validation of UPLC method .....	71
4.2.11.	<i>In vitro</i> biocompatibility study.....	72
4.2.11.1.	Cell culture conditions .....	72
4.2.11.2.	Cultivation of the HCE-T cell-based model.....	73
4.2.11.3.	MTT Assay .....	73
5.	RESULTS AND DISCUSSION .....	74
5.1.	<i>In situ</i> forming ophthalmic gel development and optimization using a Design of Experiments .....	75
5.2.	The model of temperature of gelation.....	79
5.3.	Models of rheological properties: complex viscosity and storage modulus .....	83
5.3.1.	The model of complex viscosity .....	83
5.3.2.	The model of storage modulus.....	86
5.4.	Selection of rheologically improved <i>in situ</i> forming ophthalmic gel .....	89
5.4.1.	In depth rheological characterization of <i>in situ</i> forming ophthalmic gel – oscillatory tests.....	91
5.4.2.	Dynamic viscosity evaluation by rotational rheology.....	97
5.5.	Effect of active pharmaceutical ingredients on temperature of gelation and complex viscosity.....	100
5.5.1.	Evaluation of dynamic viscosity of systems containing APIs .....	103
5.5.2.	Gelation time.....	104
5.6.	Drug release from <i>in situ</i> forming gels .....	105
5.6.1.	Validation of UPLC method for quantification of TIMO .....	106
5.6.2.	Development of <i>in vitro</i> release method .....	110
5.6.2.1.	Selection of receptor medium – solubility testing.....	110
5.6.2.2.	Membrane selection .....	110
5.6.2.3.	Discriminatory power of the method .....	113



5.6.3.	Evaluation of IVR from the optimal <i>in situ</i> forming gel.....	116
5.7.	Sterilization .....	117
5.8.	Stability study .....	121
5.9.	Biocompatibility assessment of <i>in situ</i> forming ophthalmic gel.....	123
6.	CONCLUSIONS.....	125
	REFERENCES.....	128
	BIOGRAPHY.....	142

## SUMMARY

The anatomical barriers and the tear fluid dynamics in the precorneal area have a huge effect on the eye-related drug bioavailability. *In situ* forming gels stand out as the formulation candidates for the improvement of bioavailability and efficacy of topical ophthalmic drugs. These are prepared as liquid dosage forms that undergo phase transition on eye surface to form viscoelastic gel in response to an environmental stimulus following topical administration. During formulation development, *in situ* forming ophthalmic gels need to be fine-tuned considering all the biopharmaceutical challenges of the front of the eye. The aim of this thesis was to develop temperature-responsive *in situ* forming poloxamer P407/ poloxamer P188/chitosan gel fine-tuned in terms of polymer content, temperature of gelation, viscosity and storage modulus by applying Quality by Design principles. Minimizing the total polymer content, while retaining the advantageous rheological properties, has been achieved by means of D-optimal statistical design. *In situ* forming gels were prepared by cold method and analyzed by rheological temperature sweep test. Statistical software was used to set experimental design, establish the mathematical model and analyze the collected data. Validated mathematical models enabled the selection of 4 candidates of poloxamer 407/poloxamer 188/chitosan systems, which viscoelastic behavior was studied in depth by oscillatory rheological tests under biorelevant conditions (after dilution with simulated tear fluid in the ratio of 40:7). The optimal *in situ* forming gel was selected based on minimal polymer content (P407, P188 and chitosan concentration of 14.2, 1.7 and 0.25%, w/w, respectively), favorable rheological characteristics and *in vitro* resistance to tear dilution. The formulation robustness against entrapment of active pharmaceutical ingredients (API) with different physicochemical characteristics was demonstrated using four APIs in the concentrations and combinations relevant for topical ophthalmic use. Through discriminative *in vitro* release test, adequate release profile of model drug was proven. Biocompatibility of the optimal *in situ* forming gel was confirmed employing 3D corneal epithelial cell models. In conclusion, a systematic approach to *in situ* forming gel development implemented in this thesis resulted in a stable and robust formulation characterized by ease of formulation preparation, ability for sterile filtration and autoclaving, ease of administration, accuracy of dosing, avoidance of eye-related discomfort, biocompatibility and prolonged residence at the eye surface.

**KEYWORDS:** ophthalmic drug delivery, quality by design (QbD), poloxamers, chitosan, rheology, temperature-responsive *in situ* forming gel, temperature of gelation.

## SAŽETAK

**Uvod:** Topikalna je primjena glavni put primjene oftalmičkih lijekova, a kapi za oko najčešće korišten farmaceutski oblik. Međutim, pri primjeni kapi za oko, zbog dinamičnih barijera prekornealnog područja, dolazi do brze eliminacije lijeka s površine oka. Stoga je lijek dostupan za apsorpciju kroz samo nekoliko minuta što rezultira vrlo niskom bioraspoloživošću, uglavnom manjom od 5%. Klasični tehnološki pristupi, s ciljem produljenja vremena zadržavanja lijeka na površini oka, uključuju pripremu viskoznih otopina, gelova i masti. Međutim, ti su sustavi povezani sa zamućenjem vida i otporom gibanju vjeđa pri treptanju te poteškoćama pri doziranju što umanjuje suradljivost bolesnika. Iz navedenih je razloga velika potreba za inovativnim oftalmičkim pripravcima koji bi omogućili poboljšanje suradljivosti bolesnika i terapijske učinkovitosti u odnosu na klasične farmaceutske oblike. *In situ* gelovi predstavljaju jedno od inovativnih rješenja suvremene farmaceutske tehnologije. Izrađuju se od polimera koji pokazuju reverzibilne fazne prijelaze, a zbog povoljnih reoloških svojstava nastalog gela, minimiziraju smetnje s treptanjem, osjećaj stranoga tijela u oku, kao i zamućenje vida. Takav je sustav oblikovan kao otopina lijeka pogodna za primjenu u oko jer gelira pri fiziološkim uvjetima. *In situ* oftalmički gelovi trebaju biti pomno dizajnirani s ciljem produljenja vremena zadržavanja lijeka na mjestu primjene, povećanja bioraspoloživosti i učinkovitosti. Sustavan pristup razvoju farmaceutskih proizvoda provodi se po načelima kvalitete ugrađene u dizajn proizvoda (eng. *Quality by design*, QbD). Implementacija QbD principa rezultira uspješnim razvojem farmaceutskoga proizvoda, smanjenjem troškova te skraćanjem vremena do pojave lijeka na tržištu. Cilj je ovoga doktorskoga rada razviti *in situ* gel za oftalmičku primjenu korištenjem smjese polimera (poloksamera P407, poloksamera P188 i kitozana) specifično dizajnirane u smislu ukupnoga sadržaja polimera te reoloških parametara temperature geliranja ( $T_{gel}$ ), kompleksne viskoznosti ( $\eta^*$ ) i modula pohrane ( $G'$ ).

**Metode:** *In situ* oftalmički gelovi poloksamera P407 i P188 i kitozana (CS) pripremljeni su "hladnom" metodom dok je izotoničnost postignuta dodatkom NaCl. Osmolalnost je određena metodom snižavanja ledišta, a transparentnost mjerenjem indeksa refrakcije. S obzirom da su reološka svojstva formulacije pri sobnoj temperaturi i pri temperaturi površine oka ključna za točnost doziranja, vrijeme zadržavanja lijeka na površini oka, kao i njegovo oslobađanje iz *in situ* gela, korištenjem eksperimentalnog dizajna optimirana su reološka svojstva razvijenih sustava.

Temeljem eksperimentalne situacije, odabran je D-optimalni dizajn. Koncentracije P407, P188 i kitozana odabrane su kao nezavisne varijable, dok su kao odgovori od interesa odabrane  $T_{gel}$ ,  $\eta^*$  i  $G'$  pri temperaturi površine oka ( $35^{\circ}\text{C}$ ) mjerene reološkim testom promjene temperature (engl. *temperature sweep*) pri konstantnoj kutnoj frekvenciji i smičnoj deformaciji. Statistički je softver korišten za postavljanje eksperimentalnoga dizajna, utvrđivanje modela, generiranje sekvenci i za statističku obradu prikupljenih podataka. Kao optimalni raspon za  $T_{gel}$  odabran je  $28 - 32^{\circ}\text{C}$ ; za  $G'$  vrijednost minimuma je postavljena na 5 Pa, dok se optimalni raspon za vrijednosti viskoznosti odredio na osnovu karakterizacije komercijalno dostupnih *in situ* oftalmičkih gelova. Sva su reološka mjerenja provedena na reometru povezanim s posebnom jedinicom koja osigurava točnu temperaturu mjerenja i minimalizira isparavanje uzorka.

Viskoelastična svojstva *in situ* gelova ispitivana su testom promjene sile smičnog naprezanja pri konstantnoj frekvenciji (eng. *strain sweep*). Testom promjene frekvencije (eng. *frequency sweep*) procijenila se ovisnost viskoznosti i viskoelastičnih modula o promjeni frekvencije. Evaluacija *in situ* gelova provedena je i pri biorelevantnim uvjetima (nakon razrjeđenja umjetnom suznom tekućinom u omjeru 40:7) u svrhu procjene otpornosti formulacije prema razrjeđenju suzama. Za procjenu dinamičke viskoznosti razvijenih sustava, u usporedbi s komercijalno dostupnim oftalmičkim lijekovima, korišten je rotacijski reološki test u biorelevantnim uvjetima. Robusnost razvijene formulacije prema uklapanju djelatnih tvari ispitana je evaluacijom utjecaja djelatnih tvari različitih fizičko-kemijskih svojstava na reološke karakteristike gela. Korištene su četiri oftalmičke djelatne tvari (timolol, deksametazon, dorzolamid i tobramicin) u koncentracijama i kombinacijama relevantnim za topikalnu oftalmičku primjenu.

*In vitro* oslobađanje lijeka ispitano je korištenjem vertikalne difuzijske ćelije. Za određivanje djelatne tvari u prikupljenim uzorcima korištena je tekućinska kromatografija ultravisoke djelotvornosti (UPLC). Sterilizacija odabranih formulacija provedena je filtracijom te filtracijom i autoklaviranjem. Stabilnost sterilizirane formulacije pohranjene u dobro zatvorenim bočicama pri sobnoj temperaturi tijekom šest mjeseci evaluirana je mjerenjem ključnih reoloških svojstava. Biokompatibilnost razvijenoga optimalnoga *in situ* gela ispitana je korištenjem MTT testa vijabilnosti stanica na 3D HCE-T staničnim modelima rožnice (kultiviranima na filtrima veličina pora od 3 i  $0,4\ \mu\text{m}$ ) nakon izloženosti gelu od 30 minuta.

**Rezultati:** Temeljem eksperimentalnoga plana i mjerenjem  $T_{gel}$ ,  $\eta^*$  i  $G'$  uspješno su dobiveni i validirani matematički modeli koji opisuju ovisnost mjerenih zavisnih varijabli o koncentracijama P407, P188 i kitozana. Matematičkim modelom za  $T_{gel}$  pokazan je redosljed učinaka koncentracija na odabranu varijablu: P407 (koeficijent = -13,84) > P188 (koeficijent = 6,70) > CS (koeficijent = 2,74). Negativna vrijednost koeficijenta upućuje na obrnut odnos između faktora (koncentracija) i odgovora ( $T_{gel}$ ), što za posljedicu ima da porast koncentracije P407 rezultira smanjenjem  $T_{gel}$ . Pozitivna vrijednost uočena za koeficijente vezane za koncentracije P188 i CS sugerira da povećavanjem njihovih koncentracija dolazi do pomicanja  $T_{gel}$  prema višim temperaturama. U svrhu dobivanja matematičkih modela za  $\eta^*$  i  $G'$ , podatci dobiveni mjerenjima su logaritmirani. Povećanje koncentracije P188 rezultiralo je smanjenjem  $\log(\eta^*)$  (negativan koeficijent = -1,60), dok povećanje koncentracije P407 za posljedicu ima porast  $\log(\eta^*)$  (koeficijent = 1,53). Učinak koncentracije CS na  $\log(\eta^*)$  statistički se pokazao manje značajnim od učinka koncentracija poloksamera. Slično modelu za  $\log(\eta^*)$ , povećanjem koncentracije P188 smanjivao se  $\log(G')$  (koeficijent = -0,76), dok je porast koncentracije P407 rezultirao porastom odabrane zavisne varijable (koeficijent = 2,16).

Temeljem dobivenih modela, odabrana su četiri vodeća sustava (PL1-4) koja su u detaljnoj reološkoj karakterizaciji pokazala postojanje strukture gela na temperaturi oka, ali i nakon razrjeđenja suznom tekućinom. Reološki profil razvijenih sustava sugerirao je na strukture tzv. mekih gelova koji nastaju pri srednjim koncentracijama poloksamera. Uloga kitozana, promotora mehaničke čvrstoće gela, dokazana je reološkim testom promjene frekvencije. Usporedbom dinamičkih viskoznosti razvijenih sustava s komercijalno dostupnim oftalmičkim *in situ* gelirajućim pripravcima u biorelevantnim uvjetima, utvrđeno je njihovo odgovarajuće pseudoplastično ponašanje.

S obzirom na najmanji udio polimera (P407, P188 i CS od 14,2, 1,7 i 0, 25%, *m/m*), poželjnim reološkim svojstvima ( $T_{gel} = 31,1^\circ\text{C}$ ,  $\eta^* = 2,1 \text{ Pa} \times \text{s}$ ; niskoj dinamičkoj viskoznosti pri visokim brzinama smicanja) te *in vitro* rezistentnosti na razrjeđenje suznom tekućinom ( $G' = 212,4 \text{ Pa}$  prije razrjeđenja i  $175,3 \text{ Pa}$  nakon razrjeđenja), sustav PL1 odabran kao optimalni *in situ* gel.

Procijenjen je učinak djelatnih tvari na temeljna reološka svojstva ( $T_{gel}$ ,  $\eta^*$ , dinamičku viskoznost i vrijeme geliranja) odabranog sustava PL1. Sve su djelatne tvari, s iznimkom tobramicina,

snizile  $T_{gel}$ . Najizraženiji je učinak imao deksametazon, a taj se učinak može pripisati promociji samoorganizacije P407 u sustavima koji sadrže hidrofobne djelatne tvari. Otopljene djelatne tvari (dorzolamid i timolol) pokazale su nešto slabiji učinak od deksametazona na snižavanje  $T_{gel}$ . Takav se utjecaj djelatnih tvari na  $T_{gel}$  može pripisati efektu isoljavanja. Djelatne tvari nisu značajnije utjecale na promjenu  $\eta^*$ , dok su produljile vrijeme geliranja optimalne formulacije PL1. Međutim, raspon vremena geliranja od 41,1 do 87,4 sekunde prihvatljiv je za oftalmičku primjenu.

U svrhu praćenja oslobađanja modelnoga lijeka iz optimalnoga *in situ* gela, razvijena je odgovarajuća *in vitro* metoda za ispitivanje oslobađanja. Prikladnost razvijene metode dokazana je kroz testove topljivosti, odabir najmanje rezistentne membrane i kroz evaluaciju diskriminatornosti metode. Kvantifikacijska (UPLC) je metoda validirana u skladu s ICH smjernicama. Dobiveni profil oslobađanja timolola iz *in situ* gela ukazao je na produljeno oslobađanje, značajno sporije od kontrolne otopine timolola, slično oslobađanju lijeka iz gela usporedive viskoznosti. Time je potvrđena viskoznost kao najkritičniji parametar što kontrolira oslobađanje lijeka iz te vrste pripravaka.

Ključna reološka svojstva PL1 optimalnoga *in situ* gela ispitana su prije i nakon filtracije kroz filter pora 0,2  $\mu\text{m}$  te nakon filtracije i autokalviranja (20 minuta na 121°C). Filtracija je rezultirala smanjenjem  $T_{gel}$  za oko 2°C, dok su vrijednosti  $\eta^*$  dobivene u testu promjene frekvencije povećane, što se može pripisati već poznatom utjecaju čistoće poloksamera na viskoznost njihovih gelova.

Stabilnost sterilizirane formulacije, pohranjene u dobro zatvorenim bočicama pri sobnoj temperaturi tijekom šest mjeseci, procijenjena je ispitivanjem kritičnih reoloških parametara koji mogu utjecati na performanse razvijene platforme *in vivo*. Analize  $T_{gel}$ ,  $\eta^*$  i  $G'$  ukazale su na zadržavanje bitnih reoloških svojstava razvijenoga sustava tijekom ispitanoga razdoblja.

U svrhu preliminarnoga ispitivanja biokompatibilnosti PL1 optimalnoga *in situ* gela korišteni su 3D epitelni modeli rožnice. Izloženost modela *in situ* gelu u vremenu od 30 minuta, rezultirala je smanjenjem vijabilnosti stanica manjoj od 20%, ukazujući na prikladnost razvijenoga sustava za oftalmičku primjenu.

**Zaključak:** Sustavan pristup razvoju *in situ* gelirajućeg pripravka, proveden u sklopu doktorskoga rada, kroz uspješnu primjenu D-optimalnoga statističkoga dizajna, rezultirao je sustavom smanjene ukupne koncentracije polimera, temperature geliranja u fiziološki relevantnom rasponu, pseudoplastičnog ponašanja te otpornim na razrjeđenje suznom tekućinom. Posljedično, zadržana su pozitivna reološka svojstva koja osiguravaju jednostavnost primjene, točnost doziranja te izbjegavanje nelagode nakon primjene. Razvijeni se sustav pokazao robusnim na uklapanje djelatnih tvari, što ga čini prikladnom platformom za oftalmičku primjenu djelatnih tvari različitih fizičko-kemijskih svojstava. Nadalje, razvijeni se sustav pokazao stabilan i biokompatibilan te je omogućio kontrolirano oslobađanje modelne djelatne tvari.

**KLJUČNE RIJEČI:** oftalmička primjena, kvaliteta uključena u dizajn (eng. *QbD*), poloksameri, kitozan, reologija, geliranje uzrokovano povećanjem temperature, temperatura geliranja.



# **1. INTRODUCTION**

The anatomical barriers and the tear fluid dynamics in the precorneal area of the eye have a huge effect on the eye-related drug bioavailability (1,2). This problem can be overcome by using *in situ* forming ophthalmic gels prepared from polymers that exhibit reversible phase transitions and pseudoplastic behavior to minimize interference with blinking, avoid foreign body sensation and blurring of vision (3–5). *In situ* forming ophthalmic gels need to be fine-tuned considering all the biopharmaceutical challenges of the front of the eye in order to increase drug residence time at the application site resulting in its improved bioavailability and efficacy (6). Such a system should be formulated as drug containing liquid suitable for instillation into the eye that shifts to the gel phase upon exposure to physiological conditions (7). The optimal *in situ* forming gel should be characterized by: (i) temperature of gelation in physiologically relevant range; (ii) pseudoplastic behavior that allows gel to thin during blinking, making it more comfortable and easier to spread across the eye surface (8); (iii) suitable gel strength to endure the dilution with tears. Moreover, *in vivo* performance of *in situ* forming ophthalmic gels is governed also by drug release and biocompatibility issues.

Poloxamers (trade name Pluronic®), a series of closely related block copolymers of polyethylene oxide and polypropylene oxide, have been investigated as *in situ* forming gels (9). At high concentrations of poloxamers, the aqueous solutions exhibit a dramatic change of the viscoelastic moduli and become soft solids or gels. A phase transition from liquid to gel upon reaching physiological temperatures is presently one of the most important phenomenon for their applications (10). Poloxamer 407 (P407) was mainly studied for ophthalmic delivery, however, concentrated P407 aqueous solutions (>18%, w/w) gel already at the ambient temperature (11). In that case, *in situ* forming ophthalmic gel has to be stored in refrigerator and applied cold (7), and therefore, its instillation to the front of the eye can possibly be irritating and painful.

Use of P407 in mixture with other poloxamers is considered as a strategy to decrease the P407 concentration, modulate the temperature of gelation and rheological properties of *in situ* forming gel. Among others, poloxamer 188 (P188) was shown to be a good modulator of P407 *in situ* forming gels (11–13). In previous studies, both poloxamers were used in *in situ* forming ophthalmic gels at very high total concentration, e.g. P407 and P188 in concentration of 21% and 10% (11), 16% and 14% (14), 20% and 11% (15) (w/w), respectively.

The additional improvements in the biopharmaceutical properties of poloxamer ophthalmic gels can be achieved by the presence of different additives in the formulation (16–20). Chitosan, a

biocompatible and biodegradable polycationic polymer, has been demonstrated to increase the mechanical strength and mucoadhesiveness of *in situ* forming ophthalmic gels (20). In addition, there are other benefits of including chitosan in ophthalmic formulations such as improvement of eye-related permeability due to its paracellular permeation enhancing effects (21), antimicrobial activity (22) and corneal wound healing effect (23).

The aim of this doctoral thesis was to develop stable and robust *in situ* forming ophthalmic poloxamers/chitosan gel fine-tuned in terms of polymer content and rheological properties, i.e. temperature of gelation, storage modulus and viscosity. Minimizing the total polymer content while retaining the advantageous rheological properties has been achieved by means of D-optimal statistical design. The selection of the leading candidate for drug formulation development has been based on the ability to keep its rheological properties upon dilution under biorelevant conditions. The robustness of selected mixed system has been evaluated upon entrapment of four ophthalmic active pharmaceutical ingredients (1).

## **2. THEORETICAL PART**

## 2.1. Ophthalmic drug delivery

Although evidently exposed organ, in the terms of drug delivery, eye is a specific and extremely complex from multiple perspectives. Drugs must be transported across several protective barriers regardless of which administration route is utilized (i.e. topical, subconjunctival, sub-tenon's intravitreal, peribulbar and retrobulbar administration). These barriers for effective drug absorption exist on physical, chemical and biochemical levels and each of them are active depending on the delivery route. Most of these obstacles are anatomical and physiological barriers that normally protect the eye from exogenous particles and toxicants (24). Anatomically, the eye is divided in anterior and posterior segment. The anterior segment includes approximately one-third of the eye consisting of cornea, conjunctiva, pupil, aqueous humor, iris, lens, ciliary body and the anterior portion of sclera. The posterior segment consists of vitreous humor, retina, choroid, sclera and optic nerve making up the remaining two-thirds in the back of the eye, Figure 1 (25).

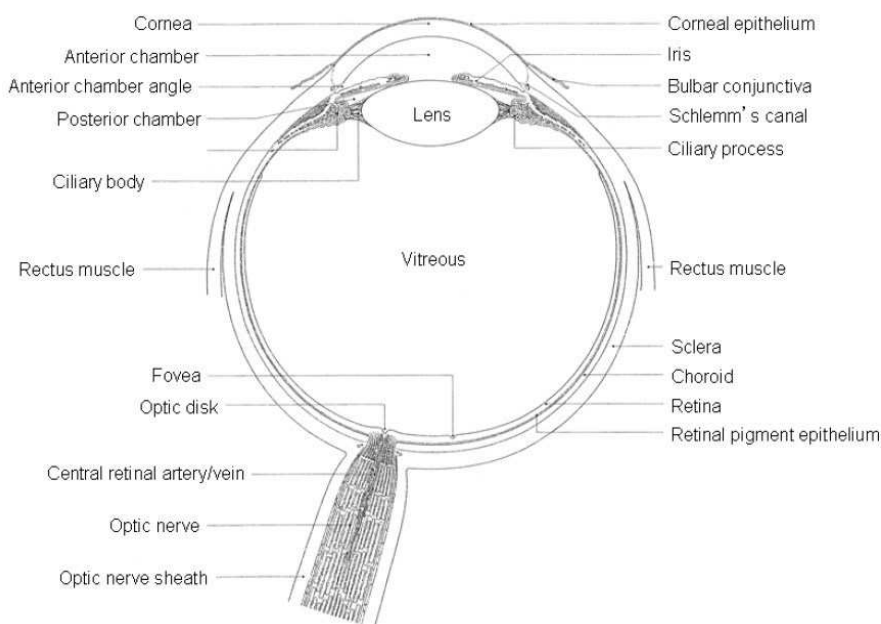


**Figure 1.** The anatomy of the eye, picture reprinted with permission from (26).

The anterior and posterior segment of the eye can be affected by various vision impairing conditions. Diseases affecting anterior segment include glaucoma, allergic conjunctivitis, anterior

uveitis and cataract while age-related macular degeneration (AMD) and diabetic retinopathy are the most prevalent diseases affecting posterior segment of the eye (27).

### **2.1.1. Topical ophthalmic drug delivery**

Topical administration is the most common drug administration route for the treatment of the anterior segment of the eye. This is due to the fact that it is the simplest, most convenient, self-administrable and non-invasive drug administration route for the management of anterior segment diseases/disorders. Drugs are delivered locally by this administration route, avoiding the blood-aqueous barrier, and the side effects and first-pass metabolism that may occur in some systemically administered drugs. Depending on the formulation and drug physiochemical properties, drugs can reach different external (cornea, conjunctiva, sclera) and internal (aqueous humor, iris, ciliary body, vitreous humor, retina, etc.) sites in the eye after topical administration (28). However, the number of protective mechanisms play the decisive role in the fate of topically administered drugs (Figure 2).

Ocular absorption of topically applied ophthalmic drugs is limited by:

- (i) rapid precorneal drug elimination
- (ii) corneal/conjunctival epithelial barrier.

Consequently, eye-related bioavailability of topically administered products is low, typically less than 5%. The major fraction of the instilled dose is usually systemically absorbed via the nasolacrimal duct or through the conjunctiva. For the treatment of diseases affecting anterior segment, the therapeutic concentrations can be achieved by frequent drug administration, however, for diseases affecting posterior segment, the intraocular levels achieved are often below minimal effective concentrations. Frequent administration is often associated with undesirable side effects caused by systemic drug absorption (2,24,29). Anterior segment diseases are mostly treated using eye drops (90% of marketed ophthalmic products) and ointments (27,28).

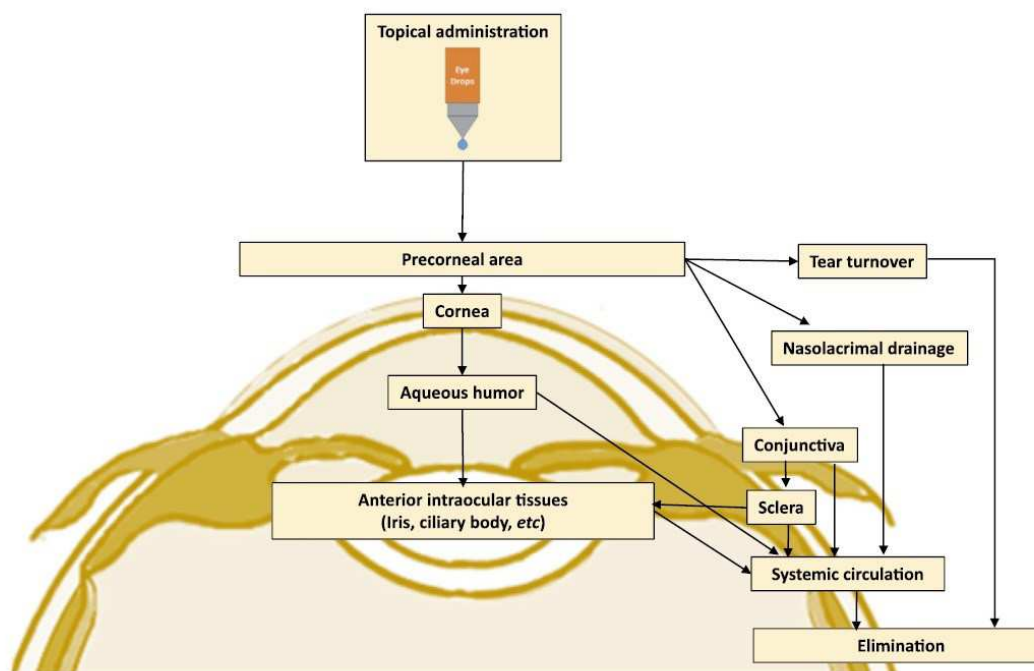


**Figure 2.** Ocular absorption and elimination pathways after topical administration, picture reprinted with permission from (28).

### *Precorneal factors*

Precorneal factors, which include tear fluid dynamics, solution drainage and nonproductive absorption, determine the residence time of the drugs on the eye surface and therefore are of great importance for eye-related drug bioavailability.

### *Tear fluid dynamics*

The tear film is a liquid layer covering the eye surface and acting as a barrier between the eye and environment (30). It is created by tears which are a complex aqueous mixture of peptides, proteins, electrolytes, lipids and small molecule metabolites (2,28). Immediately after the administration, drug/ophthalmic product is mixed with the tear film, which then presents a dynamic barrier to drug absorption. It undergoes a constant renewal and consequently limits drug residence time on the eye surface.

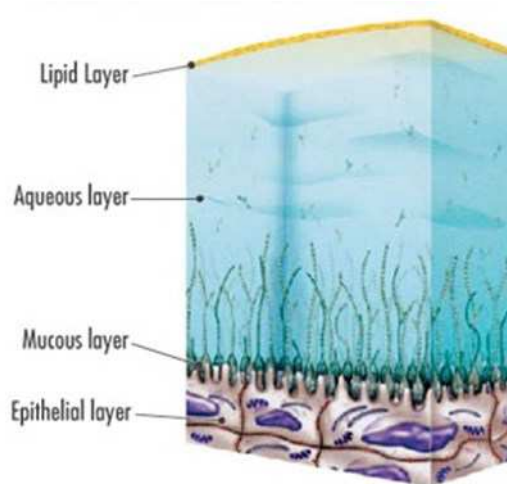


**Figure 3.** Schematic representation of tear film, picture reprinted from (31).

It is composed of three layers (Figure 3): the superficial lipid layer, the middle aqueous layer and the deep mucous layer. It plays several important roles:

- (i) it is forming and maintaining a smooth refracting surface over the cornea, as it moisturizes the environment for the epithelial cells of the cornea and conjunctiva,
- (ii) it helps with transportation of metabolic products (primarily oxygen and carbon dioxide) to and from the corneal epithelial cells,
- (iii) it provides a pathway for white blood cells in case of injury, and
- (iv) it is diluting and washing away noxious stimuli and exhibits bactericidal properties (32).

Lipids in the lipid layer of the tear film are secreted by the Meibomian glands, and they include triacylglycerols, free sterols, sterol esters and free fatty acids. The main function of lipid layer is to lower the surface tension of the tear fluid and prevent its evaporation. The aqueous portion of tear film, containing inorganic salts, glucose and urea, as well as biopolymers, proteins and glycoproteins, is secreted by the main and accessory lacrimal glands. The deepest layer of the tear film is the mucous layer. The mucous layer contains mucins, which are produced by the goblet cells of the conjunctiva. The mucins form a gel-like structure providing an easily wettable surface and thus assisting in water re-spreading after blinks (30). The mucus layer of a tear film is



restored slowly (~15 to 20 h) while the aqueous component is replaced approximately every 10 min (33).

#### *Solution drainage*

Administration of eye drops induces responsive protective mechanisms such as lacrimation and blinking, which results in more pronounced drug elimination. Commercially available eye-droppers provide average drop volume of 40  $\mu\text{l}$  (range 25–56  $\mu\text{l}$ ). Available tear volume is about 7  $\mu\text{l}$ , while conjunctival cul-de-sac can contain around 30  $\mu\text{l}$  of applied eye drop. After administration, drug has a short residence time of approximately 1–2 min at the eye surface, because of the permanent production of lacrimal fluid (0.5–2.2  $\mu\text{l}/\text{min}$ ). Even though the tear turnover rate is only approximately 1  $\mu\text{l}/\text{min}$ , the excess volume of the instilled fluid flows to the nasolacrimal duct in a couple of minutes (4).

#### *Nonproductive absorption*

In addition to tear fluid dynamics and solution drainage, systemic absorption can cause nonproductive drug removal instead of ocular absorption. Systemic absorption can occur either directly from the conjunctival sac via local blood capillaries or after the solution has arrived into the nasal cavity. Tear fluid containing the drug is transported from the lacrimal sac into the nasolacrimal duct, which empties into the nasal cavity, where the drug is then absorbed into the bloodstream. This absorption leads to drug wastage and, more importantly, possible side effects (4,24,34).

#### *Anatomical barriers*

After the topical administration, there are two main pathways of drug entry into the anterior chamber: via the cornea and via the conjunctiva. Small and lipophilic molecules (i.e. most clinically used drugs) are absorbed via the cornea, whereas large and hydrophilic molecules (e.g. new potential biotech-drugs such as protein and peptide drugs, gene medicines) are preferably absorbed through the conjunctiva and sclera. However, as mentioned previously, an important route of drug loss from the lacrimal fluid is systemic absorption through the conjunctiva.

### *Cornea*

Cornea (Figure 4) is an optically transparent and avascular tissue which acts as the principal refractive element of the eye (34). Its surface and thickness are 1.04 cm<sup>2</sup> and 0.5 mm, respectively. It comprises five layers: epithelium, Bowman's membrane, stroma, Descemet's membrane and the endothelium layer. The corneal upper layer, the epithelium, is endowed with microvilli, and covered by a charged glycocalyx, which maximizes surface area with the tear film (33). The epithelium and stroma are significant barriers to drug absorption, while endothelium participates only marginally in barrier function (35).

The permeation of drugs across corneal epithelium is a complex and dynamic process that includes passive diffusion through either a cell (transcellular) or intercellular space between the cells (paracellular), influx- and/or efflux-mediated transport by membrane proteins, endocytosis and transcytosis. Permeation is determined by both the physicochemical properties of the drug and barrier properties. Lipophilic drugs permeate via the transcellular route, while hydrophilic drugs permeate primarily via the paracellular pathway. The main physicochemical properties that determine the passive transport of drugs across cornea are:

- (i) the degree of ionization at the pH of tears;
- (ii) the drug lipophilicity (e.g. the optimal log *P* for transcorneal absorption is 2–3); and
- (iii) the charge, size and shape of the drug molecule (2).

The corneal epithelium consists of a basal layer of columnar cells, two to three layers of wing cells and one or two outermost layers of squamous polygonal shaped superficial cells (34). Epithelium is lipophilic in nature with superficial cells tightly connected by tight junctions. Tight junctions serve as a selective barrier for small hydrophilic molecules and they completely prevent the diffusion of macromolecules via the paracellular route. They are composed of a belt-like bands of intimate strands and the number of tight junction strands seems to be the most important determinant of paracellular resistance (34).

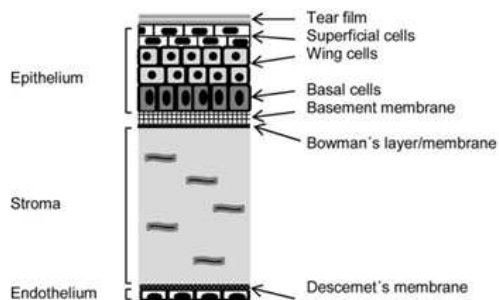


**Figure 4.** Schematic representation of corneal layers, picture reprinted with permission from (29).

From these reasons, epithelium is major obstacle for permeation of hydrophilic molecules. Compared to many other epithelial tissues (intestinal, nasal, bronchial, tracheal) corneal epithelium is relatively impermeable, but it is more permeable compared to the stratum corneum of the skin (34).

90% of corneal thickness is stroma, the hydrophilic layer containing collagen fibrils, which, due to its structure, blocks the transport of lipophilic molecules (24).

Monolayer of hexagonal cells forms the corneal innermost layer, the endothelium, separates the stroma from aqueous humor, and it is responsible for maintaining normal corneal hydration (24). Presence of endothelial leaky tight junctions allows free movements of molecules between aqueous compartments (stroma and aqueous humor) (36). From these reasons, corneal endothelium does not act as a significant barrier to the transcorneal diffusion of most drugs.

### *Conjunctiva*

The conjunctiva of the eyelids and globe is a thin, vascularized mucus membrane which forms a continuous surface area of 17.65 cm<sup>2</sup> (2), which is around 17 times bigger than the surface of cornea. Functionality of conjunctiva is related to the formation and maintenance of the tear film and in protection of the eye (34). However, in comparison to corneal, conjunctival drug absorption is considered to be nonproductive due to the presence of conjunctival blood capillaries and lymphatics, which can cause significant drug loss into the systemic circulation and, therefore, lower eye-related bioavailability. Tight junctions of the superficial conjunctival epithelium are the major barrier for drug penetration across conjunctiva. Intercellular spaces in the conjunctival epithelium are, however, wider than those in the corneal epithelium and therefore, the

conjunctival permeabilities of hydrophilic drugs are higher for an order of magnitude than their corneal permeabilities (24,34).

### *Sclera*

The sclera constitutes the posterior five-sixths of the globe and provides the structural integrity that defines the shape and length of the eye (34). The sclera mainly consists of collagen fibers and proteoglycans embedded in an extracellular matrix (24). Permeability through the sclera is considered to be comparable to that of the corneal stroma and is inversely proportional to the molecular radius of the drug. Also, charge of a drug is important because positively charged molecules permeate poorly possibly due to their binding to the negatively charged proteoglycan matrix. Drugs penetrate across the sclera through perivascular spaces, through the aqueous media of gel-like mucopolysaccharides or through empty spaces within the collagen network (34) to reach the anterior segment (trans-scleral pathway).

## 2.2. Topical ophthalmic dosage forms

The clinical performance of topical ophthalmic drug products is dependent on the interplay of the physicochemical factors of drug and delivery system along with physiological and anatomical environment of the complex eye surface. Conventional ophthalmic drug products include eye drops in form of solution or suspension and ointments mainly of the oleaginous type, and are still the mainstream treatment of anterior segment eye diseases.

Having in mind the complexity of eye surface environment and obstacles to eye-related bioavailability, formulation approaches for its improvement are to:

- (i) improve drug concentration within the formulation;
- (ii) extend retention time on eye surface;
- (iii) provide sustained drug release; and/or
- (iv) enhance corneal permeability.

To improve the drug concentration within the eye drops, the diverse solubility enhancers can be used (37). This could also allow a smaller volume of eye drop to be administered, which would then be less susceptible to removal from eye surface by solution drainage. The contact time of topical ophthalmic solutions with eye increases with the increase of formulation viscosity. Several synthetic polymers like polyvinylalcohol, polyvinylpyrrolidone, polyethylene glycol, polyacrylic acid, and many cellulose derivatives such as hypromellose and hydroxyethylcellulose, are commonly used as viscosity enhancers due to their physiologic compatibility and satisfactory physicochemical properties (38). However, increase in viscosity is followed by increase in bioavailability only to a certain extent (5).

Permeation enhancers can also be included into ophthalmic liquid formulations. They include preservatives (frequently added to multiple use ophthalmic systems and preventing microbial contamination) and surfactants (acting as drug solubilizers, and/or as spreading agents), and they modify transcorneal permeability by inducing ultrastructural changes in the corneal epithelium (39). Such molecules are, for example, ethylenediaminetetraacetic acid (EDTA), benzalkonium chloride (BAK), polyoxyethylene glycol ethers (lauryl, stearyl and oleyl), sodium taurocholate,

saponins and cremophor EL (40). However, there are safety concerns related to frequent use of these molecules (27).

Other formulation approaches to improve drug concentration within formulation, extend retention time on eye surface and provide sustained drug release include ophthalmic suspensions and emulsions. Ophthalmic suspensions are biphasic systems consisting of solid particles dispersed throughout a liquid phase (buffer), often with a help od suspending/dispersing agent (41). Suspensions are employed to deliver poorly water soluble drugs so frequently, corticosteroids are marketed in the form of suspension. Suspension particles retained in conjunctival sac subsequently improve drug retention time on eye surface and therefore the duration of action. The main challenge in their formulation, stability, efficacy and patient acceptance is the size and size distribution of particles. If not adequate, particle size can create several undesirable consequences like aggregation and resuspendability related issues. Particles in ophthalmic suspensions need to be micronized (less than 10  $\mu\text{m}$ , preferably less than 5  $\mu\text{m}$ ) to avoid irritation/foreign body sensation (42). Smaller size particle restores the drug absorbed into ocular tissues from conjunctival sac, while larger particle size helps retain particles for longer time and provide slow drug dissolution (27). Among marketed ophthalmic, suspension of dexamethasone combined with tobramycin (TobraDex<sup>®</sup>) is one of the widely used for treatment of ocular bacterial infections. Drawbacks of ophthalmic suspensions are relatively high costs and complexity of manufacturing process since sterilization can cause physical or chemical instability. From this reasons, in some cases, aseptic processing is only viable manufacturing option, which increases costs even more (43).

Ophthalmic emulsions are colloidal pharmaceutical dosage forms consisting of one phase (water/oil) dispersed in other (oil/water) with an aid of surfactants (emulsifiers) (27). An example of such system a topical corticosteroid ophthalmic emulsion of difluprednate (DUREZOL<sup>®</sup>), indicated for the treatment of inflammation and pain associated with ocular surgery, currently available in the US market (44). Positive side of ophthalmic emulsions is their lubricating nature, while drawbacks associated to these systems are related to the use of surfactants (local toxicity issues) and to physical instability (flocculation).

Eye ointments are semisolid products usually intended for application to the conjunctiva, cornea, or eyelid. Ointments offer advantages over eye drops due to the significantly prolonged retention

time on the eye surface, minimization of tear dilution, reduced nasolacrimal drainage which all results in the improvement of bioavailability (45). Ophthalmic ointments account for approximately 10% of all of the ophthalmic dosage forms in the market (46). They are associated to poor patient compliance due to the greasy feeling, discomfort reflex tearing and blurring of vision (because of the difference in refractive index between nonaqueous ointment base and tears). Therefore, they are mostly applied at night. Furthermore, drawbacks of using ophthalmic ointments are related with potential content uniformity and dosing issues (45,46).

### **2.2.1. Innovative ophthalmic drug delivery systems**

To improve eye-related drug bioavailability, there is a significant effort directed towards new drug delivery systems for ophthalmic administration (3,47–49). Innovative delivery platforms should lead to reduced dosing frequency, better patient compliance, reduced systemic adverse effects and finally improved clinical outcome. These delivery platforms include variety of drug delivery nanosystems and hydrogel-based systems.

Drug delivery nanosystems comprise nanosuspensions, nanoemulsions, polymeric micelles, nanoparticles, liposomes, niosomes, cubosomes and dendrimers (25,28,36,50–52). Using the nanosystems all the strategies to increase eye-related bioavailability can be tackled (solubility, retention time, sustained release, increased permeability).

*Nanosuspensions* consist of nanosized drug particles suspended in an appropriate dispersion medium and stabilized by polymer(s) or surfactant(s) (50). In comparison to conventional suspensions, nanosuspensions offer advantages such as faster dissolution and improved solubility of the drug, enhanced bioavailability, and reduced irritation to the eye. Nanosuspension approach provides opportunity to address many of the deficiencies associated with water insoluble drugs.

*Nanoemulsions* are biphasic dispersion of two immiscible liquids (most commonly oil-in-water), stabilized using an appropriate surfactant, suitable for the entrapment of hydrophobic drugs (51). The direct consequence of their small droplet size (20–200 nm) is their clear or hazy appearance and long-term physical stability, which differs them from milky white color and less stable coarse emulsion (51,53). Moreover, nanoemulsions possess higher solubilization capacity than simple micellar dispersions. Therefore, nanoemulsion were shown to to improve

permeability, retention time and overall eye-related bioavailability (51). The most known ophthalmic nanoemulsion is RESTASIS<sup>®</sup>, a cyclosporine nanoemulsion for treatment of dry eye.

*Polymeric micelles* (10–200 nm) are based on amphiphilic molecules or block copolymers which can generally self-assemble into organized core-corona/supramolecular structures in aqueous media at concentrations exceeding their critical micellar concentrations (CMC) (52). Polymeric micelles have shown potential for enhancing the solubility and therapeutic efficacy of poorly water soluble drugs and for protection of the drugs from degradation. Due to their small size and hydrophilic nature, micelles can efficiently permeate the corneal barriers and produce therapeutic concentrations both in the anterior as well as the posterior segment of the eye (52). To prolong the residence time at the ocular surface, polymeric micelles should intimately contact the mucus layer. Positively charged corona of polymeric micelles can enhance the interactions with negatively charged mucins at the corneal surface, facilitating precorneal retention (54).

*Nanoparticles* are particles consisting of various biodegradable materials which frequently have multifunctional surface groups, with a diameter from 10 to less than 1000 nm providing a large surface area (28). Drugs can be either encapsulated in the matrix or attached to the surface of the particle. They offer a great opportunity for efficient local delivery of drugs to the anterior segment such as permeability enhancement across the blood-aqueous barrier and cornea, longer drug contact time with ocular tissues, specific/controlled delivery of drugs to the target site and protection of drugs from degradation and metabolism. Due to their size, low irritation and sustained release properties are expected, as well as less frequent administration (55).

*Liposomes* are lipid vesicles with one or more phospholipid bilayers enclosing an aqueous core. Liposomes are adequate ophthalmic delivery systems due to the suitable biocompatibility, cell membrane-like structure and ability to encapsulate both hydrophilic and hydrophobic drugs (36). They have been investigated in ophthalmic drug delivery since 1980's. The earliest applications of liposomes were for topical drug delivery in the form of the eye drops and intravitreal injections for prolonged action (25). Although liposomes could entrap a wide range of molecules, their use is limited in topical ocular delivery because of relatively poor stability (36). Various modifications were evaluated to circumvent this drawback and one of the interesting approaches appears to be light activated liposomes which enable drug release at specified time and site with the projected laser light (25).



*Niosomes* are non-ionic surfactant vesicles structured in bilayers, ranging from 10-1000 nm, which can entrap both hydrophilic and lipophilic drugs (36). Niosomes are suitable for topical ocular delivery due to the following benefits: chemical stability, ease of surface formation and modification because of the functional groups on their hydrophilic heads; improvement of bioavailability and effectiveness in the modulation of drug release properties (32,47,55). Furthermore, they are biodegradable, biocompatible, and non-immunogenic.

*Cubosomes* are defined as nanoparticles of a liquid crystalline phase with cubic crystallographic symmetry formed by the self-assembly of amphiphilic or surfactant-like molecules (36). Glycerol monoolein is one of the most common surfactants used to make cubosomes. Cubic phases have useful properties, such as their ability to solubilize hydrophobic, hydrophilic, and amphiphilic molecules, their biodegradability by simple enzyme action and their suitability as sustained release delivery systems. Furthermore, the cubic phase is strongly bioadhesive and is thought to be a permeation enhancer (57). Several preclinical studies evaluated and showed promise for use of cubosomes as ophthalmic drug delivery systems (36,57).

*Dendrimers* are nanoscale, highly branched and reactive three-dimensional macromolecules with a high degree of molecular uniformity, narrow molecular weight distribution, specific size and interesting structural properties like internal voids and cavities and a highly functional terminal surface formed by amino, carboxyl and/or hydroxyl groups (28). In addition to the outstanding structural control, their unique property is mimicry of globular proteins. They are referred to as “artificial proteins”, based on their systematic, electrophoretic, dimensional length scaling and their biomimetic properties (58). Several preclinical studies showed their potential for ophthalmic use (28). Reports describe multiple use of dendrimers in ophthalmology for delivery of various drugs (genes, antioxidants, peptides) (36).

### 2.3. Hydrogels in ophthalmic drug delivery

Aqueous gels or hydrogels formulated using hydrophilic polymers along those based on stimuli responsive polymers (*in situ* forming gels) are in the focus for the ophthalmic drug delivery via different routes of administration (Figure 5). Hydrogels allow the incorporation of various ophthalmic drugs (hydrophilic, lipophilic and biologicals). An interesting delivery systems based on hydrogels are hydrogel contact lenses. Due to their high water content and favourable properties they are highly compatible with human tissues (47). They extend the retention time of the drug, control and extend its release to several days or even months and enhance its eye-related bioavailability to more than 50% in comparison to conventional eye drops (47). Mostly used polymers in these lenses are hydroxyethyl methacrylate, methacrylic acid, polyvinyl alcohol and silicones.

*In situ* forming gels stand out as the main candidates for topical ophthalmic drug delivery and due to their unique properties they have great market potential. They are prepared as liquid dosage forms (provides dose accuracy) which undergo phase transition on eye surface or conjunctival sac to form viscoelastic gel in response to an environmental stimulus following topical administration. The environmental stimulus can be of physical (temperature, light), chemical (pH, redox potential, ionic strength) and biological origin (inflammation, enzymes) (3,47).

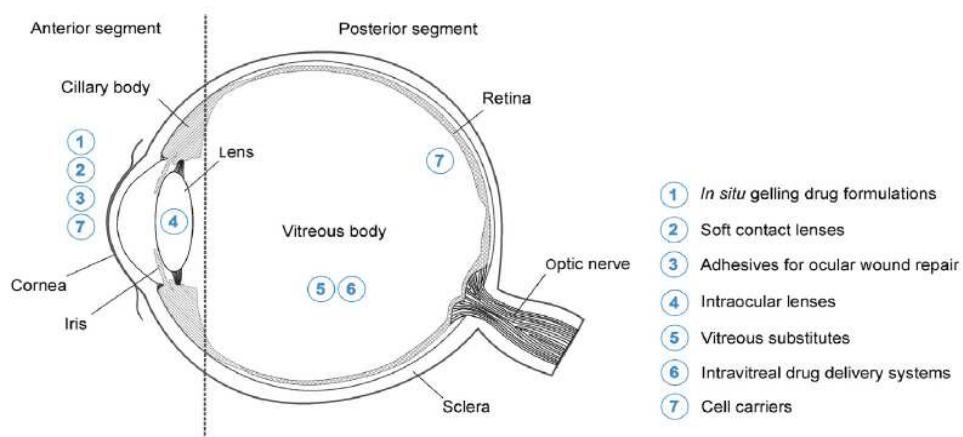


**Figure 5.** Application sites of hydrogels in ophthalmology, picture reprinted with permission from (3).

### 2.3.1. *In situ* forming ophthalmic gels

One of the solutions of innovative pharmaceutical science for efficient ophthalmic drug delivery are *in situ* forming ophthalmic gels. They are prepared from polymers that exhibit reversible phase transitions and, due to their favorable rheological properties, minimize interference with blinking, avoid foreign body sensation and blurring of vision (3–5). Such systems are formulated as drug containing liquid suitable for instillation into the eye that shifts to the gel phase upon exposure to physiological conditions (7). Till now, for the purpose of ophthalmic delivery physical and chemical stimuli such as temperature, pH and ions were investigated (4,59). These triggers can be modified to control gel formation, retention time on the eye surface and drug release (6). Since they are not preformed gels, but (viscous) solutions at administration, dosing is easier, more accurate and reproducible in comparison to the application and dosing of preformed gels. Additionally, *in situ* forming gels systems have gained major interest since no organic solvents or copolymerization agents are needed to trigger gelation (47).

Since gelling can be affected by various factors such as salt concentration, ionic strength, pH, temperature, presence of a drug, adequate characterization of *in situ* forming gels is prerequisite for their ophthalmic application. Pseudoplastic flow characteristics should be demonstrated with thixotropic properties which would assure easy spreadability across the ocular surface upon blinking and transformation to a more viscous material under low shear rate conditions to prolong the ocular residence time. Very important are safety issues which can be addressed with appropriate *in vitro* biocompatibility and *in vivo* ocular tolerability tests. Desirable properties of ideal ophthalmic gels and analytical methodology for their determination are summarized in the Table 1.

**Table 1.** Characteristics and mode of investigation of topical ophthalmic gel formulations, reprinted with permission and modified from (47).

Characteristic	Analytical methods
Clarity and optical transmittance	Visual inspection, refractive index or spectrophotometric analysis
Safety and good ocular tolerance	Observation for possible adverse effects Visual acuity Ocular tolerance (Draize, HETCAM, BCOP and histology tests) Cell-based cytotoxicity assays Isotonicity test (osmometer)
Suitable pH	Measurement of pH at biorelevant temperature
Pseudoplastic and thixotropic flow Viscoelasticity	Cone and plate in rotational or oscillation rheometer
Gelling capacity	Qualitative observation of gel formation in simulated tear fluid
Mucoadhesive properties	Polymeric mucoadhesion tests (rheometer) Bioadhesive force of the gel
Extended residence time on eye surface	Precorneal residence assessed using gamma scintigraphy
Ease and reproducibility of application	Gel consistency (rheometer), firmness and cohesiveness assessed by texture analyzer
Compatible excipients	Fourier transform infrared spectroscopy used to analyse potential drug-polymer interactions
Physical properties	Solid-state properties (X-ray powder diffraction and particle size analyzed by dynamic light scattering)
Sustained/modified drug release	<i>In vitro</i> release studies
Enhanced transocular permeation	<i>Ex vivo</i> transcorneal and transscleral permeation studies
Sterility	Direct inoculation method
Stability	Storage stability investigated

Polymers used in these systems are of natural, semisynthetic or synthetic origin, providing the unique property of significant structure conversion from viscous solution to gel upon reception of physical, chemical or biological stimulus (47). Advantages associated to hydrogels consisting of

the polymers of natural origin usually are non-toxicity, biodegradation, interaction with proteins and cells non-specific or specific binding (3). However, their potential drawbacks are weak mechanical strength, batch-to-batch inconsistency and immunogenicity. On the contrary, synthetic polymers offer well defined hydrogels in terms of network architecture, mechanical properties and prolonged stability, while they do not inherently interact with proteins or cells and their biocompatibility and biodegradability must be thoroughly assessed (3).

Polymers used in formation of *in situ* forming gels can be classified, according to the environmental stimuli that triggers sol-gel conversion, as temperature-responsive (thermoreponsive), pH or ion-responsive system (47).

Various studies have shown that these drug delivery platforms could improve the treatment of diseases affecting the surface and anterior segment of the eye, such as glaucoma, cataracts, dry eye disease, uveitis and ocular microbial infections, including conjunctivitis or keratitis. Some of these delivery platforms which are already either commercially available, or in clinical trials are summarized in the Table 2. Marketed ophthalmic products are indicated mainly for glaucoma, dry eye and ocular infections (6).

**Table 2.** *In situ* forming ophthalmic gels; either commercially available or currently in (pre)clinical trials.

Trade name	Indication	Manufacturer	Polymer(s) (mechanism of gelation)	Active ingredient	market/status
Betoptic S <sup>®</sup>	Glaucoma	Alcon <sup>®</sup>	Carbomer (pH-responsive) Amberlite <sup>®</sup> IRP-69 (ion exchange resin)	Betaxolol	On the US and EU market
Carteol <sup>®</sup> LP	Glaucoma	Bausch & Lomb, Inc.	Alginic acid (ion-responsive)	Carteolol hydrochlorate	On the EU market
Timogel <sup>®</sup>	Glaucoma	Théa PHARMA S.A.	Gellan gum (ion-responsive)	Timolol maleate	On the EU market
Timolol GFS	Glaucoma	Sandoz, Inc.	Gellan gum and xanthan gum (ion-responsive)	Timolol maleate	On the US market
Timoptic XE	Glaucoma	Merck & CO, Inc.	Gellan gum (ion-responsive)	Timolol maleate	On the US market
Timoptol <sup>®</sup> -LA	Glaucoma	Santen UK Ltd.	Gellan gum (ion-responsive)	Timolol maleate	On the UK market
Rysmon <sup>®</sup> TG	Glaucoma	Wakamoto Pharmaceutical CO., LTD.	Methylcellulose (temperature-responsive)	Timolol maleate	On the Japanese market
Refresh liquigel <sup>®</sup>	Dry eye	Allergan, Inc.	Carboxymethylcellulose sodium (temperature-responsive)	/	On the US market
REFRESH OPTIVE <sup>®</sup> Gel Drop	Dry eye	Allergan, Inc.	Carboxymethylcellulose sodium (temperature-responsive)	Glycerin	On the US market
Systane gel drops <sup>®</sup>	Dry eye	Alcon <sup>®</sup>	Hydroxypropyl-guar (pH-responsive and ion-responsive)	Polyethylene Glycol 400 Propylene Glycol	On the US and EU market
Systane <sup>®</sup> Balance	Dry eye	Alcon <sup>®</sup>	Hydroxypropyl-guar (pH-responsive)	/	On the US and EU market
TobraDex <sup>ST</sup>	Blepharitis	Alcon <sup>®</sup>	Xanthan gum (ion-responsive)	Tobramycine Dexamethasone	On the US market

Trade name	Indication	Manufacturer	Polymer(s) (mechanism of gelation)	Active ingredient	market/status
AzaSite™	Bacterial conjunctivitis	Inspire Pharmaceuticals, Inc.	Polycarbophil (pH-responsive)	Azithromycin Dexamethasone	On the US market
Besivance™	Bacterial conjunctivitis	Bausch & Lomb, Inc.	Polycarbophil (pH-responsive)	Besifloxacin	On the US, Argentina and Canadian market
AzaSite™ Plus	Ocular infections and inflammation	InSite vision, Inc.	Polycarbophil (pH-responsive) <sup>7</sup>	Azithromycin	Phase III trials (US)
AzaSite Xtra™	Ocular infections	InSite vision, Inc.	Polycarbophil (pH-responsive)	Azithromycin	GLP tox studies finished (US)
BromSite™	Ocular inflammation	Sun Pharmaceutical Industries Ltd.	Polycarbophil/ (pH-responsive)	Bromfenac	FDA approved
DexaSite™	Ocular pain and inflammation	InSite vision, Inc.	Polycarbophil (pH-responsive)	Dexamethasone	Phase III trials (US)

### 2.3.2. pH-responsive *in situ* forming gels

Ophthalmic formulations containing pH-responsive polymers (polyelectrolytes), which exhibit sol-gel phase transition in response to environmental pH changes (47) are promising tool for improvement of eye-related bioavailability. These systems exploit the difference of pH of tear fluid (7.4) and the pH of formulation. Such gels are composed of polymers with backbones containing large number of charged pendant groups (60,61). The sol-gel phase transition results from changes in the ionisation state of the weakly acidic (carboxylic or phosphoric) or weakly basic (ammonium) groups present in the polyelectrolyte (47). Common characteristic of these polyelectrolytes is pKa value between 3 and 10 which renders them suitable for pH-responsive systems (62). Most widely used pH-responsive polymers for ophthalmic formulations are polyacrylic acid and its derivatives (polymethacrylic acid, polycarbophils), chitosan and cellulose acetate phthalate (4).

Polyacrylic acid (also known as Carbomer, Carbopol) and its derivatives are anionic high molecular weight polymers whose acidic aqueous solutions are less viscous, while they are transformed into gels upon increasing the pH (Figure 6).

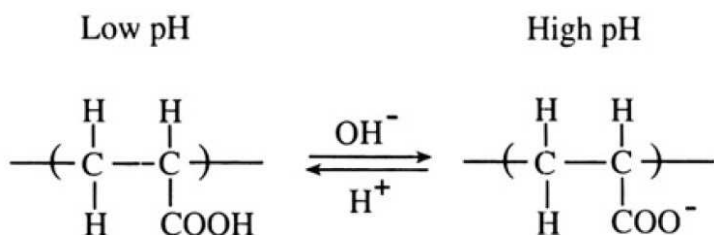


**Figure 6.** pH-dependent ionization poly(acrylic acid), picture reprinted with permission from (61).

Sol to gel transition is related to their polyanionic nature. Upon pH increase, as a result of the electrostatic repulsion of the negatively charged groups, polymers swell and gel is formed. Gel structure further entraps the drug molecules and delivers them to the environment in controllable manner. Sol-gel transitions of polyacrylic acid is dependent on the polymer molecular weight. Another beneficial feature of these polymers is mucadhesion, which is a result of physical entanglements or secondary bonds (63). Due to these favorable characteristics with positive impact on the eye related bioavailability, polyacrylic acid and its derivatives are frequently used in ophthalmic formulations (6).

Cellulose acetate phthalate is another polymer whose solutions show pH dependent gelation. It has a potential for sustained drug delivery to the eye because it is a free flowing solution at a pH of 4.4 and undergoes gelation when the pH is increased by the tear fluid to pH 7.4. This shift in pH results in almost instantaneous conversion of the fluid to a viscous gel. Gelation is triggered by neutralization of the acid groups of the polymer chain (4).

### 2.3.3. Ion-responsive *in situ* forming gels

Polymers which solutions undergo phase transition to gel in the presence of different ions are known as ion-activated polymers. The ones with the potential for ophthalmic administration are those which interact with the ions present in the tear fluid (e.g. sodium, potassium and calcium). The most widely used ion-activated polymers in ophthalmic formulations are (deacetylated) gellan gum, xanthan gum, carrageenan and alginate (4,64).

Deacetylated gellan gum (Gelrite<sup>®</sup>) is anionic polysaccharide and it composed of tetrasaccharide repeating-units (Figure 7A). Cross-linking of the negatively charged polysaccharide helices by



monovalent and divalent cations ( $\text{Na}^+$ ,  $\text{K}^+$ ,  $\text{Ca}^{2+}$ ) is driving the change of structure from sol to gel.  $\text{Na}^+$  was found to be the most gel-promoting ion *in vivo* and gel formed is liquid crystalline comprising three-fold helical chains organized in parallel fashion in an intertwined duplex stabilized by hydrogen bonds (65).

Deacetylated gellan gum and alginate are approved as pharmaceutical excipients for ophthalmic use. Gellan gum is marketed in two controlled-release glaucoma formulations called Timoptic-XE<sup>®</sup> (Merck) and Timolol GFS (Sandoz), while alginate, also for glaucoma therapy is marketed in France as Carteol LP by Laboratoire Chauvin, a Bausch and Lomb company.

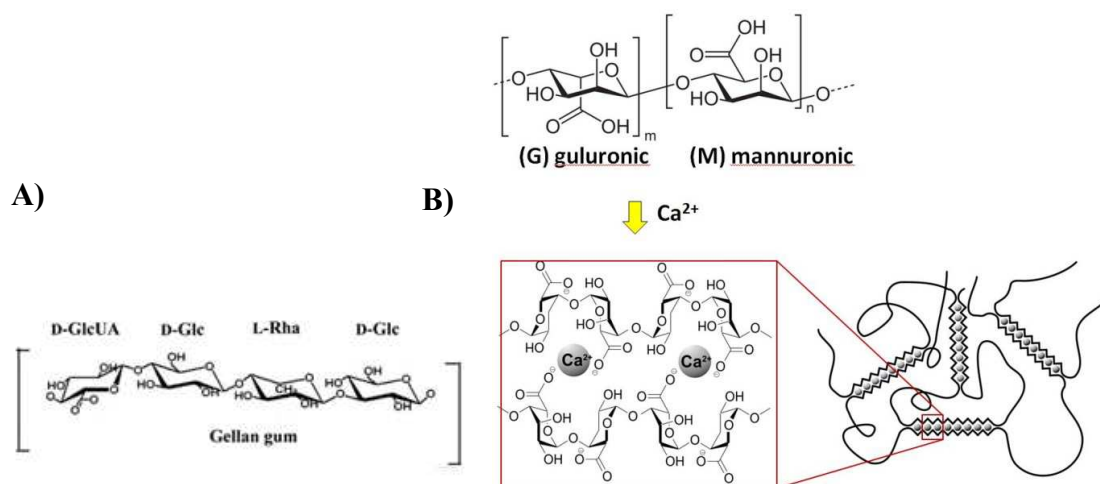


**Figure 7.** Structural formula of gellan gum (A) and alginate with mechanism of gelation in presence of  $\text{Ca}^{2+}$  (B), reprinted from (66).

Similarly to gellan gum, aqueous solutions of alginate (Figure 7B) (a natural polysaccharide extracted from brown sea algae) also form gels when instilled into the eye. Alginates, due to their excellent biodegradable, biocompatible and mucoadhesive properties and are often used as constituents of numerous drug delivery systems (67). Alginic acid is a linear and anionic block copolymer polysaccharide comprising b-D-mannuronic acid and a-L-glucuronic acid residues joined by 1,4-glycosidic linkages. Dilute aqueous solutions of alginates form strong gels on addition of di- and trivalent cations by a cooperative process involving consecutive glucuronic residues in the a-L-glucuronic acid blocks of the alginate chain.

Rupenthal et al. characterized several ion-activated polymeric systems *in vitro* and *in vivo* (64). Among number of anionic polysaccharides (gellan gum, xanthan gum, carrageenan and alginate), formulations based on gellan gum and carrageenan exhibited the most favorable characteristics in terms of phase transition, rheological and textural properties, as their viscosity significantly increased upon contact with cations of the tear fluid, thus prolonging precorneal retention time and reducing nasolacrimal drainage (64). All tested polymeric formulations were found to be non-irritant and classified as safe for *in vivo* use. Systems based on gellan gum, xanthan gum and carrageenan exhibited the most favorable characteristics in terms of precorneal retention as well as delayed release of the model hydrophilic drug (pilocarpine hydrochloride) *in vivo* (8).

#### **2.3.4. Temperature-responsive *in situ* forming gels**

The sol-gel transition of this class of *in situ* forming gels is triggered by a temperature change from storage to physiological temperature i.e. temperature of the eye surface. A literature overview of the temperature-responsive *in situ* forming ophthalmic gels is summarized in the Table 3. Summarized data show that the major driving force for sol-gel transition for temperature-responsive *in situ* forming gels is predominance of hydrophobic interactions of amphiphilic (co)polymer molecules with the temperature increase.

**Table 3.** Temperature-responsive *in situ* forming ophthalmic gels.

Temperature responsive polymer	Mechanism of gelation upon temperature increase	Polymer concentration range, w/w, %	Active ingredient (reference)
PEO-PPO-PEO <sup>1</sup> (Ploxamers)	Micelle formation occurs at the critical micellization temperature as a result of PPO block dehydration.  With increasing temperature, micellization becomes more dominant and at a definite point, micelles come into contact and no longer move (68,69).	14–42%	fluconazole (70) diclofenac sodium (15) pilocarpine (71) dorzolamide HCl (72) acyclovir (18) timolol maleate (7) rhEGF (14)
Cellulose derivative CMC, MC, HPMC <sup>2</sup>	Hydrophobic interactions among polymer chains containing methoxy groups (68,69).	1–10%	ciprofloxacin hydrochloride (73) ketorolac tromethamine (74)
Xyloglucan	Hydrophobic parts of polymer molecule aggregate to minimize the hydrophobic surface area contacting the water, causing gelation (68,69).	1.0–2.0%	pilocarpine HCl (75) ciprofloxacin (76)
PNIPAAm <sup>3</sup>	Hydrophobic interactions between polymer chains become predominant, hydrogen bonds are broken and the polymer dehydrates (68,69).	≈10%	epinephrine (77)
PLGA-PEG-PLGA <sup>4</sup>	Hydrophobic forces drive the sol-gel transition of amphiphilic polymers, to micelles, and upon further temperature increase, micelles aggregate in gel (68,69).	15–20%	dexamethasone acetate (78)

<sup>1</sup> PEO-polyethylene oxide; PPO-polypropylene oxide

<sup>2</sup> CMC-Carboxymethyl cellulose; MC-Methyl cellulose; HPMC-Hydroxypropylmethyl cellulose

<sup>3</sup> Poly N-isopropylacrilamide

<sup>4</sup> PLGA-poly(lactide-co-glycolide); PEG-polyethylene glycol

Cellulose derivatives (carboxymethyl cellulose (CMC), methyl cellulose (MC) and hydroxypropylmethyl cellulose (HPMC)) are polymers of natural origin and their solutions are exhibiting temperature triggered sol-gel phase transition (47). As temperature responsive systems, they are marketed as artificial tears or lubricating solutions and commercially available products are summarized in the Table 2.

MC and HPMC aqueous solutions form gels at concentrations ranging from 1–10%, while  $T_{gels}$  are ranging from 40–50°C and 75–90°C respectively.  $T_{gel}$  of these systems decreases with a higher degree of cellulose ether substitution or with the addition of salts or other polymers (47).

Therefore, combining cellulose derivatives with other polymers results in systems with enhanced properties to favour ophthalmic drug delivery (i.e. lower  $T_{gel}$ , enhanced viscosity) (47).

Among many other investigated polymers, poloxamers, poly N-isopropylacrilamide (PNIPAAm) and xyloglucan are frequently used as ophthalmic drug delivery systems. Aqueous solution of linear polymer PNIPAAm undergoes phase transition (precipitation) when the temperature is raised from the room temperature to about 32°C. Based on this polymer, Hsiue and coworkers developed and tested two types of glaucoma therapy thermosensitive systems containing epinephrine (77). One was the solution of linear PNIPAAm, and the other was the mixture of solution of linear PNIPAAm and suspension of crosslinked PNIPAAm nanoparticles. Both systems were biocompatible, while the latter system had more appropriate drug release profile. Results of the animal (rabbits) experiments demonstrated that the intra ocular pressure-lowering effect achieved with investigated systems lasted considerably longer than that achieved with conventional eye drops (77).

Xyloglucan is a polysaccharide which when partially degraded by  $\beta$ -galactosidase exhibits thermally reversible gelation in dilute aqueous solution, the sol-gel transition temperature varying with the degree of galactose elimination (75). Furthermore, xyloglucan possess properties such as mucoadhesivity, biocompatibility, high drug entrapment capacity and high thermal stability. This properties led to its application as desirable excipient in ophthalmic drug delivery systems (76). Miyazaki and coworkers developed xyloglucan gels with prolonged duration of miotic response following release of pilocarpine over a period of at least 4 h (75).

Biodegradable and water-soluble amphiphilic triblock copolymer of poly-(DL-lactic acid co-glycolic acid) (PLGA)-polyethylene glycol (PEG)-PLGA (PLGA-PEG-PLGA) has been applied in temperature responsive *in situ* forming gel formulations and has been widely used in parenteral delivery systems (69). Gao et al. evaluated its use for ophthalmic delivery of dexamethasone acetate (78). The results of rabbit ocular pharmacokinetics indicated that the PLGA-PEG-PLGA temperature-responsive *in situ* forming gel achieved significantly enhanced bioavailability in the anterior segment in comparison to conventional eye drops.

## 2.4. Poloxamer-based *in situ* forming ophthalmic gels

Poloxamers (trade name Pluronic<sup>®</sup>), a series of closely related block copolymers of polyethylene oxide (PEO) and polypropylene oxide (PPO) with the general formula  $\text{HO}(\text{C}_2\text{H}_4\text{O})_a(\text{C}_3\text{H}_6\text{O})_b(\text{C}_2\text{H}_4\text{O})_a\text{H}$ , have been investigated as *in situ* forming gels (9). At high concentrations of poloxamers, the aqueous solutions exhibit a dramatic change of the viscoelastic moduli and become soft solids or gels. A phase transition from liquid to gel upon reaching physiological temperatures is presently one of the most important phenomenon for their applications (79).

Poloxamer block copolymers are available in a range of molecular weights and PPO/PEO composition ratios. An attractive poloxamer as *in situ* forming ophthalmic gel is Poloxmer P407 (P407), also known as Pluronic F127. P407 has approximate block lengths of  $a = 101$  ( $\approx 70\%$  of PEO) and  $b = 56$  ( $\approx 30\%$  of PPO) and average molecular weight of about 12 600 (9840– 14,600) Da, with PEO/PPO ratio of 2:1 (80,81). It has a greater solubility in cold water relative to warm water, because of greater hydrogen bond interactions and solvation at lower temperatures (47). As a result of these molecular properties, upon temperature increase P407 converts into a colorless, optically clear and transparent gel which makes it attractive as a delivery platform for ophthalmic drugs. Ophthalmic, topical and injectable P407 formulations have shown advantageous properties by promoting stabilization and solubilization of many active pharmaceutical ingredients (APIs) (82). However, concentrated P407 aqueous solutions ( $>18\%$ , w/w) gel already at the ambient temperature (11). In that case, *in situ* forming ophthalmic gel has to be stored in refrigerator and applied cold (7) which makes its instillation to the front of the eye possibly irritating and painful.

Use of P407 in mixture with other poloxamers is considered as a strategy to decrease the P407 concentration, modulate the temperature of gelation and rheological properties of *in situ* forming gel. Among others, poloxamer 188 (P188) was shown to be a good modulator of P407 *in situ* forming gels (11–13). P188, also known as F68, has less hydrophobic properties in comparison to P407, and average molecular mass about 8400 (7680–9510) Da, while block lengths are  $a = 80$  ( $\approx 80\%$  of PEO) and  $b = 27$  ( $\approx 20\%$  of PPO), providing PEO/PPO ratio of 4:1 (81).

Studies focused on the development of *in situ* forming ophthalmic poloxamer gels are summarized in the Table 4 .

**Table 4.** *In situ* forming ophthalmic poloxamer gels.

Components in poloxamer based <i>in situ</i> forming ophthalmic gels	Concentration range of polymers, w/w, %	Total polymer concentration in optimal <i>in situ</i> forming gel w/w, %	Active ingredient (reference)
P407	18% – 25%	22%	Forskolin (83)
P407 P188	12 – 20%, 10 – 30%	30%	rhEGF (14)
P407 P188	0 – 20% 0 – 20%	20%	Fluorescein sodium Ofloxacin (84)
P407 P188	15 – 25% (w/V, %) 5 – 15% (w/V, %)	33%, 38%	Ketorolac tromethamine (85)
P407 P188 Miranol C2M Triacetin	13.65% 3.41% 4.55% 7.80%	21.61%	Dorzolamide HCl (72)
P407 P188 Carbopol 940	14 – 26%, 8 – 11% 0.1 – 0.3%	31.1%	Diclofenac sodium (15)
P407 Tween 80 Carbopol 934	15 – 20% 0.5 – 1.5% 0.1 – 0.3%	21.1%	Fluconazole (86)
P407 HPMC <sup>1</sup> MC <sup>1</sup> CMC <sup>1</sup>	15 – 25% 2% 3% 2.50%	18%	Timolol maleate (7)

Components in poloxamer based <i>in situ</i> forming ophthalmic gels	Concentration range of polymers, w/w, %	Total polymer concentration in optimal <i>in situ</i> forming gel w/w, %	Active ingredient (reference)
P407	18 – 25%	25%	without an active ingredient (87)
PEG 6000	2 – 5 %		
P407	15%	27%	Acyclovir (18)
P188	10 – 15%		
Hyaluronic acid	0.5 – 2%		
P407	21%	31%	labeled with Technetium-99m-diethylen triaminepentaacetic acid (11)
P188	10%		
Sodium hyaluronate	0.2%		
P407	16%	17%	Fluconazole (70)
CS <sup>2</sup>	0.5 – 1.5%		
P407	18%	18%	Pilocarpine HCl (88)
Gellan gum	0.1 – 1%		
P407	15 – 20%;	17.2%	Betaxolol HCl (89)
HPMC <sup>1</sup>	0.5 – 1.0%		
P407	P407 25%	28%, 30%	Pilocarpine (71)
HPMC <sup>1</sup>	HPMC 3%		
MC <sup>1</sup>	MC 5%		

<sup>1</sup> HPMC-Hydroxypropylmethyl cellulose; MC-Methyl cellulose; CMC-Carboxymethyl cellulose

<sup>2</sup> CS - Chitosan

Although poloxamers are widely investigated as potential *in situ* forming gel systems, they suffer from a drawback of having weak mechanical strength, which can lead to rapid gel erosion (7,20). To promote mechanical strength of poloxamer gels and consequently prolong their residence time and therefore eye-related bioavailability, different polymers/additives are added to their systems (7). Furthermore, since P407 mucoadhesiveness, a very important parameter for effective ophthalmic delivery, is low (90), it is frequently combined with mucoadhesive polymers such as polyacrylic acid (Carbopol) (91) and hyaluronic acid (18).

Gratieri et al. developed (20) ophthalmic *in situ* forming gel by combining poloxamer P407 and chitosan. Chitosan was added to the P407 in order to obtain adequate gel strength. The developed system had adequate mechanical and mucoadhesive properties. They demonstrated that poloxamer/chitosan formulations in a concentration of 16% of poloxamer and 0.5 – 1.5% of chitosan showed optimal gelation temperatures ( $T_{gel} \approx 32^{\circ}\text{C}$ ) and were able to withstand low shearing forces at  $35^{\circ}\text{C}$ . The mechanical properties of these formulations, especially the one containing 1% of chitosan, indicated high hardness and adhesiveness, besides showing prolonged retention. This group subsequently incorporated the antifungal agent, fluconazole, in the developed systems which resulted in prolonged API release when compared to the chitosan solution (70). The drawback of developed platform was its low resistance to dilution with simulated tear fluid. Namely, after dilution, rheological analysis revealed that the system behaved as viscoelastic solution at  $35^{\circ}\text{C}$ , indicating possible issues with controlled drug delivery.

Wei et al. evaluated the influence of P188 on P407 ophthalmic gels in concentration range from 16 – 24% for P407 and 0 – 20% for P188 (11). The mixed poloxamer solution containing 21% P407 and 10% P188 was free flowing liquid below  $25^{\circ}\text{C}$  and converted to a gel under physiological conditions. Gamma scintigraphic results demonstrated that the clearance of the *in situ* forming gel encapsulating label molecule (Technetium-99m-diethylentriamine pentaacetic acid) was significantly delayed with respect to the phosphate buffered solution, while at least a threefold increase of the precorneal retention time was achieved.

Asasutjarit et al. developed diclofenac sodium *in situ* ophthalmic gel based on P407. P188 was added to modified  $T_{gel}$  and Carbopol 940 as mucoadhesive agent (15). The optimized *in situ* gel formulation obtained from this study contained 20%/11%/0.1% (w/w/w) of P407/P188/Carbopol. It could be easily applied at the room temperature and transformed to a gel exhibiting pseudoplastic flow behavior at the precorneal temperature. *In vitro* and *in vivo* eye irritation test showed that it could be accepted as safe for ophthalmic use. In addition, *in vivo* evaluation of ophthalmic absorption indicated that formulation could increase ophthalmic bioavailability of diclofenac sodium in rabbits and reduce the frequency of administration significantly compared to a commercial product.



Fathalla et al. developed two optimal P407/P188 gels having polymer concentrations 23%/10% (w/V) and 23%/15% (w/V), respectively (85). These *in situ* gels appeared to be a promising ophthalmic delivery system for ketorolac.

In all these studies both poloxamers were used in *in situ* forming ophthalmic gels at very high total concentration, e.g. P407 and P188 in concentration of 23% and 10% and 23% and 15%, (w/V) (85) 21% and 10% (11); 16% and 14% (14); 20% and 11% (w/w) (15), respectively. Decreasing the total polymer concentration would surely have significant positive implications on economic issues and possible toxicity issues related to chronic use of poloxamer-based *in situ* forming ophthalmic gels.

## **2.5. Considerations for formulation development of poloxamer-based *in situ* forming ophthalmic gels**

*In situ* forming ophthalmic gels need to be fine-tuned considering all the biopharmaceutical challenges of the front of the eye in order to increase drug residence time at the application site resulting in its improved bioavailability and efficacy (Table 1).

The optimal poloxamer-based *in situ* forming gel should be characterized by: (i) temperature of gelation in physiologically relevant range; (ii) pseudoplastic behavior that allows gel to thin during blinking, making it more comfortable and easier to spread across the eye surface (8); (iii) suitable gel strength to endure the dilution with tears. Beside these crucial properties related to *in situ* forming gel performance, the formulation has to meet strict requirements of biocompatibility and sterility. Further criteria which can have influence on *in vivo* performance of *in situ* forming gel or patient acceptance include suitable pH, osmolality and refractive index. The eye can tolerate products over a range of pH values from about 3.0 to about 8.6, however normal tears have a pH of about 7.4 (38). Ophthalmic products may be tolerated over a fairly wide range of tonicity (0.5%–5% sodium chloride, equivalent to about 171–1711 mOsm/kg). Hypotonic solutions are better tolerated than hypertonic solutions (38). Refractive index measurements detect possible impairment of vision or discomfort to the patient after administration of eye drops. Refractive index of tear fluid is 1.340–1.360. It is recommended that eye drops should

have refractive index values not greater than 1.476 (72). However, it should be kept in mind that additives that regulate the formulation pH or osmolality can influence the rheological properties of *in situ* forming gels and the effects of their addition have to be investigated and controlled.

Additional criteria are related to the active ingredient incorporation, its availability and stability (3). Availability relates to the capability of delivering drugs at the right dose and it is closely related to the drug release rate from the formed gels. The drug release rate is mostly defined by the physicochemical properties of the active ingredient, polymer concentration, gel rheological properties and the affinity of active ingredient for the polymer network.

Last but not least, the stability of developed formulation represents a critical quality parameter, and therefore the storage conditions to insure stability and the shelf life have to be determined.

As seen from previously listed studies (Table 4), poloxamer systems show remarkable potential as *in situ* forming ophthalmic gels, however they were used at very high total concentrations. In addition to decrease the total polymer concentration, improvements in the biopharmaceutical properties of poloxamer ophthalmic gels can be achieved by the presence of different additives in the formulation (16–18,20,92), such as chitosan. These improvements of poloxamer systems result in enhanced viscoelastic properties and mechanical strength of *in situ* forming gels which consequently prolong drug residence time at site of administration (18) and could promote system resistance to dilution by tears.

## 2.6. Chitosan in ophthalmic drug delivery

Chitosan is a biocompatible and biodegradable polycationic polymer with pKa of 6.5. Its mucoadhesive properties, important for ophthalmic delivery systems, are related to the fact that below its pKa, chitosan is positively charged and electrostatically interacts with negatively charged epithelial surfaces (48). It is a heteropolymer containing both glucosamine and acetylglucosamine units (Figure 8). This polymer distinguishes from other commonly available polysaccharides due to the presence of nitrogen (93). It is not considered as one chemical entity since it can be found in a variety of forms differing in size (average molecular weight and molecular weight distribution) and degree of deacetylation (DD) and this diversity is exponentially increased by the numerous chemical modifications that have been investigated (94).

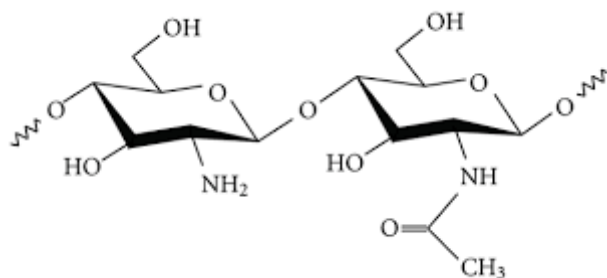


**Figure 8.** Structure of chitosan

Chitosan has already been demonstrated to increase the mechanical strength and mucoadhesiveness of poloxamer *in situ* forming ophthalmic gels (20). Furthermore, there are other benefits of including chitosan in ophthalmic formulations such as improvement of eye-related permeability due to its paracellular permeation enhancing effects (21), antimicrobial activity (22) and corneal wound healing effect (23).

Chitosan does not cause allergic reactions due to its biocompatible character and ophthalmic safety of chitosan is well documented in literature (95,96). Pioneering work in chitosan ophthalmic safety was done by Felt and coworkers (95). They studied and reported excellent ocular tolerance of chitosan in rabbit model following topical instillation of its solutions using

confocal laser scanning ophthalmoscopy combined with corneal fluorescein staining. Their conclusion was that chitosan is a well-tolerated polymer suitable for the development of ophthalmic formulations intended for topical use. There are a significant number of other studies demonstrating the ocular biocompatibility of chitosan. In addition, Pepić and coauthors studied the potential of poloxamer/chitosan micelle system as ophthalmic dexamethasone delivery system (96). *In vivo* study in rabbits showed no ocular damage or clinically abnormal signs in the cornea, conjunctiva or iris.

## 2.7. Rheological characterization of *in situ* forming gels

Hydrogels are defined by International Union of Pure and Applied Chemistry as a polymer networks that are expanded throughout their whole volume by water (97). When considering ophthalmic preparations, it is difficult to clearly draw the line between highly viscous solutions and the actual gels. One of the interesting definitions of gels is that they are systems at the upper limit of viscous preparations which are formed when high molecular weight polymers and/or high polymer concentrations are incorporated into the formulation (5).

Another definition has been made that the term "gel" should be limited to the systems which fulfil the following phenomenological characteristics:

- (i) they consist of two or more components one of which is a liquid, present in substantial quantity and
- (ii) they are soft, solid, or solid-like materials (98).

The term 'rheology' is derived from the Greek word *rheos* meaning to stream or flow. Rheology is the science of the flow and deformation of materials and describes the response of different materials to stress or shear. Many of solid materials will behave as liquids at very long times and most liquids will respond like solids at short times. They cover the spectrum of "viscoelastic materials". Rheological characterization of these materials is very important, since it provides unique insights into their microstructure (99). Characterization of the microstructure and flow properties of semisolid and liquid pharmaceuticals is essential for understanding and controlling their rheological behavior.

Moreover, definition of the solid-like characteristics of gels in terms of the dynamic mechanical properties (tested by oscillatory rheological tests) have been proposed, viz. a storage modulus,  $G'$ , which exhibits a pronounced plateau extending to times at least of the order of seconds and a loss modulus,  $G''$ , which is considerably smaller than the storage modulus in the plateau region (98).

Storage Modulus ( $G'$ , Pa) is a measure of the deformation energy stored by the sample during the shear process. After the load is removed, this energy is completely available, now acting as the driving force for the reformation process which will compensate partially or completely the

previously obtained deformation of the structure.  $G'$  presents the elastic behavior of a sample (100). Loss Modulus ( $G''$ , Pa) is a measure of the deformation energy used up by the sample during the shear process and therefore afterwards, it is lost for the sample. This energy is spent during the process of changing the material's structure, i.e. when the sample is flowing partially or completely.  $G''$  represents the viscous behavior of a material (100). Quotient of the lost and the stored deformation energy is called the loss factor or damping factor –  $\tan\delta$  (tangent value of the phase angle):

$$\tan\delta = G''/G' \quad (\text{Eq. 1})$$

According to Thomas Mezger's *The Rheology Handbook*, gels are defined as viscoelastic materials which, in oscillation rheological testing, exhibit  $G' > G''$  with  $\tan\delta < 1$ , while minimal adequate  $G'$  values for gel structures would be around 5 Pa (100). Moreover, Kojarunchitt et al. defined *soft* gels as viscoelastic systems where  $G' = G''$  (101). From all the definitions and arguments mentioned, conclusion can be made that gels can hardly be adequately defined without appropriate rheological characterization.

Two types of tests rheological tests are usually employed in investigations of viscoelastic materials- *shear tests* and *oscillatory tests*.

In order to gain reliable results, the structure of a gel must not be disturbed during its rheological characterization. Therefore, shear stress is a crucial parameter and needs to be precisely adjusted and controlled. This inherently excludes rotational rheometers from any kind of investigations on either gel formation or gel structure characteristics (102). From this reason oscillatory, tests (Figure 9) are employed. They are important since they explore the viscoelasticity of a sample providing a microstructural fingerprint that can be used to quantify stability and to sensitively refine critical aspects of product performance (103).

During the oscillatory testing the sample is subjected to a relatively small shear force or displacement applied in the form of a sinusoidal wave (Figure 9A). Oscillatory rheometers are specified to apply the bi-directional movement of the upper geometry, relative to the lower, that is required to achieve this (103). When performing full rotation, the wheel is turning over rotation angle of  $360^\circ$ . This corresponds to a complete oscillation cycle of the time dependent functions  $\tau(t)$  (shear stress),  $\gamma(t)$  (shear deformation/strain) and (shear rate)  $\dot{\gamma}(t)$ . Ever during continuous

rotation, when the wheel is passing the angle positions of  $0^\circ$  and  $180^\circ$ , the upper plate is showing the zero position and therefore,  $\gamma(t) = 0$  and also  $\tau(t) = 0$  (100).

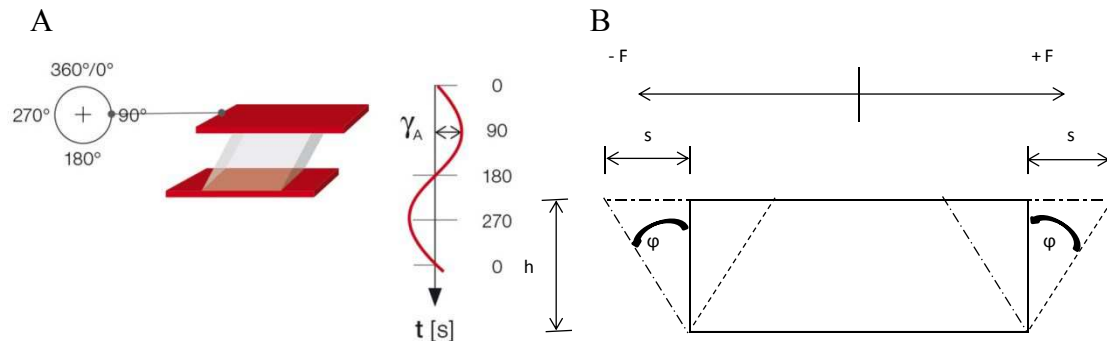


**Figure 9.** Oscillatory rheological test: A) two plates model to illustrate oscillatory shear tests, picture reprinted from (104); B) oscillatory tests: shear force  $\pm F$ , deflection path  $\pm s$  and deflection angle  $\pm \phi$  in the shear gap  $h$ , picture reprinted with permission from (100).

The velocity, however, is at maximum where  $\gamma(t) = \gamma_{\max}$ . At the angle position of  $90^\circ$ , the upper plate shows maximum deflection to the right, and at  $270^\circ$  occurs the maximum deflection to the left. Therefore,  $\gamma(t) = \gamma_{\max}$  and also  $\tau(t) = \tau_{\max}$  or  $\gamma(t) = -\gamma_{\max}$  and also  $\tau(t) = -\tau_{\max}$ , respectively (100).

A principle of oscillatory testing originates from the year 1676 when Robert Hooke (1635-1703) wrote law which described the proportionality of force and deformation for solids (ideally elastic materials):

*Deformation of solids is proportional to the applied force, i.e. the force needed to extend or compress a spring by some distance is proportional to that distance.* Resulting relation is the spring law:

$$C = F / s \quad (\text{Eq. 2})$$

Where  $F$  is the force acting on deflection path  $s$  on a spring with a constant  $C$  (measure of a stiffness). When performing oscillatory test on ideally elastic materials Hooke's law applies as follows:

$$\tau(t) = G^* \cdot \gamma(t) \quad (\text{Eq. 3})$$

with the complex modulus ( $G^*$ ) and the time dependent values of sinusoidal functions of  $\tau$  and  $\gamma$ .  $G^*$  can be described as the resistance against deformation (rigidity of material). Since

$G^* = \tau(t) / \gamma(t) = const$ , the  $\tau(t)$  curve is always in phase with the  $\gamma(t)$  curve i.e. both curves are occurring without any delay between preset and a response in the form of sine curves (100).

On the contrary to ideally elastic materials, in the oscillatory test, ideally viscous samples (or Newtonian) exhibit flow behavior described by the viscosity law or Newton's law:

$$\tau(t) = \eta^* \cdot \dot{\gamma}(t) \quad (\text{Eq.4})$$

With the complex viscosity  $\eta^*$  and the time dependent values of the sine functions of  $\tau$  and  $\dot{\gamma}$ . Complex viscosity,  $\eta^*$ , can be imagined as the viscoelastic flow resistance of a sample. Since  $\eta^* = \tau / \dot{\gamma} = const$ , the  $\tau(t)$  curve is always in phase with the  $\dot{\gamma}(t)$  curve, i.e. both curves are appearing without any delay between preset and the response, showing the same frequency. If the  $\gamma(t)$  curve is presented as a sine curve, both the  $\tau(t)$  curve and the  $\dot{\gamma}(t)$  curve are occurring as cosine curves. For samples showing ideally viscous behavior, there is a delay between the  $\tau(t)$  curve and the  $\gamma(t)$  curve with the phase shift angle  $\delta$  of  $90^\circ$  ( $\delta = \pi/2$  rad) (100). Therefore, based on their rheological behavior, *viscoelastic liquids* have phase angle equal or higher to  $90^\circ$  (Figure 11, Table 5) and exhibit higher  $G''$  than  $G'$  values in  $G' G''$  plateau region (Figure 10).

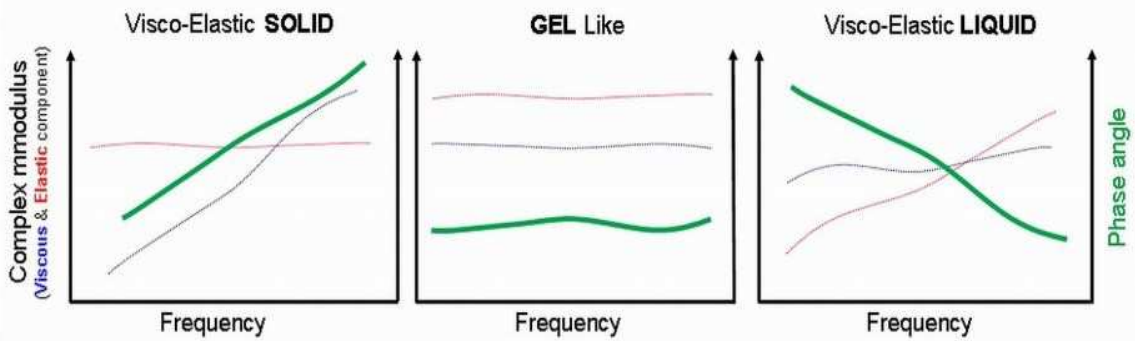


**Figure 10.** Typical oscillatory test (frequency sweep) data for samples behaving as a viscoelastic solid (as a gel or as a viscoelastic liquid), (picture reprinted from (103)).

All gel systems are viscoelastic materials since they are exhibiting viscous and elastic behavior simultaneously.

Viscoelasticity is the property of materials that exhibit both viscous and elastic characteristics when undergoing deformation. The viscous portion behaves according to Newton's law and the elastic portion behaves according to Hooke's law.



Gels, as *viscoelastic solid* materials, display a time-dependent, delayed response, whether a stress or a strain are applied as well as when the stress/strain are removed. These materials have a phase angle (late in phase response to stress or strain) between 0 and  $\pi/2$  radians (0 and 90°, Figure 11, Table 5) (100) and in  $G'$   $G''$  plateau region exhibit higher  $G'$  values (Figure 10).

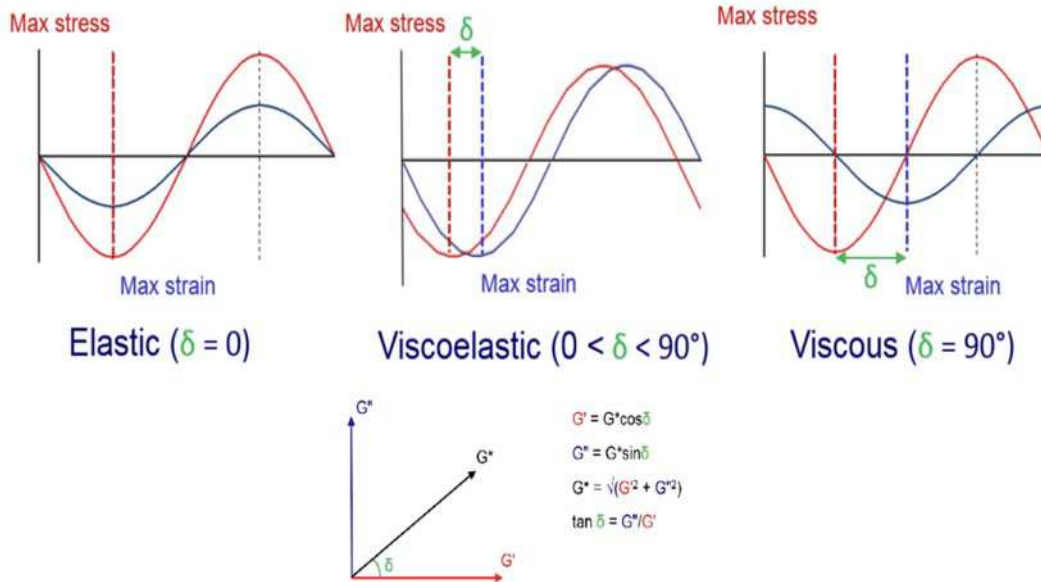


**Figure 11.** Shear stress *vs.* shear strain and resulting phase angle for elastic ( $\delta=0^\circ$ ), viscoelastic ( $0^\circ < \delta < 90^\circ$ ) and viscous ( $0 \geq 90^\circ$ ) materials, (reprinted from (103)).

On the other hand, ideally elastic materials do not have a shift in phase angle ( $\delta = 0$ , Table 5).

**Table 5.** Flow behavior of different materials with respect to  $G'$ ,  $G''$ ,  $\delta$  and  $\tan\delta$ , reprinted with permission from (100).

Ideally viscous flow behavior	Behavior of viscoelastic liquid	Viscoelastic behavior showing 50/50 ratio of the viscous and elastic portions	Behavior of viscoelastic gel or a solid	Ideally elastic deformation behavior
$\delta=90^\circ$	$90^\circ > \delta > 45^\circ$	$\delta=45^\circ$	$45^\circ > \delta > 0^\circ$	$\delta=0$
$\tan\delta \rightarrow \infty$	$\tan\delta > 1$	$\tan\delta = 1$	$\tan\delta < 1$	$\tan\delta \rightarrow 0$
$(G' \rightarrow 0)$	$G'' > G'$	$G'' = G'$	$G' > G''$	$(G'' \rightarrow 0)$

Two types of *oscillatory* tests which are commonly used for in depth characterization of gels are *strain* and *frequency sweep* analyses.

In the strain sweep (also known as amplitude sweep test) test oscillation is performed at variable strain amplitudes, while the frequency and temperature are kept at a constant value. These tests are carried out to determine the limit of linear viscoelastic (LVE) range and to evaluate mechanical spectra ( $G'$  and  $G''$ ). LVE range is the range where stress ( $\tau$ ) is directly proportional to strain ( $\gamma$ ). This term derives from the proportionality of pre-set and measured parameters (e.g. shear strain and shear stress). In a diagram, e.g. the  $G'$ -curve occurs as a straight line (100).



**Figure 12.** Schematic representation of strain sweep test (reprinted from (105)).

After determination of LVE of the sample, frequency sweep tests are commonly performed, since they provide an insight on the behavior of  $G'$ ,  $G''$  and  $\eta^*$  as a function of angular frequency, while strain ( $\gamma$ ) is kept constant in the previously determined LVE range (Figure 13). From frequency sweep analysis information about a time dependent behavior is obtained. Short term behavior is simulated by rapid motion, while long term behavior is simulated by low frequencies (100).

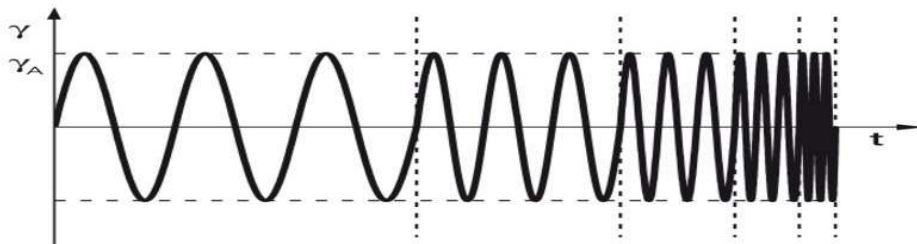


**Figure 13.** Schematic representation of frequency sweep test (reprinted from (106)).

In *rotational* tests the rheological properties of materials can be characterized in a steady simple shear flow with homogeneous regime of deformation. Basically there are two different regimes of deformation: imposition of constant rotational speed or constant torque, corresponding to *controlled shear rate* and *controlled shear stress*, respectively (107). Rotational rheology is used

to characterize the mostly complex, non-Newtonian, flow behavior of liquids, solutions, melts and dispersions. With most of the rheometers, the bob is the rotating part of the measuring system, but there are also types where the cup or the lower plate of the measuring system is set in rotational motion.

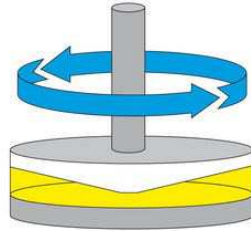


**Figure 14.** Rotational rheological test (reprinted from (108)).

Possible resulting curves, depending on nature of the tested material, are summarized in the Figure 15. Characterization and manipulation of the flow behavior of *in situ* forming gels in the experimental set up simulating conditions before and after administration to the eye surface assures their optimal performance.

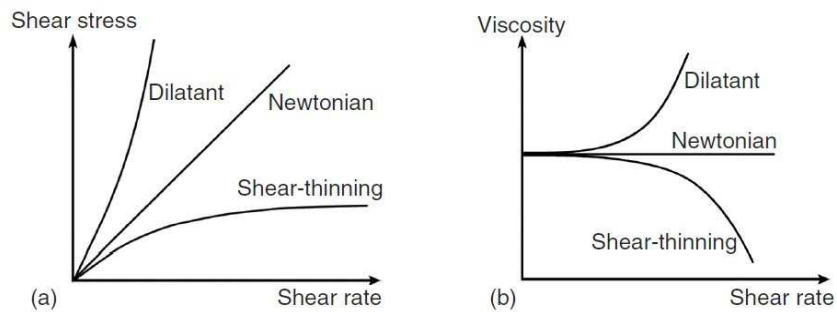


**Figure 15.** Typical flow curves for Newtonian, shear thinning and shear thickening (dilatant) fluids: (a) shear stress as a function of shear rate; (b) viscosity as a function of shear rate (picture reprinted from (107)).

As mentioned previously, gels are pseudoplastic materials. Since they are exhibiting a shear-thinning behavior, their viscosity depends on the degree of the shear load (such as blinking) – it decreases with increasing shear load, and with time, it is restored to a certain extent when the load is removed.

## **2.8. Quality by Design and Design of Experiments in pharmaceutical development**

The term Quality by Design (QbD) was suggested by the regulatory authorities (FDA, EMA) at the beginning of the new millennium, recognizing that “quality cannot be tested into products, i.e. quality should be built in by design”. This was a direct acknowledgment of the significance of quality theory in pharmaceutical development (109). QbD concept is acknowledged in pharmaceutical development due to its advantages on assurance of high quality drug products without extensive regulatory oversights (110). Implementation of this approach increases development efficiency with a successful product optimization and a robust manufacturing process, improves the communication between regulatory agencies and industry providing regulatory relief and flexibility, reduces post-approval changes and enables real-time quality control (110).

*Quality by Design* is defined as a systematic approach to development that begins with predefined objectives and emphasizes product and process understanding and process control, based on sound science and quality risk management (111).

*Pharmaceutical QbD* is a systematic, scientific, risk-based, holistic and proactive approach to pharmaceutical development that begins with predefined objectives and emphasizes product and processes understanding and process control. It means designing and developing formulations and manufacturing processes to ensure predefined product quality objectives. QbD identifies characteristics that are critical to quality from the perspective of patients, translates them into the attributes that the drug product should possess, and establishes how the critical process parameters can be varied to consistently produce a drug product with the desired characteristics (112).

*Design of Experiments* (DoE) is the main component of the statistical toolbox to use QbD in both research and industrial settings. It is considered the main systematic approach requiring the implementation of statistical thinking at the starting point of pharmaceutical development. Experimental design is a structured, organized method for determining the relationships between factors affecting a process and the output of that process. DoE, in short, means achieving process

knowledge, through the establishment of mathematical relationships between process inputs and its outputs (109) (Figure 16).

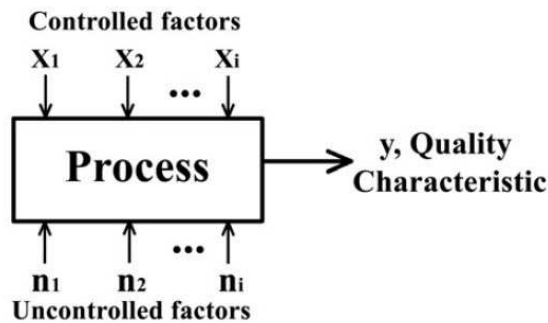


**Figure 16.** Schematic representation of process (reprinted with permission from (109)).

*Quality target product profile* (QTPP) forms the basis of design for the development of the product. Considerations for the QTPP could include intended use in clinical setting, route of administration, dosage form, delivery systems, dosage strength(s), container closure system, drug release or delivery and attributes affecting pharmacokinetic characteristics (e.g., dissolution) appropriate to the drug product dosage form being developed; drug product quality criteria (e.g., sterility, purity, stability and drug release) appropriate for the intended marketed product (111).

*Critical Quality Attribute* (CQA) is a physical, chemical, biological, or microbiological property or characteristic that should be within an appropriate limit, range, or distribution to ensure the desired product quality. CQAs are generally associated with API, excipients, intermediates (in-process materials) and drug product. Potential drug product CQAs derived from the quality target product profile and/or prior knowledge are used to guide the product and process development. Relevant CQAs can be identified by an iterative process of quality risk management and experimentation that assesses the extent to which their variation can have an impact on the quality of the drug product (111).

*Risk Assessment* is a valuable science-based process used in quality risk management that can aid in identifying which material attributes and process parameters potentially have an effect on product CQAs. Risk assessment is typically performed early in the pharmaceutical development process and is repeated as more information becomes available and greater knowledge is obtained (111).

*Design Space* is the relationship between the process inputs (material attributes and process parameters) and the critical quality attributes (111).

*Control Strategy* is designed to ensure that a product of required quality will be produced consistently (111).

### **2.8.1. DoE workflow**

The general purpose of DoE is the relation of the critical process/formulation parameters (CPP, CFP) ( $x_1, x_2, x_i$ ) with the CQAs ( $y_i$ ) through mathematical functions  $y = f(x)$ , as depicted in Figure 16. Such relationships enable the:

- determination of the most influential factors (CPPs, CFPs) among many;
- identification of optimum factor settings leading to enhanced product performance and assuring CQA values lying within specifications with minimum variability;
- elucidation of interactions between the factors, an important advantage over the conventional way of experimentation, where each factor is studied independently of the others (One-Factor-At-a-Time or OFAT experimentation)(109).

Execution of an experimental design requires seven distinct phases:

- (i) *Setting solid objectives*: clear definition of the Quality Target Product Profile (QTPP) should be done, using the knowledge base from scientific literature and technical experience, critically evaluated under the Quality Risk Management approach.
- (ii) *Selection of process variables* (factors) and *responses* (Critical Quality Attributes - CQAs): this choice is justified based on the DoE objective and should assure that the whole design is executable and appropriate for satisfying its scope.
- (iii) *Selection of an experimental design*: based on DoE objectives, screening, characterization or optimization of process and formulation, different types of designs can be chosen
- (iv) *Execution of the design*: the generated design matrix should be accurately executed, assuring that parameters not included in the design are identified and kept constant

- (v) *Checking* that the data are consistent with the experimental assumptions: DoEs are exceptionally effective in identifying outliers, arising from potential poorly executed trials.
- (vi) *Analyzing* the results: ANOVA and graphical tools are very helpful in identifying main effects of the significant factors and interactions thereof. The results are evaluated not only on a statistical basis but also versus the established theories and practically lead to process knowledge.
- (vii) *Model building and validation* - use and interpretation of the results at this step, the evaluation of the DoE outcome can support scientifically sound decision making on following actions, such as executing confirmatory runs, augmenting designs, or further proceeding with scale up and technology transfer activities (109).

Traditionally, formulations were manufactured to meet quality control tests outlined in product specifications. If the product is expected fit for commercial purpose, then it should meet quality control tests. In case of a batch failure to comply with these tests, it is reprocessed or rejected, which opens doors for regulatory questions and obvious cost related issues. Enhanced product stability decreases the amount of rejected products and reduces costs. For patients, robust pharmaceutical products increase efficacy and minimize side effects. Meanwhile, it makes it easier for governments to implement management, regulation, and supervision in the research, development, manufacturing, storage and clinical use of drugs (113).

In summary, QbD principles, when implemented, lead to a successful product development, subsequent prompt regulatory approval, reduce intensive validation burden, and significantly reduce post-approval changes (114).

## 2.9. Ocular tolerability assessment

In addition to the tests evaluating performance, early assessment of biocompatibility or ocular tolerability is crucial in development of novel ophthalmic products. The cornea and conjunctiva are susceptible to injuries and adverse ocular effects either from the administered drug or excipients used in the finished ophthalmic product. For the purpose of ocular tolerability assessment, it is important to establish adequate tests. Non clinical models used in pharmaceutical development include *in vitro* and *ex vivo* models and *in vivo* i.e. animal models.

Several tests and assays used to determine the ocular toxicity and irritation potential of ophthalmic delivery systems are recognized by regulatory agencies (47).

“*Draize rabbit eye irritation test*” uses live rabbits for the determination of range of possible eye irritation effects from chemical substances. It is accepted by the regulatory agencies. The irritation responses recorded are redness, swelling, edema, cloudiness, discharges, hemorrhage and blindness (47). The tested materials are classified based on a subjective scoring, from non-irritating to severely irritating, for their effect on the cornea, iris and conjunctiva. The main shortcomings of the Draize test is its subjectivity, poor reproducibility and the differences between the rabbit eye and the human eye (47).

“*Low-volume eye irritation test*” (*LVET*), was developed to circumvent issues related to the Draize test. The test is a modified Draize test in which the number of test material is reduced while maintaining the same scoring system of the Draize test (47).

Tests based on animal models are often criticized by public and scientific community due to the ethical concerns. Therefore, regulatory agencies have provided a set of *in vitro* and *ex vivo* tests that can potentially replace the aforementioned controversial *in vivo* eye irritation tests (47).

*In vitro* and *ex vivo* models of eye barriers enable safe and efficacious screening of formulations (48). First models are commonly based on the cells and the latter are based on tissues (115). Prerequisite for these tests is accuracy and reproducibility without the use of live animals (47). Examples of irritation assays are the isolated/enucleated organ method such as the Bovine Corneal Opacity and Permeability (BCOP) test, the non-ocular organotypic models such as Hen's Egg Test on the Chorioallantoic Membrane (HET-CAM) (a conjunctival model), and the cell-



based cytotoxic colorimetric methods such as Red Blood Cell (RBC) lysis and protein denaturation, Neutral Red Uptake (NRU) and Sulforhodamine B (SRB) assays (47).

Drawbacks related to tissue based (*ex vivo*) models are low throughput and insufficient standardization, ethical concerns and moreover, the relation from animal to human tissue is questionable (2). The cell-based models that have the correct balance between their predictability and throughput have the potential to be routinely used for assessment of eye-related biocompatibility (2,115,116). *In vitro* models may also provide mechanistic understanding of toxicity at the cellular /molecular level. Furthermore, they are capable of creating a broader range of toxicology testing capabilities such as multiple endpoints, concentrations, exposure methods and times to be better controlled and tailored accordingly (117).

Currently, most of the ocular tolerability testing is performed using cell monolayers i.e. two-dimensional (2D) cell models. Such models do not reflect 3D structure of tissues (118). Use of inadequate cell models during development can lead to selection of wrong candidates and/or formulations which can lead to great expenses in late development. Implementation of 3D cell based models, which simulate better *in vivo* physiological environment is key for successful pharmaceutical development, that is right screening of drug candidates during early phase of research and development (119).

For chemicals tested for ocular biocompatibility, as a general rule, when the cell viability of rabbit corneal epithelial cell line is  $\leq 70\%$  at two concentration levels (5% and 0.5% ), tested chemical is classified per United Nations Globally Harmonized System of Classification and Labeling of Chemicals (UN GHS) as Category 1. This category includes chemicals inducing serious eye damage or irreversible effects on the eye. However, when cell viability is  $>70\%$  at both concentrations, a test chemical is classified as UN GHS No Category, meaning that tested chemicals do not require classification for eye hazards (116).

### **3. AIMS OF THESIS**

*In situ* forming gels attract great attention as the formulation candidates for the improvement of bioavailability and efficacy of topical ophthalmic drugs. The mixtures of poloxamers 407 (gelation agent) and 188 (gelation modifier) are of interest for the development of *in situ* forming ophthalmic gels. Despite many beneficial properties of poloxamers as ophthalmic excipients, their performance is associated to weak mechanical strength, which leads to rapid erosion (7,18,20). The improvement of the mechanical strength of poloxamer gels can be achieved by the inclusion of chitosan. Chitosan is well known for its biocompatible, biodegradable and mucoadhesive properties, rendering it suitable for ophthalmic use (95).

The aim of this doctoral thesis was to develop *in situ* forming ophthalmic P407/P188/CS gel fine-tuned in terms of polymer content, temperature of gelation, storage modulus and viscosity.

Specific aims of a thesis were to optimize the formulation parameters by implementation of DoE to assure:

- (i) temperature of gelation ( $T_{gel}$ ) in physiologically relevant range;
- (ii) pseudoplastic behavior;
- (iii) suitable viscosity and storage modulus of *in situ* gel;
- (iv) resistance to dilution with simulated tear fluid;
- (v) robustness against entrapment of drugs with diverse physicochemical properties;
- (vi) controlled release of model drug.

A systematic approach (DoE) to *in situ* forming gel development has the potential to result in robust formulation characterized by ease of administration, accuracy of dosing, avoidance of eye-related discomfort and prolonged residence at the eye surface. These benefits will lead to better patient compliance, improved eye-related bioavailability and, finally, improved therapeutic outcome.

## **4. MATERIALS AND METHODS**

## 4.1. Materials

Poloxamers P407 (Kolliphor P407; EO<sub>98</sub>PO<sub>69</sub>EO<sub>98</sub>; average molecular weight (M<sub>w</sub>) 13,498 g/mol) and P188 (Lutrol micro F68; EO<sub>80</sub>PO<sub>27</sub>EO<sub>80</sub>; average M<sub>w</sub> 8902 g/mol) were purchased from BASF SE (Ludwigshafen, Germany). More than 90% deacetyled ultrapure PROTASAN<sup>TM</sup> chitosan salt (Protasan UP CL 214; M<sub>w</sub> 150,000-400,000 g/mol; viscosity 20-200 mPa × s) (CS) was obtained from NovaMatrix<sup>®</sup> (Sandvika, Norway).

Water for injection (WFI) was donated by PLIVA Croatia Ltd (Zagreb, Croatia). Ultrapure water for chromatographic analyses was produced by Ultra Clear<sup>TM</sup> UV Plus (SG Wasseraufbereitung und Regenierstation GmbH, Barsbüttel, Germany).

NaCl, NaHCO<sub>3</sub>, KCl, Na<sub>2</sub>HPO<sub>4</sub>, NaH<sub>2</sub>PO<sub>4</sub>, MgSO<sub>4</sub> × 7H<sub>2</sub>O, NaOH, KH<sub>2</sub>PO<sub>4</sub>, and CH<sub>3</sub>COONa × 3H<sub>2</sub>O, were obtained from Kemika (Zagreb, Croatia). CaCl<sub>2</sub> × 2H<sub>2</sub>O, acetonitrile (ACN), HEPES and D-glucose monohydrate were acquired from Merck (Darmstadt, Germany).

Timolol maleate (TIMO), dexamethasone (DEX), dorzolamide hydrochloride (DORZO) were kindly donated by TEVA Pharmaceutical Industries Ltd. Tobramycin (TOBRA) standard was purchased from the USP (Rockville, MD, USA).

Simulated tear fluid (STF) pH 7.4 was prepared by dissolving the following substances in double-distilled water: KCl (1.4 mg/ml), NaCl (6.8 mg/ml), NaHCO<sub>3</sub> (2.2 mg/ml) and CaCl<sub>2</sub> × 2H<sub>2</sub>O (0.08 mg/ml) (65).

Krebs-Ringer buffer (KRB) pH 7.4 was prepared by dissolving the following substances in double-distilled water: KCl (0.4 mg/ml), NaCl (6.8 mg/ml), NaHCO<sub>3</sub> (2.1 mg/ml), MgSO<sub>4</sub> × 7H<sub>2</sub>O (0.4 mg/ml), D-glucose monohydrate (1.1 mg/ml), CaCl<sub>2</sub> × 2H<sub>2</sub>O (0.52 mg/ml), NaH<sub>2</sub>PO<sub>4</sub> × 2H<sub>2</sub>O (0.158 mg/ml) and HEPES (3.575 mg/ml) (115).

50 mM phosphate buffer (PB) was prepared by dissolving KH<sub>2</sub>PO<sub>4</sub> (6.81mg/ml) and NaOH (1.56 mg/ml) in double-distilled water (120).

Hank's balanced salt solution (HBSS, pH 6) was prepared by dissolving the following substances in double-distilled water: MgSO<sub>4</sub> × 7H<sub>2</sub>O (100 mg/l), KCl (400 mg/l), NaHCO<sub>3</sub> (350 mg/l), NaCl (8000 mg/l), D-glucose monohydrate (1100 mg/l), CaCl<sub>2</sub> × 2H<sub>2</sub>O (185 mg/l) (Sigma–Aldrich),

MgCl<sub>2</sub> × 6H<sub>2</sub>O (100 mg/l), KH<sub>2</sub>PO<sub>4</sub> (60 mg/l), Na<sub>2</sub>HPO<sub>4</sub> × 2H<sub>2</sub>O (60 mg/l), and HEPES (7150 mg/l).

Final step in STF, KRB, PB and HBSS preparation was filtration of solutions (Whatman™ membrane filters, 0.2 µm, RC58, GE Healthcare Limited, Buckinghamshire, UK).

Regenerated cellulose membranes pore size of 0.2 µm and 0.45 µm (RC 0.2 and RC 0.45), polyethersulfone pore size 0.45 µm membranes (PESU 0.45) and cellulose acetate membranes with 0.8 µm pore size (CA 0.8) were obtained from Sartorius Stedim Biotech (Göttingen, Germany). Hydrophilic polyethersulfone (PES) Supor® 0.1 µm pore size membrane filters were purchased from PALL (Ann Arbor, MI, USA).

Commercially available two API-free preformed gels, TIMO-loaded *in situ* forming gel, Dexpathenone-loaded *in situ* forming gel and DEX/TOBRA-loaded *in situ* forming gel were purchased and used for analyses. All materials were used as received.

## 4.2. Methods

### 4.2.1. Preparation of *in situ* forming ophthalmic gels

*In situ* forming ophthalmic gels were prepared by slightly modified cold method (121). Briefly, appropriate amounts of all materials were weighed in a glass bottle and defined amount of previously refrigerated WFI was added. Samples were stirred (speed 400-600 rpm) in an ice bath until clear solution was obtained. In case when CS was used in mixed systems, after ice bath, additional means of ultrasound at 20-25°C (Bandelin Sonorex digital 10P, BANDELIN electronic GmbH & Co. KG, Berlin, Germany) were applied to aid its dissolution. The concentration of P407 was in the range of 10.25 – 19.30 % (w/w) while the concentration of P188 was in the range of 0 – 7.66 % (w/w). The concentration of CS was in the range of 0 – 1.29 % (w/w). Sodium chloride was used in suitable range to achieve isotonicity.

Out of four active pharmaceutical ingredients (APIs), six API-loaded *in situ* forming ophthalmic gels were prepared, namely mixed P407/P188/CS system containing: 2 % (w/w) DORZO, 0.5 % (w/w) TIMO, 2 % (w/w) DORZO and 0.5 % (w/w) TIMO, 0.1 % (w/w) DEX, 0.3 % (w/w) TOBRA, 0.05 % (w/w) DEX and 0.3 % (w/w) TOBRA. All *in situ* forming ophthalmic gels were isotonized taking into account NaCl equivalent for each API.

#### 4.2.2. Osmolality, pH and transparency determination

Osmolality was determined by the freezing point depression method (Advanced<sup>®</sup> 3D3 Single-Sample Osmometer, Advanced Instruments Inc, Norwood, Massachusetts, USA). pH was measured using PHM240 pH/Ion-Meter (Radiometer Analytical SAS, Villeurbanne, France).

The transparency of *in situ* forming ophthalmic gels was determined by measuring the refractive index (RE40 Refractometer, Mettler-Toledo, LLC, Columbus OH, USA)(122).

#### 4.2.3. Measurement of temperature of gelation and complex viscosity

The temperature sweep test was performed to determine the temperature of gelation ( $T_{gel}$ ), storage modulus ( $G'$ ), loss modulus ( $G''$ ) and complex viscosity ( $\eta^*$ ) (18,20). The rheological measurement was performed using Rheometer Anton Paar Physica MCR 301 (Figure 17A, Anton Paar GmbH, Graz, Austria) with parallel plate (PP50, Figure 17B) measuring system equipped with H-PTD 200 Truly Peltier-temperature-controlled hood (US Patent 6,571,610). Peltier heating element was connected to circulating water bath (F25-ME Refrigerated/Heating Circulator, JULABO GmbH, Seelbach, Germany). This system reduced the amount of water evaporating during the heating phase and allowed a more homogeneous temperature distribution. Samples were placed carefully on the lower plate of rheometer, measuring bob was placed in the measuring position and sample was equilibrated for 5 minutes at 5 °C. Angular frequency and strain applied were fixed at  $1\text{ s}^{-1}$  and 1 %, respectively while gap was  $d = 0.5\text{ mm}$ . Data was calculated by Rheoplus<sup>™</sup> software (Anton Paar).

$G'$ ,  $G''$  and  $\eta^*$  were recorded in the temperature range of 5–85 °C with a rate of 10 °C/min.  $T_{gel}$  is defined as the temperature point at which intersection of  $G''$  and  $G'$  curves occurs (18,100). All measurements were done in triplicate.

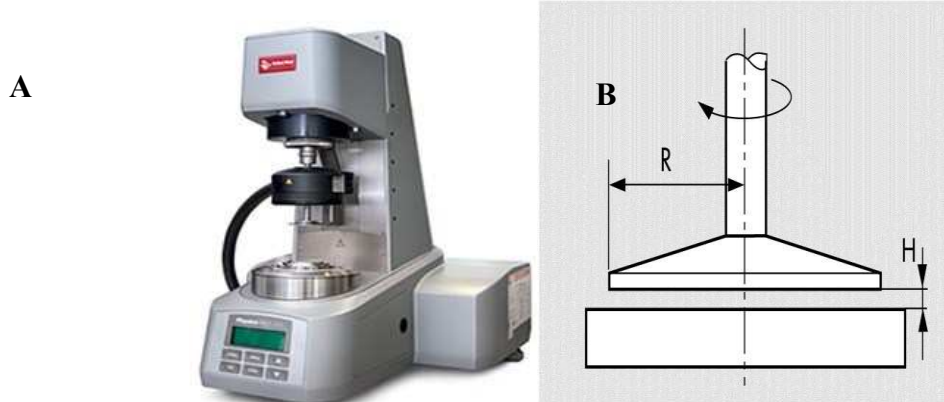


**Figure 17.** A) Anton Paar Rheometer Physica MCR 301 with H-PTD 200 Truly Peltier-temperature-controlled hood (picture reprinted from: (123)); B) parallel plate measuring system with a gap ( $H$ ) and radius ( $R$ ) (picture reprinted from (100)).

#### 4.2.4. Design of experiments

Quality by Design (QbD) principles were employed to optimize formulation parameters and evaluate their impact on  $T_{gel}$ ,  $G'$  and  $\eta^*$ . Statistical software JMP<sup>®</sup> version 12.0.1 (SAS Institute Inc., Cary, North Carolina, USA) was used to set experimental design, establish the mathematical model and analyze the collected data. Designs were generated within the class of optimal designs and D-optimality criterion was selected based on the particularities of the experimental situation.

The independent variables were the concentrations P407 (10.59 – 19.1%, w/w), P188 (0 – 7.66%, w/w) and CS (0.08 – 1.29% (w/w)), while dependent variables were  $T_{gel}$ ,  $G'$  and  $\eta^*$ . Sequential approach to experimentation was applied through screening, refining and optimizing designs (Table 6). Data set was expanded with the results of preliminary screening, consisting of five samples, which contained only P407. For the subsequent design of experiment, a new factor was added in order to explore influence of concentration levels of CS on the responses and include it into the model. Finally, preparation reproducibility was addressed in DoE by addition of three replicated samples in the last step (Table 6: Sample 23 was replicate for Sample 14; Sample 24 was replicate for Sample 15 and finally Sample 25 was replicate for Sample 16). This was done for two reasons - to evaluate the error of mixed system preparation as well as the error of the measurement.



**Table 6.** Samples prepared for DoE.

DoE	Sample*	P407	P188	CS
		(%, w/w)	(%, w/w)	(%, w/w)
Preliminary screening	1 <sup>o</sup>	11.40		
	2 <sup>o</sup>	13.80		
	3 <sup>o</sup>	15.20		
	4 <sup>o</sup>	16.90		
	5 <sup>o</sup>	19.30		
Screening	6 <sup>•</sup>	11.32	0.87	
	7 <sup>•</sup>	19.10	0.80	
	8 <sup>•</sup>	15.80	0.84	
	9 <sup>•</sup>	14.12	4.01	
	10 <sup>•</sup>	14.61	4.24	
	11 <sup>•</sup>	18.39	4.64	
	12 <sup>•</sup>	10.59	7.40	
	13 <sup>•</sup>	15.49	7.66	
Refining step (addition of CS)	14 <sup>▪</sup>	16.40	0.85	0.08
	15 <sup>▪</sup>	10.93	4.20	0.08
	16 <sup>▪</sup>	15.92	3.97	0.08
	17 <sup>▪</sup>	13.61	2.51	0.66
	18 <sup>▪</sup>	11.16	0.95	1.29
	19 <sup>▪</sup>	16.20	0.92	1.22
	20 <sup>▪</sup>	10.80	4.18	1.25
	21 <sup>▪</sup>	15.70	3.96	1.18
	22 <sup>▪</sup>	11.31	0.89	0.10
Replicate step	23 (14) <sup>□</sup>	16.40	0.84	0.09
	24 (15) <sup>□</sup>	10.93	4.21	0.09
	25 (16) <sup>□</sup>	15.88	3.97	0.08

\*<sup>o</sup>-preliminary screening, <sup>•</sup>-screening, <sup>▪</sup>-screening with addition of CS, <sup>□</sup>-optimization step

Multiple regression and analyses of variance (ANOVA) were used to evaluate experimental results (JMP<sup>®</sup> version 12.0.1). Factorial models were set to determine all main effects and interactions for the factors of interest i.e. concentrations of P407, P188 and CS. Significance of

the regression models was assessed with ANOVA. Level of significance for all tests was  $\alpha = 0.05$ .

Factor Profiling platform (JMP<sup>®</sup>) was utilized to explore and visualize estimated models, e.g. explore the shape of the response surface, find optimum settings of the factors and simulate response data.

To validate the models, the experimental values of  $T_{gel}$ ,  $G'$  and  $\eta^*$  of four optimal mixed P407/P188/CS systems were statistically compared to their predicted responses.

#### 4.2.5. Oscillatory rheological characterization – strain sweep, frequency sweep and gelation time testing

The viscoelastic behavior of *in situ* forming ophthalmic gels was investigated by strain (amplitude) sweep and frequency sweep test using the rheometer system with cone-and-plate (CP50, Figure 18) geometry with  $1^\circ$  incline. Gap of the measuring configuration was  $d = 0.05$  mm.

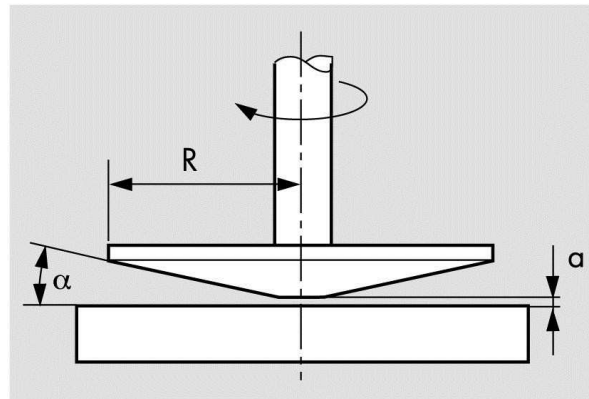


**Figure 18.** Cone and plate measuring system with a radius (R), gap a); and incline ( $\alpha$ ) (picture reprinted from (100)).

For strain sweep analysis, the angular frequency was set at 62.8 rad/s and the strain was varied from 0.001 to 1000 %. The linear viscoelastic range (LVE) at 35°C was identified as the region in which the moduli ( $G'$  and  $G''$ ) are independent of the strain.

For frequency sweep analyses strain was set at 1%, which was in the linear viscoelastic range, while the angular frequencies were in the range of 0.628-199 rad/s.

The evaluation of *in situ* forming ophthalmic gel under biorelevant conditions was performed by sample dilution with STF (40:7). The STF diluted samples were submitted to strain and frequency sweep analysis at 35°C.

Gelation time was determined as the time point at which intersection of the curves of measured  $G''$  and  $G'$  occurred (100). The samples were placed at rheometer plate preheated at 35°C. Strain (1%) was constantly in LVE range, while applied frequency was 1 Hz throughout the test.

#### **4.2.6. Rotational rheological characterization**

In order to study and compare dynamic viscosities of developed *in situ* forming gel formulations with commercially available ophthalmic products from US and EU market, rotational test with controlled shear rate (CSR) was developed and applied.

The same rheometer, Anton Paar Physica MCR 301 with cone plate (CP50, Figure 18) measuring system, Peltier element and special temperature isolated hood, as in oscillatory tests was used. Gap was  $d=0.05$  mm and angle  $1^\circ$ . Temperature was 35°C and samples were allowed to equilibrate for 5 minutes.

Viscosity profiles of samples in biorelevant conditions (diluted with STF 40:7) were measured in the shear rate range of  $0.1\text{s}^{-1} - 1000\text{ s}^{-1}$ . Similar measuring methodology was reported before (15).

#### **4.2.7. Sterilization**

Sterilization of selected *in situ* forming gel was evaluated by filtration and flitration and autoclaving. In case of sterilization by filtration samples were filtrated  $0.2\ \mu\text{m}$  through syringe filter (Spartan RC  $0.2\ \mu\text{m}$ ). Filtrated samples, placed in non-siliconized 20 ml (15 R) Type I clear glass vials sealed with Teflon 2 coated chlorobutyl rubber stoppers (Schott<sup>®</sup>), were sterilized by steam at 121°C for 20 minutes using Systec V-95 autoclave (Systec GmbH, Sandvsweg, Germany).

#### **4.2.8. Physical stability of samples at room temperature**

Selected samples of *in situ* forming gel placed in non-siliconized 20 ml (15 R) Type I clear glass vials sealed with Teflon 2 coated chlorobutyl rubber stoppers sterilized by filtration and filtration and autoclaving, as well as non sterilized control samples, were stored for 6 months at 25°C/60%RH. Key rheological properties, i.e.  $T_{gel}$  and  $(\eta^*)$  were evaluated and compared at initial and 6 months time point.

#### **4.2.9. *In vitro* release testing**

In vitro release (IVR) testing was performed using the Vision Microette (Hanson, Chatsworth, CA, USA), a commercial Franz diffusion cells apparatus equipped with six static vertical diffusion cell with 12 ml volume and 15 mm orifice (providing area for release of 1.767 cm<sup>2</sup>), an AutoFill sample collector and circulating water bath (Figure 19). Donor part of vertical cell consisted of open cell top with cap which is suitable for retaining less viscous liquids. Temperature was maintained at 35°C and stirring speed of 400 rpm assured homogenized sample in the receptor medium (STF). Sink conditions were assured. An aliquot of 2.5 ml of sample was placed on the testing membranes in donor compartment.

IVR testing of *in situ* formulations was performed during 24 hours. 1 ml of receptor medium was collected automatically at predetermined time intervals. System's rinsing volume was set at 1.5 ml to assure no carryover of an API prior each sampling point.

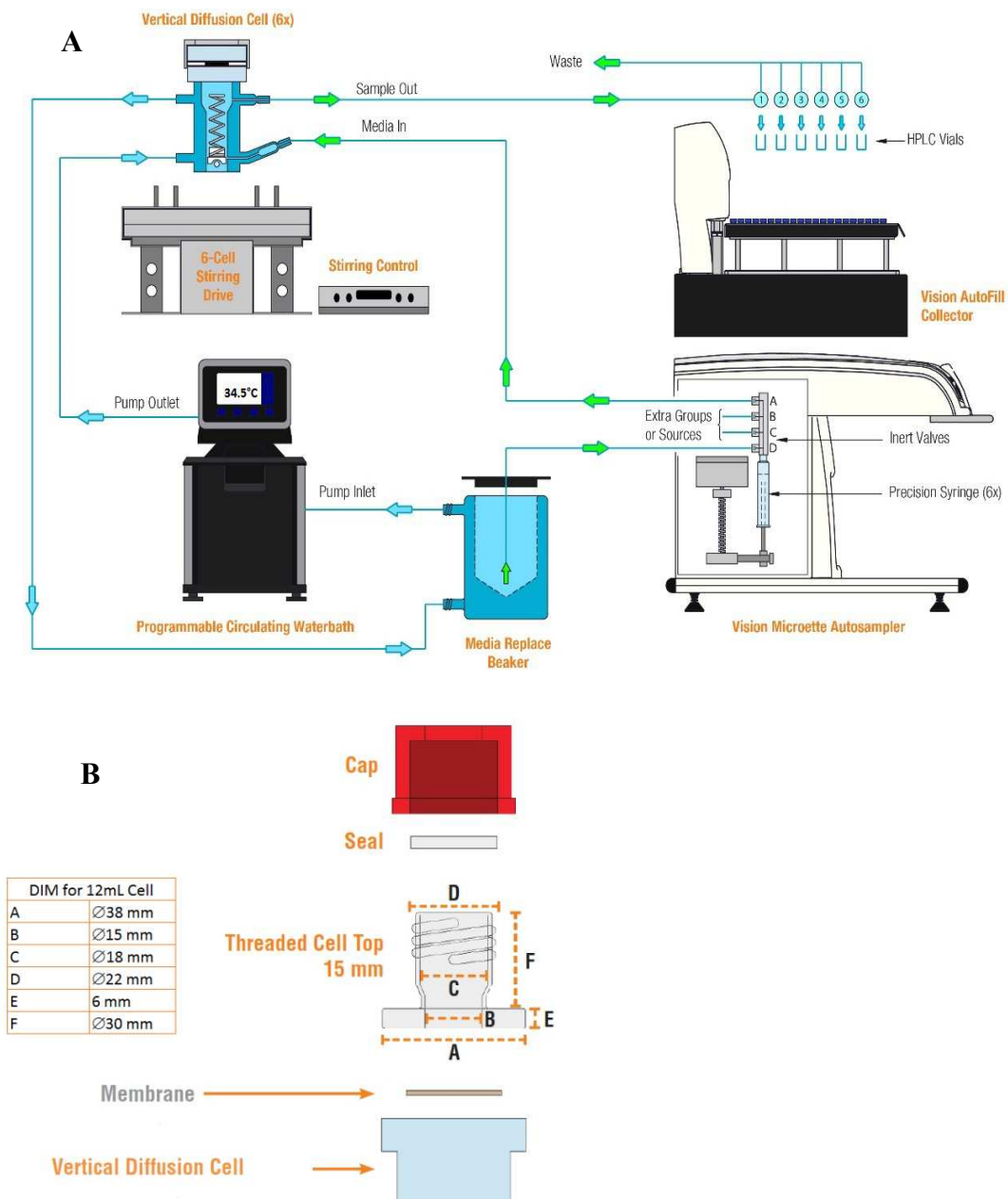


**Figure 19.** A) Franz diffusion cells apparatus used in IVR test (picture reprinted from (124)); B) Special top for less viscous fluids (picture reprinted from: (125)).

#### 4.2.9.1. Solubility testing and choice of IVR medium

Medium for IVR testing should provide sink conditions (126), meaning that medium volume should be 3-10 times the saturation solubility of the drug.

In order to evaluate the influence of different salts and buffers providing pH of solutions of 7.4 on API solubility, saturation solubility testing was performed in the following media:

1. Simulated tear fluid, STF
2. Krebs-Ringer buffer solution, KRB
3. 50 mM phosphate buffer, PB

API was added in the flasks containing 20 ml of corresponding medium. Flasks were sealed and placed on a thermostatic orbital shaker at 35°C (GFL® orbital shaker 3031, GFL Gesellschaft für Labortechnik GmbH, Burgwedel, Germany) and stirred at 75 min<sup>-1</sup> throughout 48 h. Testing was performed in triplicate for each tested medium. pH values were checked and, when needed, adjusted to 7.4 during the test.

Supernatants of saturated solutions were taken after 24 and 48 h and filtered through 0.2 µm filters (Spartan RC 0.2 µm, GE Healthcare Life Sciences, Freiburg, Germany), diluted with tested medium and analyzed by UPLC method.

#### 4.2.9.2. Membrane selection study

Five membranes summarized in Table 7 were evaluated for suitability for the IVR testing.

**Table 7.** Membranes in IVR study.

Membrane	pore size (µm)
regenerated cellulose (RC)	0.2
regenerated cellulose (RC)	0.45
polyethersulfone (PESU)	0.45
cellulose acetate (CA)	0.8
Hydrophilic polyethersulfone (PES)	0.1

Membranes were presoaked in the release medium for 12 hours before starting the test. Three tests were performed in order to choose the most suitable membrane. In the first, membranes

were screened for API adsorption at two concentration levels of API-solutions in STF (0.0801 mg/mL and 0.4005 mg/mL). API solutions were filtrated through the membranes; filtrated and non-filtrated solutions were analyzed by UPLC and ratio of their areas was calculated.

Secondly, influence of membranes on drug release from the *in situ* forming gel formulation was tested. Finally, for lead candidates, membrane's resistance to diffusion of drug from the API solutions in STF at two concentration levels (0.01 mg/mL and 2.5 mg/mL) was tested.

#### **4.2.9.3. Data presentation and statistical analysis**

For the purpose of statistical analysis for evaluation of discriminative nature of the developed IVR method, for each tested cell results were expressed as amount of drug released per membrane area ( $\mu\text{g}/\text{cm}^2$ ) versus the square root of time. The slope of the resulting line is a measure of the drug release rate.

For the purpose of this study, slopes of tested samples were calculated on at least five sampling points and samples were considered to be similar only if their slope ratios passed the first level acceptance criteria as described in the USP chapter <1724> (127,128).

For *the first stage* comparison of the batches, Mann-Whitney U test was used to calculate and evaluate the 90% confidence interval for the ratio of the slopes between the two batches (127). Each T (test sample) slope is compared to each R (reference sample) slope by calculating T/R slope ratios. If 6 cells for T and R batch are available, the 36 individual T/R ratios are then ordered from the lowest to the highest. The 8<sup>th</sup> and 29<sup>th</sup> T/R ratios represent the lower and upper limits of the 90% confidence interval for the ratio of test to reference release rates. To pass first stage testing, these ratios, when converted to percents by multiplying by 100, must be within the range of 75–133.33% (127,129).

#### **4.2.10. UPLC analyses**

Quantification of an API was done by ultra-performance liquid chromatography (UPLC). Three types of UPLC instruments were used: Agilent Infinity 1290 (Agilent, Santa Clara, CA, USA), Waters ACQUITY UPLC H and Waters ACQUITY UPLC I Class (Waters, Milford, MA, USA). Data were acquired and processed with the Empower 2 software (Waters, Milford, MA, USA).

The chromatographic separation was done on a Waters Acquity UPLC BEH Shield RP18 column (2.1x100mm, 1.7µm particle size) with the mobile phase consisting of 60% of 5 mM sodium acetate buffer (pH 4.5) and 40% ACN (v/v). Volume of injection was 5 µL and elution was isocratic. Sample temperature was maintained at 15°C, while column temperature was set at 50°C. Flow of the mobile phase was 0.6 ml/min and detection was done at 296 nm wavelength (Photodiode Array detector (PDA) was part of Waters systems and Diode Array (DAD detector) was used in the Agilent instrument).

For each sequence, standard solutions were prepared in duplicate and injected alternately. At least five standard solution injections were done in each injection sequence. System suitability was evaluated according to following criteria: relative standard deviation (RSD) of the detector response factor for all standard solution injections in the sequence is not more than 3.0%, and tailing factor of API peak is not more than 2.0.

#### **4.2.10.1. Validation of UPLC method**

The objective of validation of an analytical procedure is to demonstrate that it is suitable for its intended purpose (130). Validation of UPLC method for TIMO quantification was assessed by demonstration of specificity, linearity, accuracy, range, repeatability and standard/sample stability.

Specificity of developed method was performed by comparing chromatograms obtained with standard solution, sample solution, placebo solution, *in vitro* release medium, and mobile phase.

The linearity of an analytical method is its ability to elicit test results that are directly, or by a well-defined mathematical transformation, proportional to the concentration of analyte within a given range (130). The linearity study was designed to cover the range of about 1% to about 100% of the working concentration from IVR test. Evaluation was performed by injecting in duplicate standards spiked with P407 (14 %, w/w), P188 (2 %, w/w), NaCl (0.9%, w/w) and chitosan (0.3%, w/w) at seven concentration levels by in the range from 0.00516–0.05170 mg/ml.

The accuracy of a method expresses the closeness of agreement between true value (a reference value or a conventional true value) and the value found by analytical procedure. In practice this is related to the closeness of agreement between added (spiked) and found amount of analyte of interest (130). Method accuracy was evaluated through recovery experiment from the recovery



solutions prepared in triplicate for each level in the same concentration range as for linearity study (1%-100%).

Placebo solution containing P407 (14 % w/w), P188 (2 %, w/w), NaCl (0.9%, w/ w) and CS (0.3%, w/ w) was added to all recovery solutions. Each of three solutions, prepared for each of seven concentration levels, was injected once.

The concentration range for which the standard linearity and accuracy study met the acceptance criteria was taken as the range of the method.

Repeatability of UPLC method was established by relative standard deviation of injections of standard solutions.

The stability study was designed to evaluate the suitability of storing the standard and sample solutions at working and room temperature to ensure that they are sufficiently stable to complete the analysis within a reasonable time frame. The stability of the standard solution and sample solution was evaluated over an appropriate period of time (at least 24 hours) against freshly prepared standard solution.

#### **4.2.11. *In vitro* biocompatibility study**

The biocompatibility was assayed using corneal epithelial models based on the immortalized human corneal epithelial cell line (HCE-T) (RIKEN Cell Bank, Tsukuba, Japan). *In situ* forming gel was applied directly onto cell-based models. After the 30-minute treatment at 37°C, treated models were incubated at the room temperature for 5 minutes to induce formulation gel-sol transition. The cell surface was rinsed with Hank's balanced salt solution and exposed to air-liquid interface for the following 24 h. The cell viability was assessed by MTT test.

##### **4.2.11.1. Cell culture conditions**

HCE-T cells were cultivated in DMEM/F12 medium (Lonza, Basel, Switzerland) supplemented with fetal bovine serum (5%, Biosera, Boussens, France), insulin (5 µg/ml, Sigma-Aldrich), dimethyl sulfoxide (0.5%, Applichem), epidermal growth factor (10 ng/ml, Sigma-Aldrich) and penicillin/streptomycin/amphotericin B (Lonza) in a humidified atmosphere containing 5% CO<sub>2</sub> at 37 °C (48). The cells were subcultured at 80–90% confluence. The culture medium was changed every 48 h.

#### **4.2.11.2. Cultivation of the HCE-T cell-based model**

The HCE-T cell-based models were cultivated according to the protocol by (115). Briefly, Transwell<sup>®</sup> polycarbonate membrane cell culture inserts (0.4 and 3.0  $\mu\text{m}$  pore size, surface area 1.12  $\text{cm}^2$ , Corning B.V. Life Sciences, Amsterdam, The Netherlands) were coated with rat tail type I collagen (225  $\mu\text{g}/\text{well}$ ; Sigma-Aldrich) and human fibronectin (4  $\mu\text{g}/\text{well}$ ; Sigma-Aldrich). HCE-T cells were seeded onto the coated polycarbonate filter and were cultivated submerged in the medium until a sharp increase in transepithelial electrical resistance (TEER) was observed, after which they were exposed to the air-liquid interface (ALI) for the following 3 days. The culture medium was changed every 2 days during the submerged conditions and every day during exposure to the ALI.

#### **4.2.11.3. MTT Assay**

MTT assay was performed on the HCE-T cell-based models according to the protocol by Pauly et al. (131). The culture medium for basolateral compartment was aspirated, and the wells were transferred to a clean 12-well cell culture plate (Corning B.V. Life Sciences). The MTT (3-[4,5-dimethylthiazol-2-yl]-2,5-diphenyl tetrazolium bromide, Sigma-Aldrich) solution in culture medium (0.5  $\text{mg}/\text{ml}$ , 700  $\mu\text{L}$ ) was applied to both the apical and basolateral compartments, and the cells were incubated for 4 h at 37  $^{\circ}\text{C}$ . After the removal of the MTT solution, formazan crystals were dissolved by the addition of isopropanol (700  $\mu\text{L}$ ) to both compartments. The absorbance was measured at 570 nm by using microplate reader (1420 Multilabel counter VICTOR3, Perkin Elmer, Waltham, MA, USA).

## **5. RESULTS AND DISCUSSION**

## 5.1. *In situ* forming ophthalmic gel development and optimization using a Design of Experiments

QbD approach was applied in order to determine the minimal total concentrations of P407, P188 and CS that would yield an optimal *in situ* forming ophthalmic gel with the potential to ensure the defined formulation characteristics i.e.,  $T_{gel}$  in physiologically relevant range, storage modulus and complex viscosity which would provide controlled (prolonged) release of model drug, pseudoplastic flow behavior; which would preserve gel structure in biorelevant conditions and which would be robust against entrapment of drugs with diverse physicochemical properties.

For the establishment of the mathematical model, it was necessary to generate the data of  $T_{gel}$ ,  $G'$  and  $\eta^*$  of the sample based on the independent variables (Table 8). This was achieved by the temperature sweep test (Figure 20). In the first screening step of the applied sequential approach, influence of concentration levels of two factors (independent variables; P407 and P188 concentration) on  $T_{gel}$ ,  $G'$  and  $\eta^*$  (dependent variables) was tested. Selected independent variables were evaluated at their low, medium and high levels, which were selected based on the preliminary experiments. Based on the particular experimental conditions, a custom D-optimal design was applied to provide estimates for the effect testing with smallest standard errors, as it maximizes the information in the selected set of experimental runs with respect to a model stated (132). Two center points were included in the experimental runs to allow the testing for non-linear factor effects and estimation of the pure experimental error, and to increase the power of the experiment. A total of eight experimental runs were generated for the evaluation of the main effects and possible interactions. Accordingly, eight samples, varying in concentrations of P407 (10.59 – 19.1%, w/w) and P188 (0.8 – 7.66%, w/w) were prepared, and their  $T_{gel}$ ,  $G'$  and  $\eta^*$  were determined (Table 8). Collected data were analyzed, and significant cause-and-effect relationship was identified. Data set was expanded with the results of preliminary screening, consisting of five samples, which contain only P407 (11.4 – 19.3%, w/w)(1).

In the subsequent, refining step, CS concentration was added as an additional independent variable. Concentration ranges of factors P407 and P188 were selected based on the result

obtained in screening step, and CS concentration was evaluated in the range of 0.08 – 1.29% (w/w) based on the literature data (20,133).

D-optimal statistical design with one center point was applied. Nine experimental runs were required for analyzing the main effects and all second level interactions. Additionally, to evaluate error of mixed P407/P188/CS system preparation and measurement, three replicated runs were added to the experimental sequence (replicate step, Table 8). Based on this approach, three mathematical models were established, i.e.  $T_{gel}$ ,  $G'$  and  $\eta^*$  models, as the prerequisite for the optimization of *in situ* forming P407/P188/CS ophthalmic gel (1).

All prepared formulations had an ophthalmically acceptable osmolality, which was achieved by the addition of appropriate amounts of NaCl to the solution. Osmolality was determined by the freezing point depression method (Advanced® 3D3 Single-Sample Osmometer, Advanced Instruments Inc, Norwood, Massachusetts, USA). For CS free solutions it was in the range of 295.4 – 301.8 mOsm/kg, while for CS containing solutions it was in the range of 310.4 – 332.0 mOsm/kg. pH of tested systems was in the range of 5.8 for CS containing solutions to 6.5 for CS free solutions (1). The transparency of *in situ* forming ophthalmic gels was determined by measuring the refractive index and determined values of all systems were in the ophthalmically suitable range for eye drops (i.e. not greater than 1.476) (72).

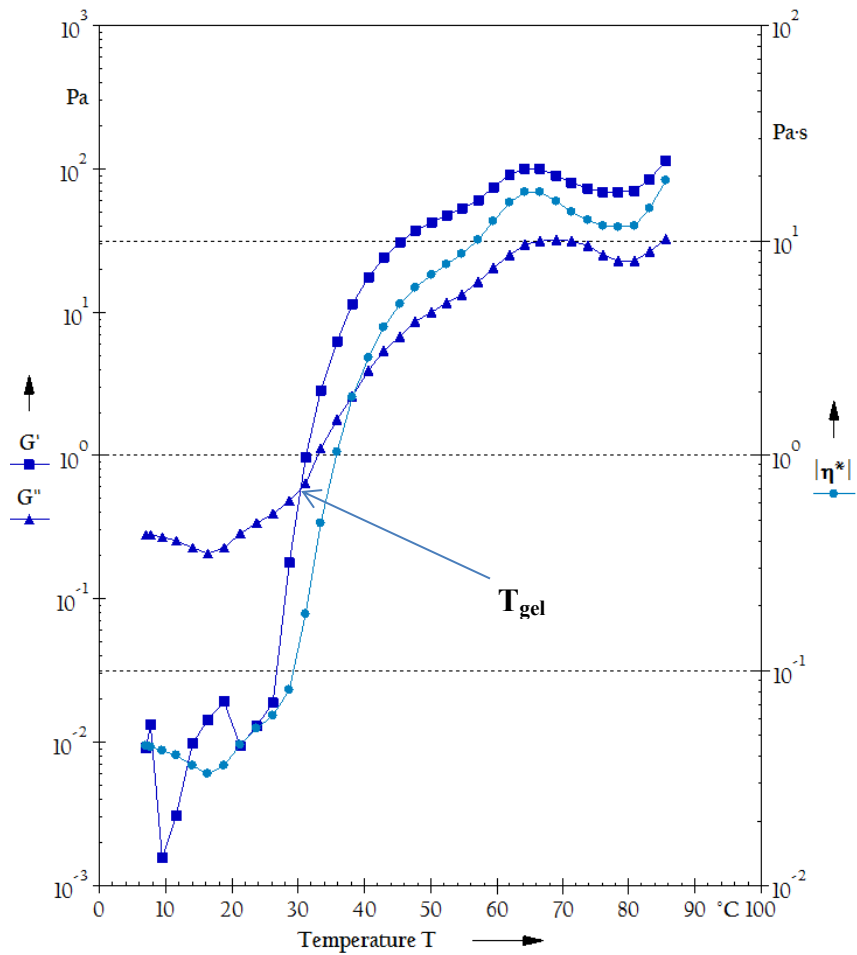


**Figure 20:** Typical temperature sweep profile of temperature responsive *in situ* forming gel ( $G'$ - squares,  $G''$ - triangles and  $\eta^*$  - circles).  $T_{gel}$  is marked with an arrow at intersection of  $G'$  and  $G''$  curves.

**Table 8.** Sample sequence from design of experiment (DoE) and corresponding experimental temperature of gelation ( $T_{gel}$ ), complex viscosity ( $\eta^*$ ), storage modulus ( $G'$ ) and damping factor ( $\tan\delta$ ), reprinted with permission from (1).

DoE	Sample*	P407	P188	CS	$T_{gel}$	$\eta^*$ <sup>1</sup>	$\log\eta^*$	$G'$ <sup>1</sup>	logG	Damping factor <sup>1</sup> ( $\tan\delta$ )	Form
		(%, w/w)	(%, w/w)	(%, w/w)	(°C)	(Pa·s)		(Pa)			
Preliminary screening	1o	11.4			<b>33.4</b>	<b>0.05</b>	-1.34	3.56	0.55	0.825	gel
	2o	13.8			<b>24.4</b>	<b>19.5</b>	1.29	119	2.08	0.259	gel
	3o	15.2			<b>24.3</b>	<b>702</b>	2.85	4320	3.64	0.206	gel
	4o	16.9			<b>20.7</b>	<b>1520</b>	3.18	9360	3.97	0.197	gel
	5o	19.3			<b>15.1</b>	<b>2430</b>	3.39	15200	4.18	0.101	gel
Screening	6•	11.32	0.87		<b>31.6</b>	<b>0.44</b>	-0.36	2.45	0.39	0.494	gel
	7•	19.1	0.8		<b>15.1</b>	<b>2370</b>	3.37	14700	4.17	0.142	gel
	8•	15.8	0.84		<b>22.5</b>	<b>277</b>	2.44	1660	3.22	0.315	gel
	9•	14.12	4.01		<b>29.8</b>	<b>2.17</b>	0.34	13.2	1.12	0.248	gel
	10•	14.61	4.24		<b>33.4</b>	<b>1.21</b>	0.08	7.01	0.85	0.413	gel
	11•	18.39	4.64		<b>22.5</b>	<b>131</b>	2.12	794	2.90	0.271	gel
	12•	10.59	7.4		<b>49.4</b>	<b>0.02</b>	-1.68	n.d.	n.d.	1E+30	solution
	13•	15.49	7.66		<b>35.1</b>	<b>0.48</b>	-0.32	4.3	0.63	0.685	gel
Refining step (addition of CS)	14•	16.4	0.85	0.08	<b>23.8</b>	<b>169</b>	2.23	975	2.99	0.425	gel
	15•	10.93	4.2	0.08	<b>52.5</b>	<b>0.02</b>	-1.61	0.0156	-1.81	9.46	solution
	16•	15.92	3.97	0.08	<b>31.1</b>	<b>7.77</b>	0.89	46.4	1.67	0.327	gel
	17•	13.61	2.51	0.66	<b>33.5</b>	<b>0.54</b>	-0.27	9.17	0.96	0.748	gel
	18•	11.16	0.95	1.29	<b>54.8</b>	<b>0.4</b>	-0.4	0.273	-0.56	9.09	solution
	19•	16.2	0.92	1.22	<b>26.3</b>	<b>26.2</b>	1.42	229	2.36	0.201	gel
	20•	10.8	4.18	1.25	<b>47.7</b>	<b>0.49</b>	-0.31	0.927	-0.03	3.14	solution
	21•	15.7	3.96	1.18	<b>33.5</b>	<b>3.32</b>	0.52	35.6	1.55	0.46	gel
	22•	11.31	0.89	0.1	<b>38.2</b>	<b>0.04</b>	-1.4	n.d.	n.d.	2.37	solution
Replicate step	23 (14) <sup>o</sup>	16.4	0.84	0.09	<b>23.9</b>	<b>1245</b>	3.1	7270.000	3.86	0.2745	gel
	24 (15) <sup>o</sup>	10.93	4.21	0.09	<b>52.4</b>	<b>0.02</b>	-1.63	0.029343	-1.53	12.4	solution
	25 (16) <sup>o</sup>	15.88	3.97	0.08	<b>31.1</b>	<b>2.36</b>	0.37	21.2	1.33	0.2935	gel

<sup>1</sup> $\eta^*$   $G'$  and  $\tan\delta$  at 35°C, determined by temperature sweep test (angular frequency and strain were 1 s<sup>-1</sup> and 1%, respectively);

n.d = not determined

## 5.2. The model of temperature of gelation

Within the established  $T_{gel}$  model, the response of interest is represented by following regression equation (1):

$$T_{gel} = 35.46 - 13.84 \times \overline{P407} + 6.70 \times \overline{P188} + 2.74 \times \overline{CS} + 7.07 \times \overline{P407} \times \overline{P188} + 9.16 \times \overline{P407} \times \overline{P188} \times \overline{CS} \quad (\text{Eq. 5})$$

where factors denoted as overlined represent centered factors, that are reduced by mean value and divided by the half of the factor range. This way of representation allows for easier interpretation of the regression results and comparison of regression coefficients (the magnitude of the factor effect). The obtained coefficient of determination between the experimental and predicted values of  $T_{gel}$  was  $R^2 = 0.93$  (Figure 21A).

Statistical analysis of the collected data revealed significant effects of P407, P188 and CS concentrations on the  $T_{gel}$  ( $p < 0.05$ ). The concentration effect impacts  $T_{gel}$  in following order: P407 (coefficient = -13.84) > P188 (coefficient = 6.70) > CS (coefficient = 2.74). The negative value of the coefficient indicates an inverse relationship between the factor (concentration) and the response ( $T_{gel}$ ), showing that increase of the P407 concentration will result in a decrease of  $T_{gel}$ . The positive value of the coefficient observed for P188 indicates that increasing the concentration of P188, shifts  $T_{gel}$  to higher values, as already reported in the literature (12,15). Similarly to P188, but to a lesser extent, the increase in CS concentration increases  $T_{gel}$ . Evidently, CS affects the onset of gelling but it does not interfere with the formation of *in situ* gel, thus, making it a suitable additive in this mixed poloxamer system (1). In the similar concentration range, CS was already shown not to induce marked changes in the  $T_{gel}$  of poloxamer systems (20).



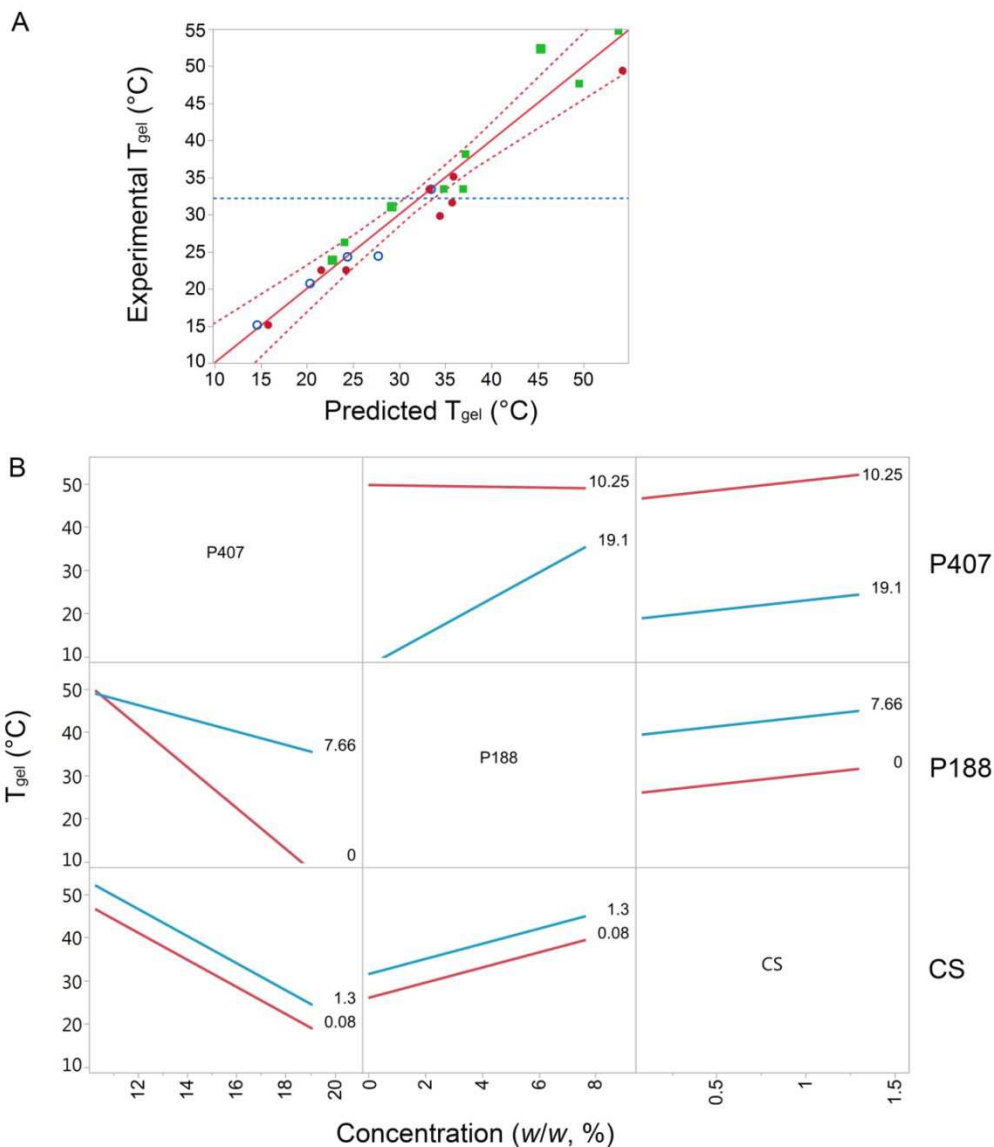


**Figure 21.** A) Experimental vs. predicted values of  $T_{gel}$ . B) Interaction profiles for  $T_{gel}$ . Factors at the borders of the concentration range tested. Red lines: lower limits of the tested concentration range (P407 10.25, P188 0, CS 0.08%, w/w); blue lines: upper limits of the tested concentration ranges (P407 19.1, P188 7.66, CS 1.3%, w/w), reprinted with permission from (1)

Significant higher order terms include the interaction between P407 and P188 (coefficient = 7.07) and the interaction among P407, P188 and CS (coefficient = 9.16). These interactions show that the effect of one factor may vary depending on the level of the other factor. P407 and P188 interaction profile suggests that the impact of P407 on the  $T_{gel}$  decrease is more pronounced at the

lower level of P188 (Figure 21B). At the other side, higher level of P407 assures more pronounced effect of P188 on the  $T_{gel}$  increase. Parallel lines on the Figure 21B indicate lack of significant interactions at lowest and highest concentration levels of the independent variables (i.e. P407 and CS, P188 and CS) (1).

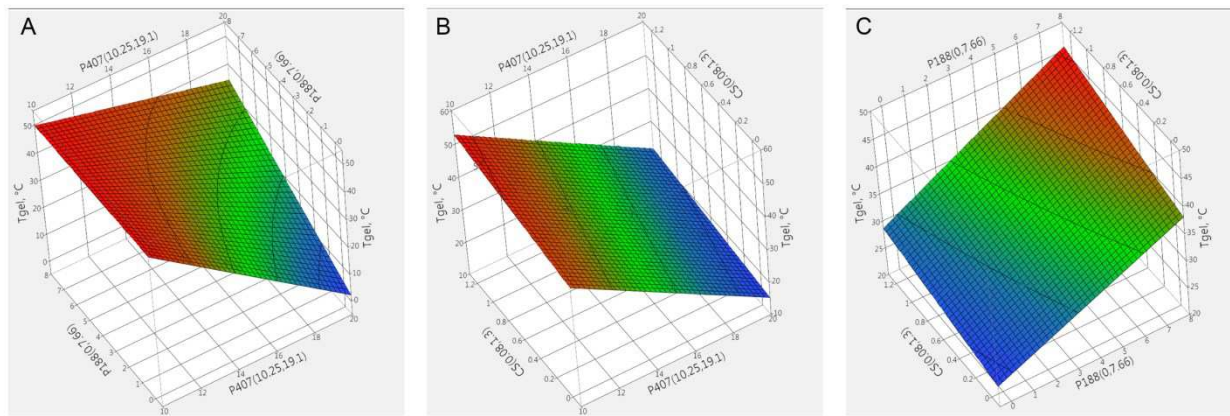


**Figure 22.** Response surface of the effects of the concentration of P407, P188 and CS on the  $T_{gel}$ . A) The 3-D response surface plot at varying concentration of P407 (10.25 – 19.1 %, w/w) and P188 (0 – 7.66 %, w/w). B) The 3-D response surface plot at varying concentration of P407 (10.25 – 19.1%, w/w) and CS (0.08 – 1.30%, w/w). C) The 3-D response surface plot at varying concentration of P188 (0 – 7.66%, w/w) and CS (0.08 – 1.30%, w/w), reprinted with permission from (1).

The response surface and contour plots shown in Figure 22 are three-dimensional feature of Figure 21B, depicting relationship of the independent variables on the response. As it can be seen in the Figs. 21B and 22A, relationship of the P407 and P188 on  $T_{gel}$  is not a straightforward. Curvatures shown on the Fig. 22A indicate that this relation is not linear (1).

These interactions reveal the complexity of interplay of the components in the measured mixed systems. This complexity of interplay is highly related to the concentration of P188 in the system as suggested by Zhang et al. who revealed the formation of two distinct populations of micelles in mixed P407/P188 systems, depending on the concentrations of polymers, as presented on the Figure 23 (12). They suggested that P188 micellization was responsible for the  $T_{gel}$  increase (Figure 23).

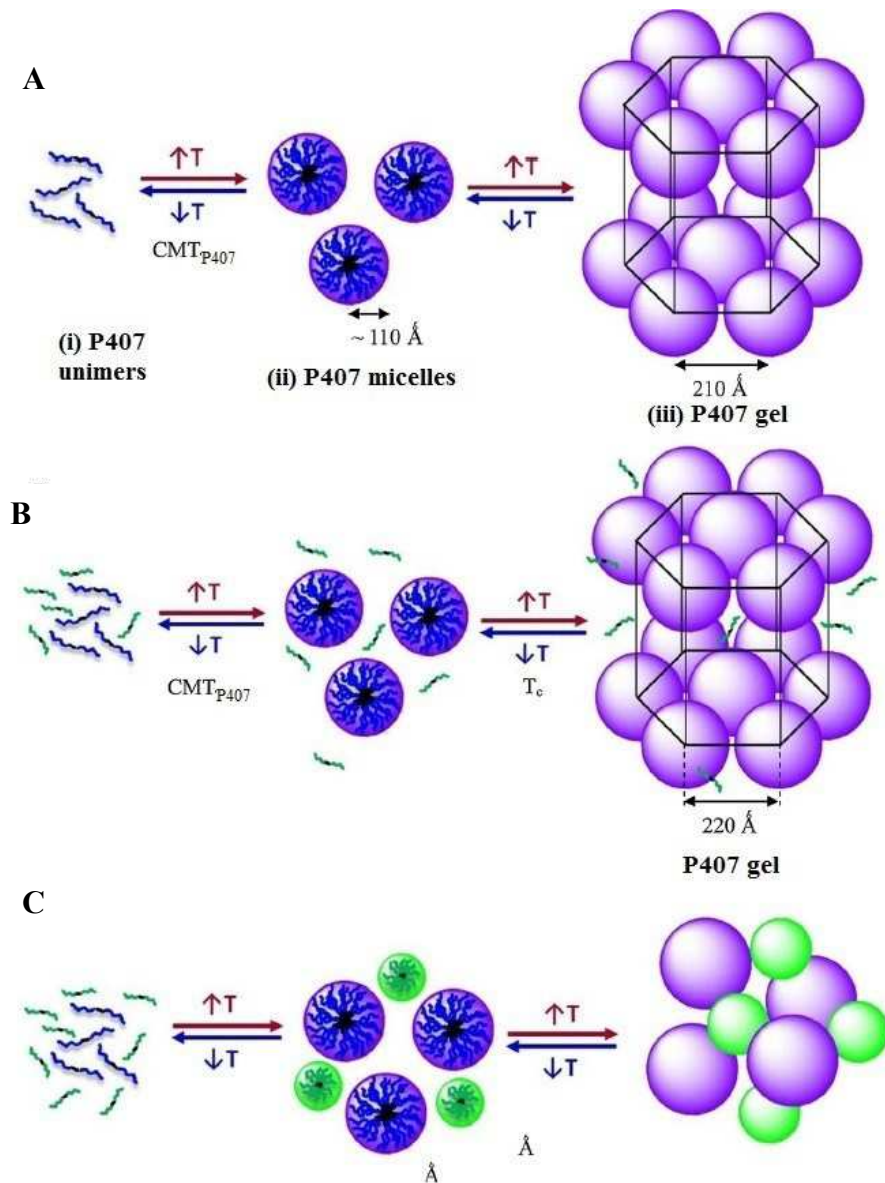


**Figure 23.** A) Proposed mechanism for micelle organization P407 (at concentration levels of 20, 17 and 16%,  $w/w$ ). B) Proposed mechanism for micelle organization for mixed solutions of P407/P188 (at 19/1, 18/2 and 17/3, %  $w/w$ ). Micellization of P188 may also occur in the segregated mixtures. The crystalline P407 phase is predominant at high temperature. C) Proposed mechanism for micelle organization for mixed solution of P407/P188 (at 10/10 and 5/15, %  $w/w$ ) when P188 concentrations were higher than the CMC in the range of investigated temperature (picture modified and reprinted with permission from (12)).

### 5.3. Models of rheological properties: complex viscosity and storage modulus

Critical attribute that determines the dosing accuracy, retention time, and drug release from *in situ* forming ophthalmic gels is formulation rheological behavior. The systems with fine-tuned rheological properties would withstand the high shear rates and tear dilution thus preventing the drainage of an API from the site of the absorption (5)

Oscillatory rheological tests provide insight into the gel microstructure. Complex viscosity is described by the ratio of the complex modulus  $G^*$  and the angular frequency  $\omega$  (100).

$$\eta^* = \frac{G^*}{\omega} \quad (\text{Eq. 6})$$

Complex modulus consists of two parts -  $G'$  and  $G''$  and their relationship is described via Pythagoras theorem (100):

$$|G^*| = \sqrt{G'^2 + G''^2} \quad (\text{Eq. 7})$$

Consequently, this relation is similar for the complex viscosity:

$$|\eta^*| = \sqrt{\eta'^2 + \eta''^2} \quad (\text{Eq. 8})$$

Complexity of this term comes from the fact that it is combination of its real part depicting viscous behavior ( $\eta'$ ) and imaginary part ( $\eta''$ ) which represents elastic behavior (100).

#### 5.3.1. The model of complex viscosity

Influence of different P407, P188 and CS concentration levels on the measured  $\eta^*$  at 35°C and angular frequency of  $1\text{s}^{-1}$  (6.28 rad/s) was investigated and mathematically described. Prior to the statistical analysis,  $\eta^*$  data were checked for normality. It was confirmed by Kolmogorov test that data follows the log-normal distribution. Thus, log transformation was applied on the measured  $\eta^*$  data (1).

In this mathematical approach, the response of interest [ $\log(\eta^*)$ ] is represented by following regression equation:

$$\log(\eta^*) = -0.37 + 1.53 \times \overline{P407} - 1.60 \times \overline{P188} - 0.55 \times \overline{P407} \times \overline{P188} - 0.76 \times \overline{P407} \times \overline{CS} + 0.70 \times \overline{CS} \times \overline{CS} + 1.56 \times \overline{P407} \times \overline{P407} \times \overline{P188} \quad (\text{Eq. 9})$$

Developed  $\eta^*$  model shows good fit between experimental and predicted logarithmic values of  $\eta^*$  with resulting coefficient of determination  $R^2 = 0.97$  (Figure 24A).

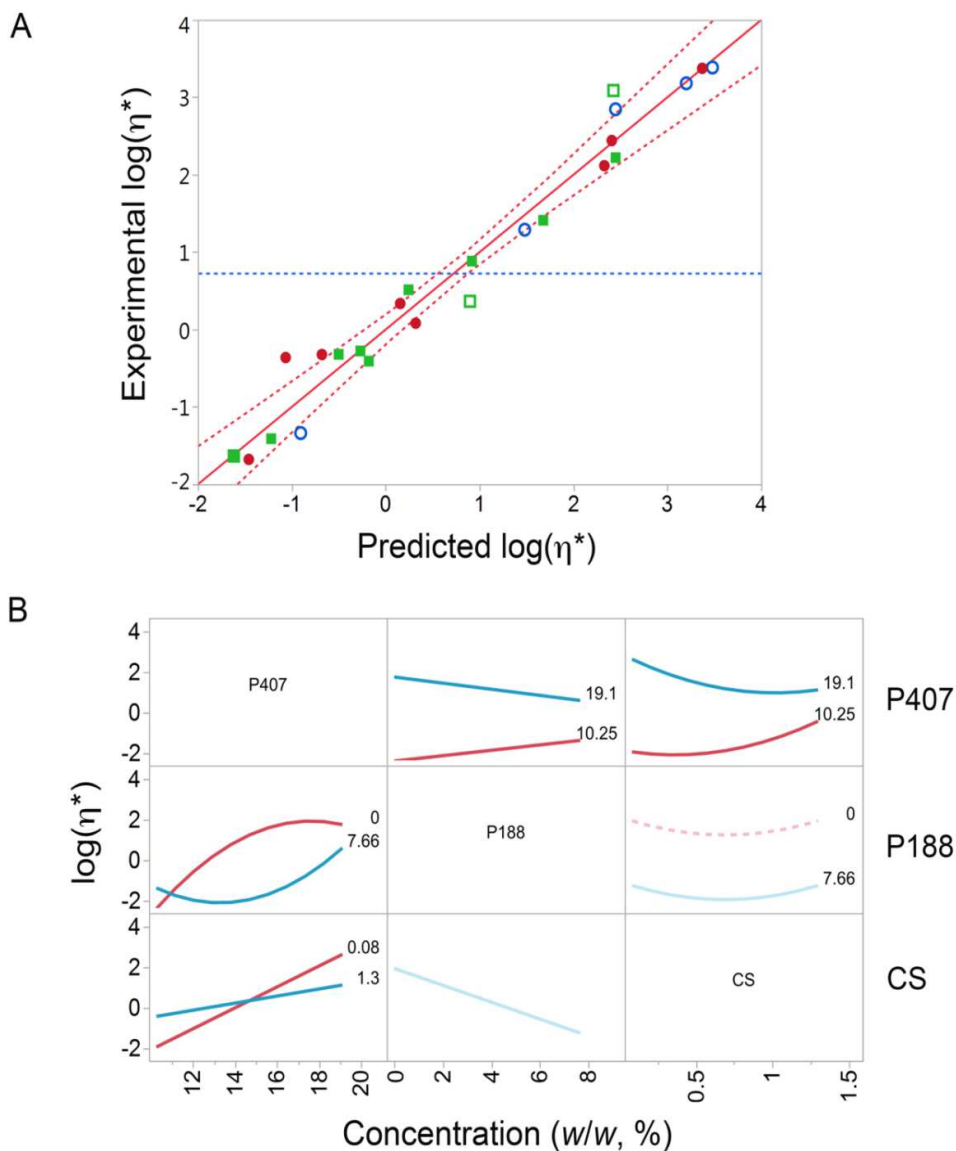


**Figure 24.** A) Experimental values vs. predicted values of  $\log(\eta^*)$ . B) Interaction Profiles for  $\log_{10}(\eta^*)$ . Factors at the borders of the concentration range tested. Red lines- lower limits of the tested concentration range (P407 10.25, P188 0, CS 0.08%, w/w); blue lines: upper limits of the tested concentration ranges (P407 19.1, P188 7.66, CS 1.3%, w/w), reprinted with permission from (1).

Statistical analysis of the collected data revealed significant effects of P188 and P407 concentrations on  $\log(\eta^*)$  ( $p < 0.05$ ). The increase of P188 concentration results in the decrease of  $\log(\eta^*)$  as revealed by its negative coefficient (coefficient = -1.60). On the contrary, the increase

of P407 concentration results in the increase of  $\log(\eta^*)$  (coefficient = 1.53). The complexity of interactions is noticed on the response surface and contour plots of P407 and P188 (Figure 25A) and P407 and CS (Figure 25 B), while less complex relationship is noticed for P188 and CS on the response (Figure 25 C; which is in agreement with the linear lines on the Figure 24B ). Namely, the interaction between P407 and CS (coefficient = -0.76) as well as between P407 and P188 (coefficient = -0.55) was observed. Concomitantly, two higher order terms were found with the positive effect on the response, namely the interaction among P407, P407 and P188 (coefficient = 1.56) and CS and CS (coefficient = 0.70) (1).

At higher level of P188, the effect of P407 on increase of  $\log(\eta^*)$  is less pronounced (Figure 25B). In contrary, the omission of P188 from the system results in faster increase of  $\log(\eta^*)$  when increasing P407 concentration (1).

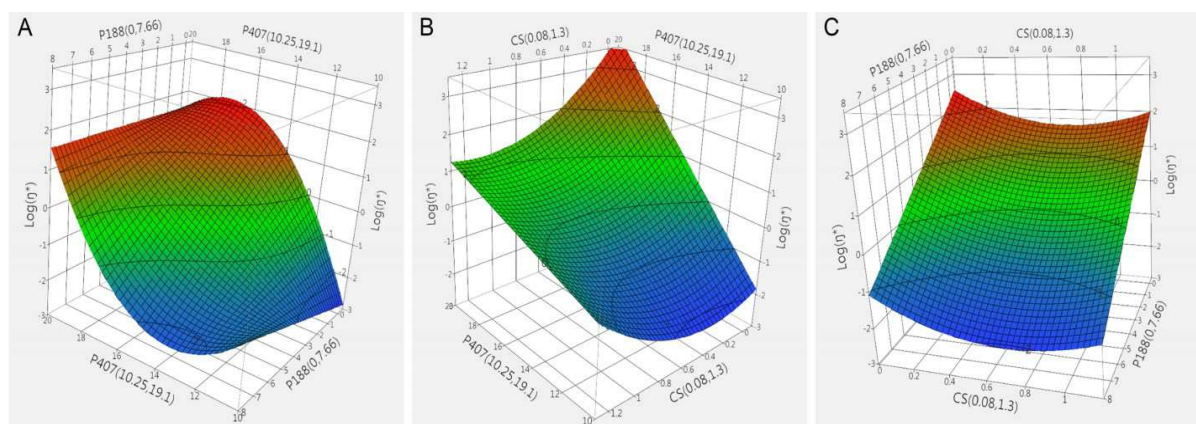


**Figure 25.** Response surface of the effects of the concentration of P407, P188 and CS on the  $\log(\eta^*)$ . A) The 3-D response surface plot at varying concentration of P407 (10.25 – 19.1%, w/w) and P188 (0 – 7.66%, w/w). B) The 3-D response surface plot at varying concentration of P407 (10.25 – 19.1%, w/w) and CS (0.08 – 1.30%, w/w). C) The 3-D response surface plot at varying concentration of P188 (0 – 7.66%, w/w) and CS (0.08 – 1.30%, w/w), reprinted with permission from (1).

CS and P407 interaction profile suggests that the impact of P407 on the  $\log(\eta^*)$  increase is more pronounced at the lower level of CS (Figure 24B). Similarly to the data presented on the Figure 24B, complexity of interactions is noticed on the response surface and contour plots of P407 and P188 (Figure 25A) and P407 and CS (Figure 25B), while less complex relationship is noticed for P188 and CS on the response; which is depicted by the linear lines on the Figure 24B

and Figure 25C. As it can be seen by comparing the response surface and contour plots images of the  $T_{gel}$  model and  $\log(\eta^*)$  model (Figure 22 and Figure 25), higher degree of complexity, i.e. curvatures, was found in the  $\log(\eta^*)$  model. This indicated the absence of linear relationship between the concentrations of three tested polymers to a response (1).

### 5.3.2. The model of storage modulus

As for the model of  $\log(\eta^*)$ , influence of different independent variables (P407, P188 and CS concentration levels) on the measured response  $G'$  at 35°C and angular frequency of  $1s^{-1}$  was tested and mathematically described. Again, Kolmogorov test confirmed that data follows the log-normal distribution, therefore log transformation was applied on the measured  $G'$  data (1).

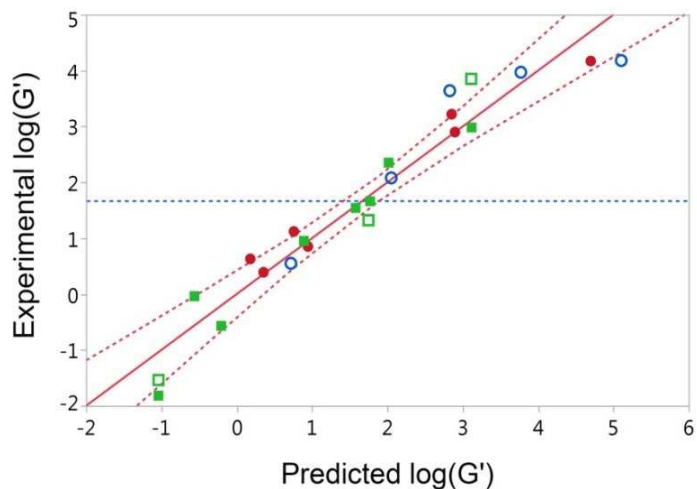
Log ( $G'$ ) is described by following regression equation (1):

$$\log(G') = 1.13 + 2.16 \times \overline{P407} - 0.77 \times \overline{P188} - 0.26 \times \overline{P407} \times \overline{CS} + 0.56 \overline{P188} \times \overline{CS} \quad (\text{Eq. 10})$$

Developed log ( $G'$ ) model exhibits suitable fit between experimental and predicted logarithmic values of  $G'$  with resulting coefficient of determination  $R^2 = 0.93$  (Figure 26A) (1).



A



B

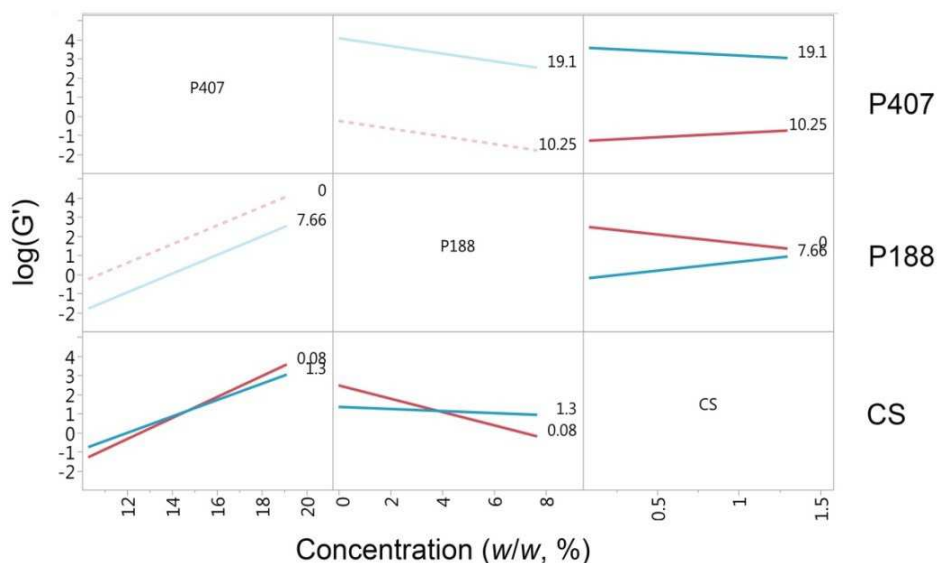


**Figure 26.** A) Experimental values vs. predicted values of  $\log(G')$ . B) Interaction Profiles for  $\log(G')$ . Factors at the borders of the concentration range tested. Red lines-lower limits of the tested concentration range (P407 10.25, P188 0, CS 0.08%, w/w); blue lines: upper limits of the tested concentration ranges P407 19.1, P188 7.66, CS 1.3%, w/w), reprinted with permission from (1).

Statistical analysis of the acquired data revealed significant effects of P407 and P188 concentrations on  $\log(G')$  ( $p < 0.05$ ), with P407 concentration having stronger effect on the response. As expected, similarly to model for  $\log(\eta^*)$ , the increase of P188 concentration results



in the decrease of  $\log(G')$  due to its negative coefficient (coefficient = -0.76). On the contrary, the increase of P407 concentration results in the increase of  $\log(G')$  (coefficient = 2.16) (1).

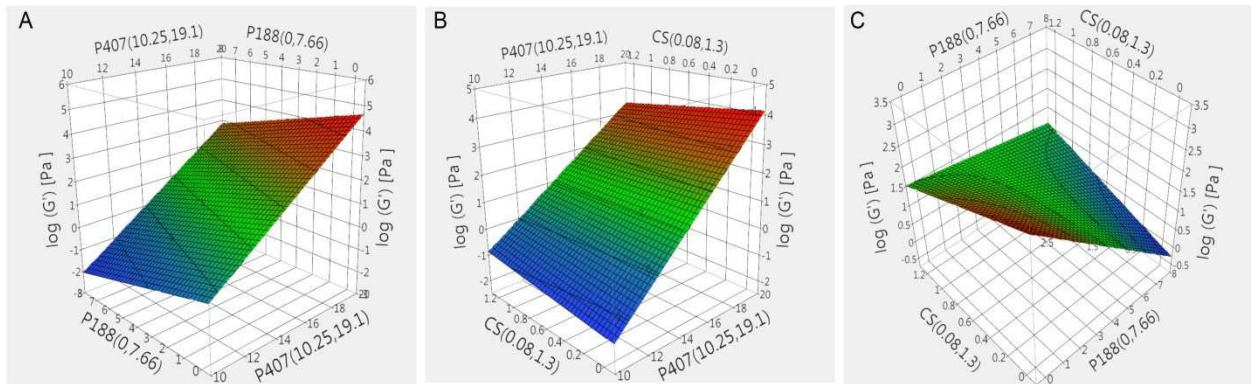


**Figure 27.** Response surface of the effects of the concentration of P407, P188 and CS on the  $\log(G')$ . A) The 3-D response surface plot at varying concentration of P407 (10.25 – 19.1 %, w/w) and P188 (0 – 7.66 %, w/w). B) The 3-D response surface plot at varying concentration of P407 (10.25 – 19.1 %, w/w) and CS (0.08 – 1.30 %, w/w). C) The 3-D response surface plot at varying concentration of P188 (0 – 7.66 %, w/w) and CS (0.08 – 1.30 %, w/w), reprinted with permission from (1).

As seen on the Figure 27 (A; B) relation between P407 and P188 and P407 and CS on the response in model appears to be relatively simple. More complex relation of P188 and CS on the  $\log(G')$  was found to be statistically significant interaction with positive effect on the dependent variable (coefficient = 0.56) (Figure 27C) (1).

Figure 26B (2D view of the Figure 27) shows that the increase of P188 at lower level of CS results in decrease of  $\log(G')$ , while this effect is not observed when CS is at highest level (1.3%, w/w). The increase in CS at low level of P188 lowers the response of interest. However, this effect is opposite at higher level of P188 (7.66%, w/w) (1).

Another interaction included in the model, but with no statistical significance, was interaction between P407 and CS having a negative impact on the response (coefficient = -0.26). Same interaction with significant negative effect was noticed in the model for  $\log(\eta^*)$  (1).

#### 5.4. Selection of rheologically improved *in situ* forming ophthalmic gel

$T_{gel}$  of innovative ophthalmic *in situ* forming gels is the most critical parameter related to efficacy and safety as well as patient compliance since it influences the accuracy of dosing, (dis)comfort associated with the instillation and residence time at the eye surface. Namely, if the system gels at room temperature, dosing would be hindered. Storage at low temperature would diminish this problem, however, the instillation of cold formulation can possibly be irritating and painful. Therefore, the optimal  $T_{gel}$  of *in situ* forming ophthalmic gel should be between 25°C, the average ambient temperature, and 35°C, the eye surface temperature (20). In this study, the optimal range of  $T_{gel}$  was set to 28 – 32 °C (1).

Viscosity is one of the key attributes for innovative ophthalmic *in situ* forming gels defining the residence time at the eye surface and drug release profile. The optimal range of viscosity is much more difficult to select in relation to  $T_{gel}$ . A wide range of viscosities reported for poloxamer-based *in situ* forming ophthalmic gels have suitable *in vivo* response (7,14,20). Therefore, we characterized the commercially available *in situ* forming ophthalmic gels with rotational test with controlled shear rate to enable the recognition of leading candidates. Oscillatory tests of selected leading candidates revealed the lower limit for  $\eta^*$  (at 35°C and 1s<sup>-1</sup>) at 1.2 Pa × s (1).

$G'$  presents the elastic behavior of a sample and it assures adequate gel stability. As minimal  $G'$  values for gel structures are around 5 Pa (100), this value was set as minimal value for this dependent variable.

Considering the optimal  $T_{gels}$ ,  $G'$  and  $\eta^*$  suggested by corresponding models, four mixed P407/P188/CS systems were selected (Table 9). The additional criterion of the selection was the lowest possible total polymer content in *in situ* forming ophthalmic gel. To validate the data obtained by the models, mixed P407/P188/CS systems were prepared.  $T_{gel}$ ,  $G'$  and  $\eta^*$  were determined by temperature sweep test and compared with predicted values (Table 9) (1). Furthermore, damping factor ( $\tan\delta$ ) factor was obtained in these measurements and values lower than 1 for all samples at 35°C, indicate presence of gel state (100).

**Table 9.** Selected mixed P407/P188/CS systems, corresponding experimental and predicted temperature of gelation ( $T_{gel}$ ), complex viscosity ( $\eta^*$ ), storage modulus ( $G'$ ) and dumping factor ( $\tan\delta$ )<sup>1</sup>, reprinted with permission from (1).

Sample	P407 (%, w/w)	P188 (%, w/w)	CS (%, w/w)	Exp. $T_{gel}$ (°C)	Pred. $T_{gel}$ (°C)	$T_{gel}$ recovery (%)	Exp. $\log(\eta^*)$ <sup>1</sup>	Pred. $\log(\eta^*)$	$\log(\eta^*)$ recovery (%)	Exp. $\log(G')$ <sup>1</sup>	Pred. $\log(G')$	$\log(G')$ recovery (%)	Damping Factor ( $\tan\delta$ )
<b>PL1</b>	14.2	1.7	0.25	31.10 ± 0.01	31.27 (29.72-32.82)	99.5	0.32 ± 0.06	0.62 (0.28-0.96)	52.4	1.15 ± 0.17	1.50 (1.26-1.74)	76.6	0.29 ± 0.03
<b>PL 2</b>	15.0	2.0	0.5	26.30 ± 0.01	28.87 (27.00-30.74)	109.77	0.81 ± 0.06	0.60 (0.06-1.14)	73.8	1.60 ± 0.06	1.75 (1.48-2.02)	91.5	0.21 ± 0.00
<b>PL3</b>	14.2	1.7	1.01	29.90 ± 1.7	35.30 (32.45-38.15)	118.06	0.66 ± 0.02	0.53 (0.09-0.97)	80.2	1.44 ± 0.09	1.18 (0.74-1.62)	122.4	0.26 ± 0.01
<b>PL4</b>	14.2	1.7	0.5	28.70 ± 0.01	32.60 (30.90-34.30)	113.59	0.61 ± 0.09	0.30 (-0.23-0.83)	48.9	1.40 ± 0.02	1.42 (1.14-1.70)	98.5	0.23 ± 0.01

Exp., experimental, presented as mean ± SD

Pred., predicted, presented as mean; values in brackets represent lower and upper limits of 95% confidence interval

<sup>1</sup> $\eta^*$  (Pa × s) and  $G'$  (Pa) at 35°C determined by temperature sweep test (angular frequency and strain were 1 s<sup>-1</sup> and 1 %, respectively)

High coefficient of determination ( $R^2 = 0.93$ ) and the overall recovery of experimental to predicted  $T_{gel}$  ( $110.23 \pm 0.08\%$ ; relative standard deviation (RSD) = 7.02%) confirmed the suitability of  $T_{gel}$  model. Similar agreement was found for  $\log(G')$  model ( $R^2 = 0.93$ ) with the average recovery of experimental to predicted of  $97.25 \pm 19.07\%$ , having slightly higher variability (RSD = 19.61%) (1). In case of  $\log(\eta^*)$  model, even better coefficient of determination ( $R^2 = 0.97$ ) was observed, and despite the lower overall recovery of experimental to predicted  $\log(\eta^*)$  ( $63.83 \pm 0.16\%$ ; RSD = 24.3%), the developed model enabled the development of mixed P407/P188/CS system with targeted viscosity ( $> 1.2 \text{ Pa} \times \text{s}$ ) (1). The higher variability of this model could be related to the heating rate-dependent kinetics of gel formation. Mixed P407/P188 systems exhibit very complex rheological behavior with internal relaxations and slow reorganizations taking place in the temperature range preceding or following the  $T_{gel}$  (Figure 23) (12). However, when ophthalmic *in situ* forming gel is applied, formulation is quickly spreaded throughout the surface of the eye and actually dramatic and the fast temperature change from room temperature (storage condition) to biologically relevant temperature is occurring *in vivo*.

#### **5.4.1. In depth rheological characterization of *in situ* forming ophthalmic gel – oscillatory tests**

In depth rheological characterization of selected mixed P407/P188/CS systems structure was performed by oscillatory rheological tests.

Oscillatory tests explore the viscoelasticity of a sample providing a microstructural fingerprint that can be used to quantify stability and to sensitively refine critical aspects of product performance (103).

Mixed P407/P188/CS systems are viscoelastic materials and they are showing viscous and elastic behavior simultaneously. Depending on their rheological behavior, viscoelastic liquids differ from viscoelastic solids. Namely, as mentioned previously, viscoelastic solid materials (such as gels) have a phase angle ( $\delta$ ) between 0 and  $\pi/2$  radians (0 and  $90^\circ$ ) and consequently  $\tan\delta$  (dumping factor, loss tangent)  $< 1$  (100).

Two types of oscillatory tests were used to characterize developed mixed systems - strain and frequency sweep analyses. In the strain sweep test oscillation is performed at variable amplitudes, while the frequency and temperature are kept at a constant value. These tests are carried out to

determine the limit of LVE range, i.e. the range where stress ( $\tau$ ) is directly proportional to strain ( $\gamma$ ); and to evaluate mechanical spectra ( $G'$  and  $G''$ ) (100).

Strain sweep analysis of developed mixed P407/P188/CS systems at 35°C are presented on the Figure 28.

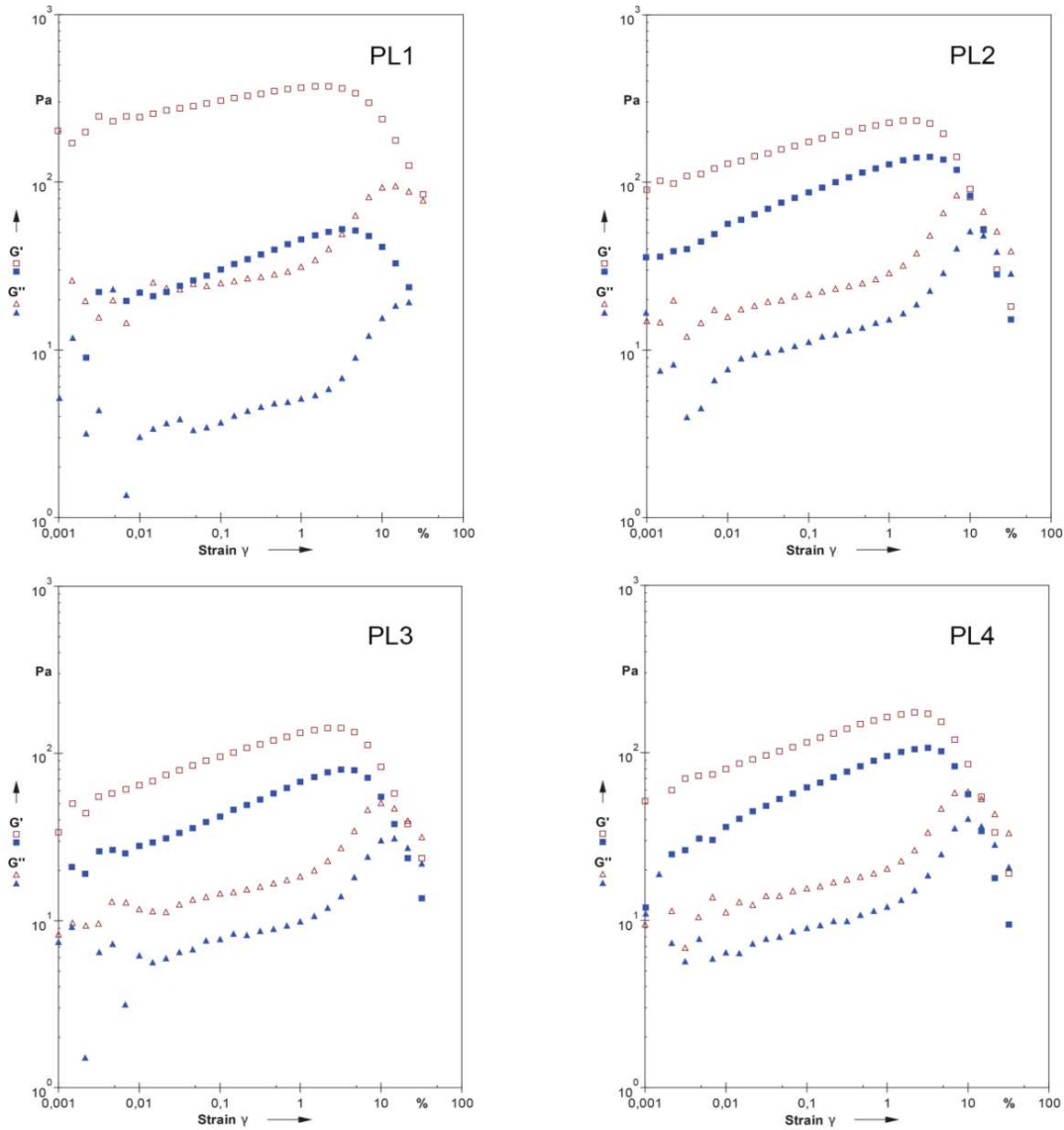


**Figure 28.** Strain sweeps (shear strain amplitude sweep) with controlled shear deformation (CSD) of selected mixed P407/P188/CS systems (PL1, PL2, PL3 and PL4) before (empty symbols, red) and after (filled symbols, blue) dilution with simulated tear fluid (STF). Storage modulus ( $G'$ ) is represented by square while loss modulus ( $G''$ ) by triangle.

Analyzing the data obtained by strain sweep studies, a typical gel-like behavior is observed, with the LVE range being maintained up to almost 3% of applied strain (Figure 28). For all samples,  $G'$  is significantly higher than  $G''$ , indicating that at 35°C elastic character of the sample is dominant and gel structure is present.

After determination of LVE of the samples, developed mixed P407/P188/CS systems were subjected to the frequency sweep analysis, which gave an insight on the behavior of  $G'$ ,  $G''$  and  $\eta^*$  as a function of angular frequency, while strain ( $\gamma$ ) is kept constant in the previously determined LVE range. Frequency sweep analysis provides information about a time dependant behavior of samples. Short term behavior is simulated by rapid motion (high frequencies), while long term behavior is simulated by low frequencies (100).

Frequency sweep measurements for all four mixed P407/P188/CS systems indicated that  $G'$  was higher than  $G''$  revealing suitable gel stability (Figure 29). Moreover, the presented rheological profile suggests the existence of soft gels known to be formed at moderate poloxamer concentration (134). This phenomenon has been ascribed to the weak attraction of spherical micelles as the solvent becomes poorer on heating.

To determine the influence of CS on the gel mechanical strength, frequency sweep analysis was carried out also for the respective control systems without CS (Figure 29). As expected, the presence of CS in mixed systems resulted in higher  $G'$  and  $G''$  values indicating increased gel mechanical strength (1). It was already suggested that the elastic characteristic of the system increased owing to an effect on microscopic diffusion within gel structure which facilitated the accommodation of unbound water and consequently micelle packaging (20).

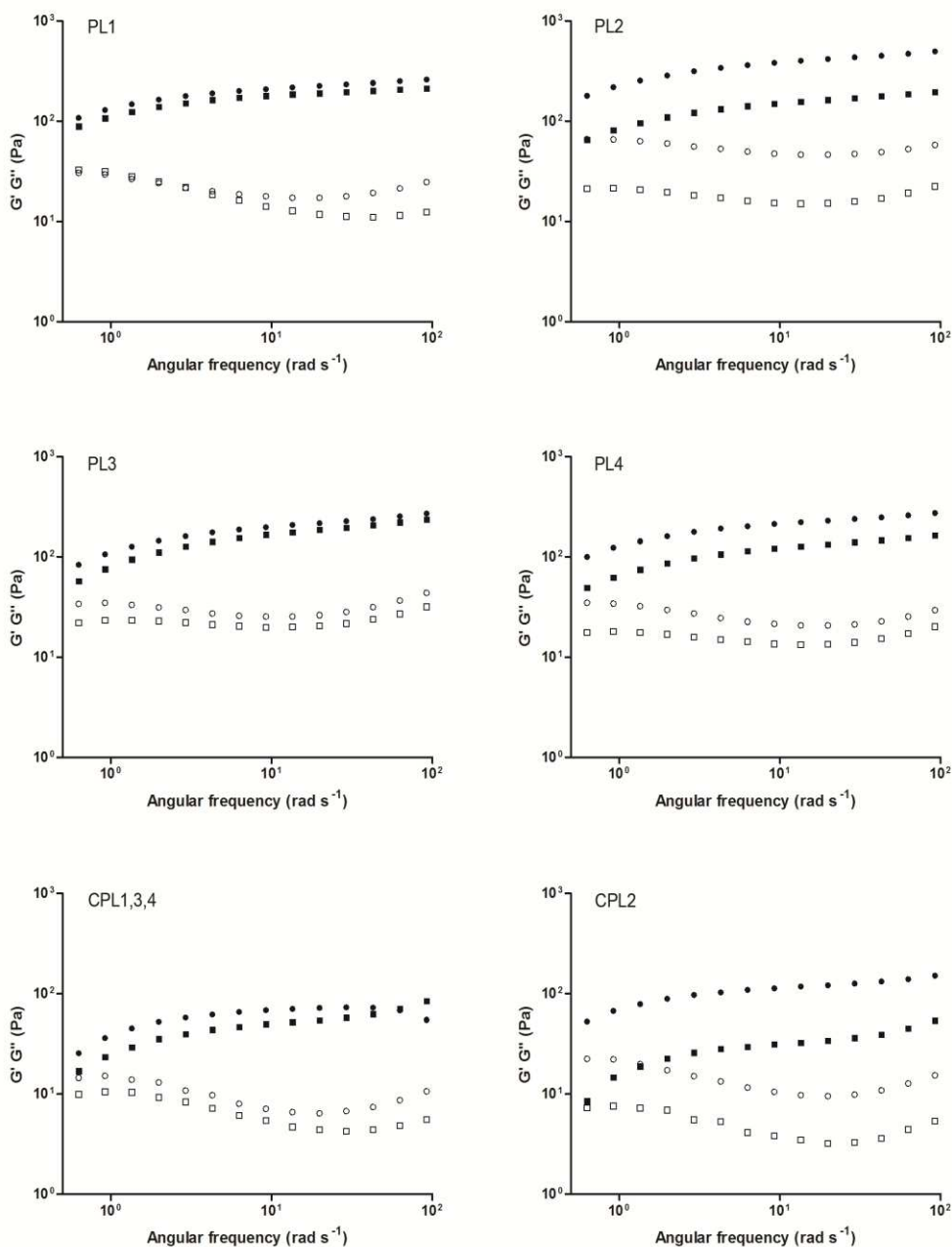


**Figure 29.** Rheological properties of selected mixed P407/P188/CS systems (PL1, PL2, PL3 and PL4) and respective controls under biorelevant conditions. Frequency sweeps analysis before (circles) and after (squares) dilution with STF: 40:7 at 35°C.  $G'$  filled symbols,  $G''$  empty symbols. Control sample for PL1, PL3 and PL4 is labeled CPL1,3,4; control sample for PL2 is labeled CPL2, reprinted with permission from (1).

Since dilution of ophthalmic product with tears is inevitable after administration *in vivo*, it is essential to evaluate their key properties in biorelevant conditions. An optimal gel system should keep its structure despite the dilution with tears. From this reasons, mixed systems were further characterized under biorelevant conditions. Therefore, dilution with STF at the ratio of 40:7 mimicking their mixing with tear fluid after instillation was done (11). Despite the dilution, mixed systems retained their ability to form gel at temperature lower than 35°C (i.e., the sample PL2 formed gel at 28.7°C, while PL1, PL3 and PL4 formed gel at 33.5°C). The observed increase in  $T_{gel}$  relative to undiluted systems can be related to both, the decrease in the total concentration of polymers and the modification of the physicochemical properties of the hydrogels in the presence of STF electrolytes (20,135).

The dilution of all mixed systems with STF resulted in no change in  $G'$  to  $G''$  ratio or their overall profile (Figure 29). Furthermore, there was no significant change in the absolute values of  $G'$  and  $G''$  in case of samples prepared with the same poloxamer concentration and different CS concentration (Figure 29; PL1, PL3 and PL4). On the contrary, comparing the mixed system PL2 (P407/P188/CS 15.0/2.0/0.5%, w/w) with PL4 (P407/P188/CS 14.2/1.7/0.5%, w/w), it may be observed that the small increase in poloxamers concentration influenced the resistance to dilution. Figure 30 shows the relationship of  $\eta^*$  and angular frequency of selected mixed P407/P188/CS systems. The decrease of  $\eta^*$  values with the increase of angular frequency arguments suitable pseudoplastic behavior of *in situ* forming ophthalmic gels (Figure 30). The viscosity profiles of all mixed systems did not change significantly upon dilution with STF suggesting the maintenance of their pseudoplastic behavior.



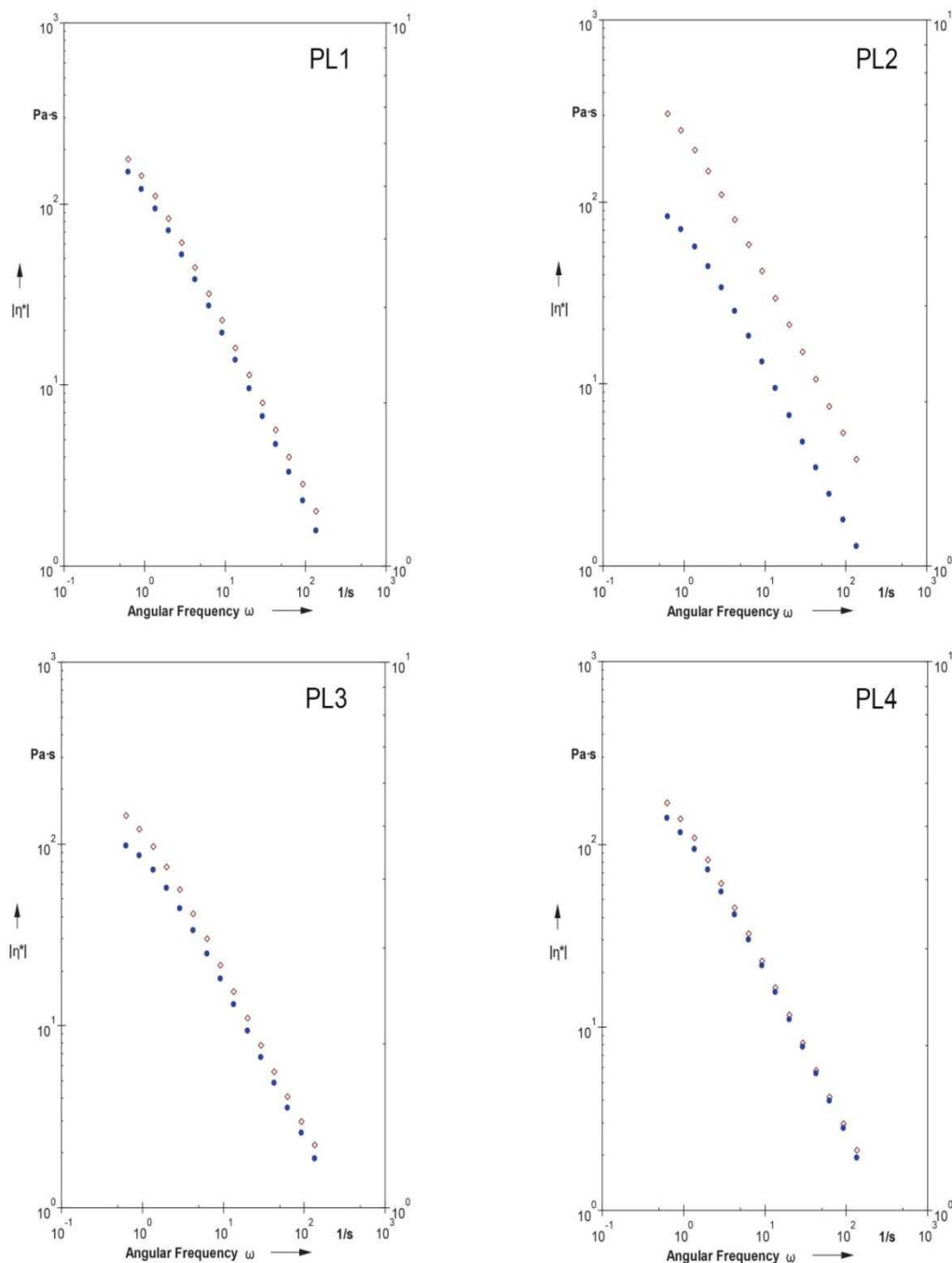


**Figure 30.** Complex viscosity ( $\eta^*$ ) of selected mixed P407/P188/CS systems as a function of angular frequency ( $\omega$ ) before (red, empty symbols) and after (blue, filled symbols) dilution with STF, reprinted with permission from (1).

Moreover, there was no marked change in the absolute values of  $\eta^*$  upon dilution except, again, in the case of PL2 sample (1).

Comparing mixed P407/P188/CS systems developed in this study with mixed P407/CS system developed by Gratieri et al. in terms of resistance to dilution, it may be concluded that P188 significantly contributed to gel stability (20). In mixed P407/CS system the concentration of P407 was higher (16%, w/w and 14%, w/w, upon dilution with STF) than in case of mixed P407/P188/CS system (14.2%, w/w and 12.09%, w/w, upon dilution with STF). However, upon dilution mixed P407/CS system behaved as viscoelastic solution at 35°C and decreased frequencies while mixed P407/P188/CS system behaved as soft gel(1).

#### **5.4.2. Dynamic viscosity evaluation by rotational rheology**

In DoE study in this thesis, oscillatory tests were used to study gel formation in order to gain reliable and conclusive results. For this purpose, the structure of a gel must not be disturbed during its rheological characterization. Therefore, shear stress is a crucial parameter and needs to be precisely adjusted and controlled. Oscillatory tests are superior to rotational tests when comes to investigations on gel formation or gel structure characteristics (102), i.e. to explore the viscoelasticity of a sample providing a microstructural fingerprint that can be used to quantify stability and to sensitively refine critical aspects of product performance.

Commercially available ophthalmic products and *in situ* forming gel formulations developed in this study are based on different polymers. Therefore, their gelation mechanisms differ which consequently results in difference in the linear viscoelastic (LVE) range and in other characteristics tested by oscillatory tests. In order to compare developed formulations with commercially available products, rotational test with controlled shear rate (CSR) was developed. Viscosity profile of samples in biorelevant conditions (diluted with STF 40:7) was measured in the shear rate range of 0.1 – 1000 s<sup>-1</sup>. Similar measuring methodology was reported before (15). Results of measurements are presented in the Table 10.

**Table 10.** Dynamic viscosity results of commercially available ophthalmic formulations and P407/P188/CS mixed systems after dilution with STF.

Shear Rate [1/s]	API-free Preformed gel 1*	API-free Preformed gel 2*	TIMO-loaded <i>in situ</i> forming gel*	Dexpanthenol loaded <i>in situ</i> forming gel*	DEX/TOBRA-loaded <i>in situ</i> forming gel*	PL 1 P407/P188/CS (% w/w 14.2/1.7/0.25)	PL 2 P407/P188/CS (% w/w 15/2/0.5)	PL 3 P407/P188/CS (% w/w 14.2/1.7/1.01)	PL 4 P407/P188/CS (% w/w 14.2/1.7/0.5)
Polymer	Gellan gum	Hydroxypropyl guar	Carbomer	HP-guar (agar gum)	Xanthan gum	Mixed systems			
0.1	2.035 ±0.007	3.545 ± 0.728	4.160 ±2.305	1.033 ±0.816	10.170 ±0.608	49.900 ±7.330	34.500 ±0.849	46.450 ±9.970	15.000 ±4.384
0.278	1.690 ±0.099	1.550 ±0.325	1.395 ±0.672	0.254 ±0.028	6.110 ±0.226	26.950 ±4.172	16.000 ±1.414	27.650 ±4.596	8.785 ±0.757
0.774	1.255 ±0.120	0.701 ±0.132	0.675 ±0.273	0.100 ±0.023	3.365 ±0.078	9.025 ±0.148	5.940 ±3.239	13.150 ±2.899	3.730 ±0.438
2.15	0.841 ±0.108	0.338 ±0.050	0.325 ±0.193	0.066 ±0.020	1.690 ±0.028	2.000 ±0.113	2.425 ±1.209	5.220 ±0.495	1.183 ±0.279
5.99	0.629 ±0.043	0.179 ±0.022	0.096 ±0.012	0.035 ±0.005	0.789 ±0.011	0.542 ±0.222	0.496 ±0.153	0.863 ±0.434	0.312 ±0.026
16.7	0.401 ±0.031	0.097 ±0.010	0.064 ±0.012	0.035 ±0.013	0.351 ±0.004	0.131 ±0.010	0.196 ±0.134	0.287 ±0.058	0.107 ±0.010
46.4	0.240 ±0.013	0.058 ±0.004	0.038 ±0.005	0.019 ±0.011	0.152 ±0.001	0.082 ±0.019	0.131 ±0.056	0.188 ±0.011	0.078 ±0.002
129	0.134 ±0.006	0.037 ±0.002	0.025 ±0.002	0.009 ±0.001	0.067 ±0.001	0.063 ±0.009	0.100 ±0.028	0.155 ±0.004	0.067 ±0.000
359	0.072 ±0.003	0.025 ±0.001	0.017 ±0.001	0.008 ±0.000	0.031 0.000	0.053 ±0.002	0.084 ±0.015	0.133 ±0.001	0.059 ±0.000
1000	0.039 ±0.002	0.017 ±0.000	0.012 ±0.000	0.006 ± 0.001	0.016 0.000	0.048 ±0.001	0.075 0.009	0.111 ±0.003	0.054 ±0.001

Values are mean [Pa·s] ± SD (n = 3)

Simulated tear fluid (STF)

As already noticed in case of oscillatory shear rheological tests, viscosities of developed mixed systems, recorded in rotational test, showed suitable pseudoplastic behavior. Dynamic viscosities of P407/P188/CS systems were higher at lower shear rates compared to commercially available

formulations, indicating adequate suitability of developed mixed systems to retain potential APIs. On the contrary, at high shear rates, viscosities dropped significantly rendering them adequate for ophthalmic use.

Based on minimal polymer content (P407, P188 and CS concentration of 14.2, 1.7 and 0.25%, w/w, respectively), favorable rheological characteristics ( $T_{gel} = 31.1\text{ }^{\circ}\text{C}$ ,  $\eta^* = 2.1\text{ Pa} \times \text{s}$ ; low dynamic viscosity at high shears) and in vitro resistance to tear dilution ( $G'$  212.4 Pa and 175.3 Pa before and after dilution, respectively), the PL1 was selected as optimal *in situ* forming gel (1).

## 5.5. Effect of active pharmaceutical ingredients on temperature of gelation and complex viscosity

The addition of APIs in the mixed P407/P188/CS system is expected to cause a modification of the physicochemical properties of *in situ* forming gels. Four ophthalmic APIs were selected in order to gain understanding of their effects on  $T_{gel}$  and  $\eta^*$  of selected PL1 *in situ* forming gel (1).

APIs were tested in the concentrations and combinations relevant for topical ophthalmic use.

*In situ* forming ophthalmic gels containing TIMO, DEX and DORZO were prepared in the same way as API free systems. For preparation of systems containing TOBRA, API was first dissolved in defined aliquot of WFI and then mixed with P407/P188/CS solution. pH was adjusted to 5.8 since addition of TOBRA increased pH of the solution. All prepared formulations had an ophthalmically acceptable osmolality, which was achieved by the addition of appropriate amounts of NaCl to the solution (1).

API-loaded P407/P188/CS systems were characterized for  $T_{gel}$  and  $\eta^*$  before and after dilution with STF (Table 11). Additionally, rotational test was performed in order to evaluate the influence of APIs on dynamic viscosity profile (1).

**Table 11.** Effect of APIs on temperature of gelation ( $T_{gel}$ ) and complex viscosity ( $\eta^*$ ), reprinted with permission from (1).

Sample	Before dilution with STF <sup>1</sup>		After dilution with STF	
	$T_{gel}$ (°C)	$\eta^*$ (Pa × s) <sup>2</sup>	$T_{gel}$ (°C)	$\eta^*$ (Pa × s) <sup>2</sup>
PL1 - DORZO	27.50 ± 1.70	7.88 ± 1.18	33.50 ± 0.01	0.67 ± 0.06
PL1 - TIMO	26.30 ± 0.01	4.90 ± 0.54	29.90 ± 1.20	2.44 ± 1.50
PL1 - DORZO/TIMO	28.70 ± 0.02	4.82 ± 1.07	32.90 ± 0.80	0.64 ± 0.10
PL1 - TOBRA	30.30 ± 1.40	1.52 ± 0.66	31.10 ± 0.01	0.52 ± 0.10
PL1 - DEX	22.60 ± 1.70	6.11 ± 0.70	28.70 ± 0.01	1.56 ± 1.16
PL1 - DEX/TOBRA	23.65 ± 3.18	6.88 ± 1.59	31.15 ± 0.07	0.639 ± 0.21
PL1	31.10 ± 1.40	2.10 ± 0.74	33.50 ± 0.70	0.37 ± 0.15

<sup>1</sup> Simulated tear fluid (STF)

<sup>2</sup> #  $\eta^*$  at 35°C determined by temperature sweep test (angular frequency and strain were 1 s<sup>-1</sup> and 1 %, respectively)

Values are mean ± SD (n = 3)

All APIs, except TOBRA, notably decreased  $T_{gel}$  in comparison with  $T_{gel}$  of PL1. This effect was highest for DEX showing the decrease of the  $T_{gel}$  for 8.5°C (1). DEX has already been shown to decrease the  $T_{gel}$  of P407 based *in situ* forming gels (136,137). Such an effect can be ascribed to the promotion of P407 self-assembly in the presence of hydrophobic drug allowing the formation of gel at lower temperatures (138). The  $T_{gel}$  of the mixed P407/P188 systems was also reported to be affected by the addition of hydrophobic APIs; the  $T_{gel}$  decreased with increasing the pH-dependent hydrophobicity of API in the systems (139). Smaller  $T_{gel}$  decrease was observed for the systems containing dissolved APIs, namely  $T_{gel}$  decreased for 4.8 and 2.4 °C in case of TIMO and DORZA, respectively. As anticipated by other authors, the decrease of  $T_{gel}$  induced by dissolved APIs could be related to the API salting out effect (140,141). Their presence could shift the concentration and/or temperature at which micelles are formed to lower values and, moreover, could affect the close-packing of micelles, resulting in  $T_{gel}$  decrease (135,139). However, despite the decrease of  $T_{gel}$  by the addition of APIs, all the samples except those with DEX formed gels at temperature higher than 25°C (1).

The  $\eta^*$  values for API-loaded PL1 were in the range of 1.52 – 7.88 Pa × s indicating no pronounced influence of API entrapment on gel viscosity (Table 11) (1).

Dilution with STF, as expected, led to the increase in  $T_{gel}$  and certain decrease in  $\eta^*$  for all the API-loaded PL1. All the samples retained their gel structure after dilution as suggested by the frequency sweep analysis (Figure 31) (1).

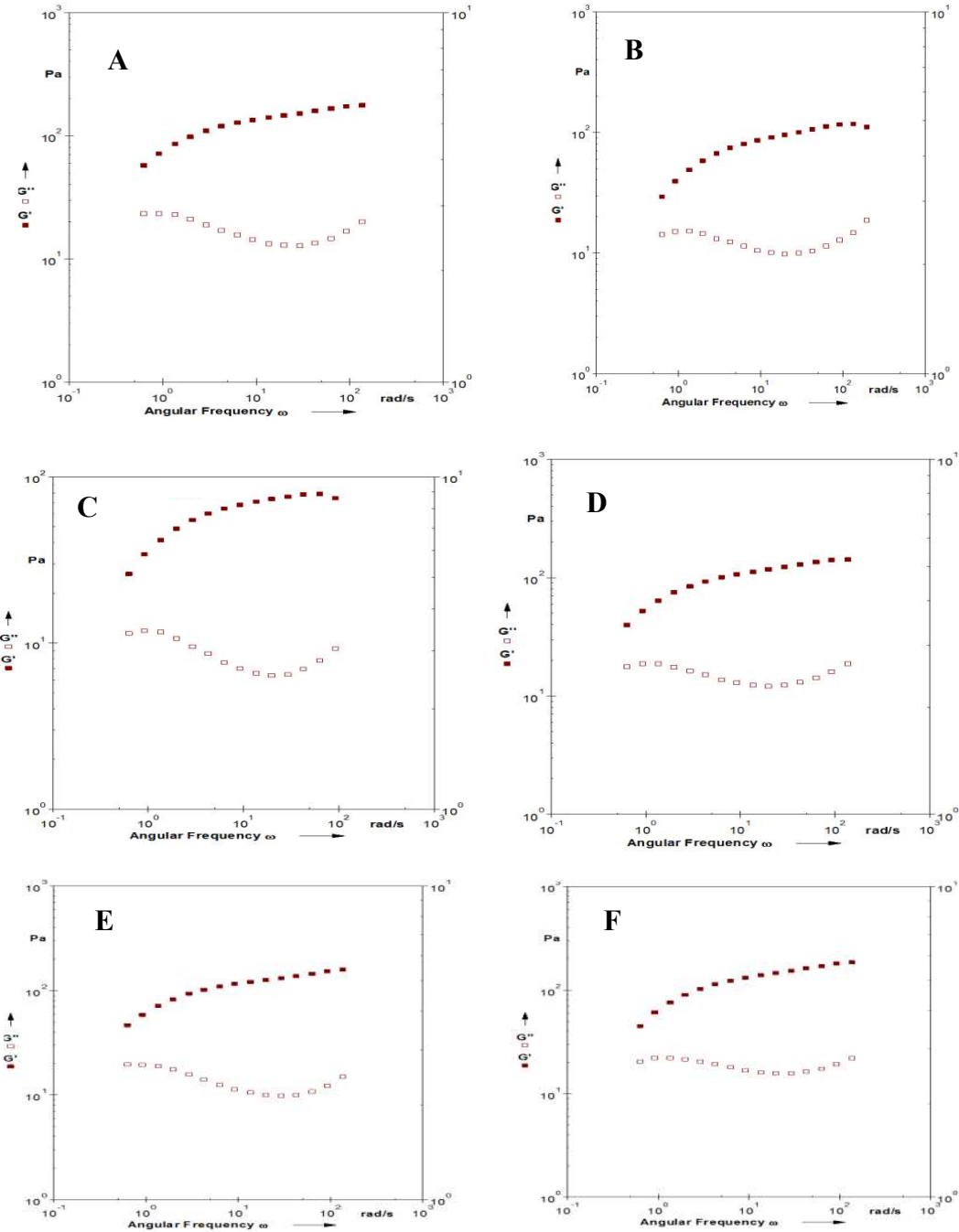


**Figure 31.** Storage (filled symbols) and loss modulus (empty symbols) of API-loaded PL-1 formulations after dilution with STF 40:7 at 35°C: A) PL1-DEX, B) PL1-TOBRA, C) PL1- DEX/TOBRA; D) PL1-DORZO; E) PL1-TIMO; F) PL1-DORZO/TIMO

### 5.5.1. Evaluation of dynamic viscosity of systems containing APIs

After dilution with STF in the ratio 40:7, dynamic (shear) viscosity profiles of mixed systems containing different APIs were recorded. Viscosity profiles of all samples showed suitable pseudoplastic behavior after dilution with STF at 35°C (Table 12).

**Table 12.** Dynamic viscosity obtained by rotational test for PL1 based formulations after dilution with STF.

Shear Rate [1/s]	PL1 [Pa × s]	PL1 - DORZO [Pa × s]	PL1 - TIMO [Pa × s]	PL1 - DORZO/ TIMO [Pa × s]	PL1- TOBRA [Pa × s]	PL1 - DEX [Pa × s]	PL1 - DEX/ TOBRA [Pa × s]
<b>0.1</b>	49.90 ±7.330	25.65 ±5.303	57.7 ±11.597	37.7 ±2.687	20.050 ±6.010	51.45 ±14.779	43.6± 11.314
<b>0.278</b>	26.950 ±4.172	16.75 ±6.293	22.7 ±4.667	19.8 ±6.505	9.275 ±0.205	23.15 ±3.748	20.7± 4.95
<b>0.774</b>	9.025 ±0.148	4.52 ±1.909	8.38 ±3.705	6.84 ±1.442	3.465 ±1.308	10.6 ±0.283	8.58 ±0.283
<b>2.15</b>	2.000 ±0.113	1.022 ±0.393	2.44 ±0.368	1.315 ±0.318	1.085 ±0.361	2.705 ±1.45	2.695 ±1.011
<b>5.99</b>	0.542 ±0.222	0.274 ±0.076	0.503 ±0.325	0.36 ±0.139	0.4075 ±0.022	0.388 ±0.151	0.305 ±0.146
<b>16.7</b>	0.131 ±0.010	0.061 ±0.007	0.075 ±0.01	0.116 ±0.006	0.12525 ±0.077	0.114 ±0.073	0.091 ±0.048
<b>46.4</b>	0.082 ±0.019	0.052 ±0.003	0.055 ±0.006	0.081 ±0.002	0.0683 ±0.124	0.058 ±0.013	0.056 ±0.011
<b>129</b>	0.063 ±0.009	0.049 ±0.002	0.048 ± 0.002	0.067 ±0.001	0.053 ±0.002	0.05 ±0.006	0.046 ±0.003
<b>359</b>	0.053 ±0.002	0.047 ±0.001	0.045 ±0.000	0.062 ±0.002	0.0443 ±0.003	0.047 ±0.004	0.041 ±0.001
<b>1000</b>	0.048 ±0.001	0.045 ±0.001	0.043 ±0.000	0.058 ±0.002	0.0398 ± 0.003	0.045 ±0.003	0.039 ±0.001

Values are mean ± SD (n = 3).

Dynamic viscosity results indicate adequate pseudoplastic behavior of developed systems in biorelevant conditions - after dilution with STF (40:7) at 35°C.



### 5.5.2. Gelation time

To gain insights in APIs influence on gelation, gelation time, namely the time point at which intersection of the curves of measured loss modulus ( $G''$ ) and the storage modulus ( $G'$ ) occurs, was determined for PL 1 systems containing APIs (1). Results are presented in the Table 13.

**Table 13.** Results of gelling time for PL1 and of PL1 systems containing APIs.

Sample	Gelation time (s)
PL1 - DORZO	68.35 ± 3.89
PL1 - TIMO	41.05 ± 3.09
PL1 - DORZO/TIMO	87.37 ± 21.70
PL1 - TOBRA	51.03 ± 13.74
PL1 - DEX	45.53 ± 13.7
PL1 - DEX/TOBRA	0.00 ± 0.00
PL 1	5.00 ± 5.00

Values are mean ± SD (n = 3).

The addition of APIs in the mixed P407/P188/CS system prolonged the gelation time in all cases except for DEX/TOBRA (1). However, the obtained gelation time values were still in the appropriate range (41.1-87.4 s) for ophthalmic administration (142,143).

Results of in depth rheological characterization (oscillatory and rotational) indicate the robustness of selected PL1 *in situ* forming gel against entrapment of APIs with different physicochemical characteristics. All samples acted as gels upon dilution and preserved pseudoplasticity (1). The decrease in  $T_{gel}$  caused by API entrapment open the possibility to further decrease the concentration of poloxamers required to obtain *in situ* forming gels with appropriate biopharmaceutical properties (144).

## 5.6. Drug release from *in situ* forming gels

*In vitro* release tests (IVRs) are an important tool for measuring changes in critical physical properties of semisolid products that may be related to their topical bioavailability (127,145). Origin of these changes could be the physicochemical characteristics of the drug substance, excipients, formulation manufacturing process, shipping and storage effects, aging and other formulation and/or process factors. Although IVRs are valuable, it is necessary to stress out that these tests cannot predict directly *in vivo* performance of the drugs because they cannot mimic physiologic reality of the biological membranes, like cornea of the eye or stratum corneum of the skin, which are usually *in vivo* rate limiting barriers to drugs bioavailability (127).

From regulatory perspective, currently the only required use of the IVR test is to determine the acceptability of minor process and/or formulation changes in approved semisolid dosage forms (129). Recently, for complex generic drugs, regulatory agencies suggest extensive *in vitro* equivalence testing as adequate substitute for expensive *in vivo* bioequivalence studies. Discriminative IVR methodology plays a critical role in this characterization package (146–148). Furthermore, for application in pharmaceutical industry method needs to be standardized and cost-effective (126). For assessment of *in vitro* drug release from nano-sized and gelling ophthalmic delivery system a variety of membrane diffusion techniques were implemented such as simple dialysis methods, dialysis methods using modified Apparatus 1 and 2 and Franz diffusion cells (126). Aim of this part of the study was to develop robust, precise and discriminative method for testing drug release from developed *in situ* ophthalmic gel formulations. From this reason, TIMO was used as a model ophthalmic drug and vertical diffusion (Franz diffusion) cell system was selected as apparatus, due to its applicability for assessment of drug release from semisolids (127).

When drug is dissolved in the drug product, as it is the case in of PL1- TIMO samples, resulting release kinetics from semisolids is described by Higuchi model (127):

$$Q = 2 \times C_o \sqrt{\frac{Dt}{\pi}} \quad (\text{Eq.11}).$$

where Q is the amount of drug released into the sink (medium) per cm<sup>2</sup>, C<sub>o</sub> is the drug concentration in the releasing matrix, and D is the drug diffusion coefficient through the matrix.

Viscosity, dominantly the ratio of the viscous and elastic properties of prepared gels, is the major critical attribute that would influence drug diffusion/release from *in situ* ophthalmic gels. Drug release would, obviously, be reversely proportional to matrix viscosity.

Parameters considered during development of IVR test in this study were: choice of IVR medium, membrane selection, sampling points and discriminatory power of the method.

#### **5.6.1. Validation of UPLC method for quantification of TIMO**

In order to adequately assess TIMO determination in IVR study, prior to the IVR testing, quantification method for TIMO using ultra performance liquid chromatography was developed, optimized and validated. Validation was designed to cover following parameters:

- specificity,
- linearity,
- accuracy,
- range,
- repeatability and
- standard/sample stability.

##### *Specificity*

During the specificity study chromatograms of mobile phase, *in vitro* release medium (STF) and placebo solution were evaluated to ensure that there is no interference with TIMO peak.

Results are presented on the Figure 32(A-E).

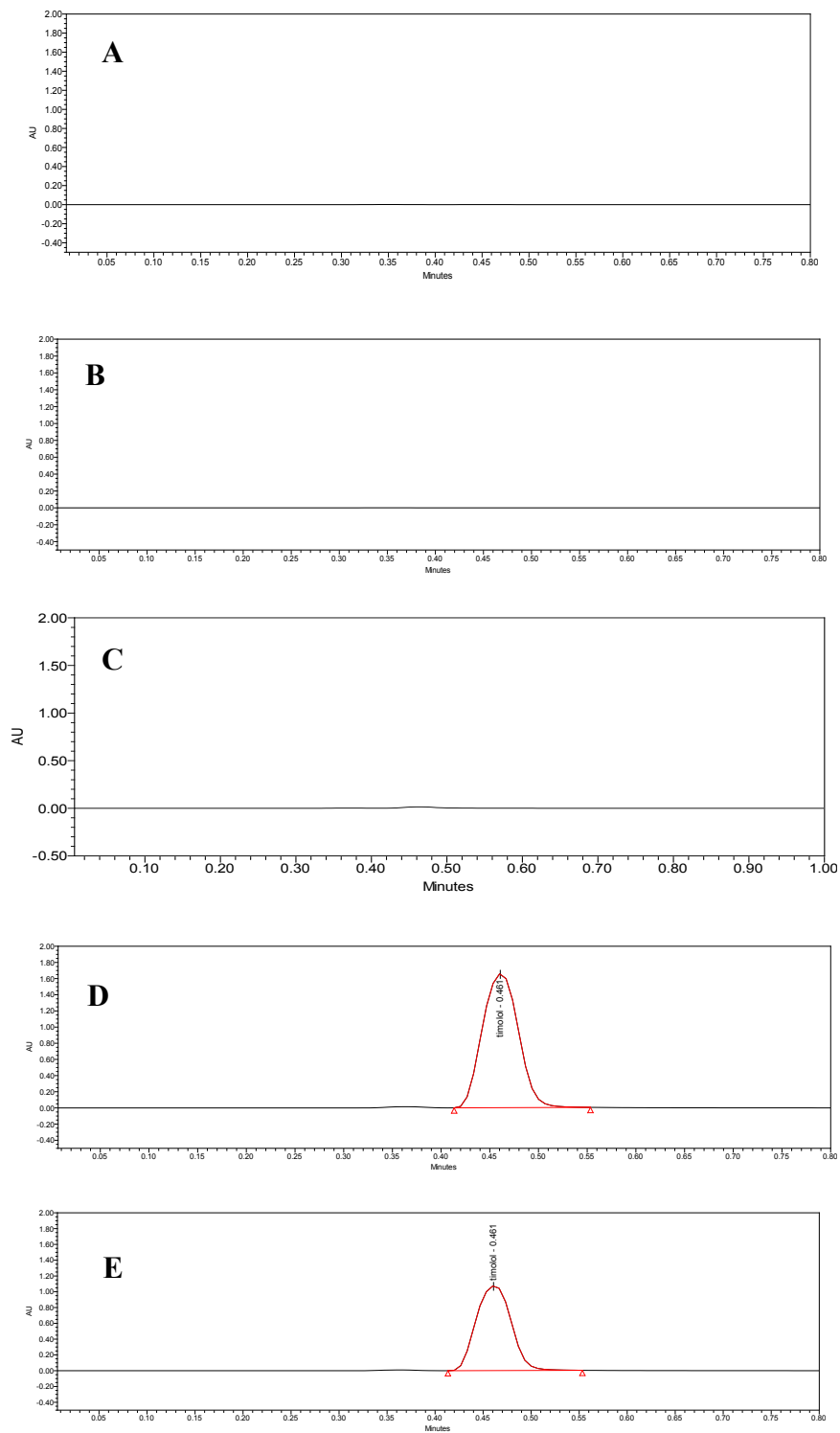


**Figure 32:** Chromatograms of A) mobile phase solution, B) STF, C) Placebo solution, D) TIMO standard solution and of E) IVR sample solution.

From all chromatograms obtained in the specificity study it is evident that STF, mobile phase and placebo do not interfere with TIMO retention time.

*Linearity*

Linearity of the detector response was evaluated in the concentration range of 0.00516 – 0.05170 mg/ml (Table 14). Following regression equation was obtained, with coefficient of determination  $R^2 > 0.999$ :

$$y = 11462861.374 x + 56163.742 \quad (\text{Eq. 12})$$

**Table 14.** Linearity results.

Level	Area	Concentration (mg/ml)
1%	58897.937	0.0052
1%	63885.278	0.0052
10%	619685.978	0.0516
10%	695850.980	0.0516
20%	1201809.472	0.1034
20%	1224370.385	0.1032
40%	2476425.186	0.2068
40%	2522467.191	0.2064
70%	4245772.080	0.3619
70%	4286297.129	0.3619
90%	5432830.553	0.4653
90%	5378213.778	0.4643
100%	5948429.986	0.5159
100%	5828232.691	0.5170
<b>SLOPE</b>		<b>11462861.37436</b>
<b>INTERCEPT</b>		<b>56163.7</b>

The 95% confidence interval of the y-intercept (-9709.11, 122036.59) includes zero, which indicates that the intercept is not statistically significant. Obtained results demonstrated a linear relationship between the detector response and the TIMO concentration in the tested range.

*Accuracy, range and repeatability of UPLC method*

Method accuracy was evaluated through recovery experiment from the solutions prepared in triplicate in the same concentration range as for linearity evaluation. Placebo solution was spiked with TIMO. Results presented in the Table 15 indicate that method, with recoveries from 99-105% and RSDs from 1-5% was found accurate for named purpose.

**Table 15.** Accuracy study results.

Level	Average recovery (%)	RSD (%)
1%	102	4
10%	105	5
20%	101	1
40%	103	3
70%	101	1
90%	101	1
100%	99	1

Repeatability was demonstrated by evaluating RSD (<3.0%) of standards injected throughout the sequences. Based on the linearity and accuracy results, the range of the developed UPLC method was found to be from 0.5 µg/ml do 516.9 µg/ml.

*Sample and standard stability*

Stability of standard and sample solutions (from IVR test) was evaluated after 24 hours (

Table 16). Both sample and standard recovery results were within the acceptance criteria for standard ( 98.0-102.0 %) and sample (95-105%), at 24 stability time point.

**Table 16.** Stability of standard and sample solution.

Time/h	RF recovery for standard solution (%)	mg/ml recovery for sample solution (%)
24	100.4 ± 1.1	101.2 ± 0.9

## 5.6.2. Development of *in vitro* release method

### 5.6.2.1. Selection of receptor medium – solubility testing

TIMO is highly soluble in water (149), therefore aqueous media were chosen as receptor media for IVR, namely STF, KRB and PB. During shake flask solubility testing for all investigated media, in the tested volume of 20 ml, it was not possible to achieve saturated TIMO solution conditions. After 48 hours of tests and large amounts of API spent, testing was stopped, and the solutions were filtrated through 0.2 µm filters, diluted with corresponding medium and quantified by the UPLC.

pH of the media was measured throughout the test and it did not change significantly after 48 hours in all evaluated media. Since equilibrium conditions could not be achieved, results are expressed as soluble *more than* stated mg/ml values (Table 17). Solubility results in all three media are comparable.

**Table 17.** Results of estimated TIMO solubility testing after 48 hours.

medium	STF	KRB	PB
estimated solubility – mg/ml	>214.2	>189.3	>201.7

On account of no significant difference in solubility of TIMO in tested media, simulated tear fluid was chosen as receptor medium, due to the highest similarity to the tears *in vivo* in comparison to other media.

### 5.6.2.2. Membrane selection

Membranes in IVR should provide inert support for sample, they must not interfere with API by adsorbing it or by impacting or controlling its release. Permeability of the membrane is described by following equation (150):

$$P = D \cdot k_p / h_m \quad (\text{Eq. 13})$$

where  $D$  is diffusional coefficient of drug through the membrane,  $k_p$  is partition coefficient between the membrane and receptor medium (fluid) and  $h_m$  is membrane thickness. Membrane

and its corresponsive stationary layer present certain diffusional resistance and therefore impact the drug release to a certain extent. It is important for a membrane to be very thin and highly porous in order to impact diffusion as little as possible.

In order to find the most appropriate membrane, five membranes were evaluated in our study. Results of the influence of tested membranes on the TIMO recovery for API adsorption are presented in the Table 18. Acceptance criterion was that recovery of filtrated solution compared to the non-filtrated solution to be 95-105%. As it is seen from the Table 18, none of the five tested membranes adsorbed significantly TIMO at both concentration levels tested (0.0801 and 0.4005 mg/ml).

**Table 18.** TIMO recoveries after membrane filtration.

Membrane	TIMO recovery (%) at 0.0801 mg/ml	TIMO recovery (%) at 0.4005 mg/ml
RC 0.2	103	98
RC 0.45	101	100
PESU 0.45	101	101
PES 0.1	102	103
CA 0.8	101	105

During an *in vitro* release experiment, drug migration from gel to receptor occurs as a series of successive diffusional steps. Since the physical properties of the product itself are of interest in IVR, diffusion/release through semisolid must be the rate limiting step of the process. From this reason, it is very important, as emphasized, that the membrane, together with the receptor medium, is highly permeable for the drug (151).

In order to choose membrane with will have lowest resistance to drug diffusion, all five membranes were used in IVR test of the PL1 formulation (0.2% TIMO). Test was done in triplicate for each membrane and results of obtained release rates (slopes) are summarized in the Table 19.



**Table 19.** TIMO release rates (slopes) using different membranes obtained in first 2 hours of test.

Membrane	slope $\pm$ SD
RC 0.2	72.72 $\pm$ 2.48
RC 0.45	68.17 $\pm$ 14.26
PESU 0.45	109.05 $\pm$ 31.61
PES 0.1	96.11 $\pm$ 1.35
CA 0.8	117.18 $\pm$ 2.20

Regenerated cellulose membranes (RC 0.2 and RC 0.45) had highest resistance to TIMO release rate, while with the use of CA 0.8 highest slopes were obtained. PESU 0.45 showed higher variability compared to other tested membranes (Table 19).

Based on data obtained in first two studies (low absorption, high diffusivity and lower variability), PES 0.1 and CA 0.8 were selected as two lead membranes of choice, and were used for study which evaluated resistance to diffusion from the TIMO solutions at two concentration levels (0.01 mg/ml and 2.5 mg/ml). For this purpose, data was evaluated by plotting % the *in vitro* released drug from the solutions versus time. Results are depicted on the Figure 33.

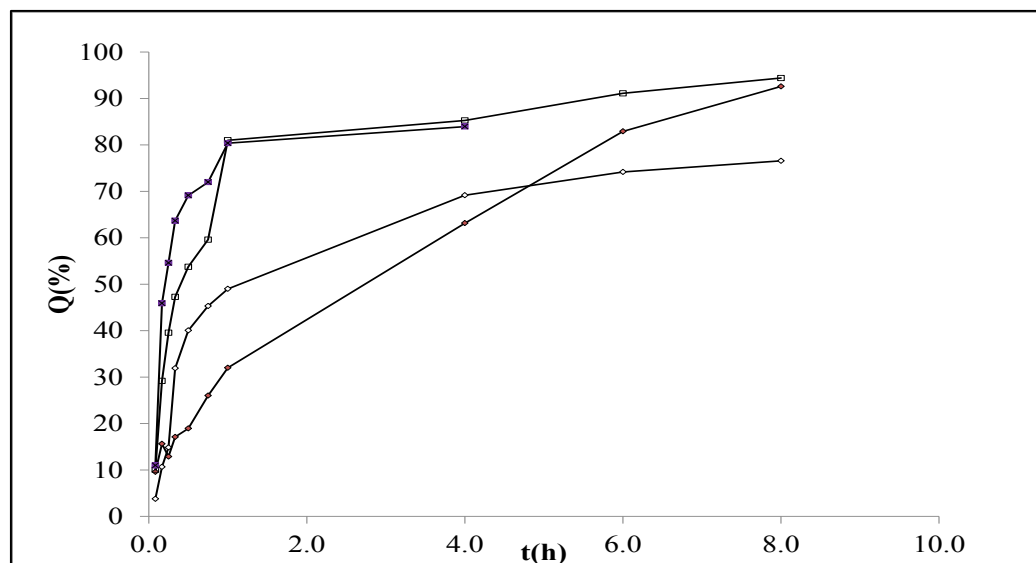


**Figure 33.** Influence of PES 0.1 (diamonds) and CA 0.8 (squares) on TIMO release at 0.01 mg/ml (filled) and 2.5 mg/ml (unfilled) concentration levels

Since higher and complete release was obtained with CA 0.8 membranes at both concentration levels, it can be concluded have that they have smaller influence on the diffusion of TIMO from solutions compared to PES 0.1 membranes. Therefore, CA 0.8 membranes were chosen as the most appropriate membranes for IVR testing.

### 5.6.2.3. Discriminatory power of the method

As emphasized, drug release form the gels would mainly depend on its diffusivity through the gel matrix. To evaluate influence of viscosity, six formulations, presented in the Table 20, were investigated during IVR method optimization.

**Table 20.** Formulations tested in IVR development.

Formulation	P407 (%, w/w)	P188 (%, w/w)	CS (%, w/w)	TIMO (%, w/w)	T <sub>gel</sub> (°C)	η* <sup>1</sup> (Pa × s)
PL1	14.2	1.7	0.25	0.1	31.1 ± 2.0	1.2 ± 0.3
PL1 -0.1	14.2	1.7	0.25	0.1	29.2 ± 1.6	1.6 ± 0.2
PL1 -0.3	14.1	1.7	0.25	0.3	28.7 ± 0.5	1.3 ± 0.5
C1	14.2	-	0.25	0.2	26.9 ± 2.2	4.12 ± 1.2
C2	11.4	-	-	0.2	31.1 ± 1.7	0.097 ± 0.07
C3	17.8	-	-	0.2	21.4 ± 1.5	1690 ± 7.1

<sup>1</sup> η\* at 35°C determined by temperature sweep test (angular frequency and strain were 1 s<sup>-1</sup> and 1%, respectively)

In order to evaluate the influence of different concentrations of P407 in formulation on drug release, two formulations, containing 0.2% of the TIMO, were compared – C2, containing 11.4% P407 and C3 which contained 17.8% P407. Formulation C3 was already gel at ambient conditions. Results are presented on the Figure 34.

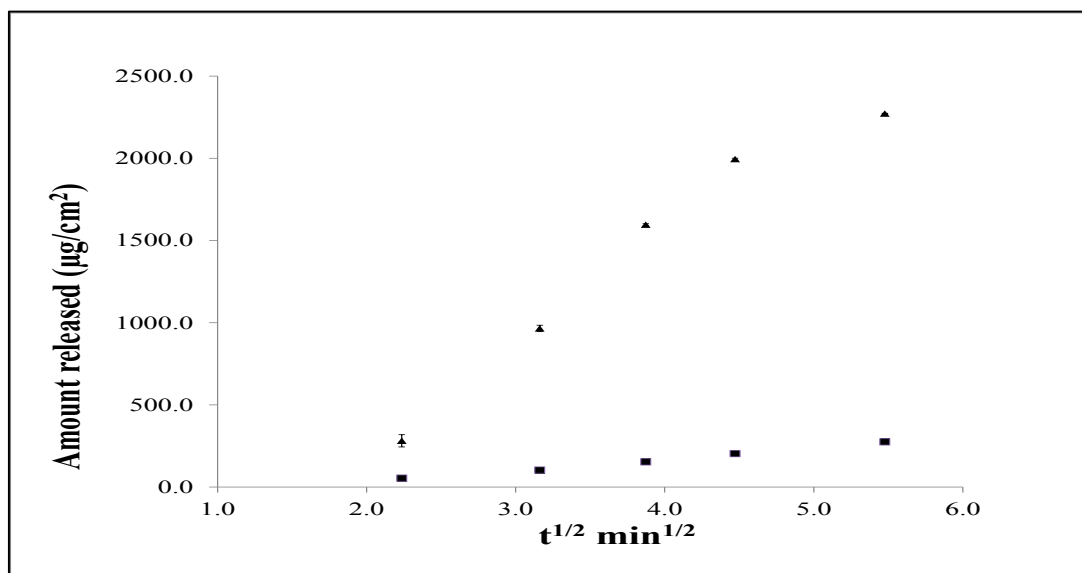


**Figure 34.** IVR of TIMO from C2 (11.4% P407, triangles) and C3 (17.8% P407, squares) (mean ±RSD).

*In vitro* release of TIMO from C2 was very fast, yielding slope (N=5) 637.73 ± 55.06 in first 30 minutes of the test, indicating that viscous property of the formulation is dominant and comparable to TIMO solutions in STF. On the contrary, slope of the formulation C3 (N=6) was 69.10 ± 8.15, indicating predominance of elastic properties, which confirmed visual observation;

sample appeared as a firm gel at ambient conditions. This predominantly elastic nature of a formulation ensured sustained release of API into the receptor. Consequently, lower and upper limits of 90% confidence interval (30 and 45.73%, respectively) were out of preset limits (75-133.33%) and absence of release rate similarity of tested formulations was indicated.

To evaluate method's sensitivity to discriminate formulations containing different concentrations of the API while amounts of excipients are kept the same, IVR testing was done on the formulations containing 0.1 (PL1-0.1%) and 0.3% (PL1-0.3%) of TIMO. Results are presented on the Figure 35. Again, Mann-Whitney's U test was used to calculate and evaluate the 90% confidence interval for the ratio of the slopes between the two batches and with the lower limit 23% and upper 52.73%, developed method successfully eliminated similarity between two tested batches differing in TIMO's concentration (151).

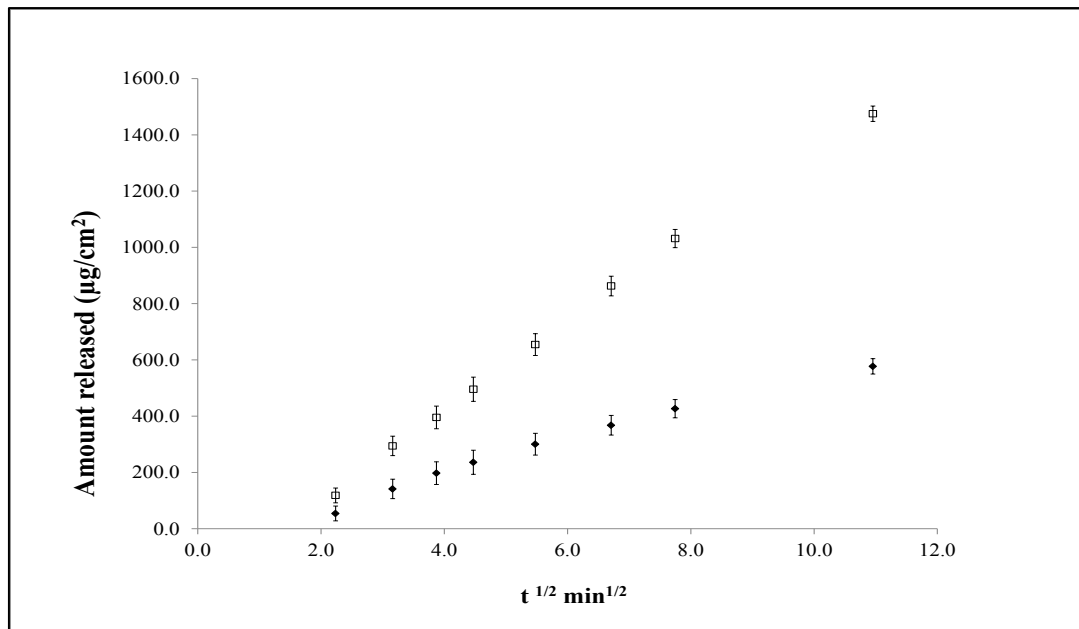


**Figure 35.** IVR of *in situ* forming gels containing different amount of TIMO: PL1-0.1% (diamonds, filled) vs PL1-0.3% (square, empty) formulations (mean  $\pm$  RSD).

Since the developed method was able to discriminate formulation differing in physicochemical properties, it was found to be suitable for assessing *in vitro* release of PL1 based *in situ* ophthalmic formulations.

### 5.6.3. Evaluation of IVR from the optimal *in situ* forming gel

As emphasized, IVR is prerequisite tool for measuring changes in critical physical properties of gels products that may be related to their topical bioavailability. Optimal *in situ* forming ophthalmic gel should exhibit adequate/prolonged release profile of the API to promote eye-related bioavailability. Viscosity is crucial attribute affecting the drug release from gel matrices. If increased, viscosity results in slower diffusion of the drug across the gel matrix and into the receptor medium (64).

Purpose of IVR study was to evaluate the influence of viscosity and/or  $T_{gel}$  related to the functional excipient concentration on the drug release rate.

The optimal *in situ* forming gel (PL1) was characterized in term of its influence on TIMO release profile. Control *in situ* forming gel C1 was characterized by  $\eta^*$  comparable to PL1, while control *in situ* forming gel C2 was characterized by  $T_{gel}$  comparable to PL1 (Table 20). TIMO solution was used as the control sample. The *in vitro* release profiles of PL1 and respective controls are shown in Figure 36.

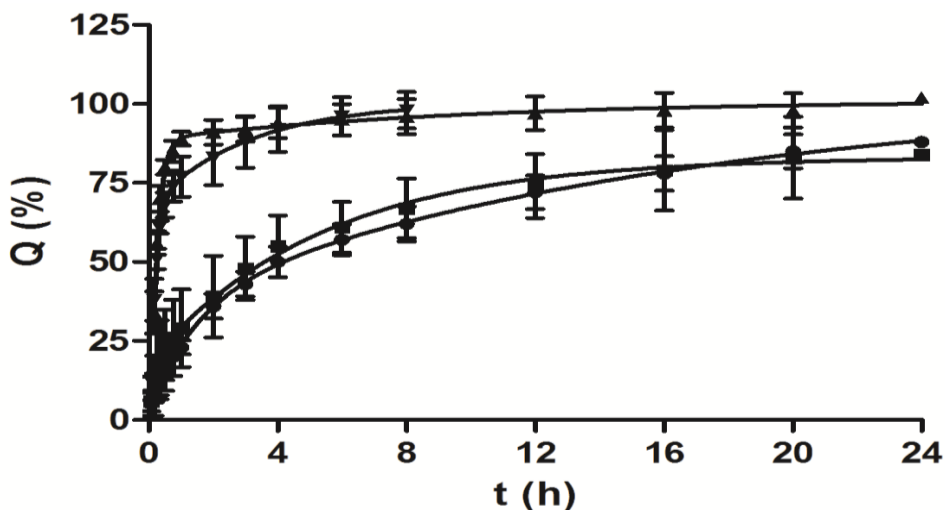


**Figure 36.** Release profiles of TIMO from PL1 (circles) and control *in situ* forming gel C1 (squares) with  $\eta^*$  comparable to PL1, control *in situ* forming gel C2 (triangle) with  $T_{gel}$  comparable to PL1 and TIMO solution (inverse triangle). The data are expressed as the mean  $\pm$  SD, reprinted with permission from (1).

*In vitro* release of TIMO from PL1 and C1 was significantly slower than from C2 and TIMO solution, confirming the viscosity as the critical factor which is governing the drug release from the gel matrix (1). Confidence interval of the slopes obtained for PL1 and C1 was calculated (75-131.2%) and confirmed similarity of drug release of tested formulations at first stage of the test. Similar observations were already reported for *in situ* forming ophthalmic gels (64,70).

## **5.7. Sterilization**

Due to specific use, ophthalmic products have the same or similar quality/safety requirements as injectables and implants (38). The goal of the sterilization process is inactivation of the bioburden without adversely affecting product quality attributes (152). Ocular infections are extremely dangerous and can rapidly lead to the loss of vision (153). Moreover, eyebaths, droppers and all other dispensers should also be sterile and controlled if packaged with the drug product (153). Therefore, manufacturing under validated conditions which assure sterility in the final container for the shelf life of the product is a prerequisite for ophthalmic products.

Commonly used methods of sterilization are steam sterilization (autoclaving), dry-heat sterilization/depyrogenation, gas sterilization, sterilization by ionizing radiation and sterilization by filtration (152). Terminal sterilization of ophthalmic products in their final containers should be adopted wherever possible. If the product is susceptible to degradation by terminal sterilization, then filtration under aseptic conditions should be considered, usually performed using a filter pore size of 0.22  $\mu\text{m}$  or less (153). Wherever possible, all components used for aseptic manufacture should be sterile, or should meet a low specified bioburden control limit (153).

Autoclaving (terminal sterilization) is the first choice for most ophthalmic solutions because of its convenience for large-scale production. However, the suitability of autoclaving in relation to physicochemical formulation stability needs to be assessed (15). Filtration is commonly used procedure in sterile production because it lowers the risk of presence of bioburden and particulates. A combination these methods is frequently used in sterile production.

Ease of formulation preparation, solubilization ability as a surfactant, a final aqueous solution and the ability for sterile filtration have made poloxamer P407 an interesting candidate for developing sterile products, specifically when controlled release of the drug is required (80).

To determine the appropriate sterilization methods, key rheological properties of the PL 1 optimal *in situ* forming gel were inspected prior and after filtration through 0.2  $\mu\text{m}$  filter, and after filtrating and autoclaving (20 minutes at 121°C). Results are presented in the Table 21.

**Table 21.** Key rheological properties of PL 1 optimal *in situ* forming gel prior and after sterilization.

Sample	$T_{\text{gel}} (^{\circ}\text{C})^1$	$\eta^*^1$ Pa $\times$ s	$G'^1$ (Pa)
PL 1	31.1 $\pm$ 0.01	2.1 $\pm$ 0.36	14.1 $\pm$ 5.2
PL 1 filtrated	28.7 $\pm$ 0.03	2.6 $\pm$ 0.41	15.9 $\pm$ 6.0
PL 1 filtrated and autoclaved	28.5 $\pm$ 0.02	2.8 $\pm$ 0.40	16.8 $\pm$ 5.7

<sup>1</sup>  $T_{\text{gel}}$ ,  $\eta^*$  and  $G'$  presented as mean  $\pm$  SD at 35°C, determined by temperature sweep test (angular frequency and strain were 1  $\text{s}^{-1}$  and 1%, respectively).

Filtration and filtration and autoclaving induced certain decrease of  $T_{\text{gel}}$  of the PL1 *in situ* forming gel ( $T_{\text{gel}}$  decreased approximately for 2°C). Moreover, certain increase in  $G'$ ,  $G''$  and  $\eta^*$  measured in the frequency sweep test was noticed for filtrated sample in comparison to non filtrated one (Figure 37). Subsequent autoclaving did not induce further changes in  $G'$ ,  $G''$  and complex viscosity in comparison to the filtered sample.

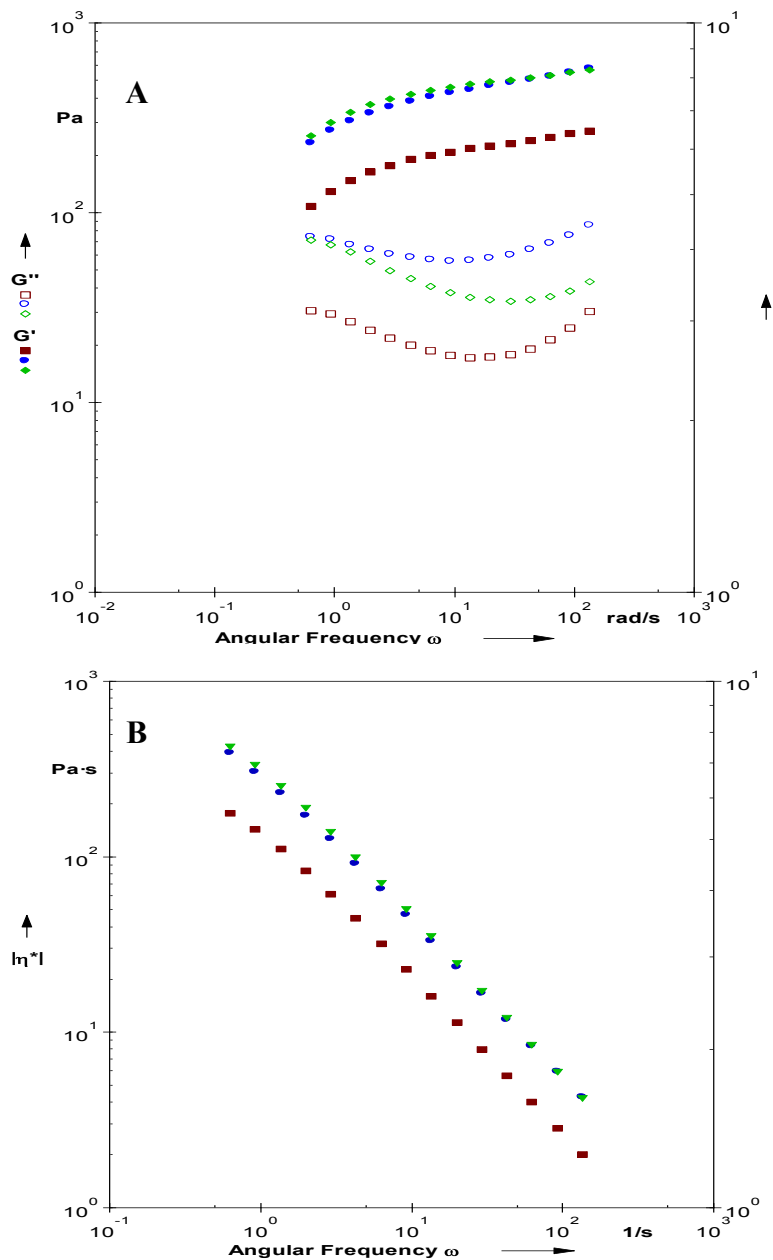


**Figure 37.** Frequency sweeps of PL 1 optimal *in situ* forming gel after sterilization. A)  $G'$  (filled symbols) and  $G''$  (non filled symbols) of non-filtered (red squares) and filtered (blue circles) sample, filtrated and autoclaved sample (green diamonds). B)  $|\eta^*|$  as function of angular frequency for non-filtered (red squares) and filtered (blue circles) sample, filtrated and autoclaved (green triangles).

This phenomenon could be related to the presence of impurities or foreign particles in the *in situ* gel solutions which could interact with micellar packaging and gelling and which can be removed



by filtration process. The use of the purer poloxamers, namely the ones with removed low molecular weight copolymer species and consequently with more uniform molecular mass distribution, was related to higher poloxamer gel viscosity (80).

In our case, impurities which are impacting the micellization and are removed by filtration process could originate from synthesis materials and from the glass or plastic packaging or other contact areas during poloxamers or *in situ* gels manufacturing.

Filtration and autoclaving process did not affect viscosity of the PL1 compared to filtration process alone, suggesting that autoclaving is applicable for the P407, as reported before (82).

In conclusion, optimal PL1 *in situ* forming gel retained its beneficial rheological properties after sterilization process, while more detailed structure analysis revealed stronger gel characteristics in comparison to non sterilized sample. These findings support applicability of developed *in situ* gel for ophthalmic use.

## 5.8. Stability study

Sterilized PL 1 optimal *in situ* forming gel, stored in well stopped glass vials, was subjected to preliminary stability study. After 6 months storage at room temperature (20-25°C), temperature and frequency sweeps were performed on an aged sample. Results are presented on the Figure 38 and Figure 39.

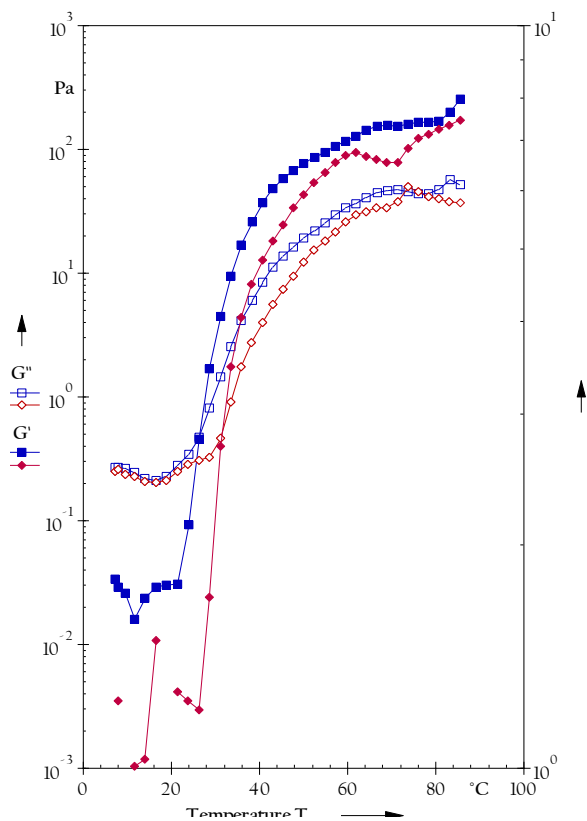


**Figure 38.** Temperature sweeps ( $G'$  filled symbols and  $G''$  empty symbols) for PL 1 optimal *in situ* forming gel at initial point (blue squares) and at 6 months stability of filtered and autoclaved sample (red, diamonds).

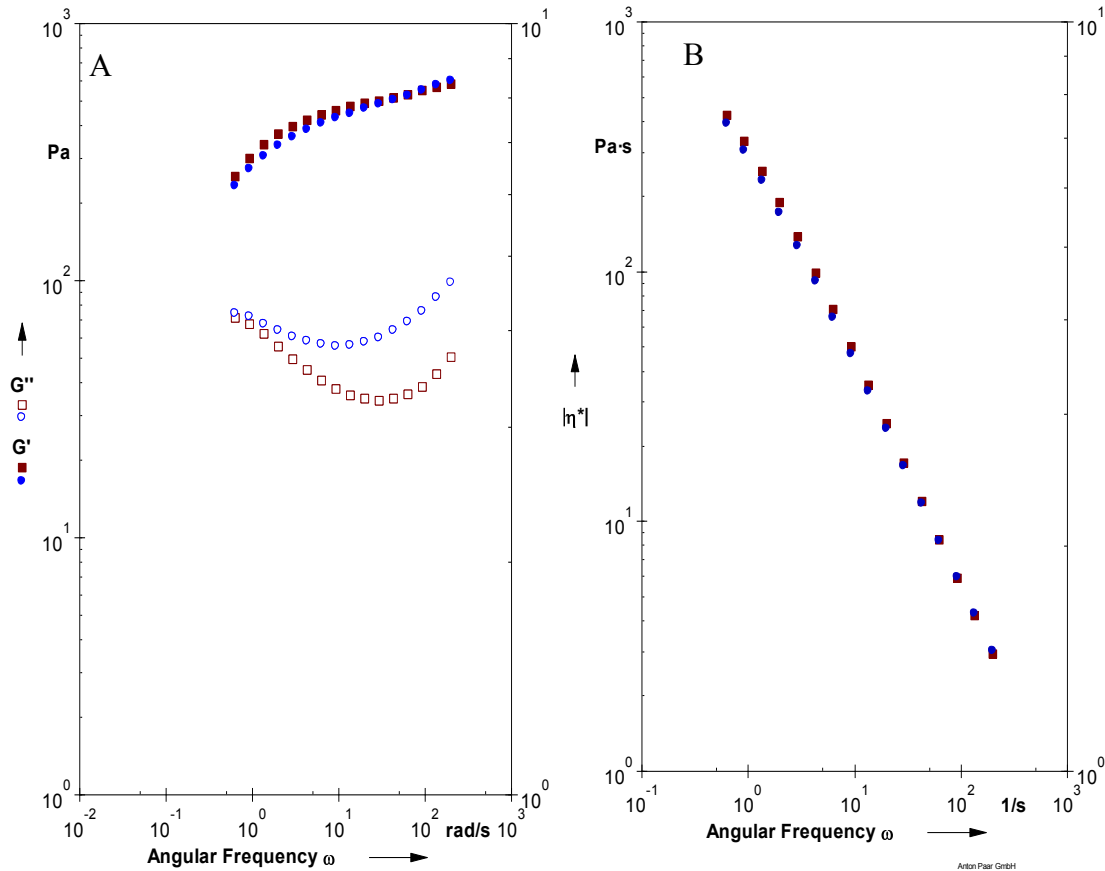


**Figure 39.** Rheological characterization of PL 1 optimal *in situ* forming gel after stability testing. A) Frequency sweep,  $G'$  (filled symbols) and  $G''$  (empty symbols): initial point (blue circles) vs. 6 months stability sample autoclaved (red squares). B) Frequency sweep,  $\eta^*$  initial point (blue circles) vs. 6 months stability sample filtered and autoclaved (red squares).

Results of the preliminary stability study results revealed that no significant change in key rheological properties ( $T_{gel}$ ,  $\eta^*$ ) was noticed for the filtered and autoclaved sample. Moreover, the rheological profiles acquired by the temperature and frequency sweeps at initial point are comparable to the results obtained for an aged sample.

## 5.9. Biocompatibility assessment of *in situ* forming ophthalmic gel

Immortalized human corneal epithelial cell line (HCE-T) is one of the most studied human derived cell lines in terms of transcorneal passive transcellular and paracellular transport, transporter expression and metabolic enzymes (115). In the preliminary ocular biocompatibility studies of developed *in situ* forming gel, simple 2D HCE-T monolayer was used to assess the formulation biocompatibility. However, exaggerated toxicity was found in comparison to *in vivo* studies (154). *In vitro* 2D models are generally characterized by certain shortcomings, such as a more pronounced susceptibility to cytotoxicity, as they replicate only a limited segment of tissue structure/function (119). Consequently, the concentration of polymers/formulation that can be safely applied to such models may be reduced in comparison to the *in vivo* system.

Despite the fact that HCE-T cell line is well defined and characterized, obstacles regarding its routine use were reported. From this reasons, Juretić et al. investigated and described two disctintive phenotypes of HCE-T models, depending on the pore size of polycarbonate membrane. Model I was multilayered HCE-T epithelium cultivated on filters with 0.4  $\mu\text{m}$  pores and Model II consisted of an apical lipophilic HCE-T epithelial monolayer and a basolateral lipophilic monolayer of migrated HCE-T cell cultivated on filters with 3  $\mu\text{m}$  pores. A polycarbonate membrane with a 3  $\mu\text{m}$  pore size (Model II) was proved to be better than a polycarbonate membrane with a 0.4  $\mu\text{m}$  pore size (Model I) for tight barrier formation with HCE-T cells (115).

In order to better predict the ocular tolerability, we employed more complex 3D corneal epithelial models to determine the formulation biocompatibility, namely Model I and Model II (115).

Cell viability was determined with the colorimetric MTT (3-[4,5-dimethylthiazol-2-yl]-2,5-diphenyl tetrazolium bromide assay (48,67,115,116). This assay measures the activity of the mitochondrial enzyme succinate dehydrogenase, which is expressed only in living cells. Acquired signal is proportional to the number of metabolically active (viable) cells (131).

Results of biocompatibility screening revealed, contrary to HCE-T epithelial monolayer, that 3D models showed biocompatibility of the tested formulation (1). Namely, 30-minute treatment resulted in decrease in 3D model cell viability lower than 20% (116).

## **6. CONCLUSIONS**

In this doctoral thesis, a QbD approach was applied in order to determine the minimal total concentrations of P407, P188 and CS that would yield an *in situ* forming ophthalmic gel with the potential to ensure the defined formulation characteristics. D-Optimal design was selected based on the particularities of experimental situation, while sequential approach to experimentation was applied through screening, refining and optimizing designs. Analysis of collected data identified significant cause and effect relationships. Mathematical models describing  $T_{gel}$ ,  $\eta^*$  and  $G'$  with a suitable fit between experimental and predicted values were established. Subsequently, all established models were validated. Concentrations of poloxamer polymers (P407 and P188) were found to have most significant effect on all responses of interest. Decrease of  $T_{gel}$  was related to the increase of P407 concentration while the increase of  $T_{gel}$  when increasing P188 concentration was related to micellization of P188. Significant higher order terms in the model for  $T_{gel}$  included the interactions between P407 and P188 and among P407, P188 and CS. Model obtained for  $\log(\eta^*)$  had higher degree of complexity in comparison to mathematical model for  $T_{gel}$ . Increase of P188 concentration resulted in the decrease of  $\log(\eta^*)$  while on the contrary, the increase of P407 concentration resulted in the increase of  $\log(\eta^*)$ . Surprisingly, impact of CS concentrations on  $\log(\eta^*)$  in the obtained model was hindered by poloxamers effect. Complexity of this model was depicted by the several interactions - two interactions with negative effect on the response (between P407 and CS and as well as between P407 and P188) and two interactions with the positive effect on the response  $\log(\eta^*)$  (among P407, P407 and P188 and between CS and CS). Mathematical model for  $\log(G')$  revealed significant effects of P407 and P188 concentrations on  $\log(G')$  with P407 concentration having stronger effect on the response. The increase of P188 concentration resulted in the decrease of  $\log(G')$  and on the contrary, the increase of P407 concentration resulted in the increase of the response. One statistically significant interaction with positive effect on the  $G'$  was between P188 and CS, while another interaction included in the model was one between P407 and CS with a negative impact on the response, similar to the model for  $\log(\eta^*)$ .

Based on the models established, four lead *in situ* forming gel platforms were selected and in depth rheologically characterized. PL1 was revealed as optimal *in situ* forming gel since it had lowest polymer content and rheological characteristics suitable for *in situ* forming gels.

Robustness of selected PL1 *in situ* forming gel against entrapment of APIs with different physicochemical characteristics was assessed by the in depth rheological characterization (oscillatory and rotational) in biorelevant conditions. Results indicated that all samples acted as gels upon dilution and preserved pseudoplasticity suggesting robustness of the platform against API entrapment. The decrease in  $T_{gel}$  caused by API entrapment opens the possibility to further decrease the concentration of poloxamers required to obtain *in situ* forming gels with appropriate biopharmaceutical properties.

A discriminative and selective *in vitro* release method was developed for characterization of the optimal *in situ* forming gel PL1 as a platform containing TIMO as model drug. Results of *in vitro* release suggested prolonged release related to viscosity of the *in situ* forming gel.

Evaluation of sterilization process by filtration and filtration and autoclaving showed no significant effect on PL1 quality attributes.

After 6 months storage at room temperature (20-25°C), temperature and frequency sweep analysis of aged sterile sample revealed no change in these critical parameters indicating adequate stability.

Biocompatibility of the optimal *in situ* forming gel (PL1) was shown on two 3D cell-based corneal epithelial models, namely multilayered HCE-T epithelium cultivated on filters with 0.4  $\mu\text{m}$  pores and model consisting of an apical lipophilic HCE-T epithelial monolayer and a basolateral lipophilic monolayer of migrated HCE-T cell cultivated on filters with 3  $\mu\text{m}$  pores.

In conclusion, a systematic approach to *in situ* forming gel development implemented in this thesis resulted in a stable and robust formulation characterized by ease of formulation preparation, ability for sterile filtration and autoclaving, ease of administration, accuracy of dosing, avoidance of eye-related discomfort, biocompatibility and prolonged residence at the eye surface. These benefits will lead to better patient compliance, improved eye-related bioavailability and, finally, improved therapeutic outcome.



## REFERENCES

1. Krtalić I, Radošević S, Hafner A, Grassi M, Nenadić M, Cetina-Čizmek B, et al. D-Optimal Design in the Development of Rheologically Improved In Situ Forming Ophthalmic Gel. *J Pharm Sci* [Internet]. 2018 Jun;107(6):1562–71. Available from: <https://doi.org/10.1016/j.xphs.2018.01.019>.
2. Pepić I, Lovrić J, Cetina-Čizmek B, Reichl S, Filipović-Grčić J. Toward the practical implementation of eye-related bioavailability prediction models. *Drug Discov Today* [Internet]. 2014;19(1):31–44. Available from: <https://doi.org/10.1016/j.drudis.2013.08.002>
3. Kirchhof S, Goepferich AM, Brandl FP. Hydrogels in ophthalmic applications. *Eur J Pharm Biopharm* [Internet]. 2015;95:227–38. Available from: <http://dx.doi.org/10.1016/j.ejpb.2015.05.016>
4. Almeida H, Amaral MH, Lobão P, Lobo JMS. In situ gelling systems: A strategy to improve the bioavailability of ophthalmic pharmaceutical formulations. *Drug Discov Today* [Internet]. 2014;19(4):400–12. Available from: <http://dx.doi.org/10.1016/j.drudis.2013.10.001>
5. Zignani M, Tabatabay C, Gurny R. Topical semi-solid drug delivery: kinetics and tolerance of ophthalmic hydrogels. *Adv Drug Deliv Rev* [Internet]. 1995;16(1):51–60. Available from: [https://doi.org/10.1016/0169-409X\(95\)00015-Y](https://doi.org/10.1016/0169-409X(95)00015-Y)
6. Destruel PL, Zeng N, Maury M, Mignet N, Boudy V. In vitro and in vivo evaluation of in situ gelling systems for sustained topical ophthalmic delivery: state of the art and beyond. *Drug Discov Today* [Internet]. 2017;22(4):638–51. Available from: <http://dx.doi.org/10.1016/j.drudis.2016.12.008>
7. El-Kamel AH. In vitro and in vivo evaluation of Pluronic F127-based ocular delivery system for timolol maleate. *Int J Pharm* [Internet]. 2002;241(1):47–55. Available from: [https://doi.org/10.1016/S0378-5173\(02\)00234-X](https://doi.org/10.1016/S0378-5173(02)00234-X)
8. Rupenthal ID, Green CR, Alany RG. Comparison of ion-activated in situ gelling systems for ocular drug delivery. Part 2: Precorneal retention and in vivo pharmacodynamic study. *Int J Pharm* [Internet]. 2011;411(1–2):78–85. Available from: <http://dx.doi.org/10.1016/j.ijpharm.2011.03.043>
9. Almeida H, Amaral MH, Lobão P, Sousa Lobo JM. Applications of poloxamers in ophthalmic pharmaceutical formulations: an overview. *Expert Opin Drug Deliv* [Internet]. 2013;10(9):1223–37. Available from: <https://doi.org/10.1517/17425247.2013.796360>
10. Trong LCP, Djabourov M, Ponton A. Mechanisms of micellization and rheology of PEO–PPO–PEO triblock copolymers with various architectures. *J Colloid Interface Sci* [Internet]. 2008;328(2):278–87. Available from: <https://doi.org/10.1016/j.jcis.2008.09.029>
11. Wei G, Xu H, Ding PT, Li SM, Zheng JM. Thermosetting gels with modulated gelation temperature for ophthalmic use: The rheological and gamma scintigraphic studies. *J Control Release* [Internet]. 2002;83(1):65–74. Available from: [https://doi.org/10.1016/S0168-3659\(02\)00175-X](https://doi.org/10.1016/S0168-3659(02)00175-X)

12. Zhang M, Djabourov M, Bourgaux C, Bouchemal K. Nanostructured fluids from pluronic® mixtures. *Int J Pharm* [Internet]. 2013;454(2):599–610. Available from: <http://dx.doi.org/10.1016/j.ijpharm.2013.01.043>
13. Qi H, Li L, Huang C, Li W, Wu C. Optimization and physicochemical characterization of thermosensitive poloxamer gel containing puerarin for ophthalmic use. *Chem Pharm Bull (Tokyo)* [Internet]. 2006;54(11):1500–7. Available from: <https://doi.org/10.1248/cpb.54.1500>
14. Kim E-Y, Zhong-Gao G, Jeong-Sook P, Li H, Han K. rhEGF / HP-beta-CD complex in poloxamer gel for ophthalmic delivery . *PubMed Commons*. 2002;233:159–167. Available from: [https://doi.org/10.1016/S0378-5173\(01\)00933-4](https://doi.org/10.1016/S0378-5173(01)00933-4)
15. Asasutjarit R, Thanasanchokpipull S, Fuongfuchat A, Veeranondha S. Optimization and evaluation of thermoresponsive diclofenac sodium ophthalmic in situ gels. *Int J Pharm* [Internet]. 2011;411(1–2):128–35. Available from: <http://dx.doi.org/10.1016/j.ijpharm.2011.03.054>
16. Qi H, Chen W, Huang C, Li L, Chen C, Li W, et al. Development of a poloxamer analogs/carbopol-based in situ gelling and mucoadhesive ophthalmic delivery system for puerarin. *Int J Pharm* [Internet]. 2007;337(1–2):178–87. Available from: <https://doi.org/10.1016/j.ijpharm.2006.12.038>
17. Shastri D, Prajapati S, Patel L. Thermoreversible mucoadhesive ophthalmic in situ hydrogel: Design and optimization using a combination of polymers. *Acta Pharm* [Internet]. 2010;60(3):349–60. Available from: <https://doi.org/10.2478/v10007-010-0029-4>
18. Mayol L, Quaglia F, Borzacchiello A, Ambrosio L, La Rotonda MI. A novel poloxamers/hyaluronic acid in situ forming hydrogel for drug delivery: Rheological, mucoadhesive and in vitro release properties. *Eur J Pharm Biopharm* [Internet]. 2008;70(1):199–206. Available from: <https://doi.org/10.1016/j.ejpb.2008.04.025>
19. Ying L, Tahara K, Takeuchi H. Drug delivery to the ocular posterior segment using lipid emulsion via eye drop administration: Effect of emulsion formulations and surface modification. *Int J Pharm* [Internet]. 2013;453(2):329–35. Available from: <http://dx.doi.org/10.1016/j.ijpharm.2013.06.024>
20. Gratieri T, Gelfuso GM, Rocha EM, Sarmiento VH, de Freitas O, Lopez RFV. A poloxamer/chitosan in situ forming gel with prolonged retention time for ocular delivery. *Eur J Pharm Biopharm* [Internet]. 2010;75(2):186–93. Available from: <http://dx.doi.org/10.1016/j.ejpb.2010.02.011>
21. Başaran E, Yazan Y. Ocular application of chitosan. *Expert Opin Drug Deliv* [Internet]. 2012;9(6):701–12. Available from: <https://doi.org/10.1517/17425247.2012.681775>
22. de la Fuente M, Raviña M, Paolicelli P, Sanchez A, Seijo B, Alonso MJ. Chitosan-based nanostructures: A delivery platform for ocular therapeutics. *Adv Drug Deliv Rev* [Internet]. 2010;62(1):100–17. Available from: <http://dx.doi.org/10.1016/j.addr.2009.11.026>

23. Tsai C, Woung L, Yen J, Tseng P, Chiou S, Sung Y, et al. Thermosensitive chitosan-based hydrogels for sustained release of ferulic acid on corneal wound healing. *Carbohydr Polym* [Internet]. 2016;135:308–15. Available from: <https://doi.org/10.1016/j.carbpol.2015.08.098>
24. Gaudana R, Ananthula HK, Parenky A, Mitra AK. Ocular Drug Delivery. *AAPS J* [Internet]. 2010;12(3):348–60. Available from: <https://doi.org/10.1208/s12248-010-9183-3>
25. Lajunen T, Nurmi R, Kontturi L, Viitala L, Yliperttula M, Murtomäki L, et al. Light activated liposomes: Functionality and prospects in ocular drug delivery. *J Control Release* [Internet]. 2016;244:157–66. Available from: <http://dx.doi.org/10.1016/j.jconrel.2016.08.024>
26. Kuno N, Fujii S. Recent advances in ocular drug delivery systems. *Polymers (Basel)* [Internet]. 2011;3(1):193–221. Available from: <https://doi.org/10.3390/polym3010193>
27. Patel A, Cholkar K, Agrahari V, Mitra AK. Ocular drug delivery systems: An overview. *World J Pharmacol* [Internet]. 2013;2(22):47–64. Available from: <http://www.wjgnet.com/esps/%5Chttp://www.wjgnet.com/2220-3192/full/%5Chttp://dx.doi.org/10.5497/wjp.v2.i2.47>
28. Janagam DR, Wu L, Lowe TL. Nanoparticles for drug delivery to the anterior segment of the eye. *Adv Drug Deliv Rev* [Internet]. 2017;122:31–64. Available from: <https://doi.org/10.1016/j.addr.2017.04.001>
29. Rönkkö S, Vellonen K-S, Järvinen K, Toropainen E, Urtti A. Human corneal cell culture models for drug toxicity studies. *Drug Deliv Transl Res* [Internet]. 2016;6(6):660–75. Available from: <https://doi.org/10.1007/s13346-016-0330-y>
30. Cwiklik L. Tear film lipid layer: A molecular level view. *Biochim Biophys Acta - Biomembr* [Internet]. 2016;1858(10):2421–30. Available from: <http://dx.doi.org/10.1016/j.bbamem.2016.02.020>
31. Collins Street Optometrists. Understanding the Tear Film and Dry Eye [Internet]. 2015 [cited 2018 May 5]. Available from: <http://www.collinsoptometrists.com.au/dry-eye-clinic/understanding-the-tear-film-and-dry-eye/>
32. du Toit LC, Pillay V, Choonara YE, Govender T, Carmichael T. Ocular drug delivery – a look towards nanobioadhesives. *Expert Opin Drug Deliv* [Internet]. 2011;8(1):71–94. Available from: <http://www.tandfonline.com/doi/full/10.1517/17425247.2011.542142>
33. McKenzie B, Kay G, Matthews KH, Knott R, Cairns D. Preformulation of cysteamine gels for treatment of the ophthalmic complications in cystinosis. *Int J Pharm* [Internet]. 2016;515(1–2):575–82. Available from: <http://dx.doi.org/10.1016/j.ijpharm.2010.03.065>
34. Järvinen K, Järvinen T, Urtti A. Ocular absorption following topical delivery. *Adv Drug Deliv Rev* [Internet]. 1995;16:3–19. Available from: [https://doi.org/10.1016/0169-409X\(95\)00010-5](https://doi.org/10.1016/0169-409X(95)00010-5)

35. Eghrari AO, Riazuddin SA, Gottsch JD. Progress in Molecular Biology and Translational Science. In: Hejtmancik JF, Nickerson JM, editors. Progress in Molecular Biology and Translational Science [Internet]. Elsevier Inc.; 2015. p. 7–23. Available from: <https://doi.org/10.1016/bs.pmbts.2015.04.001>
36. Cholkar K, Patel SP, Vadlapudi AD, Mitra AK. Novel Strategies for Anterior Segment Ocular Drug Delivery. *J Ocul Pharmacol Ther* [Internet]. 2013;29(2):106–23. Available from: <http://online.liebertpub.com/doi/abs/10.1089/jop.2012.0200>
37. Morrison PW, Khutoryanskiy V V. Advances in ophthalmic drug delivery. *Ther Deliv* [Internet]. 2014;5(12):1297–315. Available from: <http://www.future-science.com/doi/10.4155/tde.14.75>
38. United States Pharmacopeia 40. Physical Tests and Determinations <771> OPHTHALMIC PRODUCTS — QUALITY TESTS. 2017;(Second Supplement to USP 40–NF 35):8589–95.
39. Chetoni P, Burgalassi S, Monti D, Saettone MF. Ocular toxicity of some corneal penetration enhancers evaluated by electrophysiology measurements on isolated rabbit corneas. *Toxicol Vitro* [Internet]. 2003;17(4):497–504. Available from: [https://doi.org/10.1016/S0887-2333\(03\)00052-3](https://doi.org/10.1016/S0887-2333(03)00052-3)
40. Majumdar S, Hippalgaonkar K, Repka MA. Effect of chitosan, benzalkonium chloride and ethylenediaminetetraacetic acid on permeation of acyclovir across isolated rabbit cornea. *Int J Pharm* [Internet]. 2008;348(1–2):175–8. Available from: <https://doi.org/10.1016/j.ijpharm.2007.08.017>
41. United States Pharmacopeia 38. <1151> PHARMACEUTICAL DOSAGE FORMS. In 2016. p. 1278–301.
42. Kulshreshtha AK, Singh ON, Wall GM. Pharmaceutical Suspensions [Internet]. Vol. 53, *Journal of Chemical Information and Modeling*. 2013. 337 p. Available from: doi: 10.1007/978-1-4419-1087-5
43. Shargel L, Kanfer I, editors. Generic drug product development : specialty dosage forms [Internet]. New York: Taylor & Francis Inc, Informa Healthcare; 2016. Available from: <https://www.crcpress.com/Generic-Drug-Product-Development-Specialty-Dosage-Forms/Shargel-Kanfer/p/book/9780849377860>
44. Durezol [Internet]. [cited 2018 Mar 6]. Available from: [https://www.rxlist.com/durezol-drug.htm#indications\\_dosage](https://www.rxlist.com/durezol-drug.htm#indications_dosage)
45. Yellepeddi VK, Palakurthi S. Recent Advances in Topical Ocular Drug Delivery. *J Ocul Pharmacol Ther* [Internet]. 2016;32(2):67–82. Available from: <http://online.liebertpub.com/doi/10.1089/jop.2015.0047>
46. Xu X, Al-Ghabeish M, Rahman Z, Krishnaiah YSR, Yerlikaya F, Yang Y, et al. Formulation and process factors influencing product quality and in vitro performance of ophthalmic ointments. *Int J Pharm* [Internet]. 2015;493(1–2):412–25. Available from: <http://dx.doi.org/10.1016/j.ijpharm.2015.07.066>

47. Al-Kinani AA, Zidan G, Elsaid N, Seyfoddin A, Alani AWG, Alany RG. Ophthalmic gels: Past, present and future. *Adv Drug Deliv Rev* [Internet]. 2017; Available from: <https://doi.org/10.1016/j.addr.2017.12.017>
48. Hafner A, Lovrić J, Romić MD, Juretić M, Pepić I, Cetina-Čižmek B, et al. Evaluation of cationic nanosystems with melatonin using an eye-related bioavailability prediction model. *Eur J Pharm Sci* [Internet]. 2015;75:142–50. Available from: <https://doi.org/10.1016/j.ejps.2015.04.003>
49. Le Broulais C, Acar L, Zia H, Sado PA, Needham T, Leverge R. Ophthalmic drug delivery systems - Recent advances. *Prog Retin Eye Res* [Internet]. 1998;17(1):33–58. Available from: [https://doi.org/10.1016/S1350-9462\(97\)00002-5](https://doi.org/10.1016/S1350-9462(97)00002-5)
50. Ali HSM, York P, Ali AMA, Blagden N. Hydrocortisone nanosuspensions for ophthalmic delivery: A comparative study between microfluidic nanoprecipitation and wet milling. *J Control Release* [Internet]. 2011;149(2):175–81. Available from: <http://dx.doi.org/10.1016/j.jconrel.2010.10.007>
51. Singh Y, Meher JG, Raval K, Khan FA, Chaurasia M, Jain NK, et al. Nanoemulsion: Concepts, development and applications in drug delivery. *J Control Release* [Internet]. 2017;252:28–49. Available from: <http://dx.doi.org/10.1016/j.jconrel.2017.03.008>
52. Mandal A, Bisht R, Rupenthal ID, Mitra AK. Polymeric micelles for ocular drug delivery: From structural frameworks to recent preclinical studies. *J Control Release* [Internet]. 2017;248:96–116. Available from: <http://dx.doi.org/10.1016/j.jconrel.2017.01.012>
53. Hafner A, Lovrić J, Lakoš GP, Pepić I. Nanotherapeutics in the EU: an overview on current state and future directions. *Int J Nanomedicine* [Internet]. 2014;9:1005–23. Available from: <https://doi.org/10.2147/IJN.S55359>
54. Pepić I, Lovrić J, Filipović-Grčić J. How do polymeric micelles cross epithelial barriers? *Eur J Pharm Sci* [Internet]. 2013;50(1):42–55. Available from: <https://doi.org/10.1016/j.ejps.2013.04.012>
55. Sahoo SK, Dilnawaz F, Krishnakumar S. Nanotechnology in ocular drug delivery. *Drug Discov Today* [Internet]. 2008;13(3–4):144–51. Available from: <https://doi.org/10.1016/j.drudis.2007.10.021>
56. Moghassemi S, Hadjizadeh A. Nano-niosomes as nanoscale drug delivery systems: An illustrated review. *J Control Release* [Internet]. 2014;185(1):22–36. Available from: <http://dx.doi.org/10.1016/j.jconrel.2014.04.015>
57. Achouri D, Alhanout K, Piccerelle P, Andrieu V. Recent advances in ocular drug delivery. *Drug Dev Ind Pharm* [Internet]. 2013;39(11):1599–617. Available from: <https://doi.org/10.3109/03639045.2012.736515>
58. Yavuz B, Pehlivan SB, Unlu N. Dendrimeric systems and their applications in ocular drug delivery. *ScientificWorldJournal* [Internet]. 2013;2013:732340. Available from: <http://dx.doi.org/10.1155/2013/732340>

59. Agrawal AK, Das M, Jain S, Furrer P, Plazonnet B, Mayer JM, et al. *In situ* gel systems as “smart” carriers for sustained ocular drug delivery. *J Pharm Sci* [Internet]. 2000;9(1–2):383–402. Available from: <http://www.tandfonline.com/doi/full/10.1517/17425247.2012.665367>
60. Gupta P, Vermani K, Garg S. Hydrogels: from controlled release to pH-responsive drug delivery. *Drug Discov Today* [Internet]. 2002;7(10):569–79. Available from: [https://doi.org/10.1016/S1359-6446\(02\)02255-9](https://doi.org/10.1016/S1359-6446(02)02255-9)
61. Qiu Y, Park K. Environment-sensitive hydrogels for drug delivery. *Adv Drug Deliv Rev* [Internet]. 2012;64(SUPPL.):49–60. Available from: <http://dx.doi.org/10.1016/j.addr.2012.09.024>
62. Schmaljohann D. Thermo- and pH-responsive polymers in drug delivery. *Adv Drug Deliv Rev* [Internet]. 2006;58(15):1655–70. Available from: <https://doi.org/10.1016/j.addr.2006.09.020>
63. Ceulemans J, Ludwig A. Optimisation of carbomer viscous eye drops: An in vitro experimental design approach using rheological techniques. *Eur J Pharm Biopharm* [Internet]. 2002;54(1):41–50. Available from: [https://doi.org/10.1016/S0939-6411\(02\)00036-X](https://doi.org/10.1016/S0939-6411(02)00036-X)
64. Rupenthal ID, Green CR, Alany RG. Comparison of ion-activated in situ gelling systems for ocular drug delivery. Part 1: Physicochemical characterisation and in vitro release. *Int J Pharm* [Internet]. 2011;411(1–2):69–77. Available from: <http://dx.doi.org/10.1016/j.ijpharm.2011.03.042>
65. Paulsson M, Hägerström H, Edsman K. Rheological studies of the gelation of deacetylated gellan gum (Gelrite®) in physiological conditions. *Eur J Pharm Sci* [Internet]. 1999;9(1):99–105. Available from: [https://doi.org/10.1016/S0928-0987\(99\)00051-2](https://doi.org/10.1016/S0928-0987(99)00051-2)
66. Clarkson University. Responsive alginate hydrogels [Internet]. [cited 2018 Apr 30]. Available from: [http://people.clarkson.edu/~amelman/alginate\\_hydrogels.html](http://people.clarkson.edu/~amelman/alginate_hydrogels.html)
67. Dukovski Jurišić B, Plantić I, Čunčić I, Krtalić I, Juretić M, Pepić I, et al. Lipid/alginate nanoparticle-loaded in situ gelling system tailored for dexamethasone nasal delivery. *Int J Pharm* [Internet]. 2017;533(2):480–7. Available from: <https://doi.org/10.1016/j.ijpharm.2017.05.065>
68. Ruel-Gariépy E, Leroux JC. In situ-forming hydrogels - Review of temperature-sensitive systems. *Eur J Pharm Biopharm* [Internet]. 2004;58(2):409–26. Available from: <https://doi.org/10.1016/j.ejpb.2004.03.019>
69. Matanović MR, Kristl J, Grabnar PA. Thermoresponsive polymers: Insights into decisive hydrogel characteristics, mechanisms of gelation, and promising biomedical applications. *Int J Pharm* [Internet]. 2014;472(1–2):262–75. Available from: <http://dx.doi.org/10.1016/j.ijpharm.2014.06.029>
70. Gratieri T, Gelfuso GM, De Freitas O, Rocha EM, Lopez RFV. Enhancing and sustaining the topical ocular delivery of fluconazole using chitosan solution and poloxamer/chitosan in situ forming gel. *Eur J Pharm Biopharm* [Internet]. 2011;79(2):320–7. Available from: <http://dx.doi.org/10.1016/j.ejpb.2011.05.006>

71. Desai SD, Blanchard J. In vitro evaluation of pluronic F127 based controlled release ocular delivery systems for pilocarpine. *J Pharm Sci* [Internet]. 1998;87(2):226–30. Available from: <https://doi.org/10.1016/j.ejpb.2011.05.006>
72. Ammar HO, Salama HA, Ghorab M, Mahmoud AA. Development of dorzolamide hydrochloride in situ gel nanoemulsion for ocular delivery. *Drug Dev Ind Pharm* [Internet]. 2010;36(11):1330–9. Available from: <https://doi.org/10.3109/03639041003801885>
73. Charoo NA, Kohli K, Ali A. Preparation of In Situ -Forming Ophthalmic Gels of Ciprofloxacin Hydrochloride for the Treatment of Bacterial Conjunctivitis : In Vitro and In Vivo Studies. 2003;92(2):407–13. Available from: <https://doi.org/10.1002/jps.10290>
74. Bain MK, Bhowmik M, Ghosh SN, Chattopadhyay D. In Situ Fast Gelling Formulation of Methyl Cellulose for In Vitro Ophthalmic Controlled Delivery of Ketorolac Tromethamine. *J Appl Polym Sci* [Internet]. 2009;113:1241–1246. Available from: <https://doi.org/10.1002/app.30040>
75. Miyazaki S, Suzuki S, Kawasaki N, Endo K, Takahashi A, Attwood D. In situ gelling xyloglucan formulations for sustained release ocular delivery of pilocarpine hydrochloride. *Int J Pharm* [Internet]. 2001;229(1–2):29–36. Available from: [https://doi.org/10.1016/S0378-5173\(01\)00825-0](https://doi.org/10.1016/S0378-5173(01)00825-0)
76. Mahajan HS, Deshmukh SR. Development and evaluation of gel-forming ocular films based on xyloglucan. *Carbohydr Polym* [Internet]. 2015;122:243–7. Available from: <http://dx.doi.org/10.1016/j.carbpol.2015.01.018>
77. Hsiue GH, Hsu SH, Yang CC, Lee SH, Yang IK. Preparation of controlled release ophthalmic drops, for glaucoma therapy using thermosensitive poly-N-isopropylacrylamide. *Biomaterials* [Internet]. 2002;23(2):457–62. Available from: [https://doi.org/10.1016/S0142-9612\(01\)00127-2](https://doi.org/10.1016/S0142-9612(01)00127-2)
78. Gao Y, Sun Y, Ren F, Gao S. PLGA-PEG-PLGA hydrogel for ocular drug delivery of dexamethasone acetate. *Drug Dev Ind Pharm* [Internet]. 2010;36(10):1131–8. Available from: <https://doi.org/10.3109/03639041003680826>
79. Pham Trong LC, Djabourov M, Ponton A, Trong LCP, Djabourov M, Ponton A. Mechanisms of micellization and rheology of PEO–PPO–PEO triblock copolymers with various architectures. *J Colloid Interface Sci* [Internet]. 2008;328(2):278–87. Available from: <http://dx.doi.org/10.1016/j.jcis.2008.09.029>
80. Fakhari A, Corcoran M, Schwarz A. Thermogelling properties of purified poloxamer 407. *Heliyon* [Internet]. 2017;3(8):1–26. Available from: <http://dx.doi.org/10.1016/j.heliyon.2017.e00390>
81. EUROPEAN PHARMACOPOEIA 8.5. Poloxamers. 2008;2307–9.
82. Dumortier G, Grossiord JL, Agnely F, Chaumeil JC. A review of poloxamer 407 pharmaceutical and pharmacological characteristics. *Pharm Res* [Internet]. 2006;23(12):2709–28. Available from: <https://doi.org/10.3109/03639041003680826>

83. Gupta S, Samanta MK. Design and evaluation of thermoreversible in situ gelling system of forskolin for the treatment of glaucoma. *Pharm Dev Technol* [Internet]. 2010;15(4):386–93. Available from: <https://doi.org/10.3109/10837450903262033>
84. Al Khateb K, Ozhmukhametova EK, Mussin MN, Seilkhanov SK, Rakhypbekov TK, Lau WM, et al. In situ gelling systems based on Pluronic F127/Pluronic F68 formulations for ocular drug delivery. *Int J Pharm* [Internet]. 2016;502(1–2):70–9. Available from: <http://dx.doi.org/10.1016/j.ijpharm.2016.02.027>
85. M.A. Fathalla Z, Vangala A, Longman M, Khaled KA, Hussein AK, El-Garhy OH, et al. Poloxamer-based thermoresponsive ketorolac tromethamine in situ gel preparations: Design, characterisation, toxicity and transcorneal permeation studies. *Eur J Pharm Biopharm* [Internet]. 2017;114:119–34. Available from: <http://dx.doi.org/10.1016/j.ejpb.2017.01.008>
86. Lihong W, Xin C, Yongxue G, Yiyang B, Gang C. Thermoresponsive ophthalmic poloxamer/tween/carbopol in situ gels of a poorly water-soluble drug fluconazole: Preparation and in vitro-in vivo evaluation. *Drug Dev Ind Pharm* [Internet]. 2014;40(10):1402–10. Available from: <https://doi.org/10.3109/03639045.2013.828221>
87. Edsman K, Carlfors J, Petersson R. Rheological evaluation of Gelrite® in situ gels for ophthalmic use. *Eur J Pharm Sci* [Internet]. 1998;6(2):105–12. Available from: [https://doi.org/10.1016/S0928-0987\(97\)00074-2](https://doi.org/10.1016/S0928-0987(97)00074-2)
88. Dewan M, Sarkar G, Bhowmik M, Das B, Chattoapadhyay AK, Rana D, et al. Effect of gellan gum on the thermogelation property and drug release profile of Poloxamer 407 based ophthalmic formulation. *Int J Biol Macromol* [Internet]. 2017;102:258–65. Available from: <http://dx.doi.org/10.1016/j.ijbiomac.2017.03.194>
89. Geethalakshmi A, Karki R, Sagi P, Jha SK, Venkatesh DP. Temperature triggered in situ gelling system for betaxolol in glaucoma. *J Appl Pharm Sci* [Internet]. 2013;3(2):153–9. Available from: [http://japsonline.com/admin/php/uploads/804\\_pdf.pdf](http://japsonline.com/admin/php/uploads/804_pdf.pdf)
90. Akash MSH, Rehman K. Recent progress in biomedical applications of pluronic (PF127): Pharmaceutical perspectives. *J Control Release* [Internet]. 2015;209:120–38. Available from: <http://dx.doi.org/10.1016/j.jconrel.2015.04.032>
91. Cafaggi S, Russo E, Caviglioli G, Parodi B, Stefani R, Sillo G, et al. Poloxamer 407 as a solubilising agent for tolfenamic acid and as a base for a gel formulation. *Eur J Pharm Sci* [Internet]. 2008;35(1–2):19–29. Available from: <https://doi.org/10.1016/j.ejps.2008.05.010>
92. Hong-Ru Lin, K. C. Sung and W-JV. In Situ Gelling of Alginate/Pluronic Solutions for Ophthalmic Delivery of Pilocarpine. *Biomacromolecules* [Internet]. 2004;5(6):2358–2365. Available from: <https://pubs.acs.org/doi/pdf/10.1021/bm0496965>
93. Rinaudo M. Chitin and chitosan: Properties and applications. *Prog Polym Sci* [Internet]. 2006;31(7):603–32. Available from: <https://doi.org/10.1016/j.progpolymsci.2006.06.001>
94. Kean T, Thanou M. Biodegradation, biodistribution and toxicity of chitosan. *Adv Drug Deliv Rev* [Internet]. 2010;62(1):3–11. Available from: <http://dx.doi.org/10.1016/j.addr.2009.09.004>



95. Felt O, Furrer P, Mayer JM, Plazonnet B, Buri P, Gurny R. Topical use of chitosan in ophthalmology: Tolerance assessment and evaluation of precorneal retention. *Int J Pharm* [Internet]. 1999;180(2):185–93. Available from: [https://doi.org/10.1016/S0378-5173\(99\)00003-4](https://doi.org/10.1016/S0378-5173(99)00003-4)
96. Pepić I, Hafner A, Lovrić J, Pirkić B, Filipović-Grčić J. A Nonionic Surfactant/Chitosan Micelle System in an Innovative Eye Drop Formulation. *J Pharm Sci* [Internet]. 2010;99(10):4317–25. Available from: <https://doi.org/10.1002/jps.22137>
97. Slomkowski S, Alemán J V., Gilbert RG, Hess M, Horie K, Jones RG, et al. Terminology of polymers and polymerization processes in dispersed systems (IUPAC Recommendations 2011). *Pure Appl Chem* [Internet]. 2011;83(12):2229–59. Available from: <https://www.degruyter.com/view/j/pac.2011.83.issue-12/pac-rec-10-06-03/pac-rec-10-06-03.xml>
98. Almdal K, Dyre J, Hvidt S, Kramer O. Towards a phenomenological definition of the term “gel.” *Polym Gels Networks* [Internet]. 1993;1(1):5–17. Available from: [https://doi.org/10.1016/0966-7822\(93\)90020-I](https://doi.org/10.1016/0966-7822(93)90020-I)
99. Picout DR, Ross-Murphy SB. Rheology of Biopolymer Solutions and Gels. *Sci World J* [Internet]. 2003;3:105–21. Available from: <http://dx.doi.org/10.1100/tsw.2003.15>
100. Mezger TG. *The Rheology Handbook*. 4th ed. Hannover: Vincentz Network; 2014.
101. Kojarunchitt T, Baldursdottir S, Dong Y Da, Boyd BJ, Rades T, Hook S. Modified thermoresponsive Pluronic 407 and chitosan sol-gels as potential sustained-release vaccine delivery systems. *Eur J Pharm Biopharm* [Internet]. 2015;89:74–81. Available from: <http://dx.doi.org/10.1016/j.ejpb.2014.11.026>
102. Bang F, Cech T, Soergel F. Evaluating the impact of various additives upon the gel-point temperature of aqueous pluronic-based formulations. In Edinburgh, Scotland.: 42nd CRS Annual Meeting & Exposition,; 2015. Available from: [https://www.controlledreleasesociety.org/meetings/Documents/2015\\_Abstracts/100032.pdf](https://www.controlledreleasesociety.org/meetings/Documents/2015_Abstracts/100032.pdf)
103. Malvern Instruments Worldwide. Time to spec up ? Top five reasons to replace a viscometer with a rheometer [Internet]. 2016. Available from: <https://www.malvernpanalytical.com/en/learn/knowledge-center/whitepapers/WP160612FiveReasonsViscometerRheometer>
104. Mezger TG. Rheology Glossary - Oscillatory Tests [Internet]. [cited 2018 Jun 5]. Available from: [http://www.world-of-rheology.com/glossary/entries/definition/oscillatory\\_tests/](http://www.world-of-rheology.com/glossary/entries/definition/oscillatory_tests/)
105. Mezger TG. Rheology Glossary - Amplitude sweeps [Internet]. [cited 2018 Apr 30]. Available from: [http://www.world-of-rheology.com/glossary/entries/definition/amplitude\\_sweeps/](http://www.world-of-rheology.com/glossary/entries/definition/amplitude_sweeps/)
106. Mezger TG. Rheology Glossary - Frequency Sweeps [Internet]. [cited 2018 Apr 30]. Available from: [http://www.world-of-rheology.com/glossary/entries/definition/frequency\\_sweeps/](http://www.world-of-rheology.com/glossary/entries/definition/frequency_sweeps/)

107. Willenbacher N, Georgieva K. Rheology of disperse systems [Internet]. Product design and engineering: Formulation of gels and pastes. 2013. p. 7–49. Available from: [https://www.mvm.kit.edu/download/Rheology\\_of\\_disperse\\_systems\\_Buch\\_Wiley\\_2013.pdf](https://www.mvm.kit.edu/download/Rheology_of_disperse_systems_Buch_Wiley_2013.pdf)
108. Mezger TG. Rheology Glossary - Rotational Tests [Internet]. Available from: [http://www.world-of-rheology.com/glossary/entries/definition/rotational\\_tests/](http://www.world-of-rheology.com/glossary/entries/definition/rotational_tests/)
109. Politis SN, Colombo P, Colombo G, Rekkas DM. Design of experiments (DoE) in pharmaceutical development. Drug Dev Ind Pharm [Internet]. 2017;43(6):889–901. Available from: <http://dx.doi.org/10.1080/03639045.2017.1291672>
110. Simões A, Veiga F, Figueiras A, Vitorino C. A practical framework for implementing Quality by Design to the development of topical drug products: Nanosystem-based dosage forms. Int J Pharm [Internet]. 2018;548(1):385–99. Available from: <https://doi.org/10.1016/j.ijpharm.2018.06.052>
111. International Conference on Harmonisation (ICH). Pharmaceutical Development Q8. ICH Harmon Tripart Guidel [Internet]. 2009;8(August):1–28. Available from: [https://www.ich.org/fileadmin/Public\\_Web\\_Site/ICH\\_Products/Guidelines/Quality/Q8\\_R1/Step4/Q8\\_R2\\_Guideline.pdf](https://www.ich.org/fileadmin/Public_Web_Site/ICH_Products/Guidelines/Quality/Q8_R1/Step4/Q8_R2_Guideline.pdf)
112. Yu LX. Pharmaceutical Quality by Design: Product and Process Development, Understanding, and Control. Pharm Res [Internet]. 2008;25(4):781–91. Available from: <https://doi.org/10.1007/s11095-007-9511-1>
113. Li J, Qiao Y, Wu Z. Nanosystem trends in drug delivery using quality-by-design concept. J Control Release [Internet]. 2017;256(January):9–18. Available from: <http://dx.doi.org/10.1016/j.jconrel.2017.04.019>
114. Pramod K, Tahir Ma, Charoo N, Ansari S, Ali J. Pharmaceutical product development: A quality by design approach. Int J Pharm Investig [Internet]. 2016;6(3):129–38. Available from: <http://doi.org/10.4103/2230-973X.187350>
115. Juretić M, Jurišić Dukovski B, Krtalić I, Reichl S, Cetina-Čižmek B, Filipović-Grčić J, et al. HCE-T cell-based permeability model: A well-maintained or a highly variable barrier phenotype? Eur J Pharm Sci [Internet]. 2017;104:23–30. Available from: <http://dx.doi.org/10.1016/j.ejps.2017.03.018>
116. Takeuchi S, Kwon S. In Vitro Methods for Predicting Ocular Irritation [Internet]. In Vitro Toxicology. Elsevier Inc.; 2017. 209-219 p. Available from: <https://doi.org/10.1016/B978-0-12-804667-8.00011-0>
117. Wilson SL, Ahearne M, Hopkinson A. An overview of current techniques for ocular toxicity testing. Toxicology [Internet]. 2015;327:32–46. Available from: <http://dx.doi.org/10.1016/j.tox.2014.11.003>
118. Laschke MW, Menger MD. Life is 3D: Boosting Spheroid Function for Tissue Engineering. Trends Biotechnol [Internet]. 2017;35(2):133–44. Available from: <https://doi.org/10.1016/j.tibtech.2016.08.004>

119. Kathleen A. Fitzgerald, Meenakshi Malhotra, Caroline M. Curtin, Fergal J. O' Brien CMOD. Life in 3D is never flat: 3D models to optimise drug delivery. *J Control Release* [Internet]. 2015;215:39–54. Available from: <https://doi.org/10.1016/j.jconrel.2015.07.020>
120. United States Pharmacopeia 41. Solutions; Buffer solutions. 2018;5748–9.
121. Schmolka IR. Artificial Skin I . Preparation and Properties Treatment of Burns. *J Biomed Mater Res* [Internet]. 1972;6:571–82. Available from: <https://doi.org/10.1002/jbm.820060609>
122. Ammar HO, Salama HA, Ghorab M, Mahmoud AA. Nanoemulsion as a Potential Ophthalmic Delivery System for Dorzolamide Hydrochloride. *AAPS PharmSciTech* [Internet]. 2009;10(3):808–19. Available from: <http://www.springerlink.com/index/10.1208/s12249-009-9268-4>
123. OELCHECK. Dyn. viscosity (rheometer) [Internet]. Available from: <https://en.oelcheck.com/analyses/test-methods/dyn-viscosity-rheometer-greases/>
124. Hanson Research. Vision® Microette™ [Internet]. [cited 2018 Mar 5]. Available from: [http://www.hansonresearch.it/prod\\_visio\\_microette\\_en.html](http://www.hansonresearch.it/prod_visio_microette_en.html)
125. Hanson Research. Hanson Buyer ' s Guide. 2013;2014(January). Available from: <https://files.hansonresearch.com/wp-content/uploads/2015/06/99300001-Hanson-Buyers-Guide-Rev-3-14-lo-res.pdf>
126. Jug M, Hafner A, Lovrić J, Kregar ML, Pepić I, Vanić Ž, et al. An overview of in vitro dissolution/release methods for novel mucosal drug delivery systems. *J Pharm Biomed Anal* [Internet]. 2018; Available from: <https://doi.org/10.1016/j.jpba.2017.06.072>
127. United States Pharmacopeia 39. < 1724 > Semisolid Drug Products — Performance. 2013;1869–81.
128. Bao Q, Shen J, Jog R, Zhang C, Newman B, Wang Y, et al. In vitro release testing method development for ophthalmic ointments. *Int J Pharm* [Internet]. 2017;526(1–2):145–56. Available from: <http://dx.doi.org/10.1016/j.ijpharm.2017.04.075>
129. Food and Drug Administration. Semisolid Dosage Forms Scale-Up and Postapproval Changes: Chemistry, Manufacturing, and Controls; In Vitro Release Testing and In Vivo Bioequivalence Documentation [Internet]. Center for Drug Evaluation and Research. 1997. Available from: <https://www.fda.gov/downloads/drugs/guidances/ucm070930.pdf>
130. International Conference on Harmonisation of Technical Requirements for Registration of Pharmaceuticals for Human Use. ICH Harmonised Tripartite Guideline; VALIDATION OF ANALYTICAL PROCEDURES: TEXT AND METHODOLOGY Q2(R1). Vol. 1994. Geneva, Switzerland; 2005.
131. Pauly A, Meloni M, Brignole-Baudouin F, Warnet JM, Baudouin C. Multiple endpoint analysis of the 3D-Reconstituted corneal epithelium after treatment with benzalkonium chloride: Early detection of toxic damage. *Investig Ophthalmol Vis Sci* [Internet]. 2009;50(4):1644–52. Available from: <https://doi.org/10.1167/iovs.08-2992>

132. Bodea A, Leucuta SE. Optimization of hydrophilic matrix tablets using a D-optimal design. *Int J Pharm* [Internet]. 1997;153(2):247–55. Available from: [https://doi.org/10.1016/S0378-5173\(97\)00117-8](https://doi.org/10.1016/S0378-5173(97)00117-8)
133. Gupta H, Jain S, Mathur R, Mishra P, Mishra AK, Velpandian T. Sustained ocular drug delivery from a temperature and pH triggered novel in situ gel system. *Drug Deliv* [Internet]. 2007;14(8):507–15. Available from: <https://doi.org/10.1080/10717540701606426>
134. Kojarunchitt T, Hook S, Rizwan S, Rades T, Baldursdottir S. Development and characterisation of modified poloxamer 407 thermoresponsive depot systems containing cubosomes. *Int J Pharm* [Internet]. 2011;408(1–2):20–6. Available from: <http://dx.doi.org/10.1016/j.ijpharm.2011.01.037>
135. Aka-Any-Grah A, Bouchemal K, Koffi A, Agnely F, Zhang M, Djabourov M, et al. Formulation of mucoadhesive vaginal hydrogels insensitive to dilution with vaginal fluids. *Eur J Pharm Biopharm* [Internet]. 2010;76(2):296–303. Available from: <http://dx.doi.org/10.1016/j.ejpb.2010.07.004>
136. Arbelaez-Camargo D, Suñé-Negre JM, Roig-Carreras M, García-Montoya E, Pérez-Lozano P, Miñarro-Carmona M, et al. Preformulation and characterization of a lidocaine hydrochloride and dexamethasone sodium phosphate thermo-reversible and bioadhesive long-acting gel for intraperitoneal administration. *Int J Pharm* [Internet]. 2016;498(1–2):142–52. Available from: <http://dx.doi.org/10.1016/j.ijpharm.2015.12.012>
137. Meznarich NAK, Juggernauth KA, Batzli KM, Love BJ. Structural Changes in PEO- PPO -PEO Gels Induced by Methylparaben and Dexamethasone Observed Using Time-Resolved SAXS. *Macromolecules* [Internet]. 2011;44:7792–8. Available from: <https://doi.org/10.1021/ma2015358>
138. Sharma PK, Bhatia SR. Effect of anti-inflammatories on Pluronic® F127: Micellar assembly, gelation and partitioning. *Int J Pharm* [Internet]. 2004;278(2):361–77. Available from: <https://doi.org/10.1016/j.ijpharm.2004.03.029>
139. Scherlund M, Brodin A, Malmsten M. Micellization and gelation in block copolymer systems containing local anesthetics. *Int J Pharm* [Internet]. 2000;211(1–2):37–49. Available from: [https://doi.org/10.1016/S0378-5173\(00\)00589-5](https://doi.org/10.1016/S0378-5173(00)00589-5)
140. Jeong B, Kim SW, Bae YH. Thermosensitive sol-gel reversible hydrogels. *Adv Drug Deliv Rev* [Internet]. 2012;64(SUPPL.):154–62. Available from: <http://dx.doi.org/10.1016/j.addr.2012.09.012>
141. Van Hemelrijck C, Müller-Goymann CC. Rheological characterization and permeation behavior of poloxamer 407-based systems containing 5-aminolevulinic acid for potential application in photodynamic therapy. *Int J Pharm* [Internet]. 2012;437(1–2):120–9. Available from: <http://dx.doi.org/10.1016/j.ijpharm.2012.07.048>
142. Jaiswal M, Kumar M, Pathak K. Zero order delivery of itraconazole via polymeric micelles incorporated in situ ocular gel for the management of fungal keratitis. *Colloids Surfaces B Biointerfaces* [Internet]. 2015;130:23–30. Available from: <http://dx.doi.org/10.1016/j.colsurfb.2015.03.059>

143. Morsi N, Ghorab D, Refai H, Teba H. Ketorolac tromethamine loaded nanodispersion incorporated into thermosensitive in situ gel for prolonged ocular delivery. *Int J Pharm* [Internet]. 2016;506(1–2):57–67. Available from: <http://dx.doi.org/10.1016/j.ijpharm.2016.04.021>
144. Sharma PK, Reilly MJ, Bhatia SK, Sakhitab N, Archambault JD, Bhatia SR. Effect of pharmaceuticals on thermoreversible gelation of PEO-PPO-PEO copolymers. *Colloids Surfaces B Biointerfaces* [Internet]. 2008;63(2):229–35. Available from: <https://doi.org/10.1016/j.colsurfb.2007.12.009>
145. Zatz JL, Segers JD. Techniques for measuring in vitro release from semisolids. *Dissolution Technol* [Internet]. 1998;5(1):3–17. Available from: [dx.doi.org/10.14227/DT050198P3](http://dx.doi.org/10.14227/DT050198P3)
146. Food and Drug Administration. Draft Guidance on Lanreotide Acetate [Internet]. 2014. Available from: <https://www.fda.gov/downloads/Drugs/GuidanceComplianceRegulatoryInformation/Guidances/UCM406278.pdf>
147. Food and Drug Administration. Draft Guidance on Cyclosporine [Internet]. 2013. Available from: <https://www.fda.gov/downloads/Drugs/GuidanceComplianceRegulatoryInformation/Guidances/ucm358114.pdf>
148. Food and Drug Administration. Draft Guidance on Acyclovir [Internet]. 2012. Available from: <https://www.fda.gov/downloads/drugs/guidancecomplianceregulatoryinformation/guidances/ucm296733.pdf>
149. Tan G, Yu S, Pan H, Li J, Liu D, Yuan K, et al. Bioadhesive chitosan-loaded liposomes: a more efficient and higher permeable ocular delivery platform for timolol maleate. *Int J Biol Macromol* [Internet]. 2017;94:355–63. Available from: <https://doi.org/10.1016/j.ijbiomac.2016.10.035>
150. Grassi M, Grassi G, Lapasin R, Colombo I. Understanding Drug Release and Absorption Mechanisms A PHYSICAL and MATHEMATICAL APPROACH [Internet]. Boca Raton, FL, USA: CRC Press, Taylor & Francis Group; 2007. Available from: <https://www.crcpress.com/Understanding-Drug-Release-and-Absorption-Mechanisms-A-Physical-and-Mathematical/Grassi-Grassi-Lapasin-Colombo/p/book/9780849330872>
151. Lusina Kregar M, Dürriegl M, Rožman A, Jelčić Ž, Cetina-Čižmek B, Filipović-Grčić J. Development and validation of an in vitro release method for topical particulate delivery systems c. 2015;485:202–14. Available from: <https://doi.org/10.1016/j.ijpharm.2015.03.018>
152. United States Pharmacopeia. <1211> Sterilization and Sterility Assurance of Compendial Articles. *Gen Inf*. 2015;USP 40:1744–9.
153. Aulton M, Taylor K, editors. *Aulton's Pharmaceutics* [Internet]. 5th ed. Elsevier; 2017. Available from: <https://www.elsevier.com/books/aaultons-pharmaceutics/aulton/978-0-7020-7005-1>

154. Furrer B, Plazonnet, Mayer J., Gurny R. Application of in vivo confocal microscopy to the objective evaluation of ocular irritation induced by surfactants. *Int J Pharm* [Internet]. 2000;207(1–2):89–98. Available from: [https://doi.org/10.1016/S0378-5173\(00\)00540-8](https://doi.org/10.1016/S0378-5173(00)00540-8)

## **BIOGRAPHY**

Iva Krtalić (née Ujdur) was born on January 2<sup>nd</sup> 1982 in Metković, Croatia. She finished elementary school and the Mathematical gymnasium in Metković. She graduated from the Faculty of Pharmacy and Biochemistry, University of Zagreb, in 2005.

Since 2006 she works for PLIVA Croatia Ltd. in Generic Research and Development in Zagreb. From 2006 till 2013 she worked as a Researcher - Analyst and specialized for development and validation of standard and innovative *in vitro* release methods for modified release parenteral products and oral dosage forms.

In 2008 she enrolled in postgraduate doctoral study “Pharmaceutical-Biochemical Sciences” at the Faculty of Pharmacy and Biochemistry, University of Zagreb and in 2012 she joined project “Development of *in vitro* and *ex vivo* models for permeability testing of new topical ophthalmic formulations“ (Partnership in research: 04.01/56, Croatian science foundation and PLIVA Croatia Ltd.). Her doctoral thesis research was conducted as a part of this project.

Since 2013 she works as Principal scientist, Analytical Project Leader where she contributes scientifically to the development of complex sterile drug products.

She co-authored three peer-reviewed papers and participated in different international scientific workshops and conferences.

#### **List of Publications:**

**Krtalić I.**, Radošević S., Hafner A., Grassi M, Nenadić M., Cetina-Čižmek B., Filipović-Grčić J., Pepić I., Lovrić J. D-Optimal Design in the Development of Rheologically Improved In Situ Forming Ophthalmic Gel, *Journal of Pharmaceutical Sciences*, 2018;107:1562-1571.

Jurišić Dukovski, B., Plantić, I., Čunčić, I., **Krtalić, I.**, Juretić, M., Pepić, I., Lovrić, J., Hafner, A. Lipid/alginate nanoparticle-loaded in situ gelling system tailored for dexamethasone nasal delivery. *International Journal of Pharmaceutics*, 2017;533:480-487.



Juretić, M., Jurišić Dukovski, B., **Krtalić, I.**, Reichl, S., Cetina-Čižmek, B., Filipović-Grčić, J., Lovrić, J., Pepić, I. HCE-T cell-based permeability model: A well- maintained or a highly variable barrier phenotype? *European Journal of Pharmaceutical Sciences*, 2017;104:23-30

## Basic documentation card

University of Zagreb

Faculty of Pharmacy and Biochemistry

Department of Pharmaceutical Technology

A. Kovačića 1, 10000 Zagreb, Croatia

PhD thesis

### DEVELOPMENT OF INNOVATIVE *IN SITU* FORMING GELS FOR TOPICAL OPHTHALMIC DELIVERY

Iva Krtalić

#### SUMMARY

The anatomical barriers and the tear fluid dynamics in the precorneal area have a huge effect on the eye-related drug bioavailability. *In situ* forming gels stand out as the formulation candidates for the improvement of bioavailability and efficacy of topical ophthalmic drugs. These are prepared as liquid dosage forms that undergo phase transition on eye surface to form viscoelastic gel in response to an environmental stimulus following topical administration. During formulation development, *in situ* forming ophthalmic gels need to be fine-tuned considering all the biopharmaceutical challenges of the front of the eye. The aim of this thesis was to develop temperature-responsive *in situ* forming poloxamer P407/ poloxamer P188/chitosan gel fine-tuned in terms of polymer content, temperature of gelation and viscosity by applying Quality by Design principles. Minimizing the total polymer content, while retaining the advantageous rheological properties, has been achieved by means of D-optimal statistical design. *In situ* forming gels were prepared by cold method and analyzed by rheological temperature sweep test. Statistical software was used to set experimental design, establish the mathematical model and analyze the collected data. Validated mathematical models enabled the selection of 4 candidates of poloxamer 407/poloxamer 188/chitosan systems, which viscoelastic behavior was studied in depth by oscillatory rheological tests under biorelevant conditions. The optimal *in situ* forming gel was selected based on minimal polymer content, favorable rheological characteristics and *in vitro* resistance to tear dilution. The formulation robustness against entrapment of active pharmaceutical ingredients (API) with different physicochemical characteristics was demonstrated using four APIs in the concentrations and combinations relevant for topical ophthalmic use. Through discriminative *in vitro* release test, adequate release profile of model drug was proven. Biocompatibility of the optimal *in situ* forming gel was confirmed employing 3D corneal epithelial cell models. In conclusion, a systematic approach to *in situ* forming gel development implemented in this thesis resulted in a stable and robust formulation characterized by ease of formulation preparation, ability for sterile filtration and autoclaving, ease of administration, accuracy of dosing, avoidance of eye-related discomfort, biocompatibility and prolonged residence at the eye surface.

The thesis is deposited in the Central Library of Faculty of Pharmacy and Biochemistry.

Thesis includes: 144 pages, 39 figures, 21 tables and 154 references. Original is in English language

Keywords: ophthalmic drug delivery, quality by design (QbD), poloxamers, chitosan, rheology, temperature-responsive *in situ* forming gel, temperature of gelation.

Menthor: **Jasmina Lovrić, Ph.D.** Associate Professor, Faculty of Pharmacy and Biochemistry, University of Zagreb

Reviewers: **Jelena Filipović-Grčić, Ph.D.** Full Professor, Faculty of Pharmacy and Biochemistry, University of Zagreb  
**Branka Zorc, Ph.D.** Full Professor, Faculty of Pharmacy and Biochemistry, University of Zagreb  
**Marijana Erceg, Ph.D.** Research associate, PLIVA Croatia Ltd.

Thesis accepted: October 24<sup>th</sup> 2018.

## Temeljna dokumentacijska kartica

Sveučilište u Zagrebu

Farmaceutsko-biokemijski fakultet

Zavod za farmaceutsku tehnologiju

A. Kovačića 1, 10000 Zagreb, Hrvatska

Doktorski rad

### RAZVOJ INOVATIVNIH *IN SITU* GELIRAJUĆIH PRIPRAVAKA ZA TOPIKALNU PRIMJENU OFTALMIČKIH LIJEKOVA

Iva Krtalić

#### SAŽETAK

Pri primjeni kapi za oko, zbog dinamičnih barijera prekornealnog područja, dolazi do brze eliminacije lijeka s površine oka. *In situ* gelovi predstavljaju jedno od inovativnih rješenja suvremene farmaceutske tehnologije za poboljšanje terapijske učinkovitosti topikalnih oftalmičkih lijekova. Takvi su sustavi oblikovani kao otopina lijeka, pogodna za topikalnu primjenu, a koja gelira izlaganjem fiziološkim uvjetima. *In situ* oftalmički gelovi trebaju biti pomno dizajnirani s ciljem produljenja vremena zadržavanja lijeka na mjestu primjene, povećanja bioraspoloživosti i učinkovitosti. Cilj je ovoga doktorskoga rada bio razviti *in situ* gel za oftalmičku primjenu korištenjem smjese polimera (poloksamera P407, poloksamera P188 i kitozana) specifično dizajnirane u smislu ukupnoga sadržaja polimera, temperature geliranja ( $T_{gel}$ ), kompleksne viskoznosti ( $\eta^*$ ) i reološkoga parametra modula pohrane ( $G'$ ). Korištenjem D-optimalnoga statističkoga eksperimentalnog dizajna optimirana su reološka svojstva razvijenih sustava uz smanjenje ukupne koncentracije korištenih polimera. *In situ* oftalmički gelovi poloksamera pripremljeni su "hladnom" metodom te analizirani reološkim testom promjene temperature. Statistički je softver korišten za postavljanje eksperimentalnoga dizajna, utvrđivanje modela, generiranje sekvenci i za statističku obradu prikupljenih podataka. Temeljem validiranih modela, odabrana su četiri vodeća poloksamer 407/poloksamer 188/kitozan sustava, čije je viskoelastično ponašanje ispitano u detaljnoj reološkoj karakterizaciji. S obzirom na najmanji udio polimera, poželjna reološka svojstva te *in vitro* rezistentnost na razrjeđenje suznom tekućinom, miješani je sustav PL1 odabran kao optimalni *in situ* gel. Prikladnost razvijenoga sustava kao platforme za uklapanje djelatnih tvari različitih fizikalno-kemijskih svojstava je dokazana je dodatkom četiri djelatne tvari u koncentracijama i kombinacijama relevantnim za topikalnu oftalmičku primjenu. Odgovarajući profil oslobađanja djelatne tvari iz PL1 platforme pokazan je diskriminatornom *in vitro* metodom oslobađanja. Biokompatibilnosti PL1 optimalnoga *in situ* gela pokazana je na 3D epitelnim modelima rožnice. Sustavan pristup razvoju *in situ* gela, proveden u sklopu doktorskoga rada, rezultirao je stabilnom i robusnom formulacijom, koju karakterizira jednostavna priprava, mogućnost sterilizacije te svojstva koja omogućuju jednostavnost primjene, točnost doziranja, izbjegavanje nelagode nakon primjene, biokompatibilnost i produljeno zadržavanje na površini oka.

Rad je pohranjen u Centralnoj knjižnici Farmaceutsko-biokemijskog fakulteta Sveučilišta u Zagrebu.

Rad sadrži: 144 stranice, 39 slika, 21 tablicu i 154 literaturna navoda. Izvornik je na engleskom jeziku

Ključne riječi: oftalmička primjena, kvaliteta uključena u dizajn (eng. QbD), poloksameri, kitozan, reologija, geliranje uzrokovano povećanjem temperature, temperatura geliranja.

Mentor: **Dr. sc. Jasmina Lovrić**, *izvanredni profesor, Farmaceutsko-biokemijski fakultet Sveučilišta u Zagrebu.*

Ocjenjivači: **Dr.sc. Jelena Filipović-Grčić**, *redoviti profesor, Farmaceutsko-biokemijski fakultet Sveučilišta u Zagrebu.*  
**Dr.sc. Branka Zorc**, *redoviti profesor, Farmaceutsko-biokemijski fakultet Sveučilišta u Zagrebu.*  
**Dr.sc. Marijana Erceg**, *znansvena suradnica, PLIVA Hrvatska d.o.o.*

Rad prihvaćen: 24. listopada 2018.



Pharmaceutics, Drug Delivery and Pharmaceutical Technology

## D-Optimal Design in the Development of Rheologically Improved *In Situ* Forming Ophthalmic Gel



Iva Krtalić<sup>1</sup>, Senka Radošević<sup>1</sup>, Anita Hafner<sup>2</sup>, Mario Grassi<sup>3</sup>, Mirta Nenadić<sup>2</sup>, Biserka Cetina-Čižmek<sup>1</sup>, Jelena Filipović-Grčić<sup>2</sup>, Ivan Pepić<sup>2</sup>, Jasmina Lovrić<sup>2,\*</sup>

<sup>1</sup> R&D, PLIVA Croatia Ltd, TEVA Group Member, Prilaz baruna Filipovića 25, 10000 Zagreb, Croatia

<sup>2</sup> Department of Pharmaceutical Technology, University of Zagreb, Faculty of Pharmacy and Biochemistry, A. Kovačića 1, 10000 Zagreb, Croatia

<sup>3</sup> Department of Engineering and Architecture (DIA), University of Trieste, Via Alfonso Valerio 6/A, I 34127 Trieste, Italy

### ARTICLE INFO

#### Article history:

Received 8 September 2017

Revised 29 December 2017

Accepted 24 January 2018

Available online 5 February 2018

#### Keywords:

ophthalmic drug delivery  
quality by design (QbD)  
chitosan  
rheology  
gel

### ABSTRACT

*In situ* forming ophthalmic gels need to be fine tuned considering all the biopharmaceutical challenges of the front of the eye in order to increase drug residence time at the application site resulting in its improved bioavailability and efficacy. The aim of this study was to develop *in situ* forming ophthalmic poloxamer P407/poloxamer P188/chitosan gel fine tuned in terms of polymer content, temperature of gelation, and viscosity. Minimizing the total polymer content while retaining the advantageous rheological properties has been achieved by means of D-optimal statistical design. The optimal *in situ* forming gel was selected based on minimal polymer content (P407, P188, and chitosan concentration of 14.2%, 1.7%, and 0.25% w/w, respectively), favorable rheological characteristics, and *in vitro* resistance to tear dilution. The optimal *in situ* forming gel was proved to be robust against entrapment of active pharmaceutical ingredients making it a suitable platform for ophthalmic delivery of active pharmaceutical ingredients with diverse physicochemical properties.

© 2018 American Pharmacists Association®. Published by Elsevier Inc. All rights reserved.

### Introduction

The anatomical barriers and the tear fluid dynamics in the precorneal area of the eye have a huge effect on the eye-related drug bioavailability.<sup>1</sup> This problem can be overcome by using *in situ* forming ophthalmic gels prepared from polymers that exhibit reversible phase transitions and pseudoplastic behavior to minimize interference with blinking and avoid foreign body sensation and blurring of vision.<sup>2-4</sup> *In situ* forming ophthalmic gels need to be fine tuned considering all the biopharmaceutical challenges of the front of the eye in order to increase drug residence time at the application site resulting in its improved bioavailability and efficacy.<sup>5</sup> Such a system should be formulated as drug containing liquid suitable for instillation into the eye that shifts to the gel phase upon exposure to physiological conditions.<sup>6</sup> The optimal *in situ* forming gel should be characterized by: (1) temperature of gelation ( $T_{gel}$ ) in physiologically relevant range; (2) pseudoplastic behavior that

allows gel to thin during blinking, making it more comfortable and easier to spread across the eye surface<sup>7</sup>; (3) suitable gel strength to endure the dilution with tears. Moreover, *in vivo* performance of *in situ* forming ophthalmic gels is governed also by drug release and biocompatibility issues.

Poloxamers (Pluronic®), a series of closely related block copolymers of polyethylene oxide and polypropylene oxide, have been investigated as *in situ* forming gels.<sup>8</sup> At high concentrations of poloxamers, the aqueous solutions exhibit a dramatic change of the viscoelastic moduli and become soft solids or gels. A phase transition from liquid to gel upon reaching physiological temperatures is presently one of the most important phenomena for their applications.<sup>9</sup> Poloxamer 407 (P407) was mainly studied for ophthalmic delivery, however, concentrated P407 aqueous solutions (>18%, w/w) gel already at the ambient temperature.<sup>10</sup> In that case, *in situ* forming ophthalmic gel has to be stored in refrigerator and applied cold,<sup>6</sup> and therefore, its instillation to the front of the eye can possibly be irritating and painful.

The use of P407 in mixture with other poloxamers is considered as a strategy to decrease the P407 concentration and to modulate the temperature of gelation and rheological properties of *in situ* forming gel. Among others, poloxamer 188 (P188) was shown to be a good modulator of P407 *in situ* forming gels.<sup>10-12</sup> In previous studies, both poloxamers were used in *in situ* forming ophthalmic

This article contains supplementary material available from the authors by request or via the Internet at <https://doi.org/10.1016/j.xphs.2018.01.019>.

\* Correspondence to: Jasmina Lovrić (Telephone: +385 1 63 94 763; Fax: +385 1 46 12 691).

E-mail address: [jlovric@pharma.hr](mailto:jlovric@pharma.hr) (J. Lovrić).

<https://doi.org/10.1016/j.xphs.2018.01.019>

0022-3549/© 2018 American Pharmacists Association®. Published by Elsevier Inc. All rights reserved.

gels at very high total concentration, for example, P407 and P188 in concentration of 21% and 10%,<sup>10</sup> 16% and 14%,<sup>13</sup> 20% and 11%<sup>14</sup> (w/w), respectively.

The additional improvements in the biopharmaceutical properties of poloxamer ophthalmic gels can be achieved by the presence of different additives in the formulation.<sup>15–19</sup> Chitosan, a biocompatible and biodegradable polycationic polymer, has been demonstrated to increase the mechanical strength and mucoadhesiveness of *in situ* forming ophthalmic gels.<sup>19</sup> In addition, there are other benefits of including chitosan in ophthalmic formulations such as improvement of eye-related permeability due to its paracellular permeation enhancing effects,<sup>20</sup> antimicrobial activity,<sup>21</sup> and corneal wound healing effect.<sup>22</sup>

The aim of this study was to develop *in situ* forming ophthalmic poloxamers/chitosan gel fine tuned in terms of polymer content and rheological properties, that is, temperature of gelation, storage modulus, and viscosity. Minimizing the total polymer content while retaining the advantageous rheological properties has been achieved by means of D-optimal statistical design. The selection of the leading candidate for drug formulation development has been based on the ability to keep its rheological properties upon dilution under biorelevant conditions. The robustness of selected mixed system has been evaluated upon entrapment of 4 ophthalmic active pharmaceutical ingredients (APIs).

## Materials and Methods

### Materials

Poloxamers P407 (Kolliphor P407; EO<sub>98</sub>PO<sub>69</sub>EO<sub>98</sub>; average molecular weight ( $M_w$ ) 13,498 g/mol) and P188 (Lutrol micro F68; EO<sub>80</sub>PO<sub>27</sub>EO<sub>80</sub>; average  $M_w$  8902 g/mol) were purchased from BASF SE (Ludwigshafen, Germany). More than 90% deacetylated ultrapure PROTASAN™ chitosan salt (Protasan UP CL214;  $M_w$  150,000–400,000 g/mol; viscosity 20–200 mPa × s) (CS) was obtained from NovaMatrix® (Sandvika, Norway). Timolol maleate (TIMO), dexamethasone (DEX), dorzolamide hydrochloride (DORZO) were kindly donated by TEVA Pharmaceutical Industries Ltd. Tobramycin (TOBRA) standard was purchased from the United States Pharmacopeia (Rockville, MD).

Simulated tear fluid (STF), pH 7.4, was prepared by dissolving the following substances in double-distilled water: KCl (1.4 mg/mL), NaCl (6.8 mg/mL), NaHCO<sub>3</sub> (2.2 mg/mL), and CaCl<sub>2</sub> × 2H<sub>2</sub>O (0.08 mg/mL).<sup>23</sup> Final step in STF preparation was filtration of solution (Whatman™ membrane filters, 0.2 μm, RC58; GE Healthcare Limited, Buckinghamshire, UK).

Cellulose acetate 0.8 μm membranes for *in vitro* release (IVR) test (CA 0.8) were obtained from Sartorius Stedim Biotech (Göttingen, Germany).

### Preparation of In Situ Forming Ophthalmic Gels

*In situ* forming ophthalmic gels were prepared by slightly modified cold method.<sup>24</sup> Briefly, appropriate amounts of all materials were weighed in a glass bottle and defined amount of previously refrigerated water for injection (WFI; PLIVA Croatia Ltd.) was added. Samples were stirred (speed 400–600 rpm) in an ice bath until clear solution was obtained. In case when CS was used in mixed systems, after ice bath, additional means of ultrasound at 20°C–25°C (Bandelin Sonorex digital 10P; BANDELIN electronic GmbH & Co. KG, Berlin, Germany) was applied to aid its dissolution. All prepared systems had an ophthalmically acceptable osmolality, which was achieved by the addition of appropriate amounts of NaCl to the solution. Osmolality was determined by the freezing point depression method (Advanced® 3D3 Single-Sample Osmometer; Advanced Instruments Inc., Norwood, MA). For CS-free solutions, it

was in the range of 295.4–301.8 mOsm/kg, whereas for CS-containing solutions, it was in the range of 310.4–332.0 mOsm/kg. pH was measured using PHM240 pH/Ion Meter (Radiometer Analytical SAS, Villeurbanne, France) and was in the range of 5.8 for CS-containing solutions to 6.5 for CS-free solutions. The transparency of *in situ* forming ophthalmic gels was determined by measuring the refractive index (RE40 Refractometer; Mettler-Toledo, LLC, Columbus, OH). Refractive index of all systems was in the ophthalmically suitable range for eye drops (i.e., not greater than 1.476<sup>25</sup>).

Out of 4 APIs, 6 API-loaded *in situ* forming ophthalmic gels were prepared, namely mixed P407/P188/CS system containing: 2% (w/w) DORZO, 0.5% (w/w) TIMO, 2% (w/w) DORZO, and 0.5% (w/w) TIMO, 0.1% (w/w) DEX, 0.3% (w/w) TOBRA, 0.05% (w/w) DEX and 0.3% (w/w) TOBRA. *In situ* forming ophthalmic gels containing TIMO, DEX, and DORZO were prepared in same way as API-free systems. For preparation of systems containing TOBRA, API was first dissolved in defined aliquot of WFI and then mixed with P407/P188/CS solution. pH was adjusted to 5.8 since addition of TOBRA increased pH of the solution. All *in situ* forming ophthalmic gels were isotonized taking into account NaCl equivalent for each API.

### Measurement of Temperature of Gelation and Complex Viscosity

The temperature sweep test was performed to determine the  $T_{gel}$ , the temperature dependence of complex viscosity ( $\eta^*$ ) and the temperature dependence of storage ( $G'$ ) and loss modulus ( $G''$ ).<sup>17,26</sup> The rheological measurement was performed using Rheometer Anton Paar Physica MCR 301 (Anton Paar GmbH, Graz, Austria) with parallel plate (PP50) measuring system equipped with H-PTD 200 Truly Peltier temperature-controlled hood (U.S. Patent 6,571,610) connected to circulating water bath (JULABO GmbH, Seelbach, Germany). Samples were equilibrated at 5°C for 5 min. Angular frequency and strain applied were fixed at 1 s<sup>-1</sup> and 1%, respectively, whereas gap was  $d = 0.5$  mm. Data were calculated by Rheoplus™ software (Anton Paar).

$G'$ ,  $G''$ , and  $\eta^*$  were recorded in the temperature range of 5°C–85°C with a rate of 10°C/min.  $T_{gel}$  is defined as the temperature point at which intersection of  $G''$  and  $G'$  curves occurs.<sup>17,27</sup> All measurements were done in triplicate.

### Design of Experiments

Quality by Design principles were employed to optimize formulation parameters and evaluate their impact on  $T_{gel}$ ,  $G'$ , and  $\eta^*$ . Statistical software JMP®, version 12.0.1, (SAS Institute Inc., Cary, NC) was used to set of experimental design, establish the mathematical models, and analyze the collected data. Designs were generated within the class of optimal designs, and D-optimality criterion was selected based on the particularities of the experimental situation.

The independent variables were the concentration of P407, P188, and CS, whereas dependent variables were  $T_{gel}$ ,  $G'$ , and  $\eta^*$  obtained from temperature sweep test. Sequential approach to experimentation was applied through screening, refining, and optimizing designs (Table 1). Data set was initiated with the results of preliminary screening, consisting of 5 samples, which contained only P407. For the subsequent design of experiment (refining), a new factor was added in order to explore influence of concentration levels of CS on the responses and include it into the model. Finally, to evaluate the error of mixed system preparation and measurement, 3 replicated samples were added.

Data were checked for the basic assumptions needed for the statistical test. Normality of the data was tested with Kolmogorov test. Log-transformed response variables  $G'$  and  $\eta^*$  were fitted

**Table 1**  
Sample Sequence From Design of Experiment (DoE) and Corresponding Experimental Temperature of Gelation ( $T_{gel}$ ), Complex Viscosity ( $\eta^*$ ), Storage Modulus ( $G'$ ), and Damping Factor

DoE	Sample <sup>a</sup>	P407	P188	CS	$T_{gel}$ (°C)	$\eta^*$ (Pa × s)	$\log \eta^*$	$G'$	$\log G'$	Damping Factor ( $\tan \delta$ )	Form
		(%, w/w)	(%, w/w)	(%, w/w)				(Pa)			
Preliminary screening	1o	11.4			33.4	0.05	-1.34	3.56	0.55	0.825	Gel
	2o	13.8			24.4	19.5	1.29	119	2.08	0.259	Gel
	3o	15.2			24.3	702	2.85	4320	3.64	0.206	Gel
	4o	16.9			20.7	1520	3.18	9360	3.97	0.197	Gel
	5o	19.3			15.1	2430	3.39	15,200	4.18	0.101	Gel
Screening	6●	11.32	0.87		31.6	0.44	-0.36	2.45	0.39	0.494	Gel
	7●	19.1	0.8		15.1	2370	3.37	14,700	4.17	0.142	Gel
	8●	15.8	0.84		22.5	277	2.44	1660	3.22	0.315	Gel
	9●	14.12	4.01		29.8	2.17	0.34	13.20	1.12	0.248	Gel
	10●	14.61	4.24		33.4	1.21	0.08	7.01	0.85	0.413	Gel
	11●	18.39	4.64		22.5	131	2.12	794	2.90	0.271	Gel
	12●	10.59	7.4		49.4	0.02	-1.68	n.d.	n.d.	1E+30	Solution
	13●	15.49	7.66		35.1	0.48	-0.32	4.30	0.63	0.685	Gel
Refining step (addition of CS)	14■	16.4	0.85	0.08	23.8	169	2.23	975	2.99	0.425	Gel
	15■	10.93	4.2	0.08	52.5	0.02	-1.61	0.0156	-1.81	9.46	Solution
	16■	15.92	3.97	0.08	31.1	7.77	0.89	46.4	1.67	0.327	Gel
	17■	13.61	2.51	0.66	33.5	0.54	-0.27	9.17	0.96	0.748	Gel
	18■	11.16	0.95	1.29	54.8	0.4	-0.4	0.27	-0.56	9.09	Solution
	19■	16.2	0.92	1.22	26.3	26.2	1.42	229	2.36	0.201	Gel
	20■	10.8	4.18	1.25	47.7	0.49	-0.31	0.93	-0.03	3.14	Solution
	21■	15.7	3.96	1.18	33.5	3.32	0.52	35.6	1.55	0.46	Gel
	22■	11.31	0.89	0.10	38.2	0.04	-1.4	n.d.	n.d.	2.37	Solution
Replicate step	23 (14) <sup>o</sup>	16.4	0.84	0.09	23.9	1245	3.1	7270	3.86	0.2745	Gel
	24 (15) <sup>o</sup>	10.93	4.21	0.09	52.4	0.02	-1.63	0.03	-1.53	12.4	Solution
	25 (16) <sup>o</sup>	15.88	3.97	0.08	31.1	2.36	0.37	21.20	1.33	0.2935	Gel

<sup>a</sup> o-preliminary screening, ●-screening, ■-screening with addition of CS, <sup>o</sup>-optimization step; n.d., not determined.

using a regression model. Logarithmic transformation was found as optimal within Box-Cox power transformation for the responses  $G'$  and  $\eta^*$  so the usual regression assumptions of normality and homogeneity of variance were more closely satisfied.

Multiple regression and ANOVAs were used to evaluate experimental results (JMP® version 12.0.1). Factorial models were set to determine all main effects and interactions for the factors of interest, that is, concentrations of P407, P188, and CS. Significance of the regression models was assessed with ANOVA. Level of significance for all tests was  $\alpha = 0.05$ . Factor Profiling platform (JMP®) was utilized to explore and visualize estimated models, for example, to explore the shape of the response surface, find optimum settings of the factors, and simulate response data.

To validate the models, the experimental values of  $T_{gel}$ ,  $G'$ , and  $\eta^*$  of 4 optimal mixed P407/P188/CS systems were statistically compared with their predicted responses.

#### Strain and Frequency Sweep Testing

The viscoelastic behavior of *in situ* forming ophthalmic gels was investigated by strain sweep and frequency sweep test using the rheometer system with cone-and-plate (CP50) geometry with 1° incline. Gap in the measuring configuration was  $d = 0.05$  mm. For strain sweep analysis, the angular frequency was set at 62.8 rad/s, and the strain was varied from 0.001% to 1000%. The linear viscoelastic (LVE) range at 35°C was identified as the region in which the moduli are independent of the strain. For frequency sweep analyses, strain was set at 1%, which was in the LVE range, whereas the angular frequencies were in the range of 0.628-199 rad/s.

Gelation time was determined as the time point at which intersection of the curves of measured  $G''$  and  $G'$  occurred.<sup>27</sup> The samples were placed at rheometer plate preheated at 35°C. Strain (1%) was constantly in LVE range, whereas applied frequency was 1 Hz throughout the test.

The evaluation of *in situ* forming ophthalmic gel under biorelevant conditions was performed by sample dilution with STF

(40:7). The STF diluted samples were submitted to strain and frequency sweep analysis at 35°C.

#### In Vitro Release Study

IVR testing was performed using the Vision Microette (Hanson, Chatsworth, CA), a commercial Franz diffusion cell apparatus equipped with 6 static vertical diffusion cell with 12 mL volume and 15 mm orifice (providing area for release of 1.767 cm<sup>2</sup>), an AutoFill sample collector and circulating water bath. Donor part of vertical cell consisted of open cell top with cap which is suitable for retaining less viscous liquids. Temperature was maintained at 35°C, and stirring speed of 400 rpm assured homogenized sample in the receptor medium (STF). Sink conditions were assured. An aliquot of 2.5 mL of sample was placed on the CA 0.8 membranes in donor compartment. Suitability of CA 0.8 membranes (low drug adsorption and low diffusion resistance) was demonstrated in the membrane selection study (data not shown).

IVR testing of *in situ* formulations was performed during 24 h. One milliliter of samples was collected automatically at pre-determined time intervals. System's rinsing volume was set at 1.5 mL to assure no carryover of an API prior each sampling point. Quantification of TIMO was done by ultraperformance liquid chromatography as detailed in the [Supplementary Materials and Methods](#).

#### In Vitro Biocompatibility Study

The biocompatibility was assayed using corneal epithelial models based on the immortalized human corneal epithelial cell line (HCE-T) (RIKEN Cell Bank, Tsukuba, Japan). The cultivation of HCE-T cell-based models was performed as detailed in the [Supplementary Materials and Methods](#). The mixed P407/P188/CS system was applied directly onto cell-based models. After the 30-min treatment at 37°C, treated models were incubated at the room temperature for 5 min to induce formulation gel-sol



transition. The cell surface was rinsed with Hank's balanced salt solution and exposed to air-liquid interface for the following 24 h. The cell viability was assessed by MTT (3-[4,5-dimethylthiazol-2-yl]-2,5-diphenyl tetrazolium bromide) test according to the protocol by Pauly et al.<sup>28</sup> as detailed in the [Supplementary Materials and Methods](#).

## Results and Discussion

### In Situ Forming Ophthalmic Gel Optimization Using a Design of Experiment

The aim of the employed Quality by Design approach was to determine the minimal total concentrations of P407, P188, and CS that would yield an *in situ* forming ophthalmic gel with the potential to ensure the defined formulation characteristics. For the establishment of the mathematical model, it was necessary to generate the data of  $T_{gel}$ ,  $G'$ , and  $\eta^*$  of the sample based on the independent variables (Table 1). In the screening step of the applied sequential approach, influence of concentration levels of 2 factors (independent variables; P407 and P188 concentration) on  $T_{gel}$ ,  $G'$ , and  $\eta^*$  (dependent variables) was tested. Based on the particular experimental conditions, a custom D-optimal design was applied to provide estimates for the effect testing with smallest standard errors, as it maximizes the information in the selected set of experimental runs with respect to a model stated.<sup>29</sup> Two center points were included in the experimental runs to allow the testing for nonlinear factor effects and estimation of the pure experimental error and to increase the power of the experiment. A total of 8 experimental runs were generated for the evaluation of the main effects and possible interactions. Accordingly, 8 samples, varying in concentrations of P407 (10.59%-19.1%, w/w) and P188 (0.8%-7.66%, w/w), were prepared, and their  $T_{gel}$ ,  $G'$ , and  $\eta^*$  were determined (Table 1). Collected data were analyzed, and significant cause-and-effect relationship was identified. Data set was expanded with the results of preliminary screening, consisting of 5 samples, which contain only P407 (11.4%-19.3%, w/w).

In the subsequent, refining step, CS concentration was added as an additional independent variable. Concentration ranges of factors P407 and P188 were selected based on the result obtained in screening step, and CS concentration was evaluated in the range of 0.08%-1.29% (w/w) based on the literature data.<sup>19,30</sup> D-optimal statistical design with 1 center point was applied. Nine experimental runs were required for analyzing the main effects and all second-level interactions. Additionally, to evaluate error of mixed P407/P188/CS system preparation and measurement, 3 replicated runs were added to the experimental sequence (replicate step). Based on this approach, 3 mathematical models were established, that is,  $T_{gel}$ ,  $G'$ , and  $\eta^*$  models, as the prerequisite for the optimization of *in situ* forming P407/P188/CS ophthalmic gel.

### The Model of Temperature of Gelation

Within the established  $T_{gel}$  model, the response of interest is represented by following regression equation:

$$T_{gel} = 35.46 - 13.84 \times \overline{P407} + 6.70 \times \overline{P188} + 2.74 \times \overline{CS} + 7.07 \times \overline{P407} \times \overline{P188} + 9.16 \times \overline{P407} \times \overline{P188} \times \overline{CS} \quad (1)$$

where factors denoted as overlined represent centered factors, that is reduced by mean value and divided by the half of the factor

range. The obtained coefficient of determination between the experimental and predicted values of  $T_{gel}$  was  $R^2 = 0.93$  (Fig. S1a).

Statistical analysis of the collected data revealed significant effects of P407, P188, and CS concentrations on the  $T_{gel}$  ( $p < 0.05$ ). The concentration effect impacts  $T_{gel}$  in following order: P407 (coefficient = -13.84) > P188 (coefficient = 6.70) > CS (coefficient = 2.74). The negative value of the coefficient indicates an inverse relationship between the factor (concentration) and the response ( $T_{gel}$ ), showing that increase of the P407 concentration will result in a decrease of  $T_{gel}$ . The positive value of the coefficient observed for P188 indicates that increasing the concentration of P188 shifts  $T_{gel}$  to higher values, as already reported in the literature.<sup>11,14</sup> Similar to P188, but to a lesser extent, the increase in CS concentration increases  $T_{gel}$ . Evidently, CS affects the onset of gelling, but it does not interfere with the formation of *in situ* gel, thus, making it a suitable additive in this mixed poloxamer system. In the similar concentration range, CS was already shown not to induce marked changes in the  $T_{gel}$  of poloxamer systems.<sup>19</sup>

Significant higher order terms include the interaction between P407 and P188 (coefficient = 7.07) and the interaction among P407, P188, and CS (coefficient = 9.16). These interactions, shown as response surface and contour plots (Figs. 1a-1c), indicate that one factor may vary depending on the level of the other factor. P407 and P188 interaction profile suggests that the impact of P407 on the  $T_{gel}$  decrease is more pronounced at the lower level of P188 (Fig. S1b). At the other side, higher level of P407 assures more pronounced effect of P188 on the  $T_{gel}$  increase. Curvatures shown on the Figure 1a indicate that this relation is not linear. These interactions reveal the complexity of interplay of the components in the measured mixed systems. The complexity of interplay is highly related to the concentration of P188 in the system as suggested by Zhang et al.<sup>11</sup> who revealed the formation of 2 distinct populations of micelles in mixed P407/P188 systems. They suggested that P188 micellization was responsible for the  $T_{gel}$  increase.

### Models of Rheological Properties: Complex Viscosity and Storage Modulus

Critical attribute that determines the dosing accuracy, retention time, and drug release from *in situ* forming ophthalmic gels is formulation rheological behavior. The systems with fine-tuned rheological properties would withstand the high shear rates and tear dilution thus preventing the drainage of an API from the site of the absorption.<sup>4</sup>

### The Model of Complex Viscosity

We investigated and mathematically described the influence of different P407, P188, and CS concentration levels on the measured  $\eta^*$  at 35°C and angular frequency of 1 s<sup>-1</sup>. Before the statistical analysis,  $\eta^*$  data were checked for normality. Kolmogorov test confirmed that data follow the log-normal distribution. Thus, log transformation was applied on the measured  $\eta^*$  data.

In this mathematical approach, the response of interest [ $\log(\eta^*)$ ] is represented by following regression equation:

$$\log(\eta^*) = -0.37 + 1.53 \times \overline{P407} - 1.60 \times \overline{P188} - 0.55 \times \overline{P407} \times \overline{P188} - 0.76 \times \overline{P407} \times \overline{CS} + 0.70 \times \overline{CS} \times \overline{CS} + 1.56 \times \overline{P407} \times \overline{P407} \times \overline{P188} \quad (2)$$

Developed  $\eta^*$  model shows good fit between experimental and predicted logarithmic values of  $\eta^*$  with resulting coefficient of determination  $R^2 = 0.97$  (Fig. S2a).

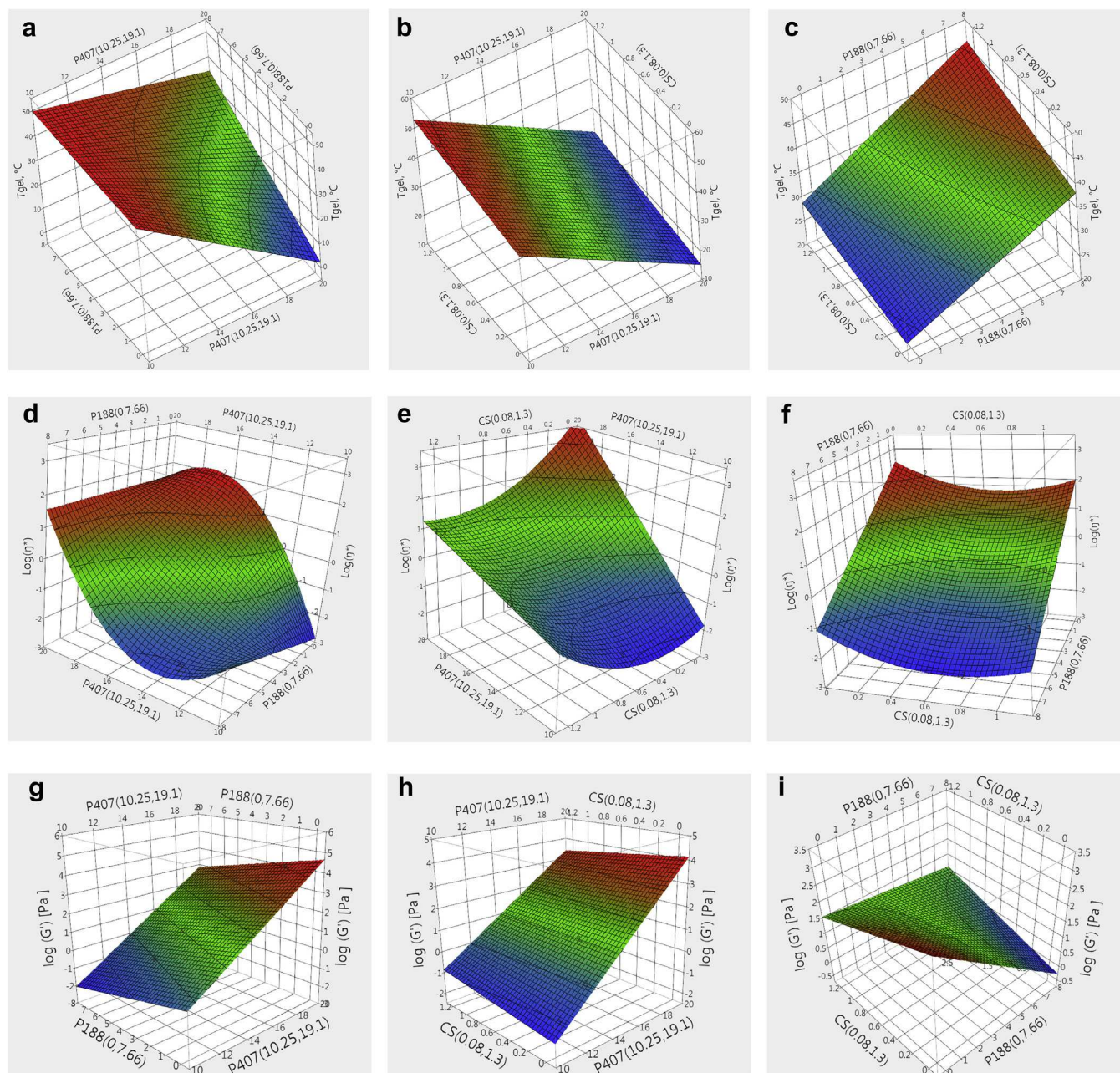


**Figure 1.** Response surface of the effects of the concentration of P407, P188, and CS on the  $T_{gel}$  (a-c),  $\log_{10}(\eta^*)$  (d-f), and  $\log_{10}(G')$  (g-i). (a) Effect of concentration of P407 and P188 on  $T_{gel}$ . (b) Effect of concentration of P407 and CS on  $T_{gel}$ . (c) Effect of concentration of P188 and CS on  $T_{gel}$ . (d) Effect of concentration of P407 and P188 on  $\log_{10}(\eta^*)$ . (e) Effect of concentration of P407 and CS on  $\log_{10}(\eta^*)$ . (f) Effect of concentration of P188 and CS on  $\log_{10}(\eta^*)$ . (g) Effect of concentration of P407 and P188 on  $\log_{10}(G')$ . (h) Effect of concentration of P407 and CS on  $\log_{10}(G')$ . (i) Effect of concentration of P188 and CS on  $\log_{10}(G')$ .

Statistical analysis of the collected data revealed significant effects of P188 and P407 concentrations on  $\log(\eta^*)$  ( $p < 0.05$ ). The increase of P188 concentration results in the decrease of  $\log(\eta^*)$  as revealed by its negative coefficient (coefficient =  $-1.60$ ). On the contrary, the increase of P407 concentration results in the increase of  $\log(\eta^*)$  (coefficient =  $1.53$ ). The complexity of interactions is noticed on the response surface and contour plots of P407 and P188 (Fig. 1d) and P407 and CS (Fig. 1e), whereas less complex relationship is noticed for P188 and CS on the response (Fig. 1f; which is in agreement with the linear lines on Fig. S2b). The model indicated 2 interactions with negative effect on the response. Namely, these were interaction between P407 and CS (coefficient =  $-0.76$ ) as well as between P407 and P188 (coefficient =  $-0.55$ ). Concomitantly,

2 higher order terms were found with the positive effect on the response, namely the interaction among P407, P407, and P188 (coefficient =  $1.56$ ), and CS (coefficient =  $0.70$ ). At higher level of P188, the effect of P407 on increase of  $\log(\eta^*)$  is less pronounced (Fig. S2b). In contrary, the omission of P188 from the system results in faster increase of  $\log(\eta^*)$  when increasing P407 concentration. CS and P407 interaction profile suggests that the impact of P407 on the  $\log(\eta^*)$  increase is more pronounced at the lower level of CS (Fig. S2b). As it can be seen by comparing the response surface and contour plot images of the  $T_{gel}$  model and  $\log(\eta^*)$  model (Figs. 1a-1c and 1d-1f), higher degree of complexity, that is curvatures, was found in the  $\log(\eta^*)$  model. This indicated the absence of linear relationship between the concentrations of 3 tested polymers to a response.



### The Model of Storage Modulus

As for the  $\log(\eta^*)$ , influence of different independent variables (P407, P188, and CS concentration levels) on the measured response  $G'$  at 35°C and angular frequency of  $1 \text{ s}^{-1}$  was tested and mathematically described. Again, Kolmogorov test confirmed that data follow the log-normal distribution; therefore, log transformation was applied on the measured  $G'$  data.

$\log(G')$  is described by following regression equation:

$$\log(G') = 1.13 + 2.16 \times \overline{P407} - 0.77 \times \overline{P188} - 0.26 \times \overline{P407} \times \overline{CS} + 0.56 \overline{P188} \times \overline{CS} \quad (3)$$

Developed  $\log(G')$  model exhibits suitable fit between experimental and predicted logarithmic values of  $G'$  with resulting coefficient of determination  $R^2 = 0.93$  (Fig. S3a).

Statistical analysis of the acquired data revealed significant effects of P407 and P188 concentrations on  $\log(G')$  ( $p < 0.05$ ), with P407 concentration having stronger effect on the response. As expected, similar to the model for  $\log(\eta^*)$ , the increase of P188 concentration results in the decrease of  $\log(G')$  due to its negative coefficient (coefficient =  $-0.76$ ). On the contrary, the increase of P407 concentration results in the increase of  $\log(G')$  (coefficient = 2.16). As seen on the Figures 1g and 1h, relation between P407 and P188 and P407 and CS on the response in model appears to be relatively simple. More complex relation of P188 and CS on the  $\log(G')$  was found to have statistically significant interaction with positive effect on the dependent variable (coefficient = 0.56) (Fig. 1i).

The increase of P188 at lower level of CS results in decrease of  $\log(G')$ , whereas this effect is not observed when CS is at highest level (1.3%, w/w). The increase in CS at low level of P188 lowers the response of interest. However, this effect is opposite at higher level of P188 (7.66%, w/w).

Another interaction included in the model, but with no statistical significance, was interaction between P407 and CS, having a negative impact on the response (coefficient =  $-0.26$ ). Same interaction with significant negative effect was noticed in the model for  $\log(\eta^*)$ .

### Selection of Rheologically Improved In Situ Forming Ophthalmic Gel

$T_{\text{gel}}$  of innovative ophthalmic *in situ* forming gels is the most critical parameter related to efficacy and safety as well as patient compliance since it influences the accuracy of dosing, (dis)comfort associated with the instillation, and residence time at the eye surface. Namely, if the system gels at room temperature, dosing would be hindered. Storage at low temperature would diminish this problem; however, the instillation of cold formulation can possibly be irritating and painful. Therefore, the optimal  $T_{\text{gel}}$  *in situ* forming ophthalmic gel should be between 25°C, the average ambient temperature, and 35°C, the eye surface temperature.<sup>19</sup> In our study, the optimal range of  $T_{\text{gel}}$  was set to 28°C-32°C.

Viscosity is one of the key attributes for innovative ophthalmic *in situ* forming gels defining the residence time at the eye surface and drug release profile. The optimal range of viscosity is much more difficult to select in relation to  $T_{\text{gel}}$ . A wide range of viscosities reported for poloxamer-based *in situ* forming ophthalmic gels have suitable *in vivo* response.<sup>6,13,19</sup> Therefore, we characterized the commercially available *in situ* forming ophthalmic gels with rotational test with controlled shear rate (Supplementary Materials) to enable the recognition of leading candidates. Oscillatory tests of selected leading candidates revealed the lower limit for  $\eta^*$  (at 35°C and  $1 \text{ s}^{-1}$ ) at  $1.2 \text{ Pa} \times \text{s}$ .

**Table 2**  
Selected Mixed P407/P188/CS Systems, Corresponding Experimental and Predicted Temperature of Gelation ( $T_{\text{gel}}$ ), Complex Viscosity ( $\eta^*$ ), Storage Modulus ( $G'$ ), and Damping Factor ( $\tan\delta$ )

Sample	P407 (% w/w)	P188 (% w/w)	CS (% w/w)	Exp. $T_{\text{gel}}$ (°C)	Pred. $T_{\text{gel}}$ (°C)	$T_{\text{gel}}$ Recovery (%)	Exp. $\log(\eta^*)^a$	Pred. $\log(\eta^*)^a$	$\log(\eta^*)$ Recovery (%)	Exp. $\log(G')^a$	Pred. $\log(G')^a$	$\log(G')$ Recovery (%)	Damping Factor ( $\tan\delta$ )
PL1	14.2	1.7	0.25	31.10 ± 0.01	31.27 (29.72-32.82)	99.5	0.32 ± 0.06	0.62 (0.28-0.96)	52.4	1.15 ± 0.17	1.53 (1.29-1.78)	76.6	0.29 ± 0.03
PL2	15.0	2.0	0.5	26.30 ± 0.01	28.87 (27.00-30.74)	109.77	0.81 ± 0.06	0.60 (0.06-1.14)	73.8	1.60 ± 0.06	1.75 (1.48-2.02)	91.5	0.21 ± 0.00
PL3	14.2	1.7	1.01	29.90 ± 1.7	35.30 (32.45-38.15)	118.06	0.66 ± 0.02	0.53 (0.09-0.97)	80.2	1.44 ± 0.09	1.18 (0.74-1.62)	122.4	0.26 ± 0.01
PL4	14.2	1.7	0.5	28.70 ± 0.01	32.60 (30.90-34.30)	113.59	0.61 ± 0.09	0.30 (-0.23 to 0.83)	48.9	1.40 ± 0.02	1.42 (1.14-1.70)	98.5	0.23 ± 0.01

Exp., experimental, presented as mean ± SD.

Pred., predicted, presented as mean; values in brackets represent lower and upper limits of 95% CI.

<sup>a</sup>  $\eta^*$  ( $\text{Pa} \times \text{s}$ ) and  $G'$  (Pa) at 35°C determined by temperature sweep test (angular frequency and strain were  $1 \text{ s}^{-1}$  and 1%, respectively).

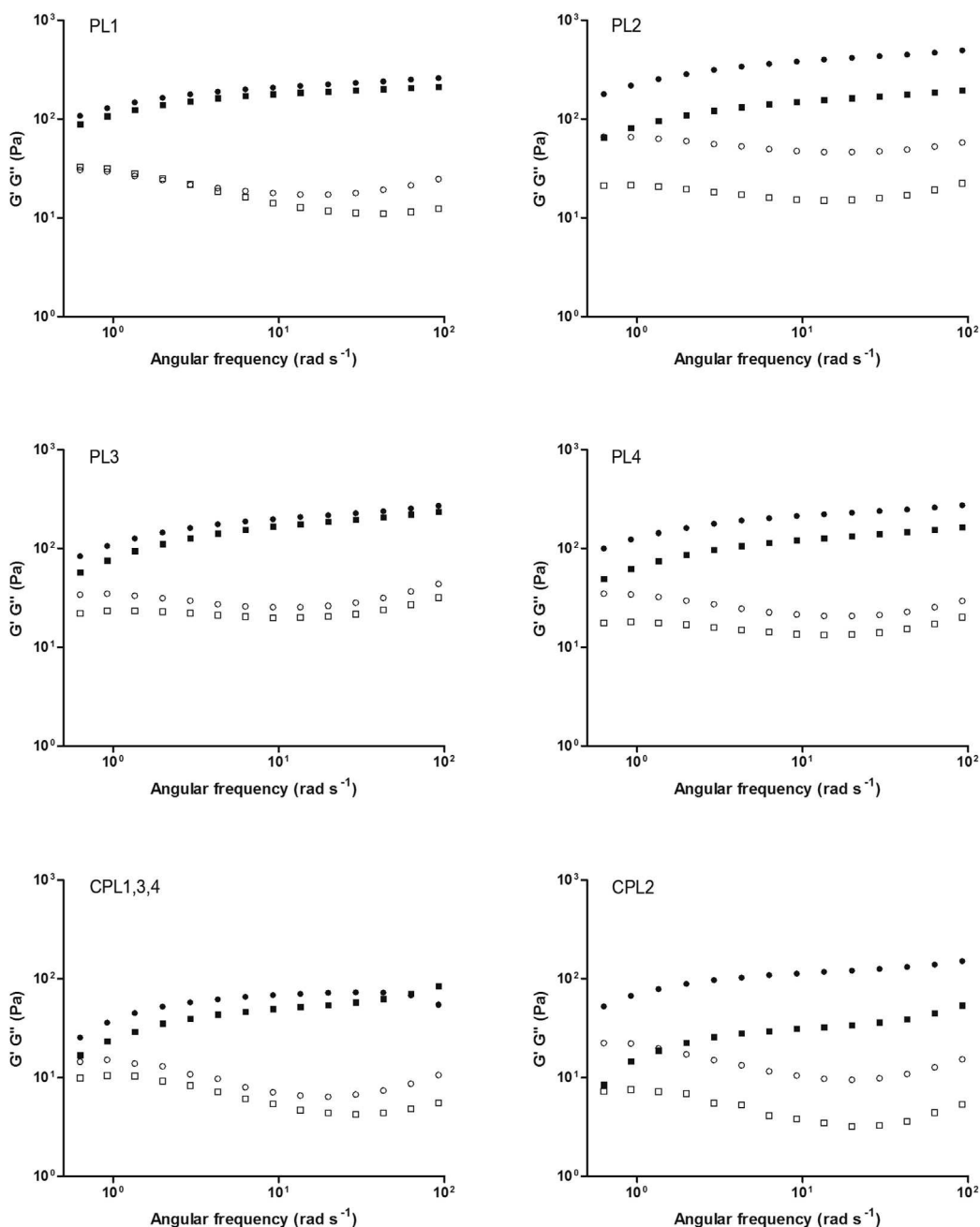


**Figure 2.** Rheological properties of selected mixed P407/P188/CS systems (PL1, PL2, PL3, and PL4) and respective controls under biorelevant conditions. Frequency sweeps analysis before (circles) and after (squares) dilution with simulated tear fluid (STF) 40:7 at 35°C.  $G'$  filled symbols,  $G''$  empty symbols. Control sample for PL1, PL3, and PL4 is labeled CPL1, CPL3, CPL4; control sample for PL2 is labeled CPL2.

$G'$  is a measure of the deformation energy stored by the sample during the shear process. After the load is removed, this energy is completely available, now acting as the driving force for the reformation process which will compensate partially or completely the previously obtained deformation of the structure.  $G'$  presents the elastic behavior of a sample, and it assures adequate gel stability. As minimal  $G'$  values for gel structures are around 5 Pa,<sup>27</sup> this value was set as minimal value for this dependent variable.

Considering the optimal  $T_{gel}$ ,  $G'$  and  $\eta^*$  suggested by corresponding models, 4 mixed P407/P188/CS systems were selected (Table 2). The additional criterion of the selection was the lowest possible total polymer content in *in situ* forming ophthalmic gel. To validate the data obtained by the models, mixed P407/P188/CS

systems were prepared.  $T_{gel}$ ,  $G'$ , and  $\eta^*$  were determined by temperature sweep test and compared with predicted values (Table 2).

High coefficient of determination ( $R^2 = 0.93$ ) and the overall recovery of experimental to predicted  $T_{gel}$  ( $110.23 \pm 0.08\%$ ; relative standard deviation [RSD] = 7.02%) confirmed the suitability of  $T_{gel}$  model. Similar agreement was found for  $\log(G')$  model ( $R^2 = 0.93$ ) with the average recovery of experimental to predicted  $T_{gel}$  of  $97.25 \pm 19.07\%$ , having slightly higher variability (RSD = 19.61%). In case of  $\log(\eta^*)$  model, even better coefficient of determination ( $R^2 = 0.97$ ) was observed, and despite the lower overall recovery of experimental to predicted  $\log(\eta^*)$  ( $63.83 \pm 0.16\%$ ; RSD = 24.3%), the developed model enabled the development of mixed P407/P188/CS system with targeted viscosity ( $>1.2 \text{ Pa} \times \text{s}$ ). The higher variability

**Table 3**  
Effect of Active Pharmaceutical Ingredients on Temperature of Gelation ( $T_{gel}$ ) and Complex Viscosity ( $\eta^*$ )

Variable	Before Dilution With STF		After Dilution With STF	
	$T_{gel}$ (°C)	$\eta^*$ (Pa × s) <sup>a</sup>	$T_{gel}$ (°C)	$\eta^*$ (Pa × s) <sup>a</sup>
PL1–DORZO	27.50 ± 1.70	7.88 ± 1.18	33.50 ± 0.01	0.67 ± 0.06
PL1–TIMO	26.30 ± 0.01	4.90 ± 0.54	29.90 ± 1.20	2.44 ± 1.50
PL1–DORZO/TIMO	28.70 ± 0.02	4.82 ± 1.07	32.90 ± 0.80	0.64 ± 0.10
PL1–TOBRA	30.30 ± 1.40	1.52 ± 0.66	31.10 ± 0.01	0.52 ± 0.10
PL1–DEX	22.60 ± 1.70	6.11 ± 0.70	28.70 ± 0.01	1.56 ± 1.16
PL1–DEX/TOBRA	23.65 ± 3.18	6.88 ± 1.59	31.15 ± 0.07	0.639 ± 0.21
PL1	31.10 ± 1.40	2.10 ± 0.74	33.50 ± 0.70	0.37 ± 0.15

Values are mean ± SD ( $n = 3$ ).

<sup>a</sup>  $\eta^*$  at 35°C determined by temperature sweep test (angular frequency and strain were 1 s<sup>-1</sup> and 1%, respectively).

of this model could be related to the heating rate-dependent kinetics of gel formation. Mixed P407/P188 systems exhibit very complex rheological behavior with internal relaxations and slow reorganizations taking place in the temperature range preceding or following the  $T_{gel}$ .<sup>11</sup> However, the fast temperature change is the one expected *in vivo*.

#### In Depth Rheological Characterization of In Situ Forming Ophthalmic Gel

With the aim of in depth rheological characterization, selected mixed P407/P188/CS systems were subjected to frequency sweep analysis. Strain sweep analysis was carried out to determine the limit of LVE range, that is, the range where stress is directly proportional to strain.

Frequency sweep analysis gives an insight on the behavior of  $G'$ ,  $G''$ , and  $\eta^*$  as a function of angular frequency. The frequency sweep measurements for all 4 mixed P407/P188/CS systems indicated that  $G'$  was higher than  $G''$  revealing suitable gel stability (Fig. 2). Moreover, the presented rheological profile suggests the existence of soft gels known to be formed at moderate poloxamer concentration.<sup>31</sup> This phenomenon has been ascribed to the weak attraction of spherical micelles as the solvent becomes poorer on heating.

To determine the influence of CS on the gel mechanical strength, frequency sweep analysis was carried out also for the respective control systems without CS (Fig. 2). As expected, the presence of CS in mixed systems resulted in higher  $G'$  and  $G''$  values indicating increased gel mechanical strength. It was already suggested that the elastic characteristic of the system increased owing to an effect on microscopic diffusion within gel structure which facilitated the accommodation of unbound water and consequently micelle packaging.<sup>19</sup>

Mixed systems were further characterized under biorelevant conditions, that is, diluted with STF at the ratio of 40:7 mimicking their mixing with tear fluid after instillation.<sup>10</sup> Despite the dilution, mixed systems retained their ability to form gel at temperature lower than 35°C (i.e., the sample PL2 formed gel at 28.7°C, whereas PL1, PL3, and PL4 formed gel at 33.5°C). The observed increase in

$T_{gel}$  relative to undiluted systems (Table 2) can be related to both the decrease in the total concentration of polymers and the modification of the physicochemical properties of the hydrogels in the presence of STF electrolytes.<sup>19,32</sup>

The dilution of all mixed systems with STF resulted in no change in  $G'$  to  $G''$  ratio or their overall profile (Fig. 2). Furthermore, there was no significant change in the absolute values of  $G'$  and  $G''$  in case of samples prepared with the same poloxamer concentration and different CS concentration (Fig. 2; PL1, PL3, and PL4). On the contrary, comparing the mixed system PL2 (P407/P188/CS 15.0/2.0/0.5%, w/w) with PL4 (P407/P188/CS 14.2/1.7/0.5%, w/w), it may be observed that the small increase in poloxamer concentration influenced the resistance to dilution.

The decrease of  $\eta^*$  values with the increase of angular frequency arguments suitable pseudoplastic behavior of *in situ* forming ophthalmic gels. The viscosity profiles of all mixed systems did not change significantly upon dilution with STF suggesting the maintenance of their pseudoplastic behavior (Fig. S4). Moreover, there was no marked change in the absolute values of  $\eta^*$  upon dilution except, again, in the case of PL2 sample.

Comparing our mixed P407/P188/CS systems with mixed P407/CS system developed by Gratieri et al.<sup>19</sup> in terms of resistance to dilution, it may be concluded that P188 significantly contributed to gel stability. In mixed P407/CS system the concentration of P407 was higher (16%, w/w and 14%, w/w, upon dilution with STF) than in case of mixed P407/P188/CS system (14.2%, w/w and 12.09%, w/w, upon dilution with STF). However, upon dilution mixed P407/CS system behaved as viscoelastic solution at 35°C and decreased frequencies while mixed P407/P188/CS system behaved as soft gel.

Based on minimal polymer content (P407, P188, and CS concentration of 14.2%, 1.7% and 0.25%, w/w, respectively), favorable rheological characteristics ( $T_{gel} = 31.1^\circ\text{C}$ ,  $\eta^* = 2.1 \text{ Pa} \times \text{s}$ ) and *in vitro* resistance to tear dilution ( $G' 212.4 \text{ Pa}$  and  $175.3 \text{ Pa}$  before and after dilution, respectively), the PL1 was selected as optimal *in situ* forming gel.

#### Effect of Active Pharmaceutical Ingredients on Temperature of Gelation and Complex Viscosity

The addition of APIs in the mixed P407/P188/CS system is expected to cause a modification of the physicochemical properties of *in situ* forming gels. Four ophthalmic APIs were selected in order to gain understanding of their effects on  $T_{gel}$  and  $\eta^*$  of selected PL1 *in situ* forming gel. We tested APIs in the concentrations and combinations relevant for topical ophthalmic use. API-loaded P407/P188/CS systems were characterized for  $T_{gel}$  and  $\eta^*$  before and after dilution with STF (Table 3). All APIs, except TOBRA, notably decreased  $T_{gel}$  in comparison with  $T_{gel}$  of PL1. This effect was highest for DEX showing the decrease of the  $T_{gel}$  for 8.5°C. DEX has already been shown to decrease the  $T_{gel}$  of P407-based *in situ* forming gels.<sup>33,34</sup> Such an effect can be ascribed to the promotion of P407 self-assembly in the presence of hydrophobic drug allowing the formation of gel at lower temperatures.<sup>35</sup> The  $T_{gel}$  of the mixed P407/P188 systems was also reported to be affected by the addition

**Table 4**  
Samples Tested in the IVR Study

Sample	Description/Composition	$T_{gel}/^\circ\text{C}$	$\eta^*$ (Pa × s)
PL1	14.2% P407, 1.7%P188, 0.25% CS, 0.2% TIMO (w/w)	31.1 ± 2.0	1.2 ± 0.3
C1	14.2% P407, 0.25% CS, 0.2% TIMO (w/w)	26.9 ± 2.2	4.12 ± 1.2
C2	11.4% P407, 0.2% TIMO (w/w)	31.1 ± 1.7	0.097 ± 0.07
TIMO solution	TIMO solution in STF, 2.5 mg/mL	n/a	n.m.

$\eta^*$  at 35°C determined by temperature sweep test (angular frequency and strain were 1 s<sup>-1</sup> and 1%, respectively).

n/a, not applicable; n.m., not measured.

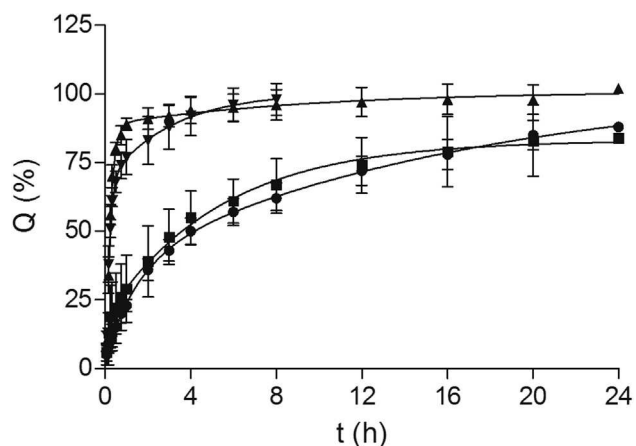


**Figure 3.** Release profiles of TIMO from PL1 (circles) and control *in situ* forming gel C1 (squares) with  $\eta^*$  comparable to PL1, control *in situ* forming gel C2 (triangle) with  $T_{gel}$  comparable to PL1 and TIMO solution (inverse triangle). The data are expressed as the mean  $\pm$  SD ( $n = 5$ ).

of hydrophobic APIs; the  $T_{gel}$  decreased with increasing the pH-dependent hydrophobicity of API in the systems.<sup>36</sup> Smaller  $T_{gel}$  decrease was observed for the systems containing dissolved APIs, namely  $T_{gel}$  decreased for 4.8°C and 2.4°C in case of TIMO and DORZA, respectively. As anticipated by many authors, the decrease of  $T_{gel}$  induced by dissolved APIs could be related to the API salting-out effect.<sup>37,38</sup> Their presence could shift the concentration and temperature at which micelles are formed to lower values and, moreover, could affect the close packing of micelles, resulting in  $T_{gel}$  decrease.<sup>32,36</sup> However, despite the decrease of  $T_{gel}$  by the addition of APIs, all the samples except those with DEX formed gels at temperature higher than 25°C. The addition of APIs in the mixed P407/P188/CS system prolonged the gelation time in all cases except for DEX/TOBRA. However, the obtained gelation time values were still in the appropriate range (41.1-87.4 s) for ocular administration.<sup>39,40</sup>

The  $\eta^*$  values for API-loaded PL1 were in the range of 1.52-7.88 Pa  $\times$  s indicating no pronounced influence of API entrapment on gel viscosity (Table 3).

Dilution with STF, as expected, led to the increase in  $T_{gel}$  and certain decrease in  $\eta^*$  for all the API-loaded PL1. All the samples retained their gel structure after dilution as suggested by the frequency sweep analysis (data not shown).

These results indicate the robustness of selected PL1 *in situ* forming gel against entrapment of APIs with different physico-chemical characteristics. The decrease in  $T_{gel}$  caused by API entrapment open the possibility to further decrease the concentration of poloxamers required to obtain *in situ* forming gels with appropriate biopharmaceutical properties.<sup>41</sup>

#### Drug Release From In Situ Forming Gel

IVR study was performed to investigate the influence of viscosity related to the functional excipient concentration on the drug release rate. The optimal *in situ* forming gel (PL1) was characterized in terms of its influence on drug release profile. For that purpose, TIMO was selected as the model drug and incorporated in PL1 in the lowest efficient dose. Control *in situ* forming gel C1 was characterized by  $\eta^*$  comparable to PL1, whereas control *in situ* forming gel C2 was characterized by  $T_{gel}$  comparable to PL1 (Table 4). TIMO solution was also used as the control sample. The IVR profiles of PL1 and respective controls are shown in Figure 3. IVR of TIMO from PL1 and C1 was significantly slower than from C2 and TIMO solution

indicating viscosity as the critical factor influencing drug release. Similar observations were already reported for *in situ* forming ophthalmic gels.<sup>26,42</sup>

#### Biocompatibility Assessment of In Situ Forming Ophthalmic Gel

Biocompatibility of the optimal *in situ* forming gel (PL1) was assessed by using 2 3D cell-based corneal epithelial models, namely multilayered HCE-T epithelium cultivated on filters with 0.4  $\mu$ m pores and model consisting of an apical lipophilic HCE-T epithelial monolayer and a basolateral lipophilic monolayer of migrated HCE-T cell cultivated on filters with 3  $\mu$ m pores.<sup>43</sup> In the preliminary studies, simple 2D HCE-T monolayer was used to assess the formulation biocompatibility. However, exaggerated toxicity was found in comparison to *in vivo* studies.<sup>44</sup> *In vitro* 2D models are generally characterized by certain shortcomings, such as a more pronounced susceptibility to cytotoxicity, as they replicate only a limited segment of tissue structure/function.<sup>45</sup> Consequently, the concentration of polymers/formulation that can be safely applied to such models may be reduced in comparison to the *in vivo* system. Therefore, we employed more complex 3D corneal epithelial models to screen the formulation biocompatibility. Contrary to HCE-T epithelial monolayer, 3D models revealed biocompatibility of the formulation tested. Namely, 30-min treatment resulted in decrease in 3D model cell viability lower than 20%.

#### Conclusions

In this study, we developed *in situ* forming gel characterized by  $T_{gel}$  in physiologically relevant range, pseudoplastic behavior and resistance to dilution. D-optimal design was successfully applied to reduce the total polymer content in *in situ* forming P407/P188/CS gel while retaining its advantageous rheological properties. The developed system was proved to be robust against entrapment of APIs making it a suitable platform for ophthalmic delivery of active pharmaceutical ingredients with diverse physicochemical properties. Moreover, the developed *in situ* forming ophthalmic gel was proved to provide prolonged drug release in relation to the system viscosity.

#### ACKNOWLEDGMENTS

This work was supported by a Partnership in Research project 04.01/56 funded by the Croatian Science Foundation and PLIVA Croatia LTD.

#### References

- Pepić I, Lovrić J, Cetina-Cizmek B, Reichl S, Filipović-Grcić J. Toward the practical implementation of eye-related bioavailability prediction models. *Drug Discov Today*. 2014;19(1):31-44.
- Kirchhof S, Goepferich AM, Brandl FP. Hydrogels in ophthalmic applications. *Eur J Pharm Biopharm*. 2015;95(Pt B):227-238.
- Almeida H, Amaral MH, Lobao P, Lobo JM. *In situ* gelling systems: a strategy to improve the bioavailability of ophthalmic pharmaceutical formulations. *Drug Discov Today*. 2014;19(4):400-412.
- Zignani M, Tabatabay C, Gurny R. Topical semisolid drug-delivery - kinetics and tolerance of ophthalmic hydrogels. *Adv Drug Deliv Rev*. 1995;16(1):51-60.
- Destruel PL, Zeng N, Maury M, Mignet N, Boudy V. *In vitro* and *in vivo* evaluation of *in situ* gelling systems for sustained topical ophthalmic delivery: state of the art and beyond. *Drug Discov Today*. 2017;22(4):638-651.
- El-Kamel AH. *In vitro* and *in vivo* evaluation of Pluronic F127-based ocular delivery system for timolol maleate. *Int J Pharm*. 2002;241(1):47-55.
- Rupenthal ID, Green CR, Alany RG. Comparison of ion-activated *in situ* gelling systems for ocular drug delivery. Part 2: precorneal retention and *in vivo* pharmacodynamic study. *Int J Pharm*. 2011;411(1-2):78-85.
- Almeida H, Amaral MH, Lobao P, Sousa Lobo JM. Applications of poloxamers in ophthalmic pharmaceutical formulations: an overview. *Expert Opin Drug Deliv*. 2013;10(9):1223-1237.



9. Trong LCP, Djabourov M, Ponton A. Mechanisms of micellization and rheology of PEO-PPO-PEO triblock copolymers with various architectures. *J Colloid Interf Sci.* 2008;328(2):278-287.
10. Wei G, Xu H, Ding PT, Li SM, Zheng JM. Thermosetting gels with modulated gelation temperature for ophthalmic use: the rheological and gamma scintigraphic studies. *J Control Release.* 2002;83(1):65-74.
11. Zhang M, Djabourov M, Bourgaux C, Bouchemal K. Nanostructured fluids from pluronic(R) mixtures. *Int J Pharm.* 2013;454(2):599-610.
12. Qi H, Li L, Huang C, Li W, Wu C. Optimization and physicochemical characterization of thermosensitive poloxamer gel containing puerarin for ophthalmic use. *Chem Pharm Bull (Tokyo).* 2006;54(11):1500-1507.
13. Kim EY, Gao ZG, Park JS, Li H, Han K. rhEGF/HP-beta-CD complex in poloxamer gel for ophthalmic delivery. *Int J Pharm.* 2002;233(1-2):159-167.
14. Asasutjarit R, Thanasanchokpipull S, Fuongfuchai A, Veeranondha S. Optimization and evaluation of thermoresponsive diclofenac sodium ophthalmic in situ gels. *Int J Pharm.* 2011;411(1-2):128-135.
15. Qi H, Chen W, Huang C, et al. Development of a poloxamer analogs/carbopol-based in situ gelling and mucoadhesive ophthalmic delivery system for puerarin. *Int J Pharm.* 2007;337(1-2):178-187.
16. Shastri DH, Prajapati ST, Patel LD. Thermoreversible mucoadhesive ophthalmic in situ hydrogel: design and optimization using a combination of polymers. *Acta Pharm.* 2010;60(3):349-360.
17. Mayol L, Quaglia F, Borzacchiello A, Ambrosio L, La Rotonda MI. A novel poloxamers/hyaluronic acid in situ forming hydrogel for drug delivery: rheological, mucoadhesive and in vitro release properties. *Eur J Pharm Biopharm.* 2008;70(1):199-206.
18. Lin HR, Sung KC, Vong WJ. In situ gelling of alginate/pluronic solutions for ophthalmic delivery of pilocarpine. *Biomacromolecules.* 2004;5(6):2358-2365.
19. Gratieri T, Gelfuso GM, Rocha EM, Sarmiento VH, de Freitas O, Lopez RF. A poloxamer/chitosan in situ forming gel with prolonged retention time for ocular delivery. *Eur J Pharm Biopharm.* 2010;75(2):186-193.
20. Basaran E, Yazan Y. Ocular application of chitosan. *Expert Opin Drug Deliv.* 2012;9(6):701-712.
21. de la Fuente M, Ravina M, Paolicelli P, Sanchez A, Seijo B, Alonso MJ. Chitosan-based nanostructures: a delivery platform for ocular therapeutics. *Adv Drug Deliv Rev.* 2010;62(1):100-117.
22. Tsai CY, Woung LC, Yen JC, et al. Thermosensitive chitosan-based hydrogels for sustained release of ferulic acid on corneal wound healing. *Carbohydr Polym.* 2016;135:308-315.
23. Paulsson M, Hagerstrom H, Edsman K. Rheological studies of the gelation of deacetylated gellan gum (Gelrite) in physiological conditions. *Eur J Pharm Sci.* 1999;9(1):99-105.
24. Schmolka IR. Artificial skin. I. Preparation and properties of pluronic F-127 gels for treatment of burns. *J Biomed Mater Res.* 1972;6(6):571-582.
25. Ammar HO, Salama HA, Ghorab M, Mahmoud AA. Development of dorzolamide hydrochloride in situ gel nanoemulsion for ocular delivery. *Drug Dev Ind Pharm.* 2010;36(11):1330-1339.
26. Gratieri T, Gelfuso GM, de Freitas O, Rocha EM, Lopez RF. Enhancing and sustaining the topical ocular delivery of fluconazole using chitosan solution and poloxamer/chitosan in situ forming gel. *Eur J Pharm Biopharm.* 2011;79(2):320-327.
27. Mezger TG. *The Rheology Handbook.* 4th ed. Hannover, Germany: Vincentz Network; 2014.
28. Pauly A, Meloni M, Brignole-Baudouin F, Warnet JM, Baudouin C. Multiple endpoint analysis of the 3D-reconstituted corneal epithelium after treatment with benzalkonium chloride: early detection of toxic damage. *Invest Ophthalmol Vis Sci.* 2009;50(4):1644-1652.
29. Bodea A, Leucuta SE. Optimization of hydrophilic matrix tablets using a D-optimal design. *Int J Pharm.* 1997;153(2):247-255.
30. Gupta H, Jain S, Mathur R, Mishra P, Mishra AK, Velpandian T. Sustained ocular drug delivery from a temperature and pH triggered novel in situ gel system. *Drug Deliv.* 2007;14(8):507-515.
31. Chaibundit C, Ricardo NM, Ricardo NM, et al. Aqueous gels of mixtures of ionic surfactant SDS with pluronic copolymers P123 or F127. *Langmuir.* 2009;25(24):13776-13783.
32. Aka-Any-Grah A, Bouchemal K, Koffi A, et al. Formulation of mucoadhesive vaginal hydrogels insensitive to dilution with vaginal fluids. *Eur J Pharm Biopharm.* 2010;76(2):296-303.
33. Arbelaez-Camargo D, Sune-Negre JM, Roig-Carreras M, et al. Preformulation and characterization of a lidocaine hydrochloride and dexamethasone sodium phosphate thermo-reversible and bioadhesive long-acting gel for intraperitoneal administration. *Int J Pharm.* 2016;498(1-2):142-152.
34. Meznarich NAK, Juggernaut KA, Batzli KM, Love BJ. Structural changes in PEO-PPO-PEO gels induced by methylparaben and dexamethasone observed using time-resolved SAXS. *Macromolecules.* 2011;44(19):7792-7798.
35. Sharma PK, Bhatia SR. Effect of anti-inflammatories on Pluronic F127: micellar assembly, gelation and partitioning. *Int J Pharm.* 2004;278(2):361-377.
36. Scherlund M, Brodin A, Malmsten M. Micellization and gelation in block copolymer systems containing local anesthetics. *Int J Pharm.* 2000;211(1-2):37-49.
37. Jeong B, Kim SW, Bae YH. Thermosensitive sol-gel reversible hydrogels. *Adv Drug Deliv Rev.* 2002;54(1):37-51.
38. van Hemelrijck C, Muller-Goymann CC. Rheological characterization and permeation behavior of poloxamer 407-based systems containing 5-aminolevulinic acid for potential application in photodynamic therapy. *Int J Pharm.* 2012;437(1-2):120-129.
39. Jaiswal M, Kumar M, Pathak K. Zero order delivery of itraconazole via polymeric micelles incorporated in situ ocular gel for the management of fungal keratitis. *Colloids Surf B Biointerfaces.* 2015;130:23-30.
40. Morsi N, Ghorab D, Refai H, Teba H. Ketorolac tromethamine loaded nano-dispersion incorporated into thermosensitive in situ gel for prolonged ocular delivery. *Int J Pharm.* 2016;506(1-2):57-67.
41. Sharma PK, Reilly MJ, Bhatia SK, Sakhitab N, Archambault JD, Bhatia SR. Effect of pharmaceuticals on thermoreversible gelation of PEO-PPO-PEO copolymers. *Colloids Surf B Biointerfaces.* 2008;63(2):229-235.
42. Rupenthal ID, Green CR, Alany RG. Comparison of ion-activated in situ gelling systems for ocular drug delivery. Part 1: physicochemical characterisation and in vitro release. *Int J Pharm.* 2011;411(1-2):69-77.
43. Juretic M, Jurisic Dukovski B, Krtalic I, et al. HCE-T cell-based permeability model: a well-maintained or a highly variable barrier phenotype? *Eur J Pharm Sci.* 2017;104:23-30.
44. Furrer P, Plazonnet B, Mayer JM, Gurny R. Application of in vivo confocal microscopy to the objective evaluation of ocular irritation induced by surfactants. *Int J Pharm.* 2000;207(1-2):89-98.
45. Fitzgerald KA, Malhotra M, Curtin CM, O'Brien FJ, O'Driscoll CM. Life in 3D is never flat: 3D models to optimise drug delivery. *J Control Release.* 2015;215:39-54.



# Lipid/alginate nanoparticle-loaded *in situ* gelling system tailored for dexamethasone nasal delivery



Bisera Jurišić Dukovski<sup>a</sup>, Ivana Plantić<sup>a</sup>, Ivan Čunčić<sup>a</sup>, Iva Krtalić<sup>b</sup>, Marina Juretić<sup>a</sup>, Ivan Pepić<sup>a</sup>, Jasmina Lovrić<sup>a</sup>, Anita Hafner<sup>a,\*</sup>

<sup>a</sup> University of Zagreb, Faculty of Pharmacy and Biochemistry, Department of Pharmaceutical Technology, Zagreb, Croatia

<sup>b</sup> R&D, PLIVA Croatia Ltd, TEVA Group Member, Zagreb, Croatia

## ARTICLE INFO

### Article history:

Received 14 January 2017

Received in revised form 4 May 2017

Accepted 27 May 2017

Available online 31 May 2017

### Keywords:

Nasal delivery

*In situ* gelling

Alginate

Amidated pectin

Dexamethasone

## ABSTRACT

In this study, we suggest the development of nanoparticle loaded *in situ* gelling system suitable for corticosteroid nasal delivery. We propose lipid/alginate nanoparticles (size  $252.3 \pm 2.4$  nm, polydispersity index 0.241, zeta-potential  $-31.7 \pm 1.0$  mV, dexamethasone (Dex) content  $255 \pm 7 \mu\text{g ml}^{-1}$ ) dispersed in pectin solution ( $5 \text{ mg ml}^{-1}$ ) that undergoes a sol-gel phase transition triggered by  $\text{Ca}^{2+}$  present in nasal mucosa. The viscoelasticity of gel obtained by mixing nanoparticle suspension in pectin continuous phase with simulated nasal fluid (1:1 V/V) is characterised by a log-linear shear thinning viscosity behaviour. Observed viscosity corresponds to the range of viscosities of nasal mucus at physiological as well as under disease conditions. Nanoparticle-loaded gel was biocompatible with the selected epithelial cell model and, in comparison to dexamethasone solution, provided reduction in Dex release ( $t_{50\%}$  2.1 h and 0.6 h, respectively) and moderated transepithelial permeation *in vitro* ( $P_{\text{app}}$   $7.88 \pm 0.15$  and  $9.73 \pm 0.57 \times 10^{-6} \text{ cm s}^{-1}$ , respectively). In conclusion, this study showed the potential of the proposed system to provide local therapeutic effect upon administration of a lower corticosteroid dose and minimize the possibility for adverse effects as it can be easily sprayed as solution and delivered beyond nasal valve, ensure prolonged contact time with nasal mucosa upon gelation, and moderate corticosteroid release and permeation.

© 2017 Elsevier B.V. All rights reserved.

## 1. Introduction

Chronic rhinosinusitis is one of the most commonly diagnosed chronic nasal illnesses worldwide (Fokkens et al., 2012). The site of inflammation and potential nasal polyp growth is located beyond the nasal valve. Nasal polyps are grape-like structures which affect about 20% people with chronic rhinosinusitis and cause symptoms of prominent nasal obstruction and reduction/loss of smell. Chronic rhinosinusitis with nasal polyps can be treated with pharmacotherapy, but in more severe cases it may be necessary to remove nasal polyps by endoscopic sinus surgery. Unfortunately, post-surgical recurrence is common because the underlying inflammatory process fails to be addressed (Martino et al., 2015).

The mainstream treatment for patients with nasal polyps are corticosteroids. Even though oral corticosteroids are effective, they can cause well known side effects including suppression of hypothalamic-pituitary-adrenal axis, osteoporosis,

hyperglycaemia, gastrointestinal bleeding, hypocalcaemia, insomnia, hypertension, cataracts and glaucoma. Therefore, topical nasal corticosteroids are the natural choice for patients with nasal polyps. However, to reduce polyp size, nasal steroid must reach the inflammation site in sufficient quantities. Therefore, lately high-dose topical nasal corticosteroids have been suggested and have shown promising results as well as less systemic effects than oral corticosteroids. High-dose topical nasal corticosteroids are thought to penetrate the sinus cavities at an increased dose and therefore allow for greater control of polyp growth (Martino et al., 2015). However, long term use of high topically applied doses could be related to adverse effects such as changes in serum cortisol levels and intraocular pressure.

The current interests are focused on the development of nasal delivery device that could ensure corticosteroid delivery beyond the nasal valve, i.e. to the site where nasal polyps occur (Hansen et al., 2010; Vlckova et al., 2009). However, in addition to nasal delivery device, characteristics of formulation also impact therapeutic outcome. In this study, we suggest the development of nanoparticle loaded *in situ* gelling system able to provide an

\* Corresponding author at: A. Kovačića 1, 10000 Zagreb, Croatia.  
E-mail address: [ahafner@pharma.hr](mailto:ahafner@pharma.hr) (A. Hafner).

optimal nasal deposition, prolonged residence time and prolonged corticosteroid release. More particularly, we propose lipid/alginate nanoparticles dispersed in pectin solution that undergoes a sol-gel phase transition triggered by  $\text{Ca}^{2+}$  present in nasal mucosa. Anionic polysaccharides are known for their biocompatibility and biodegradability, and are therefore often used as constituents of numerous drug delivery systems. Both alginate and pectin show mucoadhesive properties. Their adhesion to mucus layers and increased elasticity of mucus secretions is based on the interpenetration with mucin chains (Fuongfuchat et al., 1996). The electrostatic repulsion between alginate/pectin and mucin due to the same charge may cause an uncoiling of polymer chains and facilitate chain entanglement and bond formation (Joergensen et al., 2011; Wattanakorn et al., 2010). Pectin solutions form gels in the presence of  $\text{Ca}^{2+}$  at the concentration expected at the nasal mucosa. Ionotropic gelation of polymer chains results in a highly ordered three-dimensional network with “egg-box” junction zones (Watts and Smith, 2009).

Nanoparticle loaded *in situ* gelling system can be easily sprayed as a solution and, with appropriate device, delivered to the site of inflammation. The  $\text{Ca}^{2+}$  triggered gel formation in the nasal cavity would ensure prolonged contact time with nasal mucosa. Such biopharmaceutical properties, along with the prolonged corticosteroid release from lipidic matrix nanoparticles, would allow local therapeutic effect upon administration of a lower corticosteroid dose, minimizing the possibility for adverse effects.

## 2. Materials and methods

### 2.1. Materials

Sodium alginate PRONOVA UP LVG (low viscosity; L-gulonate (G)/D-mannuronate (M) Ratio  $\geq 1.5$ ) was purchased from NovaMatrix<sup>®</sup>, Norway. Lecithin S100 was obtained from Lipoid, Germany. Di-methyldioctadecylammonium bromide (DDAB) was purchased from Sigma-Aldrich, Germany. Dexamethasone (Dex) was obtained from Sanofi Aventis, France. Low methylester (LM) amidated pectin CF 025 (pectin; degree of esterification (DE) 23–28%; degree of amidation (DA) 22–25%) was kindly donated by Herbstreith&Fox, Germany. Sodium dodecyl sulphate (SDS) was obtained from Merck, Germany. Acetonitrile (ACN), tetrahydrofuran (THF) and methanol, gradient grade for liquid chromatography, were purchased from Merck, KGaA, Germany. 0.2  $\mu\text{m}$  Spartan<sup>™</sup> regenerated cellulose filters were obtained from Whatman, United Kingdom. Simulated Nasal Fluid (SNF) was prepared as an aqueous solution containing 150.0 mmol NaCl (Kemig, Croatia), 40.0 mmol KCl (Kemig, Croatia) and 5.3 mmol  $\text{CaCl}_2 \times 2\text{H}_2\text{O}$  (Sigma-Aldrich, Germany) per litre (Martinac et al., 2005). Hank's balanced salt solution (HBSS, pH 7.4) was prepared by dissolving the following substances in double-distilled water:  $\text{MgSO}_4 \times 7\text{H}_2\text{O}$  (0.4 mM), KCl (5.4 mM),  $\text{NaHCO}_3$  (4.2 mM), NaCl (136.9 mM), D-glucose monohydrate (5.6 mM) (all purchased from Kemig, Croatia),  $\text{CaCl}_2 \times 2\text{H}_2\text{O}$  (1.3 mM) (Sigma-Aldrich, Germany),  $\text{MgCl}_2 \times 6\text{H}_2\text{O}$  (0.5 mM) (Merck KGaA, Germany),  $\text{KH}_2\text{PO}_4$  (0.4 mM) (Kemika, Croatia),  $\text{Na}_2\text{HPO}_4 \times 2\text{H}_2\text{O}$  (0.3 mM) (Fluka Chemie AG, Switzerland) and HEPEs (30.0 mM) (AppliChem, Germany) (Hafner et al., 2015) and it was used for nanoparticle biocompatibility assessment. Hank's balanced salt solution with 5.3 mM  $\text{Ca}^{2+}$  (HBSS- $\text{Ca}^{2+}$ ; pH 7.4) was prepared by dissolving KCl (5.4 mM),  $\text{NaHCO}_3$  (4.2 mM), NaCl (136.9 mM), D-glucose monohydrate (5.6 mM) (all purchased from Kemig, Croatia),  $\text{KH}_2\text{PO}_4$  (0.4 mM) (Kemika, Croatia),  $\text{Na}_2\text{HPO}_4 \times 2\text{H}_2\text{O}$  (0.3 mM) (Fluka Chemie AG, Switzerland) and  $\text{CaCl}_2 \times 2\text{H}_2\text{O}$  (5.3 mM) (Sigma-Aldrich, Germany) in double-distilled water and was used for *in vitro* permeability study. Ultrapure water for chromatographic analyses was produced by Ultra Clear<sup>™</sup> UV Plus (SG Wasseraufbereitung und Regenerierstation GmbH, Germany).

### 2.2. Preparation of lipid/alginate nanoparticles

Lipid components, lecithin and DDAB were dissolved in 96% ethanol. Concentration of lecithin in ethanolic solution was  $25\text{ mg ml}^{-1}$ , while lecithin to DDAB weight ratio was 50:0.7, 50:1, 50:3 or 50:5. Dex was dissolved in the ethanolic solution of lipids at the concentration of  $5\text{ mg ml}^{-1}$ , i.e. at lecithin to Dex weight ratio of 5:1. Alginate was solubilised in distilled water at concentration of  $10\text{ mg ml}^{-1}$  and the aliquot of alginate solution (0.5 ml) was further diluted with distilled water to a volume of 23 ml. Dex-loaded nanoparticles were obtained by injection of 2 ml of ethanolic lipid/Dex solution (syringe inner diameter of 0.75 mm) into 23 ml of diluted alginate solution under magnetic stirring (900 rpm). A final alginate concentration of  $200\text{ }\mu\text{g ml}^{-1}$  and lecithin to alginate weight ratio of 10:1 was obtained in the prepared nanoparticle suspensions. Dex that precipitated during nanoparticle production was separated by filtration using 0.45  $\mu\text{m}$  membrane filters (Millipore<sup>®</sup>, Switzerland).

Dex-free lipid and lipid/alginate nanoparticles were prepared by the injection of ethanolic lipid solution into distilled water and diluted aqueous solution of alginate, respectively, and were used as controls when appropriate.

### 2.3. Determination of Dex loading

About 0.5 g of resuspended samples containing nanoparticles was accurately weighed in 25 ml volumetric flask. 2 ml of tetrahydrofuran (THF) and 10 ml of diluent (60% methanol/40% ultrapure water, V/V) was added into the flask and sample was placed on the ultrasonic bath. After 20 min of sonication sample was checked for transparency visually and filled with diluent up to the total volume of 25 ml. Prior Ultra-Performance Liquid Chromatography (UPLC) analysis described in the Section 2.11, all samples were filtrated through 0.2  $\mu\text{m}$  Spartan<sup>™</sup> regenerated cellulose filters.

### 2.4. Physical characterization of the particle size and surface charge

The size and zeta potential of nanoparticles were measured by Photon Correlation Spectroscopy (PCS) using Zetasizer 3000 HS (Malvern Instruments, Malvern, UK). For that purpose nanoparticle samples were diluted with 0.45  $\mu\text{m}$  filtered distilled water and 10 mM NaCl solution, respectively. Zeta-potential measurements were performed at 25 °C. Samples were placed in the electrophoretic cell, where a potential of 150 mV was established.

### 2.5. The preparation of *in situ* forming nanoparticle-loaded gel

Pectin was dissolved in distilled water at the concentration of  $40\text{ mg ml}^{-1}$ . Pectin solution was added to the nanoparticle suspension to the final pectin concentration of  $5\text{ mg ml}^{-1}$ . Nanoparticle suspension with pectin in continuous phase was then mixed with SNF in volume ratio of 1:1, which resulted in instantaneous gel formation.

### 2.6. Rheological evaluation

The rheological behaviour of *in situ* forming nanoparticle-loaded gel was determined by frequency sweep test using Rheometer Anton Paar Physica MCR 301 (Anton Paar GmbH, Austria) with cone plate (CP25) measuring system equipped with H-PTD 200 Truly Peltier-temperature-controlled hood (US Patent 6,571,610). Peltier heating element was connected to circulating water bath (F25-ME Refrigerated/Heating Circulator, JULABO GmbH, Germany). Sample was placed carefully on the lower plate of rheometer, measuring bob was placed in the measuring position

and sample was equilibrated for 5 min at 37 °C. Gap was set to  $d = 0.05$  mm, and angle was 1°. The strain applied was in the linear viscoelastic range (at 0.3%) while the angular frequencies were in the range of 0.628–199 rad/s. The elastic moduli ( $G'$ ), viscous moduli ( $G''$ ) and complex viscosity ( $\eta^*$ ) were recorded. Data were calculated by Rheoplus™ software (Anton Paar).

Zero shear viscosity at 37 °C of the NP suspension in pectin continuous phase prior gelling was determined by creep test. A shear stress (10 Pa) was applied to the sample in a dynamic shear rheometer for a duration long enough (15 min) that the deformation reaches a constant value, which corresponds to steady state flow. Zero shear viscosity was calculated by the Rheoplus™ software by fitting the shear stress versus shear rate data using the Carreau's model (Mezger, 2014).

Shear viscosity profile of samples equilibrated for five minutes at 37 °C was determined by the means of rotational rheology using the same measurement bob as in creep and oscillatory tests in the shear rate range of  $0.01 \text{ s}^{-1}$ – $1000 \text{ s}^{-1}$ .

## 2.7. In vitro release studies

The release of Dex from nanoparticles and nanoparticle-loaded gel was assessed by the dialysis technique under sink conditions over 5 h.

### 2.7.1. Release profile of Dex from lipid/alginate nanoparticles

The appropriate volume of nanoparticle suspension containing 400 µg of Dex was placed into a cellulose acetate dialysis bag (Spectra/Por® 4 Dialysis Tubing, MWCO 12–14 kDa, Medicell International Ltd., UK). The dialysis bag was sealed from both sides and immersed into 30 ml of receptor medium (0.03% w/w, aqueous SDS solution) at 25 °C that was magnetically stirred at 180 rpm. At scheduled time intervals, the aliquots (2 ml) were withdrawn and replaced with equal amounts of receptor medium. Withdrawn samples were analysed for the Dex content by UPLC method described in the Section 2.11. All experiments were performed in triplicate.

### 2.7.2. Release profile of Dex from nanoparticle-loaded pectin gel

Nanoparticle-loaded gel obtained at pectin concentration of  $2.5 \text{ mg ml}^{-1}$  and  $\text{Ca}^{2+}$  concentration of 2.65 mM was placed into the dialysis bag in a volume containing 200 µg of Dex. The dialysis bag was immersed into 30 ml of 2.65 mM  $\text{CaCl}_2$  solution at 25 °C that was magnetically stirred at 180 rpm. Equal concentration of  $\text{Ca}^{2+}$  in the formulation and the receptor medium ensured gel stability over the experiment. Sampling and the Dex content analysis was performed as described in the Section 2.7.1.

## 2.8. Cell culture conditions

Caco-2 cells (American Type Culture Collection [ATCC], USA) were cultured in DMEM medium with 4500 mg/L glucose, L-glutamine and sodium bicarbonate, without sodium pyruvate (Sigma-Aldrich, Germany) supplemented with 10% foetal bovine serum (Biosera, France), nonessential amino acids (Lonza, Switzerland) and penicillin/streptomycin/amphotericin B (Lonza, Switzerland). Cells were passaged at 80–90% confluence. The medium was changed every 48 h. Cultures were maintained at 95% humidity and 37 °C in an atmosphere of 5%  $\text{CO}_2$ .

## 2.9. Cell viability study

Caco-2 cells were seeded onto 96-well plates (Corning Inc, USA) at a density of  $1.5 \times 10^4$  cells per well and allowed to reach confluence over 2 days.

### 2.9.1. Nanoparticle biocompatibility assessment

Suspensions of nanoparticles were diluted with HBSS (pH 7.4), obtaining final nanoparticle concentration of 50–400 µg ml<sup>-1</sup> with respect to lecithin. The cells were exposed to the nanoparticle suspensions for 2 h at 37 °C. Cells incubated in HBSS were used as a negative control. After 2 h of treatment with nanoparticles, the cells were washed twice with HBSS and incubated with fresh medium (100 µl/well) for 24 h. Cell viability was determined with the colorimetric MTT (3-[4,5-dimethylthiazol-2-yl]-2,5-diphenyl tetrazolium bromide, Sigma-Aldrich, Germany) assay. A total of 10 µl of MTT stock solution (5 mg ml<sup>-1</sup>) in Phosphate buffered saline without  $\text{Ca}^{2+}$  and  $\text{Mg}^{2+}$  (PBS) (Lonza, Switzerland) was added to each well, and the cells were then incubated for 1 h at 37 °C. Afterwards, the medium was removed, cells were lysed and formazan was dissolved with isopropanol. The amount of formazan was quantified spectrophotometrically at 570 nm (1420 Multilabel counter VICTOR3, Perkin Elmer, USA).

### 2.9.2. Nanoparticle-loaded gel biocompatibility assessment

Caco-2 cells were treated with nanoparticle-loaded gel prepared by mixing nanoparticle suspension in pectin continuous phase with SNF at volume ratio of 1:1. The cells were exposed to gel for 2 h at 37 °C. Cells incubated in SNF were used as negative control. Cell viability was determined as reported in the Section 2.9.1.

## 2.10. In vitro permeability through epithelial model barrier

Caco-2 cells were seeded onto the polycarbonate 12-well Transwell® inserts (0.4 µm mean pore size, 1.12 cm<sup>2</sup> surface area, Corning Costar Inc., USA) at density of  $2.5 \times 10^4$  cells per well and grown for 21–29 days. The cells were cultured with cell culture medium volume of 0.5 ml in the apical and 1.5 ml in the basolateral compartment. The culture medium was changed every other day and 12–24 h prior to the permeability experiment. The trans-epithelial electrical resistance (TEER) of the monolayers was measured using epithelial volt/ohm meter EVOM equipped with STX-2 chopstick electrode (WPI Inc., USA) to determine the formation of the monolayers and their integrity. The permeability studies were carried out in HBSS- $\text{Ca}^{2+}$ . Tested samples were nanoparticle-loaded gel (prepared as reported in the Section 2.5. with the only difference that instead of SNF, HBSS- $\text{Ca}^{2+}$  was used) and nanoparticle suspensions diluted with HBSS- $\text{Ca}^{2+}$  to Dex concentration of 60 and 112 µg ml<sup>-1</sup>. Solutions of Dex (60 µg ml<sup>-1</sup>) in HBSS- $\text{Ca}^{2+}$  and ethanol/HBSS- $\text{Ca}^{2+}$  (3%, w/w) were used as controls. The ethanol content in nanoparticle suspensions was adjusted to 3% (w/w) which was equal to the ethanol content in the nanoparticle-loaded gel. Prior to the experiment, the monolayers were washed with HBSS- $\text{Ca}^{2+}$ , after which HBSS- $\text{Ca}^{2+}$  was placed into the apical (0.5 ml) and basolateral (1.5 ml) compartments. The cell monolayers were then incubated for 30 min at 37 °C. At the beginning of the experiment, the apical compartment was emptied and 0.5 ml of the test sample was added. Samples (0.4 ml) were taken from the basolateral compartment at regular time intervals over 120 min and replaced with the same volume of fresh thermostated HBSS- $\text{Ca}^{2+}$  (37 °C). During the permeability experiment monolayers were incubated at 37 °C and 50 rpm on a horizontal orbital shaker. At the end of the experiment, the samples in the apical compartments were also collected. All experiments were done in triplicate. Samples were analysed for Dex content using UPLC (Section 2.11). The apparent permeability coefficients ( $P_{\text{app}}$ ) were calculated according to the following equation:

$$P_{\text{app}} = \frac{\partial Q}{\partial t} \times \frac{1}{AC_0}$$



**Table 1**

The composition of ethanolic and aqueous solutions used for the preparation of Dex-loaded lipid/alginate nanoparticles.

Samples	Lecithin (mg)	DDAB (mg)	DEX (mg)	Alginate (mg)
DN1	50	0.7	10	5
DN2	50	1	10	5
DN3	50	3	10	5
DN4	50	5	10	5
Ethanolic solution (2 ml)			Aqueous solution (23 ml)	

where  $\frac{\partial Q}{\partial t}$  is the steady-state flux,  $A$  is the surface area of the permeation barrier and  $C_0$  is the initial concentration of Dex in the apical compartment (Hubatsch et al., 2007).

### 2.11. Quantitative determination of Dex

The quantitative determination of Dex was performed by Ultra-Performance Liquid Chromatography (UPLC). Two types of UPLC instruments were used: Agilent Infinity 1290 (Agilent, USA) and Waters ACQUITY UPLC H Class (Waters, USA). Data were acquired and processed with the Empower 2 software (Waters, USA). The chromatographic separation of dexamethasone was done on a Waters Acquity UPLC BEH Shield RP18 column (2.1 × 100 mm, 1.7 μm particle size). Photodiode Array detector (PDA) was part of the Waters systems and Diode Array (DAD detector) was used in the Agilent instrument.

The quantitative determination of Dex in the samples from basolateral compartments in permeability and receiver compartments in *in vitro* release studies was performed on Waters ACQUITY UPLC H Class instrument using isocratic UPLC method. The mobile phase consisted of 68% of 5 mM sodium acetate buffer (pH 4.5) and 32% of ACN (V/V). The column temperature was set at 55 °C. The flow rate of the mobile phase was 0.7 ml/min and detection was at 254 nm wavelength. The samples were analysed undiluted.

The quantitative determination of Dex in the samples from apical compartments in permeability studies and the samples from dialysis bag in *in vitro* release studies was performed on Agilent Infinity 1290 instrument by the gradient UPLC method. The mobile phase consisted of 50% of 5 mM sodium acetate buffer (pH 4.5) and 50% of ACN (V/V) at 0 min, 25% of 5 mM sodium acetate buffer (pH 4.5) and 75% of ACN (V/V) at 0.2 min and 100% of ACN at 1.0 min. The column temperature was set at 55 °C. The flow rate of the mobile phase was 0.7 ml/min and detection was at 254 nm wavelength. The samples were prepared in the same manner as for determination of Dex loading (Section 2.3).

Prior analysis all samples were filtrated through 0.2 μm Spartan™ regenerated cellulose filters. The volume of injection was 10 μl. For each sequence standard solutions were prepared in duplicate and injected alternately. At least five standard solution injections were done in each injection sequence. System suitability

was evaluated according to the following criteria: relative standard deviation (RSD) of the detector response factor for all standard solution injections in the sequence is not more than 2.0%, and tailing factor of dexamethasone peak is not more than 2.0. Both UPLC methods were checked and found to be suitable for linearity, accuracy, repeatability and specificity at relevant concentration ranges.

### 2.12. Statistical analysis

Statistical data analyses were performed on all data by a 1-way ANOVA followed by multiparametric Tukey's post-hoc test with  $P < 0.05$  as the minimal level of significance. Calculations were performed with the GraphPad Prism program (GraphPad Software, Inc., San Diego, USA; www.graphpad.com).

The closeness between the two *in vitro* release profiles was evaluated based on the similarity factor ( $f_2$ ), as described previously (Blazevic et al., 2016). The mean cumulative amounts of drug released of the two formulations were compared at each time point. The release profiles were evaluated as similar when  $f_2 > 50$  (Xie et al., 2015).

## 3. Results and discussion

### 3.1. Characterisation of nanoparticles

The detailed composition of lipid/alginate nanoparticles proposed as nasal delivery platform for dexamethasone is shown in Table 1. Lecithin S100 was selected as the main lipid component to ensure drug entrapment and control over Dex release. Incorporation of DDAB (cationic lipid) provided the positive net charge of the lipid mixture to enable electrostatic interaction with alginate, i.e. the formation of negatively charged nanoparticles. Such nanoparticles are suitable for the proposed route of administration as they are unperturbed by the presence of the mucin (Griffiths et al., 2015).

The main characteristics of the nanoparticles prepared are given in Table 2. Dex-loaded lipid/alginate nanoparticles were successfully prepared with all lecithin/DDAB weight ratios employed. Mean diameter of Dex-loaded nanoparticles ranged between  $109.1 \pm 3.1$  nm and  $258.6 \pm 2.4$  nm while zeta-potential was between  $-14.2 \pm 0.3$  mV and  $-31.7 \pm 1.0$  mV. Negative zeta-potential values indicated the presence of alginate at the surface of nanoparticles. The increase in DDAB content led to the increase in positive net charge of the lipid mixture (data not shown) and stronger interaction with alginate, resulting in an increase of both the nanoparticle size and the negative surface charge. Dex loading induced a slight reduction in the nanoparticle size, suggesting the possible influence of Dex on the nanoparticle structuring. However, no significant difference between Dex-loaded and Dex-free nanoparticle surface charge has been observed. Thus it

**Table 2**

The main characteristics of Dex-loaded (DN) and Dex-free (N) lipid/alginate nanoparticles.

Sample	DDAB/lecithin ratio (w/w)	Dex content (μg ml <sup>-1</sup> )	Size (nm)	PDI	Zeta-potential (mV)
DN1 (N1)	0.7/50	218 ± 3	109.1 ± 3.1 (129.7 ± 1.2)	0.540 (0.531)	-14.2 ± 0.3 (-16.0 ± 0.4)
DN2 (N2)	1/50	207 ± 1	129.1 ± 2.5 (134.9 ± 4.4)	0.514 (0.610)	-21.9 ± 0.5 (-19.5 ± 0.3)
DN3 (N3)	1/50	204 ± 7	258.6 ± 4.2 (278.9 ± 1.4)	0.343 (0.519)	-26.5 ± 0.3 (-24.9 ± 0.6)
DN4 (N4)	5/50	255 ± 7	252.3 ± 2.4 (276.6 ± 4.6)	0.241 (0.374)	-31.7 ± 1.0 (-30.6 ± 1.0)

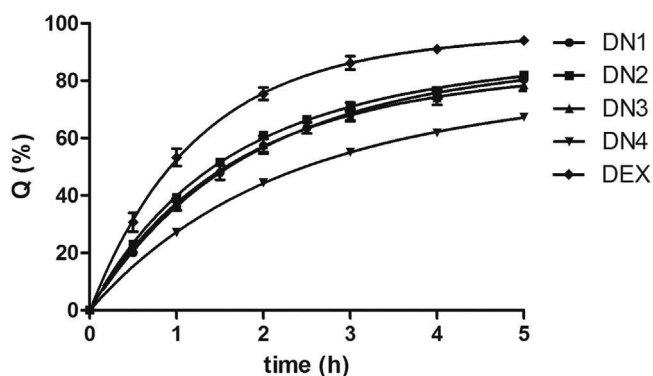


**Fig. 1.** Release profiles of Dex from lipid/alginate nanoparticles in water containing SDS (0.03%, w/w). The profile of Dex diffusion from the SDS aqueous solution (0.03%, w/w) across the dialysis membrane is also presented. Data are expressed as the mean  $\pm$  SD ( $n=3$ ).

can be concluded that Dex was entrapped within the lipid domains of nanoparticles, exerting no influence on nanoparticle surface characteristics. The highest Dex entrapment efficiency (63.8%) was obtained for nanoparticles prepared with the highest DDAB content (DN4). Furthermore, the same nanoparticles were characterised by the lowest polydispersity index and the largest negative zeta potential value ( $-31.7 \pm 1.0$  mV) that assured physical stability of nanoparticle suspension.

### 3.2. In vitro release of Dex from nanoparticles

Dex release profiles from nanoparticles was determined using the dialysis technique with SDS aqueous solution (0.03%, w/w) as a receptor medium. The profile of Dex diffusion from the SDS aqueous solution (0.03%, w/w) across the dialysis membrane was also determined, in order to assess the influence of resistance of the dialysis membrane to Dex diffusion on overall Dex release rate.

All lipid/alginate nanoparticles were characterised by prolonged Dex release and a significantly lower release rate than that observed for Dex solution (Fig. 1). This particularly refers to DN4 nanoparticles that showed the potential to ensure prolonged Dex delivery *in vivo*.

### 3.3. Evaluation of lipid/alginate nanoparticle biocompatibility

The biocompatibility of topical drug delivery nanosystems with biological cell membranes at the application site is partially governed by the surface characteristics of the nanoparticles, as the possible toxic effect can be the consequence of the interaction between nanoparticles and the cell surface. In general, negatively charged nanoparticles are compatible with cell membranes and are not likely to produce membrane disruption and cytotoxic effects. Nanoparticle cytotoxicity can also be the consequence of nanoparticle internalisation by cells (Verma and Stellacci, 2010).

Alginate and lecithin are generally regarded as safe, and are used in the development of numerous topical drug delivery systems. Alginate is negatively charged in the physiological pH range of nasal mucosa. Lecithin S100 is mainly composed of phosphatidyl choline that is primary natural constituent of biological membranes. However, the main concern is related to the potential dose-dependent cellular toxicity of cationic lipid present in the lipid mixture (Lv et al., 2006).

The biocompatibility of lipid/alginate nanoparticles was investigated using Caco-2 cells. Despite its intestinal origin, the Caco-2 cell line has already been used to screen the biopharmaceutical properties of drug delivery systems intended for nasal

administration (Ekelund et al., 2005; Hafner et al., 2009; Mao et al., 2005). In the biocompatibility study, the concentration of nanoparticles was expressed as the concentration of lecithin in the system, and ranged from 50 to 400  $\mu\text{g ml}^{-1}$ . Cell viability assay showed no toxic effects of nanoparticles at the concentration range tested and during the 2 h exposure (Fig. 2). In addition, alginate-free lipid nanoparticles, characterised by the positive surface charge proportional to DDAB content, were used as controls and were also shown not to influence the cell viability at DDAB concentration range tested (0.7–40  $\mu\text{g ml}^{-1}$ ; data not shown). Such concentration of DDAB is in the range for which there are literature reports of cytotoxic *in vitro* effect (Scarioti et al., 2011). It can be concluded that the presence of a high portion of phosphatidylcholine in alginate-free lipid NP hindered DDAB cytotoxicity. Cortesi et al. have already observed significantly lower cytotoxicity of DDAB when it was incorporated into liposomes (phosphatidylcholine:cholesterol:DDAB 8:2:1 mol/mol/mol) in comparison to micellar solution (Cortesi et al., 1996).

Physico-chemical characteristics, *in vitro* release profile and biocompatibility of DN4 nanoparticles provided the rationale to denote this formulation as the lead one (termed as NP further in the text).

### 3.4. The preparation of in situ forming NP-loaded gel

Aqueous solutions and suspensions present favourable nasal formulations, since very predictive and controlled dispersion and deposition pattern within the nasal cavity can be achieved by appropriately designed nasal delivery device. However, the main drawback refers to the limited residence time at the nasal mucosa which can be overcome by the development of *in situ* gelling systems (Karavasili and Fatouros, 2016). In the system proposed by this study, *in situ* gelling properties were provided by the addition of pectin known for its ability to form gels in contact with  $\text{Ca}^{2+}$  ions present in the nasal mucosa. NP-loaded gel was prepared by mixing NP suspension in pectin continuous phase with SNF at volume ratio of 1:1. Since the nasal epithelial lining fluid was estimated to be  $136 \pm 17 \mu\text{l}$  (Kaulbach et al., 1993) and nasal formulations are administered in small volumes, ranging from 25 to 200  $\mu\text{l}$  with 100  $\mu\text{l}$  being most common (Romeo et al., 1998), the selected ratio of 1:1 between SNF and NP suspension in pectin continuous phase simulates well the conditions *in vivo*. The  $\text{Ca}^{2+}$  concentration in simulated nasal fluid used in this study (5.3 mM) corresponds to the  $\text{Ca}^{2+}$  concentration in nasal fluid determined in healthy volunteers ( $5 \pm 1$  mM) (Vanthanouvong and Roomans, 2004). The ratio of 1:1 between SNF and NP suspension in pectin

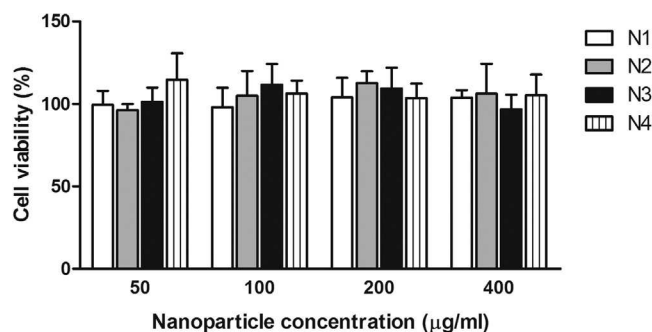


**Fig. 2.** Caco-2 cell viability (%) determined by MTT after 2 h of incubation with lipid/alginate nanoparticle suspension diluted in HBSS pH 7.4 obtaining final nanoparticle concentration of 50–400  $\mu\text{g ml}^{-1}$  with respect to lecithin (mean values  $\pm$  S.D.,  $n=3$ ).

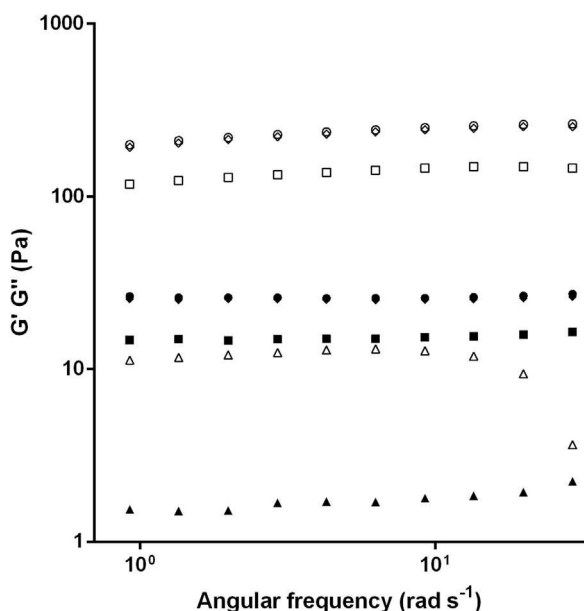


**Fig. 3.** Elastic ( $G'$ ; open symbol) and viscous ( $G''$ ; filled symbol) modulus as a function of angular frequency of different gels obtained at pectin concentration of  $2.5 \text{ mg ml}^{-1}$  and  $2.65 \text{ mM Ca}^{2+}$ : NP-loaded pectin gel (circle), pectin/alginate gel in the presence of ethanol (4%, v/v) (square), pectin gel in the presence of ethanol (3%, w/w) (rhomb) and pectin gel (triangle).

continuous phase resulted in final pectin concentration of  $2.5 \text{ mg ml}^{-1}$  and  $\text{Ca}^{2+}$  concentration of  $2.65 \text{ mM}$ .

Apart from pectin- $\text{Ca}^{2+}$  interaction, the impact of interaction of pectin and alginate present at the surface of nanoparticles, as well as with alginate in the free form, on the rheological properties of *in situ* forming pectin gel should be expected. Namely, microstructure and rheological behaviour of pectin/alginate mixed gels have already been studied (Walkenstrom et al., 2003). The properties of polymers such as alginate  $\alpha$ -L-guluronate (G) content and pectin degree of esterification and amidation affected the alginate/pectin mixed gel network density and rheological properties.

The frequency sweep measurements of NP-loaded gel and relevant controls are shown in Fig. 3. Among gels prepared in the presence of ethanol (3%, w/w), the complex formulation containing NPs in pectin gel and NP-free pectin gel showed equal rheological behaviour. However, slightly lower elastic and viscous modulus were recorded for NP-free pectin/alginate gel. The observed decrease can be ascribed to the interaction of pectin and alginate in simple mixed system. It has already been reported that mixing of LM amidated pectin and high G alginate resulted in gels with the impaired elastic modulus (Walkenstrom et al., 2003). The absence of impact of alginate on the rheological behaviour of NP-loaded pectin gel can be ascribed to alginate immobilization at the nanoparticle surface. Compared to the gels prepared in the presence of ethanol, significantly lower elastic and viscous modulus were observed for ethanol free pectin gel (Fig. 3). The influence of ethanol on viscoelastic properties can be ascribed to the decrease in polarity of the solvent and consequent decrease in interactions between polymer and solvent molecules (Guo et al., 2016).

NP-loaded gel is characterised by a log-linear decrease of complex viscosity. For angular frequencies between  $0.922$  and  $92.9 \text{ rad/s}$ , the viscosity decreased from  $219.00$  to  $2.14 \text{ Pa.s}$ . Observed complex viscosity corresponds to the range of viscosities of nasal mucus at physiological as well as under disease conditions (Lai et al., 2009).

Zero shear viscosity of the system prior gelling was determined by creep test, at the end of the stress phase, when steady state flow behaviour was reached. Zero shear viscosity ( $\eta_0$ ) was  $114.17 \pm 0.38 \text{ Pa.s}$ . This relatively high value of viscosity at zero shear indicates that the NP system would have adequate suspension stability and would not tend to settle due to the gravity. Shear viscosity profile showed pseudoplastic behaviour of the system prior gelling. The significant decrease in viscosity was observed with increasing shear rate. At shear rates above  $1 \text{ s}^{-1}$  the viscosity stabilized at values of  $3.5 \times 10^{-3} \text{ Pa.s}$ . Such a behaviour assures good sprayability, since, for example, the approximate shear rate for dispensing nasal spray from plastic squeeze bottle is  $20,000 \text{ s}^{-1}$  (Block, 2012).

### 3.5. In vitro release of Dex from NP-loaded pectin gel

The release profiles of Dex from NP-loaded gel and relevant controls (NP suspension and solution) were determined with  $\text{CaCl}_2$  solution ( $2.65 \text{ mM}$ ) as a receptor medium. Equal concentration of  $\text{Ca}^{2+}$  in the gel formulation and the receptor medium was a prerequisite to ensure pectin gel stability over the experiment. SDS was omitted from the receptor medium as it precipitates in the presence of divalent cations (Rodriguez et al., 2001).

Results obtained clearly showed that Dex entrapment in nanoparticles significantly retarded Dex release in comparison to Dex solution (Fig. 4) ( $t_{50\%}$  1.7 h and 0.6 h, respectively;  $f_2 = 37.8$ ), confirming the findings obtained with SDS solution as receptor medium. However, incorporation of Dex loaded nanoparticles in pectin gel provided only scarce reduction in Dex release in comparison to Dex-loaded nanoparticle suspension (Fig. 4) ( $t_{50\%}$  2.1 h and 1.7 h, respectively;  $f_2 = 55.9$ ). These results suggest that Dex release from NP is the rate-limiting step that governed the overall Dex release profile from NP-loaded gel. The possible better control over the drug release can be achieved by gel of fine tuned stiffness and mesh size or binding affinity of the drug to the gel constituents. However, such an approach requires a gel matrix tailoring for each specific drug (Nowald et al., 2017; Watts and Smith, 2009). In addition, extensive reduction in release rate could be unfavorable as it could impair the therapeutic effect.

### 3.6. Evaluation of NP-loaded gel biocompatibility

Pectin is described as “generally regarded as safe” due to the long history of usage in pharmaceutical and food products (Watts and Smith, 2009). LM pectin has already been used in PecFent<sup>®</sup>, an innovative nasal fentanyl formulation (Watts et al., 2013). As expected, NP-loaded pectin gel prepared in this study, was shown not to induce the decrease in cell viability under experimental

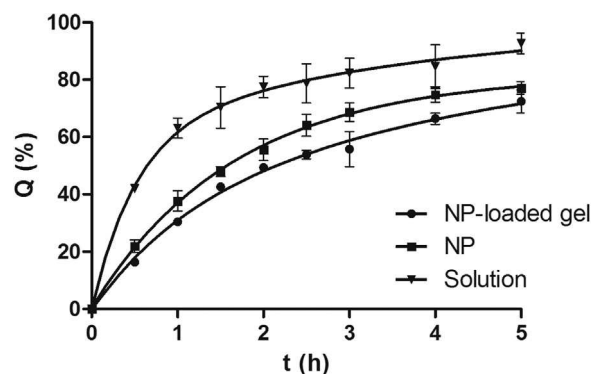


**Fig. 4.** Release profiles of Dex from NP and NP-loaded gel in  $\text{CaCl}_2$  solution ( $2.65 \text{ mM}$ ). The profile of Dex diffusion from the solution across the dialysis membrane is also presented. Data are expressed as the mean  $\pm$  SD ( $n=3$ ).

**Table 3**

Permeation of Dex across Caco-2 monolayer from solution in HBSS-Ca<sup>2+</sup> and ethanol/HBSS-Ca<sup>2+</sup> (3%, w/w), NP suspension in HBSS-Ca<sup>2+</sup>, NP-loaded pectin gel presented by apparent permeability coefficients ( $P_{app}$ ). Data are expressed as the mean  $\pm$  SD ( $n = 3$ ). Statistically significant differences between NP-loaded pectin gel and Dex solution in HBSS were observed ( $P < 0.05$ ).

Sample	Dex content ( $\mu\text{g mL}^{-1}$ )	$P_{app}$ ( $10^{-6} \text{ cm s}^{-1}$ )	Attenuation factor <sup>a</sup>
Dex/HBSS-Ca <sup>2+</sup>	60	9.73 $\pm$ 0.57	
Dex/EtOH/HBSS-Ca <sup>2+</sup>	60	9.68 $\pm$ 0.68	1.00
NP	60	8.89 $\pm$ 0.50	0.91
NP	112	9.12 $\pm$ 0.09	0.94
NP-loaded pectin gel	112	7.88 $\pm$ 0.15	0.81

<sup>a</sup> Attenuation factor represents the ratio of  $P_{app}$  of dexamethasone from the tested sample and  $P_{app}$  of dexamethasone from HBSS solution.

conditions employed and was proven to be biocompatible with the selected epithelial cell model (data not shown).

### 3.7. In vitro permeability through epithelial model barrier

NP-loaded *in situ* gelling system is designed in a way to control the release of the drug over time ensuring prolonged activity and at the same time limiting the absorption through nasal mucosa. In order to assess the potential of proposed system to influence Dex transmucosal permeation, we determined the apparent permeability coefficients ( $P_{app}$ ) of Dex from NP-loaded gel, NP suspension and solution across Caco-2 monolayer (Table 3). HBSS-Ca<sup>2+</sup> and ethanol/HBSS-Ca<sup>2+</sup> (3% w/w) Dex solutions were used as controls. The results obtained suggested no influence of ethanol at concentration tested on Dex permeation.  $P_{app}$  values for both Dex solutions were comparable to the value reported in the literature (Beck et al., 2007). Dex permeation tended to decrease with the incorporation into nanoparticles compared to the Dex solution, but the difference observed was shown to be statistically insignificant. At the same time NP suspension provided significant reduction in Dex release compared to Dex solution ( $t_{50\%}$  1.7 h and 0.6 h, respectively;  $f_2 = 37.8$ ). These results lead to the conclusion that permeation is not fully controlled by the drug release. One of the possible mechanisms that could contribute to Dex permeation across the model epithelial barrier is the internalisation of Dex-loaded nanoparticles. Mechanisms of internalisation/endocytosis of polymeric and lipidic nanoparticles have been well described in the literature and were shown to be highly dependent on the physicochemical properties of the nanoparticles such as size and zeta-potential (Beloqui et al., 2016). Nanoparticles characterised by similar mean diameter and surface charge as nanoparticles developed in this study were readily internalised by different epithelial cells. Namely, carboxylated chitosan grafted nanoparticles with mean diameter of 300 nm and zeta-potential of  $-35$  mV were shown to be internalised and transported across Caco-2 cell monolayers (He et al., 2012). PLGA nanoparticles coated with Carbopol with mean diameter of 285.9 nm and zeta-potential of  $-25.7$  mV were characterised by enhanced internalisation in comparison to uncoated PLGA nanoparticles (mean diameter about 250 nm and zeta-potential about  $-18$  mV) (Surassmo et al., 2015). The enhanced internalisation of Carbopol coated PLGA nanoparticles has been ascribed to the enhanced adhesion forces related to the large amount of Carbopol carboxylic groups.

Statistically significant Dex permeation decrease in comparison to solution was achieved upon the entrapment of Dex-loaded nanoparticles into gel formed in contact with Ca<sup>2+</sup> ( $P = 0.004$ ). The observed behaviour can partially be ascribed to retarded diffusion of Dex-loaded nanoparticles through gel matrix which could

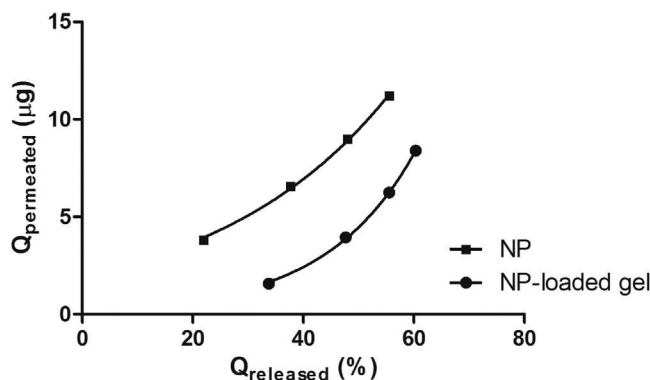


**Fig. 5.** Correlation between cumulative amount of Dex permeated across epithelial Caco-2 cell model and cumulative amount of Dex released from NP suspension and NP-loaded pectin gel.

moderate nanoparticle cell internalisation and contribute to the decrease of Dex  $P_{app}$ . Nanoparticle diffusion through the polymer matrix is hindered by the presence of the polymer network fibres or chains and their possible interactions with nanoparticle surface (de Kort et al., 2015). Diffusion-related nanoparticle cell internalisation in case of biopolymer gel matrix systems was already shown for doxorubicin-loaded PLGA/PEG nanoparticles and 3D collagen system cell cultures (Biondi et al., 2013). The overall attenuation factor of 0.81, obtained for NP-loaded gel in relation to Dex solution (Table 3), is comparable to those reported for Dex-loaded nanoparticle-coated microparticles (Beck et al., 2007).

In order to further analyse the mechanisms of Dex permeation control, we correlated data obtained by *in vitro* permeation and release studies for NP suspension and NP-loaded pectin gel with Dex content of  $112 \mu\text{g mL}^{-1}$ . Fig. 5 presents the exponential correlation between cumulative amount of Dex permeated across epithelial cell model and cumulative amount of Dex released for NP suspension and NP-loaded pectin gel, indicating that Dex permeation is related to the concentration of the Dex released at the site of absorption. Similar results were already obtained for Dex-loaded nanoparticle-coated microparticles (Beck et al., 2007). However, the shift between the correlation curves obtained for NP suspension and NP-loaded gel suggested the existence of another factor influencing the Dex permeation across the model epithelial barrier. More specifically, in case of NP suspension, each cumulative amount of Dex released was correlated with higher amount of Dex permeated than in case of NP-loaded pectin gel. This supports the already mentioned assumption that Dex permeation could also be related to cell internalisation of Dex-loaded nanoparticles, and that such process might be hindered by nanoparticle incorporation into pectin gel.

## 4. Conclusions

Herein we propose nanoparticle loaded *in situ* gelling system for corticosteroid effective nasal delivery for the treatment of chronic rhinosinusitis with nasal polyps. Such a sprayable system bears the potential to: (i) allow corticosteroid delivery beyond the nasal valve where the polyps occur and, after sol-gel transition triggered by Ca<sup>2+</sup>, (ii) ensure prolonged local action of corticosteroid due to prolonged residence time at the site of application and moderate corticosteroid release and permeation. The proposed study gives an *in vitro* proof-of-concept for the potential of developed system to provide efficient local corticosteroid delivery/effect. However, for the final proof-of-concept, the study must be extended to an appropriate *in vivo* model.



## Acknowledgement

This work was supported by a project entitled “Development of *in vitro* models for early biopharmaceutical characterization of drug delivery nanosystems” (BM072) which was funded by the University of Zagreb.

## References

- Beck, R.C., Pohlmann, A.R., Hoffmeister, C., Gallas, M.R., Collnot, E., Schaefer, U.F., Guterres, S.S., Lehr, C.M., 2007. Dexamethasone-loaded nanoparticle-coated microparticles: correlation between *in vitro* drug release and drug transport across Caco-2 cell monolayers. *Eur. J. Pharm. Biopharm.* 67, 18–30.
- Beloqui, A., des Rieux, A., Preat, V., 2016. Mechanisms of transport of polymeric and lipidic nanoparticles across the intestinal barrier. *Adv. Drug Deliv. Rev.* 106, 242–255.
- Biondi, M., Guarnieri, D., Yu, H., Belli, V., Netti, P.A., 2013. Sub-100 nm biodegradable nanoparticles: *in vitro* release features and toxicity testing in 2D and 3D cell cultures. *Nanotechnology* 24, 045101.
- Blazevic, F., Milekic, T., Romic, M.D., Juretic, M., Pepic, I., Filipovic-Grcic, J., Lovric, J., Hafner, A., 2016. Nanoparticle-mediated interplay of chitosan and melatonin for improved wound epithelialisation. *Carbohydr. Polym.* 146, 445–454.
- Block, L.H., 2012. Rheology. In: Felton, L. (Ed.), *Remington Essential of Pharmaceutics*. Pharmaceutical Press, London, pp. 393–410.
- Cortes, R., Esposito, E., Menegatti, E., Gambari, R., Nastruzzi, C., 1996. Effect of cationic liposome composition on *in vitro* cytotoxicity and protective effect on carried DNA. *Int. J. Pharm.* 139, 69–78.
- Ekelund, K., Osth, K., Pahlstorp, C., Bjork, E., Ulvenlund, S., Johansson, F., 2005. Correlation between epithelial toxicity and surfactant structure as derived from the effects of polyethyleneoxide surfactants on caco-2 cell monolayers and pig nasal mucosa. *J. Pharm. Sci.* 94, 730–744.
- Fokkens, W.J., Lund, V.J., Mullol, J., Bachert, C., Alobid, I., Baroody, F., Cohen, N., Cervin, A., Douglas, R., Gevaert, P., Georgalas, C., Goossens, H., Harvey, R., Hellings, P., C. H., N. J., Joos, G., Kalogjera, L., Kern, B., Kowalski, M., D. P., Riechelmann, H., Schlosser, R., B. S., Thomas, M., Toskala, E., Voegels, R., Wang, D. Y., Wormald, P.J., 2012. European position paper on rhinosinusitis and nasal polyps 2012. *Rhinology* 50, 1–298.
- Fuongfuchat, A., Jamieson, A.M., Blackwell, J., Gerken, T.A., 1996. Rheological studies of the interaction of mucins with alginate and polyacrylate. *Carbohydr. Res.* 284, 85–99.
- Griffiths, P.C., Cattoz, B., Ibrahim, M.S., Anuonye, J.C., 2015. Probing the interaction of nanoparticles with mucin for drug delivery applications using dynamic light scattering. *Eur. J. Pharm. Biopharm.* 97, 218–222.
- Guo, X.M., Meng, H.C., Tang, Q., Pan, R.Q., Zhu, S.M., Yu, S.J., 2016. Effects of the precipitation pH on the ethanolic precipitation of sugar beet pectins. *Food Hydrocolloid* 52, 431–437.
- Hafner, A., Lovric, J., Voinovich, D., Filipovic-Grcic, J., 2009. Melatonin-loaded lecithin/chitosan nanoparticles: physicochemical characterisation and permeability through Caco-2 cell monolayers. *Int. J. Pharm.* 381, 205–213.
- Hafner, A., Lovric, J., Romic, M.D., Juretic, M., Pepic, I., Cetina-Cizmek, B., Filipovic-Grcic, J., 2015. Evaluation of cationic nanosystems with melatonin using an eye-related bioavailability prediction model. *Eur. J. Pharm. Sci.* 75, 142–150.
- Hansen, F.S., Djupesland, P.G., Fokkens, W.J., 2010. Preliminary efficacy of fluticasone delivered by a novel device in recalcitrant chronic rhinosinusitis. *Rhinology* 48, 292–299.
- He, C., Yin, L., Tang, C., Yin, C., 2012. Size-dependent absorption mechanism of polymeric nanoparticles for oral delivery of protein drugs. *Biomaterials* 33, 8569–8578.
- Hubatsch, I., Ragnarsson, E.G., Artursson, P., 2007. Determination of drug permeability and prediction of drug absorption in Caco-2 monolayers. *Nat. Protoc.* 2, 2111–2119.
- Joergensen, L., Klosgen, B., Simonsen, A.C., Borch, J., Hagesaether, E., 2011. New insights into the mucoadhesion of pectins by AFM roughness parameters in combination with SPR. *Int. J. Pharm.* 411, 162–168.
- Karavasili, C., Fatouros, D.G., 2016. Smart materials: *in situ* gel-forming systems for nasal delivery. *Drug Discov. Today* 21, 157–166.
- Kaulbach, H.C., White, M.V., Igarashi, Y., Hahn, B.K., Kaliner, M.A., 1993. Estimation of nasal epithelial lining fluid using urea as a marker. *J. Allergy Clin. Immunol.* 92, 457–465.
- Lai, S.K., Wang, Y.Y., Wirtz, D., Hanes, J., 2009. Micro- and macrorheology of mucus. *Adv. Drug Deliv. Rev.* 61, 86–100.
- Lv, H., Zhang, S., Wang, B., Cui, S., Yan, J., 2006. Toxicity of cationic lipids and cationic polymers in gene delivery. *J. Control. Release* 114, 100–109.
- Mao, S., Germershaus, O., Fischer, D., Linn, T., Schnepf, R., Kissel, T., 2005. Uptake and transport of PEG-graft-trimethyl-chitosan copolymer-insulin nanocomplexes by epithelial cells. *Pharm. Res.* 22, 2058–2068.
- Martinac, A., Filipovic-Grcic, J., Perissutti, B., Voinovich, D., Pavelic, Z., 2005. Spray-dried chitosan/ethylcellulose microspheres for nasal drug delivery: swelling study and evaluation of *in vitro* drug release properties. *J. Microencapsul.* 22, 549–561.
- Martino, B.J., Church, C.A., Seiberling, K.A., 2015. Effect of intranasal dexamethasone on endogenous cortisol level and intraocular pressure. *Int. Forum Allergy Rhinol.* 5, 605–609.
- Mezger, T.G., 2014. Frequency sweeps. In: Mezger, T.G. (Ed.), *The Rheology Handbook*. 4th ed. Vincentz Network, Hanover, Germany, pp. 159–176.
- Nowald, C., Kasdorf, B.T., Lieleg, O., 2017. Controlled nanoparticle release from a hydrogel by DNA-mediated particle disaggregation. *J. Control. Release* 246, 71–78.
- Rodriguez, C.H., Lowery, L.H., Scamehorn, J.F., Harwell, J.H., 2001. Kinetics of precipitation of surfactants. I. Anionic surfactants with calcium and with cationic surfactants. *J. Surfactants Deterg.* 4, 1–14.
- Romeo, V.D., deMeireles, J., Sileno, A.P., Pimplaskar, H.K., Behl, C.R., 1998. Effects of physicochemical properties and other factors on systemic nasal drug delivery. *Adv. Drug Deliv. Rev.* 29, 89–116.
- Scarioti, G.D., Lubambo, A., Feitosa, J.P., Sierakowski, M.R., Bresolin, T.M., de Freitas, R.A., 2011. Nanocapsule of cationic liposomes obtained using *in situ* acrylic acid polymerization: stability, surface charge and biocompatibility. *Colloids Surf. B Biointerfaces* 87, 267–272.
- Surassmo, S., Saengkrit, N., Ruktanonchai, U.R., Suktham, K., Woramongkolchai, N., Wutikhun, T., Puttipatkhachorn, S., 2015. Surface modification of PLGA nanoparticles by carbopol to enhance mucoadhesion and cell internalization. *Colloids Surf. B Biointerfaces* 130, 229–236.
- Vanthanouvong, V., Roomans, G.M., 2004. Methods for determining the composition of nasal fluid by X-ray microanalysis. *Microsc. Res. Tech.* 63, 122–128.
- Verma, A., Stellacci, F., 2010. Effect of surface properties on nanoparticle-cell interactions. *Small* 6, 12–21.
- Vlckova, I., Navratil, P., Kana, R., Pavlicek, P., Chrbolka, P., Djupesland, P.G., 2009. Effective treatment of mild-to-moderate nasal polyposis with fluticasone delivered by a novel device. *Rhinology* 47, 419–426.
- Walkenstrom, P., Kidman, S., Hermansson, A.M., Rasmussen, P.B., Hoegh, L., 2003. Microstructure and rheological behaviour of alginate/pectin mixed gels. *Food Hydrocolloid* 17, 593–603.
- Wattanakorn, N., Asavapichayont, P., Nunthanid, J., Limmatvapirat, S., Sungthongjeen, S., Chantasart, D., Sriamornsak, P., 2010. Pectin-based bioadhesive delivery of carbenoxolone sodium for aphthous ulcers in oral cavity. *AAPS PharmSciTech* 11, 743–751.
- Watts, P., Smith, A., 2009. PecSys: *in situ* gelling system for optimised nasal drug delivery. *Expert Opin. Drug Deliv.* 6, 543–552.
- Watts, P., Smith, A., Perelman, M., 2013. Nasal delivery of fentanyl. *Drug Deliv. Transl. Res.* 3, 75–83.
- de Kort, D.W., van Duynhoven, J.P.M., Van As, H., Mariette, F., 2015. Nanoparticle diffusometry for quantitative assessment of submicron structure in food biopolymer networks. *Trends Food Sci. Technol.* 42, 13–26.
- Xie, F., Ji, S., Cheng, Z., 2015. *In vitro* dissolution similarity factor (*f*<sub>2</sub>) and *in vivo* bioequivalence criteria, how and when do they match? Using a BCS class II drug as a simulation example. *Eur. J. Pharm. Sci.* 66, 163–172.